RHODIUM-CATALYZED REACTIONS OF (*Z*)-2-EN-4-YNE ACETATES WITH ARYLBORONIC ACIDS

A Thesis Submitted to
the Graduate School of Engineering and Sciences of
İzmir Institute of Technology
in Partial Fulfillment of the Requirements for the Degree of

MASTER OF SCIENCE

in Chemistry

by
Erman KARAKUŞ

July 2011
İZMİR

ACKNOWLEDGEMENTS

First of all, I would like to thank my supervisor Prof. Dr. Levent Artok for his patient guidance, encouragement and excellent advice throughout this study. This thesis could not have been written without his astute guidance. It was honor to study with him.

Also I would like to thank all old and new members of İYTE organic research group, Gürkan Eray Akpınar, Fırat Ziyanak and Ezgi Şule Karagöz. I would like to extend special thanks to Muhammed Üçüncü for his support, help and friendship for seven years.

Special thanks to Assoc. Prof. Dr. Hayati Türkmen and Assist. Prof. Dr. Mustafa Emrullahoğlu for participating as committee member and for reviewing my work.

I would like to thank to the Dr. Hüseyin Özgener for FT-IR analyses, Dr. Özge Aksın-Artok for HRMS analyses, Işın Özçelik, Salih Günnaz (Ege University) and Dr. Wolf Hiller (Dortmund Universtiy of Technology) for NMR analyses. Also I would like to thank Assoc. Prof. Dr. Nuran Elmacı and Sıla Karaca for computational calculations.

I would like to express my thanks to my family and my best friends, Yalçın Savran and Ege Ermin for their love, motivation, continuous support and prayers.

Finally, I would like to thank specially to my beloved Ayşenur Çataler for her love, support and encouragement. She was always gentle and patient to me when I felt tired and confused during this study.

ABSTRACT

RHODIUM-CATALYZED REACTIONS OF (*Z*)-2-EN-4-YNE ACETATES WITH ARYLBORONIC ACIDS

This study is the first example of rhodium(I)-catalyzed arylative S_N2" type reaction of (*Z*)-2-en-4-yne acetates with arylboronic acids leading to *E*-configured vinyl-allenes with an aryl moiety.

The coordinative interaction of the rhodium with carbonyl oxygen promoted the δ-elimination of Rh(I)-OAc from the alkenylrhodium intermediate in both *syn*- and *anti*-modes, with the *syn*-elimination being the major path. DFT calculations revealed that a conformer of this intermediate which can lead to the *E*-configured vinylallene product via the *syn*-elimination mode, is energetically the most favorable conformer. The rhodium-catalyzed procedure is not applicable to reactions involving (*E*)-configured enyne acetates, because the geometry of the alkenylrhodium intermediate that is derived from the corresponding *E*-enyne acetate would not allow such coordinative interaction to occur.

ÖZET

(*Z*)-2-EN-4-İN ASETATLARIN ARİLBORONİK ASİTLERLE RODYUM-KATALİZLİ TEPKİMELERİ

Bu çalışma (*Z*)-2-en-4yne asetatların arilboronik asitler ile rodyum(I) katalizli arilatif S_N2" tipi reaksiyonları sonucunda *E*-konfigürasyonuna sahip, aril grubu içeren vinil allenlerin oluşmasını gösteren ilk örnektir.

Rodyumun karbonil oksijeni ile koordinatif etkileşimi Rh(I)-OAc kompleksinin alkenilrodyum ara ürününden δ-ayrılma yapmasını hem *syn* hem de *anti* biçiminde, desteklemektedir. Ancak syn ayrılma ürünü ana üründür. DFT hesaplamaları syn-ayrılma yoluyla elde edilen *E*-konfigürasyonuna sahip vinilallenin ara ürününün enerji açışından en uygun konformasyon olduğunu göstermiştir. E-konfigürasyonuna sahip enin asetatların rodyum katalizli tepkimeleri uygulanabilir değildir. Bunun nedeni *E*-enin asetatın oluşturduğu alkenilrodyum ara ürününün geometrik yapısı karbonil oksijeniyle koordinatif etkileşimin oluşmasına izin vermez.

TABLE OF CONTENTS

LIST OF FIGURES viii

LIST OF TABLES x

CHAPTER 1. INTRODUCTION 1

CHAPTER 2. TRANSITION METAL-CATALYZED REACTIONS OF ORGANOBORONS 3

2.1. Organoborons 3

2.2. Catalytic Cycle of Rh and Group 10 Metals 4

2.2.1. Structural Properties of Aryl-Rhodium Complexes 6

2.3. Rhodium-Catalyzed Addition of Organoborons to Cyclic and Acyclic Enones 7

2.4. Rhodium-Catalyzed Reactions of Organoborons to Aldehydes 8

2.5. Rhodium-Catalyzed Reactions of Organoborons with Alkenes, Alkynes and Their Derivatives 9

CHAPTER 3. ALLENES 15

3.1. What is allene? 15

3.2. Allenes in Use 15

3.2. Synthesis of Vinyl Allenes 17

3.2.1. Synthesis of Vinyl Allenes with Grignard Reagents 17

3.2.2. Synthesis of Vinylallenes with Organocopper Reagents 18

3.2.3. Rhodium-Catalyzed Asymmetric 1,6-Addition of Aryltitanates to Enynones Giving Axially Chiral Allenes 19

3.2.4. Palladium-Catalyzed Alkoxycarbonylation of (*Z*)-2-En-4-yne Carbonates Leading to 2,3,5-Trienoates 19

3.2.5. Palladium-Catalyzed 1,5-Substitution Reactions of 2-En-4-yne Carbonates with Organoboronic Acids 20

CHAPTER 4. EXPERIMENTAL STUDY 21
4.1. General Procedures for Drying the Solvents and Synthesis of Catalysts 21
4.2. Synthesis of Substrates 21
4.2.1. Synthesis of *Z*-Enyne Acetates 1b, 1c, 1g, 1h, and *E*-1a : 21
4.2.2. Synthesis of *Z*-Enyne Acetates 1c-1e 23
4.2.3. Synthesis of non-2-en-4-yn-3ylbenzene 25
4.2.4. Synthesis of Methyl (*R,Z*)-4-methylhept-3-en-5-yn-2-yl acetate [(*R,Z*)-1a] 25
4.3. Characterization of Reactants 26
4.4. General Procedure for Arylation Reactions 32
4.5. Characterization of Products 32
4.6. Computational Details 40

CHAPTER 5. RESULTS AND DISCUSSION.....41

CHAPTER 6. CONCLUSION 49

REFERENCES. 50

APPENDICES
APPENDIX A. ^{1}H NMR and ^{13}CNMR SPECTRUMS OF REACTANTS 54
APPENDIX B. MASS SPECTRUMS OF REACTANTS 82
APPENDIX C. FTIR SPECTRUMS OF REACTANTS 96
APPENDIX D. ^{1}H NMR and ^{13}CNMR SPECTRUMS OF PRODUCTS.....110
APPENDIX E. MASS SPECTRUMS OF PRODUCTS.....141
APPENDIX F. FTIR SPECTRUMS OF PRODUCTS 157
APPENDIX G. HPLC CHROMATOGRAMS OF REACTANT AND PRODUCTS.....173
APPENDIX H. GC CHROMATOGRAMS OF RACEMIC AND ENANTIOMERICALLY PURE (R,Z)-4-METHYLHEPT-3-EN-5-YN-2-OL……...182
APPENDIX I. COMPUTATIONAL CALCULATIONS DATA……...187

LIST OF FIGURES

Figure **Page**

Figure 2.1. The structure of organoboron compounds..... 3
Figure 2.2. Possible catalytic cycle for Ni, Pd and Pt..... 5
Figure 2.3. Possible catalytic cycles for Rh-catalyst 6
Figure 2.4. Rhodium-aryl complexes characterized crystallographically 6
Figure 2.5. Effect of o-substituent 7
Figure 2.6. Rh-catalyzed addition reaction of boronic acids to enones..... 7
Figure 2.7. Enantioselective Rh-catalyzed reaction of boronic acids with enones..... 8
Figure 2.8. Rh-catalyzed addition reaction of boronic acids to aldehydes.....8
Figure 2.9. Reaction mechanism of Rh-catalyzed reaction of boronic acids to aldehyde 8
Figure 2.10. Rh-catalyzed multiple alkylation on aromatic ring 9
Figure 2.11. Rh-catalyzed coupling reactions of alkenes with arylboronic acids 9
Figure 2.12. Rh-catalyzed addition of boronic acids to the fluoroalkylated electrondeficient olefins 10
Figure 2.13. Rh catalyzed hydroarylation of alkynes 10
Figure 2.14. The proposed mechanism for Rh-catalyzed hydroarylation of alkynes 10
Figure 2.15. Rh catalyzed addition of arylboronic acids to pyridine substituted alkynes 11
Figure 2.16. Rh-catalyzed coupling of *ortho*-carbonylated arylboronic acids and alkynes 11
Figure 2.17. Rh-catalyzed reaction of phenylboronic acids with alkynyl oxiranes..... 12
Figure 2.18. Proposed mechanism for the Rh-catalyzed reaction of phenylboronic acids with alkynyl oxiranes..... 12
Figure 2.19. Possible mechanism of Rh catalyzed addition and β-acetate elimination reaction in both anti and *syn* modes..... 13
Figure 2.20. Asymmetric Rh catalyzed enantioselective 1,6-addition of arylboronic acids to enynamides..... 14

Figure 3.1. Cumulated Diene (Allene)..... 15
Figure 3.2. Configurational determination of chiral allene. 15
Figure 3.3. Activity of axial chirality 16
Figure 3.4. The vinylallene pheromone (Pheromone of Acanthoscelides obtectus) isolated from male dried bean beetles 16
Figure 3.5. Synthesis of vinylallene insect phreromone 17
Figure 3.6. The reaction of chloro-enynes with grignard reagent 17
Figure 3.7. Reactions of enyne acetates with lithium dialkylcuprates..... 18
Figure 3.8. Reactions of enyne oxiranes with lithium dialkylcuprates..... 18
Figure 3.9. Synthesis of chiral allenylalkenyl silyl enol ethers. 19
Figure 3.10. Pd(0)-catalyzed alkoxycarbonylation of *Z*-enyne carbonates 19
Figure 3.11. Pd(0)-catalyzed 1,5-substitution reactions of enyne carbonates 19
Figure 4.1. Synthesis of Z-Enyne Acetates 1a, 1b, 1f, 1g, and *E*-1a 21
Figure 4.2. Synthesis of Z-Enyne Acetates 1c-1e..... 23
Figure 4.3. Synthesis of non-2-en-4-yn-3ylbenzene..... 25

Figure 4.4. (*Z*)-4-methylhept-3-en-5-yn-2-yl acetate 27
Figure 4.5. (*Z*)-4-methyldec-3-en-5-yn-2-yl acetate 27
Figure 4.6. (*Z*)-6-cyclohexyl-4-methylhex-3-en-5-yn-2-yl acetate 27
Figure 4.7. (*Z*)-4-butyldec-3-en-5-yn-2-yl acetate 28
Figure 4.8. (*Z*)-4-phenyldec-3-en-5-yn-2-yl acetate 28
Figure 4.9. (*Z*)-7-methyldec-6-en-8-yn-5-yl acetate 29
Figure 4.10. (*Z*)-2,5-dimethyloct-4-en-6-yn-3-yl acetate 29
Figure 4.11. (Z)-4-methyl-6-(trimethylsilyl)hex-3-en-5-yn-2-yl acetate 30
Figure 4.12. (*Z*)-4-methyl-6-phenylhex-3-en-5-yn-2-yl acetate 30
Figure 4.13. (*Z*)-4,7,7-trimethyloct-3-en-5-yn-2-yl acetate 30
Figure 4.14. (*Z*)-dec-3-en-5-yn-2-yl acetate 31
Figure 4.15. (*Z*)-3-methylnon-2-en-4-ynyl acetate 31
Figure 4.16. (*E*)-4-methylhept-3-en-5-yn-2-yl acetate 32
Figure 4.17. (*E*)- 2-phenyl-4-methylhepta-2,3,5-triene 32
Figure 4.18. ((*E*)-2-(4-(trifluoromethyl)-phenyl)-4-methylhepta-2,3,5-triene 33
Figure 4.19. (*E*)-2-(4-acetylphenyl)-4-methylhepta-2,3,5-triene 33
Figure 4.20. (*E*)-2-(4-meyhylphenyl)-4-methylhepta-2,3,5-triene 34
Figure 4.21. (*E*)-2-(3-meyhylphenyl)-4-methylhepta-2,3,5-triene 34
Figure 4.22. (*E*)-2-(3-chlorophenyl)-4-methylhepta-2,3,5-triene 35
Figure 4.23. (*E*)-2-(2-methoxyhenyl)-4-methylhepta-2,3,5-triene 35
Figure 4.24. (*E*)- 2-(2-naphthyl)-4-methylhepta-2,3,5-triene 36
Figure 4.25. (*E*)- 2-(3-thienyl)-4-methylhepta-2,3,5-triene 36
Figure 4.26. (*E*)- 6-phenyl-4-methyldeca-2,4,5-triene 37
Figure 4.27. (*E*) 1-cyclohexyl-1-phenyl-3-methyl-hexa-1,2,4-triene 37
Figure 4.28. (*E*)-5-phenyl-7-(prop-1-enyl)undeca-5,6-diene 38
Figure 4.29. (*E*)-4,6-diphenyl-deca-2,4,5-triene 38
Figure 4.30. (*E*)-4-methyl-2-phenyl-deca-2,3,5-triene 39
Figure 4.31. (*E*)-4,7-dimethyl-2-phenyl-octa-2,3,5-triene 39
Figure 5.1. Conjugated enynes without leaving group 45
Figure 5.2. Stereochemistry of Rh(I)-Catalyzed Arylation of (*R,Z*)-2-En-4-Yne Acetate. 45
Figure 5.3. Rh(I)-Catalyzed Arylation of (*E*)- 4-methylhept-3-en-5-yn-2-yl acetate 46
Figure 5.4. The structure of intermediate II which was subjected to dft calculations (hydrogens atoms are omitted for clarity) 47
Figure 5.5. Optimized conformers for the intermediate II (hydrogen atoms are omitted for clarity and the energy values are relative energies) 48

LIST OF TABLES

Table **Page**

Table 6.1. Effect of Base and Water Additives on the Rh(I)-Catalyzed Reaction of *Z*-Enyne Acetate 1a with Phenylboronic Acid…….42

Table 6.2. Rh(I)-Catalyzed Reaction of the *Z*-Enyne Acetate 1a with Organoboronic Acids……..…….43

Table 6.3. Rh(I)-Catalyzed Reaction of *Z*-Enyne Acetates with Phenylboronic Acids……44

CHAPTER 1

INTRODUCTION

Studies on transition metal catalyzed reactions have suddenly increased over the last two decades for the formation of C-C bonds. Rhodium-catalyzed addition reactions to different type of unsaturated systems are one of the examples of C-C bond forming process. Organometallic reagents such as Grignard, organocopper, organolithium, and organozinc are classical nucleophilic reagents for carbon-carbon coupling reactions. However, these reagents are of various restrictions in their utilization, because they are air and moisture sensitive, have very short shelf-live, and tolerates only few electrophilic groups. Thus, use of these reagents requires strict anhydrous conditions and inert atmosphere.

Due to above mentioned disadvantages of organometallic reagents, organoboron reagents bearing aryl and alkenyl groups are preferred for the transition metal catalyzed C-C bond forming reactions. Organoboron reagents are highly stable to oxygen and moisture, easy-to-handle without special precautions, and allow application of a wide range of reactive functional groups.

Organoboron reagents readily undergo transmetalation with rhodium species to produce arylrhodium(I) structures that have ability to induce the nucleophilic arylation of electrophilic sides (Fagnou and Lautens 2003; Sakai, et al. 1997).

There are many different methods for Rh-catalyzed reactions of organoboronic reagents with unsaturated systems in the literature (Fagnou and Lautens 2003; Hayashi and Yamasaki 2003; Miura, et al. 2007; Murakami and Igawa 2002; Nishimura, et al. 2010; Sakai, et al. 1997; Sakuma, et al. 2000). In 1999, It was reported that (*E*)-2-en-4-yne acetates react with different type of lithium cuprates leading to alkylated *E*- and *Z*-isomeric mixtures of vinylallenes (Purpura and Krause 1999). In 2002, Murakami and Igawa reported that propargyl acetates react with phenylboronic acids in the presence of rhodium(I) catalyst to produce allenic product with β-oxygen elimination.

Within the context of this thesis, we developed a new method for the rhodium catalyzed arylative reaction of (*Z*)-2-en-4-yne acetates with arylboronic acids to produce

E-configured vinyl-allenes. This method offered simple and mild conditions a obtaining the single diastreomer of allenic products.

CHAPTER 2

TRANSITION METAL-CATALYZED REACTIONS OF ORGANOBORONS

2.1. Organoborons

Chemical compounds bearing a functional group such as aryl or alkyl on the boron atoms are called organoborons. The term organoborons refers to a compound which has at least one C-B bond. Despite not having any C-B bonds, trialkoyxboranes are also categorized as organoboron. Boron atom is capable of forming stable covalent bond like carbon atom. Trivalent boron compounds provide electrophilic property with trigonal planar structure. However, further addition of a bond to boron produces tetravalent boron compound having tetrahedral structure and shows nucleophilic property (Figure 3.1).

Boron compounds can be used in many useful chemical reactions such as asymmetric synthesis, metal-catalysis, acid-catalysis, multicomponent reactions, biological and medical applications and in many areas from pharmaceuticals to materials because of electronic, structural and reactivity properties of organoborons.

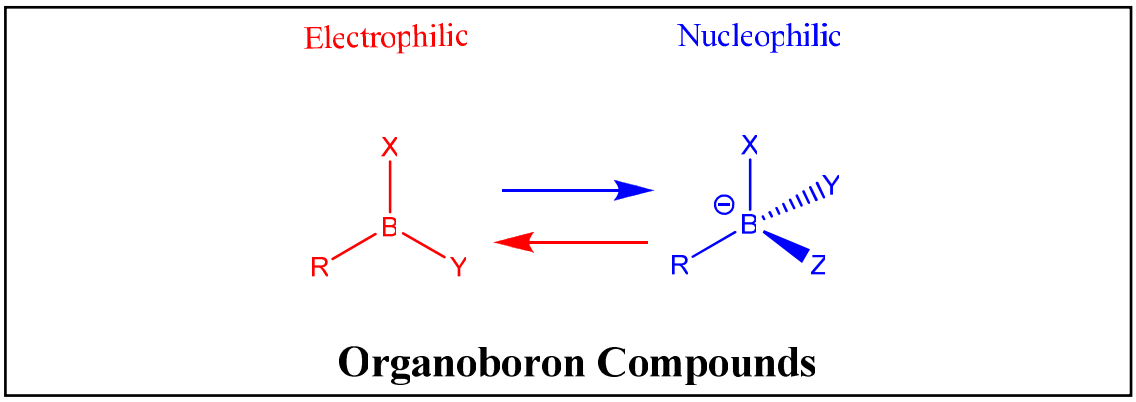

Figure 2.1. The structure of organoboron compounds
(Source: Petasis 2007)

2.2. Catalytic Cycle of Rh and Group 10 Metals

Transition metal catalyzed reactions provide very important contribution in the art of chemical synthesis. Unprecedented selectivity and new types of bond constructions have raised metal-mediated reactions. Transition metals can catalyze multistep reactions and this behavior is the one of the most important asset for them. They show variable oxidation states with finely controlled and tunable redox potentials because of changing the d-orbital energies and spacing with different ligands.

In the literature, there are many examples of transition-metal-catalyzed conjugate addition reactions of organoborons to the unsaturated systems.

Palladium(0)-catalyzed conjugate addition of aromatics to α,β-unsaturated compounds with sodium tetraphenylborate and arylboronic acids was performed in the presence of antimony (III) chloride (Cho, et al. 1995). In 2006, it was reported that conjugate addition of arylboronic acids to α,β-unsaturated carbonyl compounds proceeded with high yields in the presence of a palladium/bipyridine catalyst in aqueous media (Lin and Lu 2006). 2,4-Diarylquinolines were synthesized via the Pd-catalyzed hydroarylation of α,ß -ynones with organoboron derivatives (Arcadi, et al. 2008).

It was reported that palladium-catalyzed ring-opening addition of various arylboronic acids to heterobicyclic alkenes such as aza- and oxabicyclic alkenes resulted in formation of the corresponding products in excellent yields (Lautens and Dockendorff 2003).

In 2003, first palladium catalyzed reaction of organoboronic acids to alkynes have been reported (Oh, et al. 2003).

In 2007, it was published arylation of aromatic aldehydes with arylboroxines in the presence of Ni-phosphine ligand (Arao, et al. 2007).

When general catalytic cycle for Ni, Pd and Pt are investigated, it is observed that catalytic cycle moves around between (0) and (II) oxidation states and transmetalation can only occur with the metal(II) species in the cycle (Figure 2.2). If it is desired to viable reactions, a suitable electrophilic component must be incorporated that will oxidatively add to the metal(0) complex to produce the organometal(II) species.

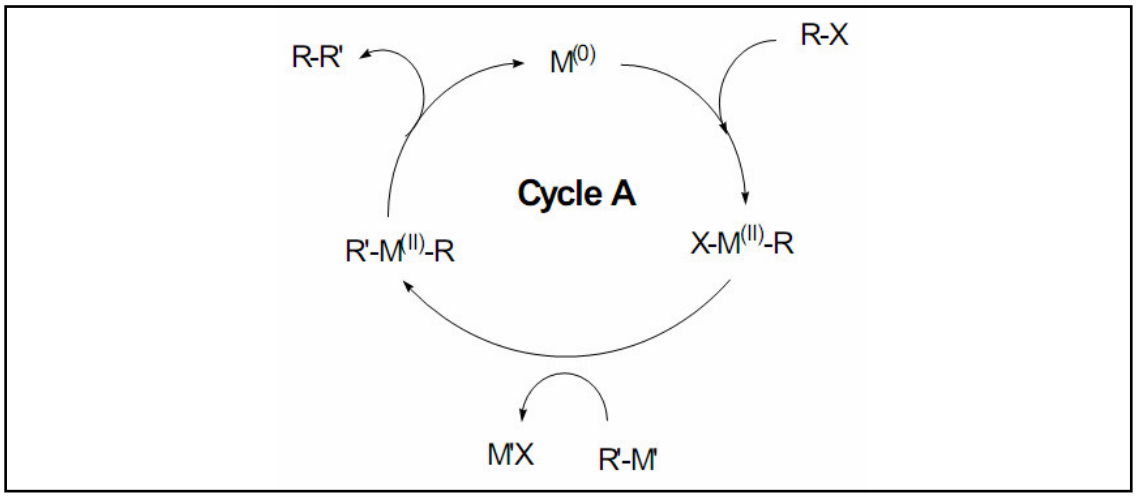

Figure 2.2. Possible catalytic cycle for Ni, Pd and Pt
(Source: Fagnou and Lautens 2003)

In the past twenty years, there has been dramatic increase in the use of transition metal-catalyzed reactions for the organic synthesis. Recently, much attention is given to rhodium catalysts in constructing carbon-carbon bond, since the rhodium-catalyzed reactions provide milder and more benign protocols.

Rhodium demonstrates interesting and different catalytic properties when the catalytic cycle is compared with group 10 metals such as Ni, Pd and Pt. Rhodium typically moves around between the (I) and (III) oxidation states in catalytic reactions with organometallic reagent. Transmetalation can occur with rhodium(I) and an organometallic compound to generate an organorhodium(I) which is capable of reacting in new ways. Addition of a suitable electrophile will produce a catalytic cycle (cycle B) as illustrated in Figure 2.3, which involves an oxidative addition. Alternatively, the organorhodium complex can be couple with an unsaturated unit of an organic compound as illustrated in cycle C. The outcome of cycle C is a net R and, H-addition across the unsaturated unit.

A wide variety of organometallic compounds reacts with rhodium(I) halides to generate rhodium-aryl complexes.

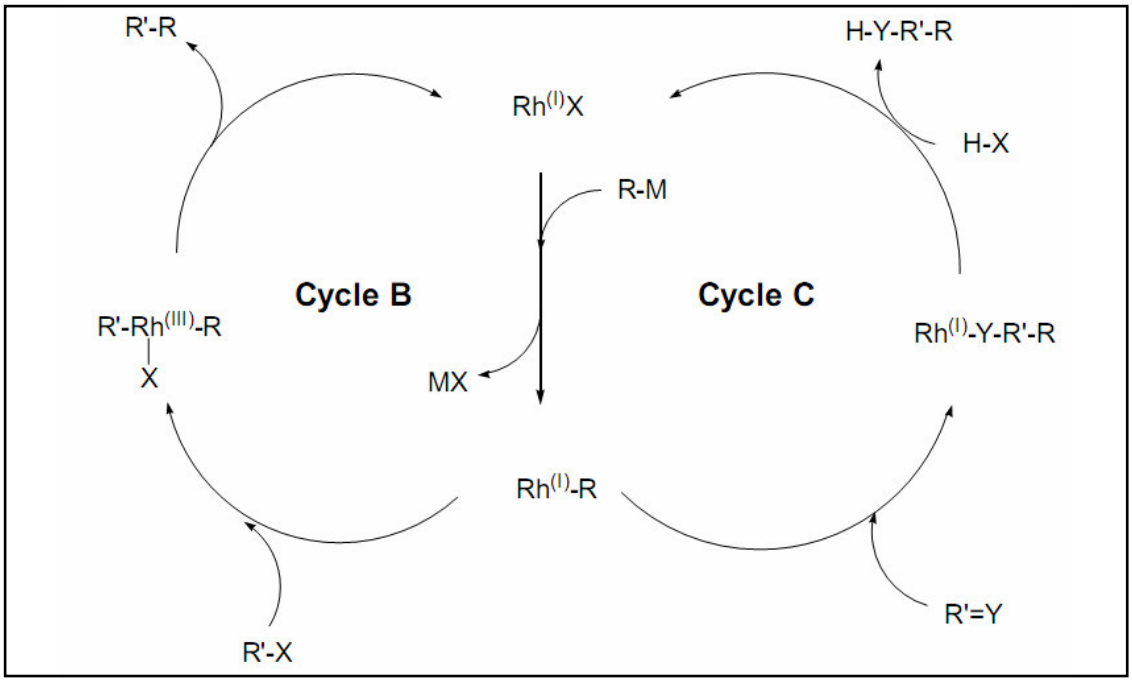

Figure 2.3. Possible catalytic cycles for Rh-catalyst
(Source: Fagnou and Lautens 2003)

2.2.1. Structural Properties of Aryl-Rhodium Complexes

Different type of crystal structure of aryl-rhodium complexes have been obtained with various kinds of ligands. Steric interactions between aryl group and adjacent ligand can be minimized by proper orientation. Aryl ring should be orthogonal to the square plane of the complex (Figure 2.4).

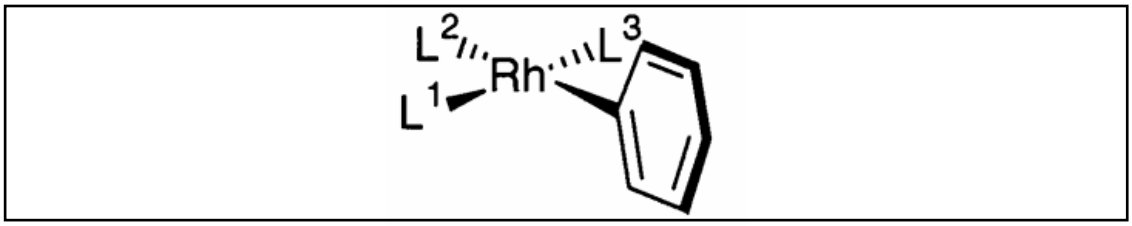

Figure 2.4. Rhodium-aryl complexes characterized crystallographically
(Source: Fagnou and Lautens 2003)

It can be seen that *ortho*-substituent on the arene situated below or above the square plane to prevent the empty coordination sites (Figure 2.5). The rate of associative

ligand process slows down with these complexes when bulky *ortho*-substituents are present.

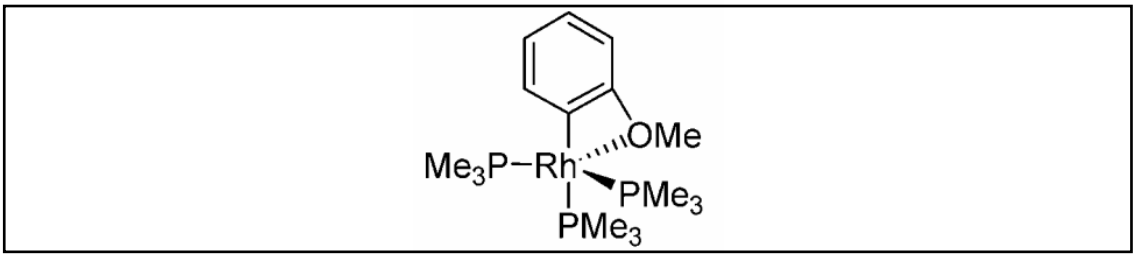

Figure 2.5. Effect of *o*-substituent
(Source: Fagnou and Lautens 2003)

2.3. Rhodium-Catalyzed Addition of Organoborons to Cyclic and Acyclic Enones

The first study in this research area was achieved in 1997. It was reported that Rh(I) complexes catalyze 1,4-addition of aryl and alkenylboronic acids to conjugated enones in aqueous solvents to give excellent yield (Sakai, et al. 1997) (Figure 2.6). Different type of ligands were investigated by using $[Rh(acac)(CO)_2]$ as the rhodium(I) source. Bis(phosphine) ligands having large bite angles gave rise the best results. The presence of water also was necessary to provide a good reactivity.

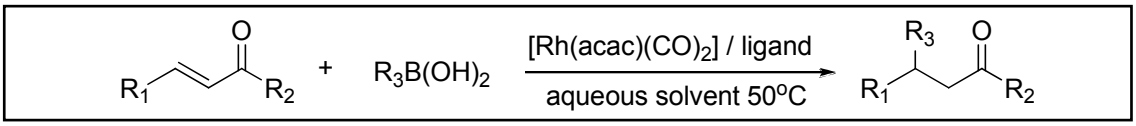

Figure 2.6. Rh-catalyzed reaction of boronic acids to enones
(Source: Sakai, et al. 1997)

In 1998, the reaction conditions were modified for example the reaction temperature was elevated from 50 ^{o}C to 100 ^{o}C, and the rhodium source was changed from $[Rh(acac)(CO)_2]$ to $[Rh(acac)(C_2H_4)_2]$ Furthermore high enantioselectivities could be achieved by using a chiral ligand such as (S)-BINAP (Takaya, et al. 1998) (Figure 2.7).

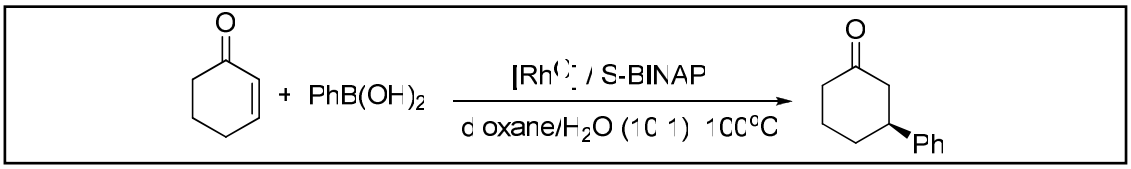

Figure 2.7. Enantioselective Rh-catalyzed reaction of boronic acids with enones (Source: Takaya, et al. 1998)

2.4. Rhodium-Catalyzed Reactions of Organoborons with Aldehydes

It was demonstrated that the rhodium-catalyzed reaction of organoboronic acids with aldehydes gave secondary alcohols in good yields (Sakai, et al. 1998) (Figure 2.8).

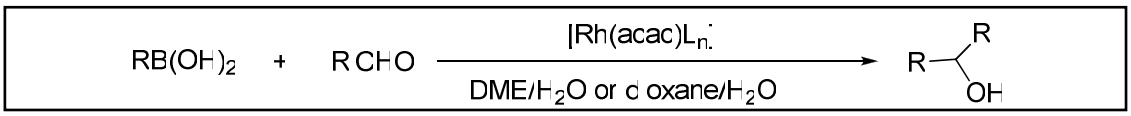

Figure 2.8. Rh-catalyzed addition reaction of boronic acids to aldehydes (Source: Sakai, et al. 1998)

They proposed a mechanism which involves a nucleophilic attack of the aryl group on the arylrhodium(I) species (Figure 2.9).

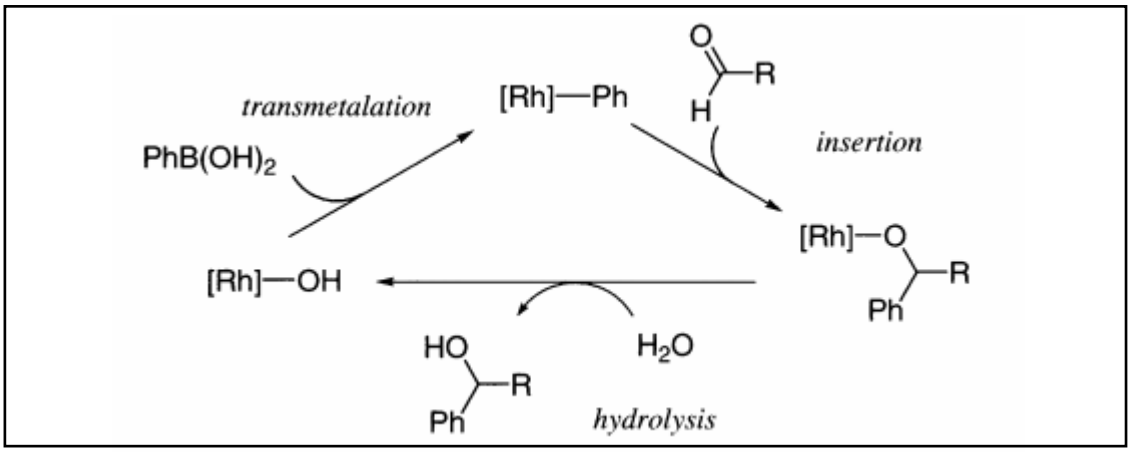

Figure 2.9. The reaction mechanism of Rh-catalyzed reaction of boronic acids with aldehydes. (Source: Takaya, et al. 1998)

Excellent catalytic activity was obtained in the addition of arylboronic acids to aldehydes with cationic rhodium complexes of certain nitrogen-containing ligands (Moreau, et al. 2001). In 2004, it was reported that the addition of arylboronic acids to aldehydes with novel Rh-carbene complexes led to high yields (Özdemir, et al. 2004).

2.5. Rhodium-Catalyzed Reactions of Organoborons with Alkenes, Alkynes and Their Derivatives

An interesting multiple alkylation reaction which is also called merry-go-round reaction was demonstrated (Oguma, et al. 2000). They synthesized a unique class of sterically encumbered aromatic molecules by Rh-catalyzed multistep arylation reaction with arylboronic acids (Figure 2.10).

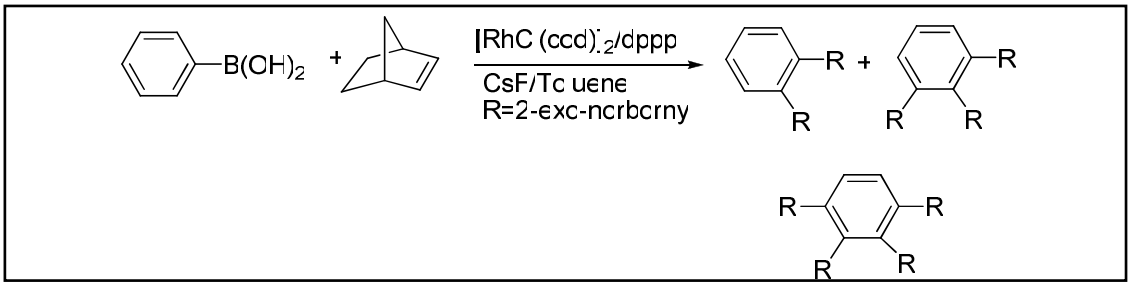

Figure 2.10. Rh-catalyzed multiple alkylation on aromatic ring
(Source: Oguma, et al. 2000)

The rhodium-catalyzed reaction of arylboronic acids with olefins was achieved by using water soluble phosphine ligand, disulfonated triphenylphosphine (TPPDS) and trisulfonated triphenylphosphine (TPPTS) (Lautens, et al. 2001) (Figure 2.11).

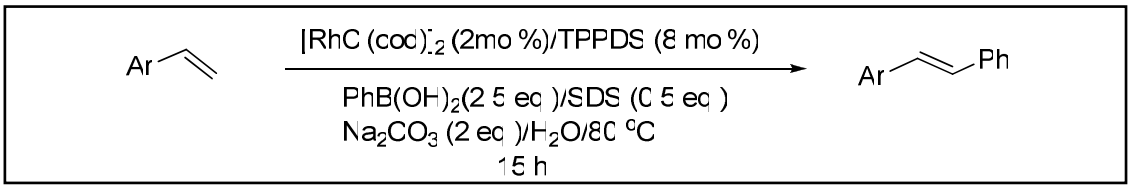

Figure 2.11. Rh-catalyzed coupling reactions of alkenes with arylboronic acids
(Source: Lautens, et al. 2001)

It was published in 2008 that the rhodium(I)-catalyzed reaction of fluoroalkylated electron deficient olefins with arylboronic acids gave rise to 1,4-addition products in good yields and high selectivities in the presence of (S)-BINAP in a toluene/water solvent system (Konno, et al. 2008) (Figure 2.12).

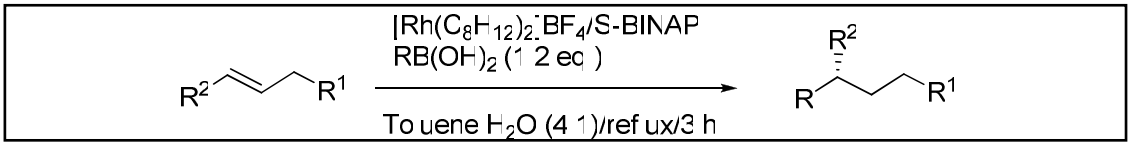

Figure 2.12. Rh-catalyzed 1,4-addition of boronic acids to the fluoroalkylated electrondeficient olefins (Source: Konno, et al. 2008)

Alkynes give addition reaction with arylboronic acids similar to the alkenes. It was reported that the rhodium-catalyzed hydroarylation reaction of internal alkynes lead to trisubstituted alkenes in high yields (Hayashi, et al. 2001) (Figure 2.13).

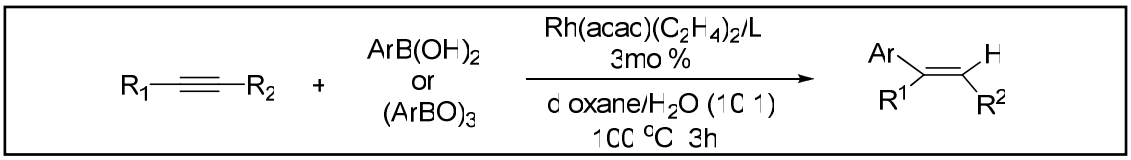

Figure 2.13. Rh catalyzed hydroarylation of alkynes (Source: Hayashi, et al. 2001)

Also, in this study it was proved that 1,4-shift of rhodium took place from 2-aryl-1-alkenylrhodium to 2-alkenylarylrhodium intermediate in the proposed mechanism of the reaction (Figure 2.14).

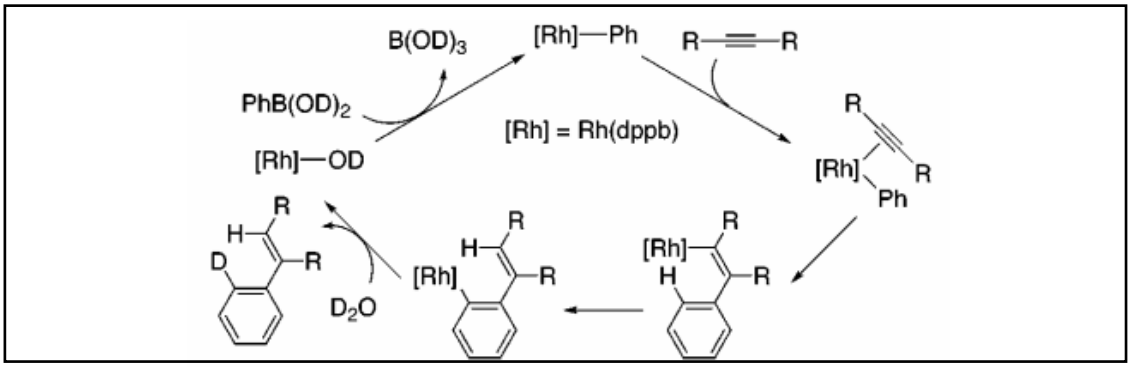

Figure 2.14. The proposed mechanism for Rh-catalyzed hydroarylation of alkynes (Source: Hayashi, et al. 2001)

Alkynyl heteroaromatic compounds reacted with arylboronic acids in the presence of rhodium catalyst to form trisubstituted alkenes as addition products in a high regioselectivity (Figure 2.15) (Lautens, et al. 2001).

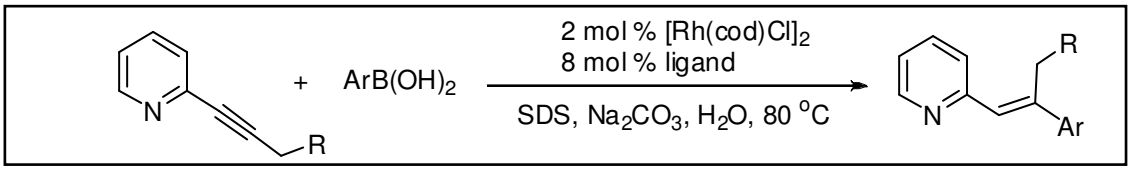

Figure 2.15. Rh catalyzed addition of arylboronic acids to pyridine substituted alkynes (Source: Lautens, et al. 2001)

In this study, they observed that the method is applicable only to alkynes in which alkynyl group is attached to *ortho* position whereas those bearing alkynyl group at the *meta* and *para* positions were completely unreactive toward the rhodium-catalyzed procedure..

Hayashi and his coworkers reported that the rhodium-catalyzed regioselective coupling reaction of alkynes with *orto*-carbonylated arylboronic acids under mild conditions led to indenols in relatively high enantioselectivities (Shintani, et al. 2005).

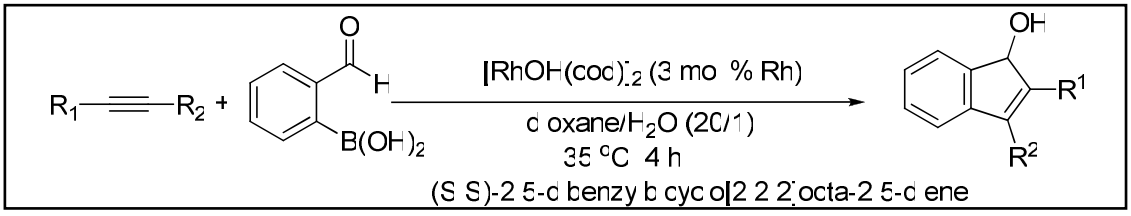

Figure 2.16. Rh-catalyzed coupling of *ortho*-carbonylated arylboronic acids and alkynes (Source: Shintani, et al. 2005)

It was also reported that the rhodium-catalyzed recation of alkynyl oxiranes with arylboronic acids leads to α-allenols diastereoselectively(Miura, et al. 2007a) (Figure 2.17).

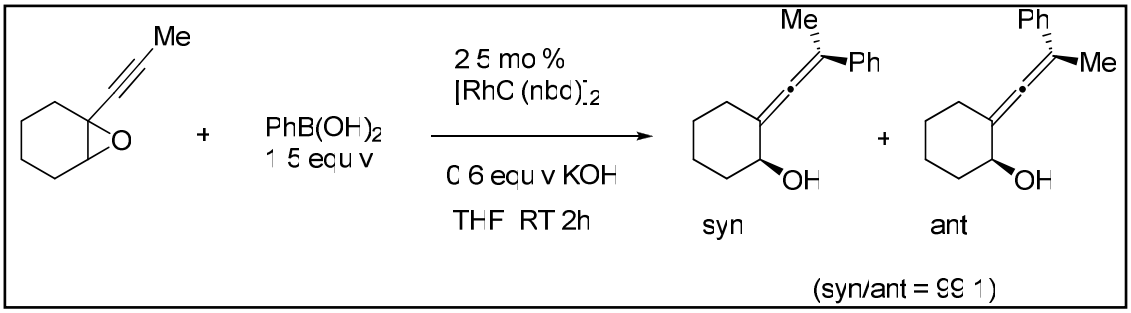

Figure 2.17. Rh-catalyzed reaction of phenylboronic acids with alkynyl oxiranes (Source: Miura, et al. 2007)

The mechanism explains the stereoselective formation of *syn* addition product. Firstly, a phenylrhodium(I) species is generated by transmetalation. Then, *cis* 1,2-addition of the phenylrhodium(I) species to alkynyl oxirane forms the alkenylrhodium(I) intermediate. Precoordination of oxygen atom of the oxirane ring with rhodium provides high stereoselectivity. β-Oxygen elimination takes place to open the oxirane ring (Figure 2.18).

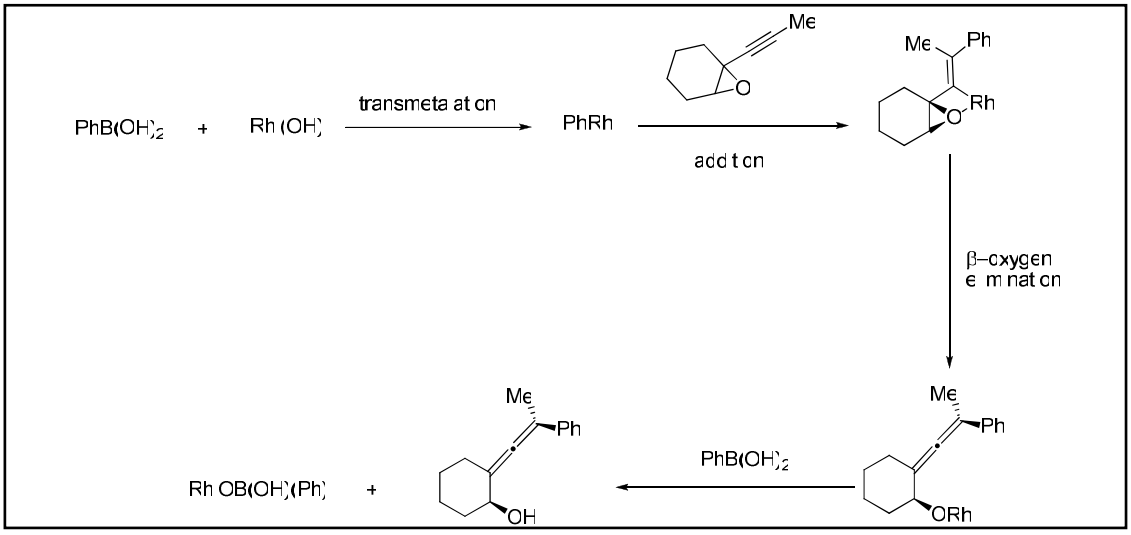

Figure 2.18. Proposed mechanism for the Rh-catalyzed reaction of phenylboronic acids with alkynyl oxiranes. (Source: Miura, et al. 2007).

It was found when using an enantiomerically enriched alkynyl oxiranes that the reaction proceeded with complete central-to-axial chirality transfer (Miura, et al. 2009).

In 2002, it was demonstrated that the Rh-catalyzed reaction of phenylboronic acid to a chiral proargyl acetate produces an allene (Murakami and Igawa 2002). This

study also provided that β-AcO elimination of an organorhodium(I) complex took place with both *syn* and *anti* modes (Figure 2.19).

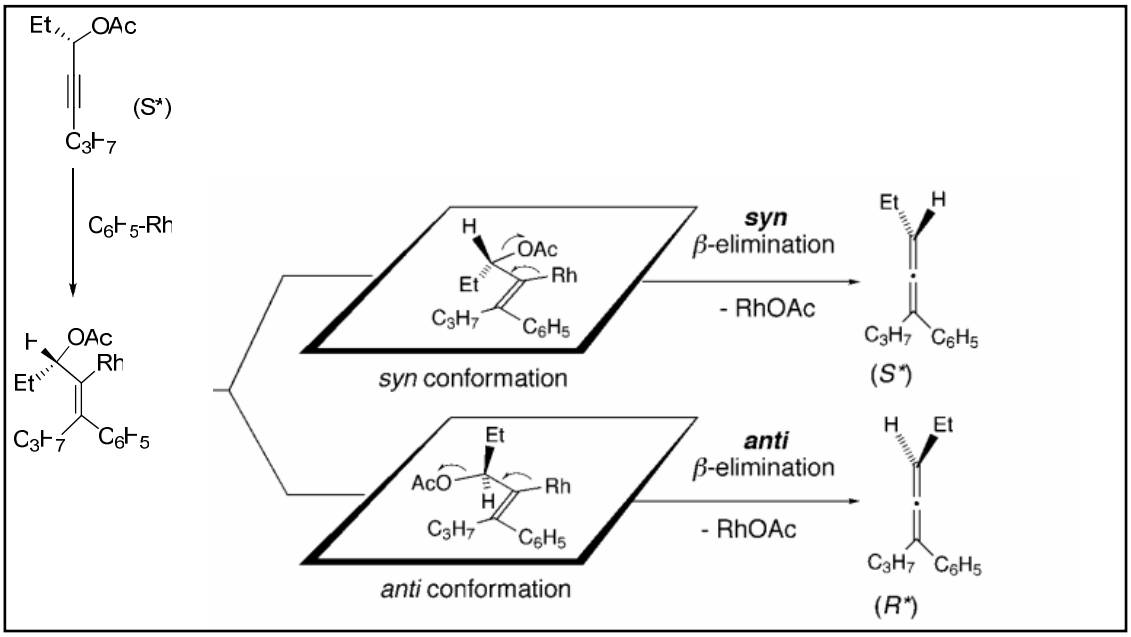

Figure 2.19. Possible mechanism of Rh catalyzed addition and β-acetate elimination reaction in both *anti* and *syn* modes. (Source: Murakami and Igawa 2002)

In this study, an allylic acetate is formed by simple addition to carbon-carbon triple bond without changing optical configuration. This result shows that allylic cation does not form from intermediate of allylic acetate. Thus, β-AcO elimination proceeds through E_2 type pathway (*anti*-coplanar conformation is preferred) instead of E_1. Solvent is very important effect for the configurational selectivity of the process. When the reaction is performed in methanol, the (R)-allene is the major enantiomer (31% ee), while in ethanol, the (S)-allene formation predominated (17% ee). The reason can be resulted from solvent polarity and steric effects.

It was reported in 2010 that the asymmetric Rh-catalyzed enantioselective 1,6-addition of arylboronic acids to enynamides leads to axially chiral allenylsilanes (Nishimura, et al. 2010) (Figure 2.20).

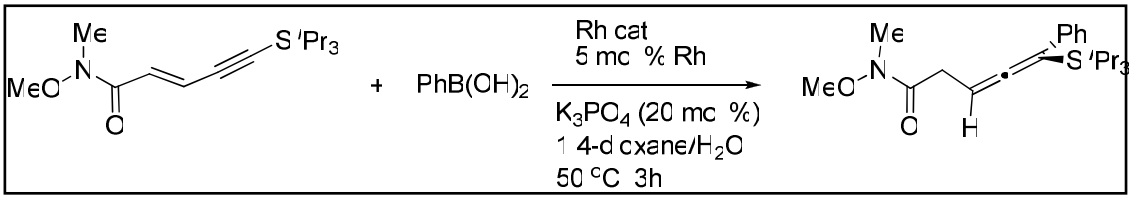

Figure 2.20. Asymmetric Rh catalyzed enantioselective 1,6-addition of arylboronic acids to enynamides (Source: Nishimura, et al. 2010).

CHAPTER 3

ALLENES

3.1. What is Allene?

Hydrocarbons having a central sp hybridized carbon atom which is connected to two other sp^2 hybridized carbon atoms is called allene, also known as cumulated diene (Figure 3.1).

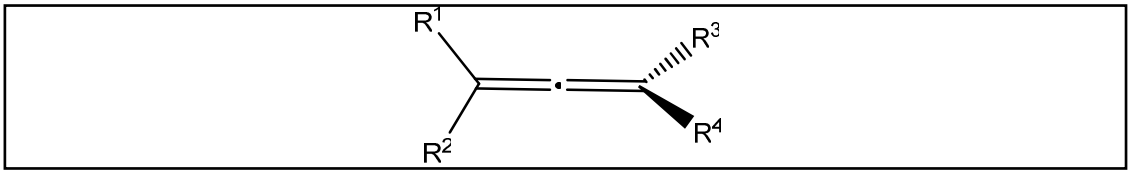

Figure 3.1. Cumulated Diene (Allene)

The structure of allenes looks like elongated tetrahedron and they are chiral when terminal carbon atoms possess two different substituents. The absolute configuration of chiral allenes can be assigned according to the sign (clockwise or counterclockwise) of rotation, they can be assigned as *R* or *S* (Figure 3.2).

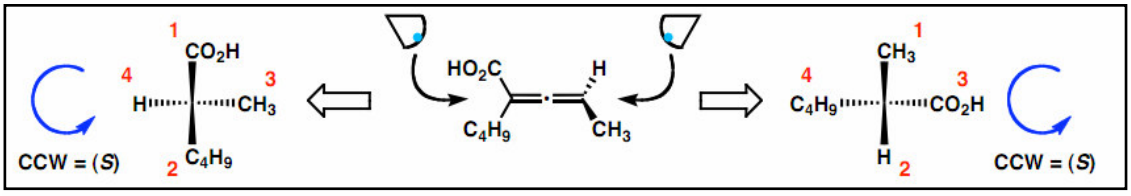

Figure 3.2. Configurational determination of chiral allene.

3.2. Allenes in Use

Allenes are very interesting and useful molecules exhibiting pharmacological activities. They also exist as natural products. Thus, the chemistry of allenes becomes very popular and attractive area for scientists. The scientists try to isolate and characterize new allenic natural products and also they try to discover efficient procedure to synthesize enantiomerically pure allene molecules.

Allenes having functional groups show impressive activities as mechanism-based enzyme inhibitors, cytotoxic, or antiviral agents.

Axial chiralty of allenes is very important for their biological activity. For example, R-(-)-adenallene has anti-HIV activity whereas S-(+)-adenallene has no anti-HIV activity (Zemlicka 1997) (Figure 3.3).

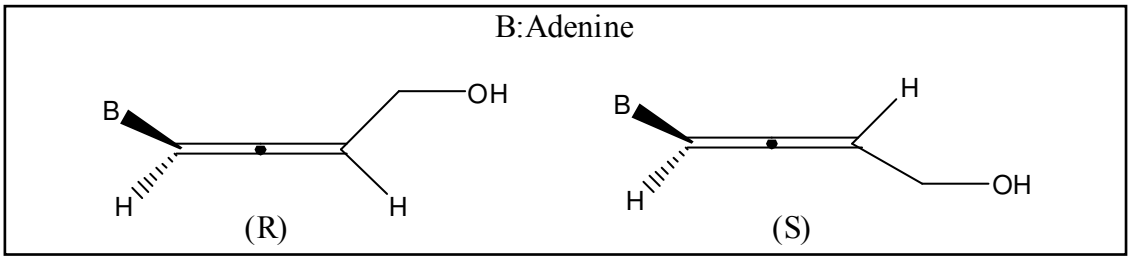

Figure 3.3. Activity of axial chirality
(Source: Zemlicka 1997)

As a natural product, an insect pheromone (Pheromone of Acanthoscelides obtectus) isolated from male dried bean beetles is an interesting allenic product which was discovered in 1970 by Horler.

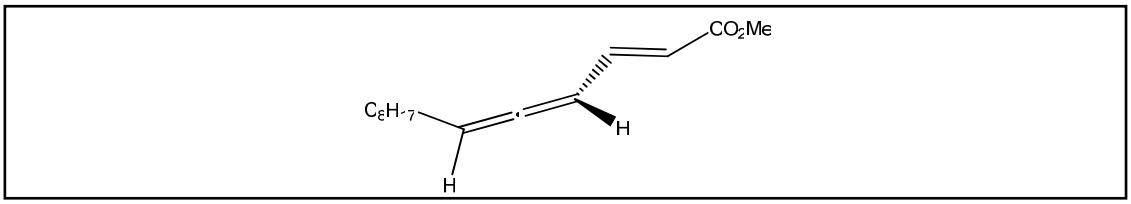

Figure 3.4. The vinylallene pheromone (Pheromone of Acanthoscelides obtectus) isolated from male dried bean beetles (Source: Horler 1970)

This pheromone can also be obtained synthetically with the palladium-catalyzed S_N2'-substitution reaction of the bromodiene with dimethyl malonate in the presence of cesium *tert*-butanolate and catalytic amounts of the chiral ligand (*R*)-segphos to lead dicarboxylated allene with 77% ee and following decarboxylation and selenoxide-mediated dehydrogenation processes (Ogasawara, et al. 2005) (Figure 3.5).

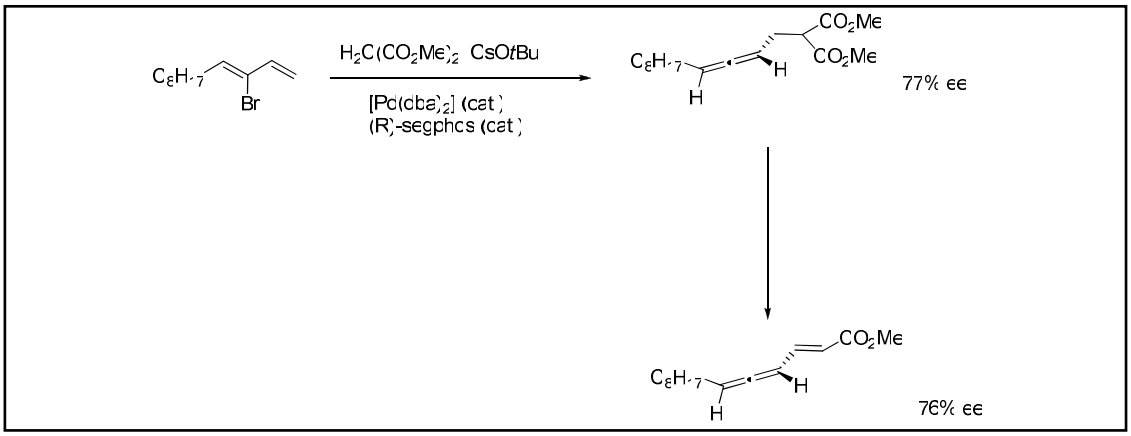

Figure 3.5. Synthesis of vinylallene insect phreromone
(Source: Ogasawara, et al. 2005)

3.2. Synthesis of Vinyl Allenes

3.2.1. Synthesis of Vinyl Allenes with Grignard Reagents

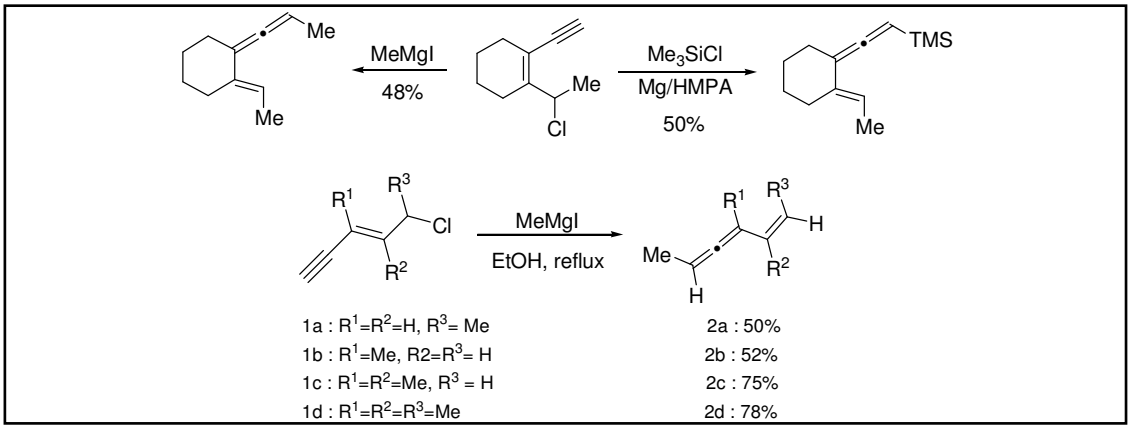

Figure 3.6. The reaction of chloro-enynes with grignard reagents
(Source: Gore and Dulcere 1972)

It was found that MeMgI or $Me_3SiMgCl$ reacted with 2,4-enyne halides to lead the E/Z mixture of vinyl allenes (Gore and Dulcere 1972) (Figure 3.6).

Formation of vinyallene is a limited process with Grignard reagent since use of this method is not applicable for other Grignard reagents.

3.2.2. Synthesis of Vinylallenes with Organocopper Reagents

In 1999, it was reported that (*E*)-2-en-4-yne acetates can effectively undergo S_N2'' type alkylation with various lithium cuprates affording an *E*- and *Z*- isomeric mixture of vinylallenes (Purpura and Krause 1999) (Figure 3.7).

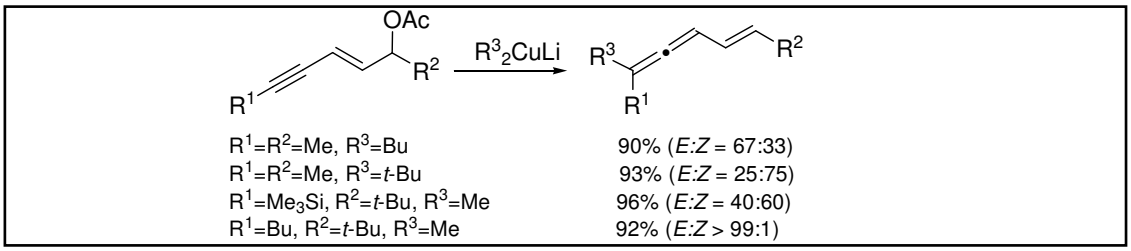

Figure 3.7. Reactions of enyne acetates with lithium dialkylcuprates
(Source: Purpura and Krause 1999)

This method can also be applied for the reactions of enyne oxiranes leading vinylallenols. When the terminal oxirane was used as a substrate, only *E*-isomer of desired product was formed, however, *E* and *Z* isomeric mixture of vinylallenols were obtained when alkyl substituted oxirane was used (Figure 3.8).

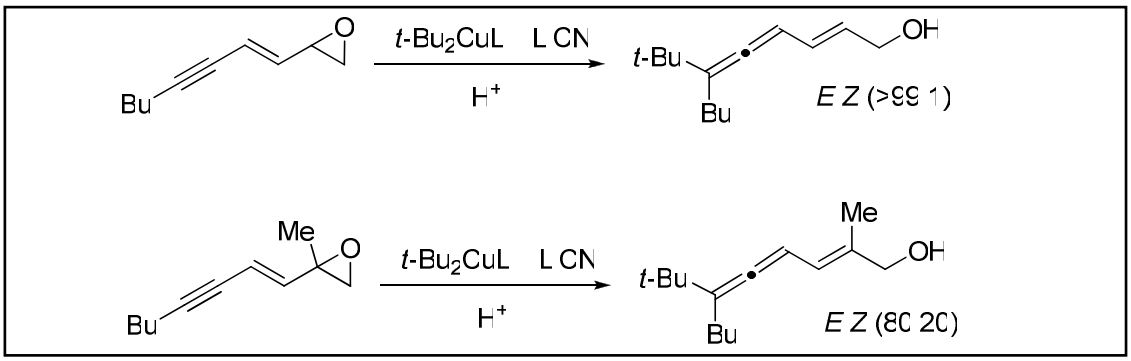

Figure 3.8. Reactions of enyne oxiranes with lithium dialkylcuprates
(Source: Purpura and Krause 1999)

3.2.3. Rhodium-Catalyzed Asymmetric 1,6-Addition of Aryltitanates to Enynones Giving Axially Chiral Allenes

It was reported that the addition of aryltitane reagents to 3-alkynyl-2-en-1-ones in the presence of chlorotrimethylsilane and rhodium-(R)-segphos as a catalyst led to high yields of axially chiral allenylalkenyl silyl enol ethers (Hayashi and Yamasaki 2003) (Figure 3.9).

.

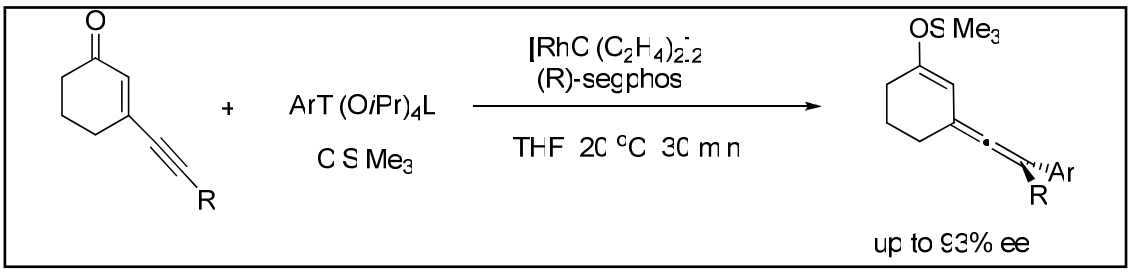

Figure 3.9. Synthesis of chiral allenylalkenyl silyl enol ethers
(Source: Hayashi and Yamasaki 2003)

3.2.4. Palladium-Catalyzed Alkoxycarbonylation of (*Z*)-2-En-4-yne Carbonates Leading to 2,3,5-Trienoates

It was recently reported that (*Z*)-2-en-4-yne carbonates gave carbonylation reaction in the presence of a balloon pressure of CO in an alcohol and palladium catalyst to lead vinylallenyl esters. According to NMR analyses, *E*-configured vinylallenyl esters were achieved in high yields (Akpinar, et al. 2011) (Figure 4.10).

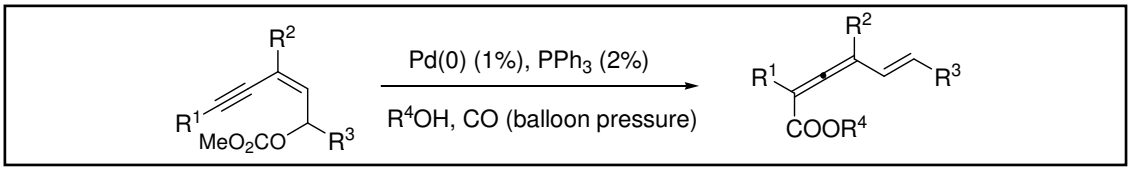

Figure 3.10. Pd(0)-catalyzed alkoxycarbonylation of Z-enyne carbonates
(Source: Akpinar, et al. 2011)

In this study, chirality transfer was also examined and no center-to-axis chirality transfer selectivity was shown with this method an enantiomeriallyc enriched enyne carbonate (94.5 % ee) led to racemic mixture of desired product.

3.2.5. Palladium-Catalyzed 1,5-Substitution Reactions of 2-En-4-yne Carbonates with Organoboronic Acids

It was recently published that 2-en-4-yne carbonates gave 1,5-substitution reactions with organoboronic acids to lead arylated vinylallenes. The palladium-catalyzed method, which proceeds through formation of vinylallenylpalladium intermediate, is applicable for both (*E*)- and (*Z*)- configured enyne carbonates and appeared to have wider scope for both organoboronic acids and enyne substrates (Üçüncü, et al. 2011).

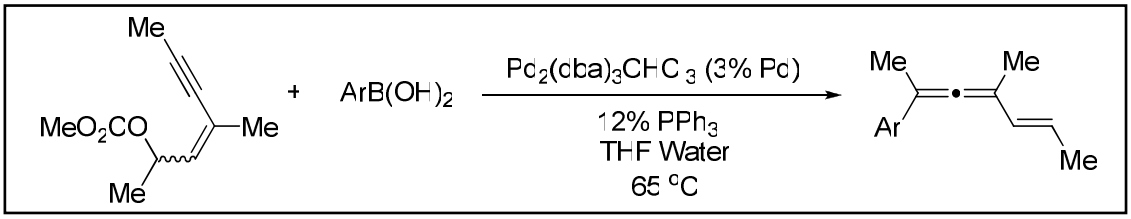

Figure 3.11. Pd(0)-catalyzed 1,5-substitution reactions of enyne carbonates (Source: Üçüncü, et al. 2011)

No center-to-axis chirality transfer selectivity could be demonstrated with the existing method, as in the case for the Pd(0)-catalyzed alkoxycarbonylation applications with these substrates (Akpinar, et al. 2011). The relevant reaction of an enantio-enriched enyne carbonate (*R*,*Z*) (94.5% *ee*) with phenylboronic acid led to a racemic mixture of the product.

CHAPTER 4

EXPERIMENTAL STUDY

4.1. General Procedures for Drying the Solvents and Synthesis of Catalysts

Tetrahydrofuran (THF), dimethylformamide (DMF), and dichloromethane (DCM) solvents were all purified by a solvent purification system (MBRAUN SPS-800). Et_2O was distilled from benzophenone-ketyl under argon prior to use. The $[RhCl(cod)]_2$ (Giordano, et al. 2007) and $[RhOH(cod)]_2$ (Uson, et al. 2007) complexes were synthesized in laboratory.

4.2. Synthesis of Substrates

4.2.1. Synthesis of *Z*-Enyne Acetates 1b, 1c, 1g, 1h, and *E*-1a :

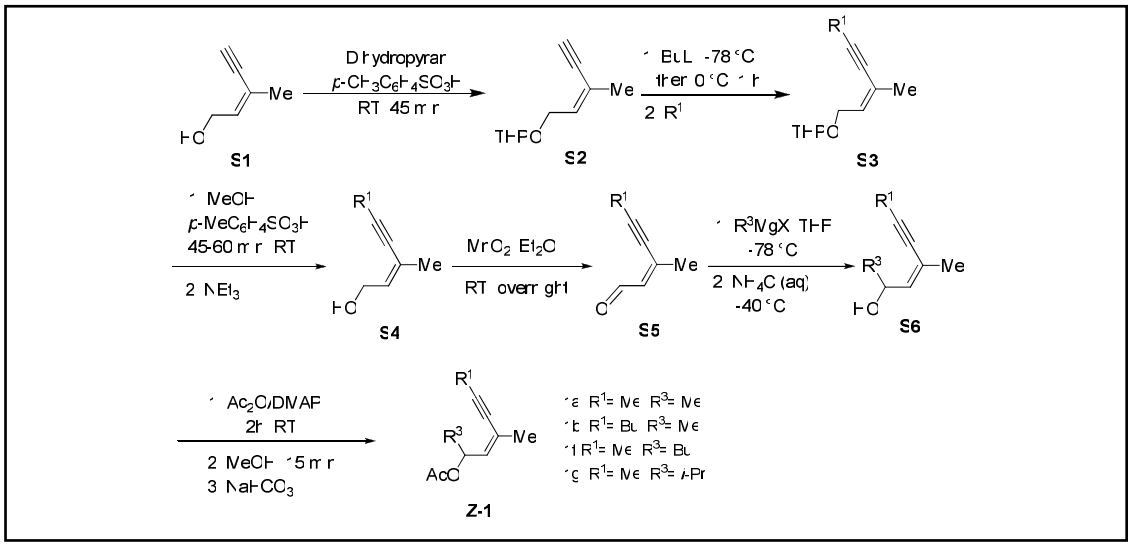

Figure 4.1. Synthesis of Z-Enyne Acetates 1a, 1b, 1f, 1g, and *E*-1a

To the mixture of commercially available, (*Z*)-pent-2-en-4-yn-1-ol (**S1**) (1.6 g, 20 mmol) and 3,4-dihydropyran (2.2 mL) was added *p*-toluenesulfonic acid (44 mg,

0.02 mmol) and then stirred for 45 min at room temperature. Then, the mixture was diluted with 40 mL of dry THF under argon and cooled to -78 °C. At that temperature, a 24 mmol hexane solution of BuLi (1.6 M, 15 mL) was added dropwise via a syringe. After stirring the reaction mixture for 1 h at 0 °C, 2.5 mL of alkyl iodide (≈40 mmol) was added dropwise. The mixture was stirred overnight at room temperature when the alkyl halide used was MeI, or 2 days at 50 °C when BuI was used. The reaction was quenched by the addition of saturated NH_4Cl (*aq*) solution and the reaction solution was extracted with Et_2O. The organic phase was washed with water, dried over MgSO4, filtered, and concentrated under reduced pressure. The residue was used in the following step without any other purification. (Betzer, et al. 1997)

To a solution of the preceding crude compound (**S3**) in methanol (60 mL) *p*-toluenesulfonic acid (1.2 g, 6 mmol) was added and the resulting solution stirred at RT for 45-60 min. Then, triethylamine was added (1.8 mL), and the solution was concentrated under reduced pressure. The mixture was taken into dichloromethane and washed with water. The combined extracts were washed with brine, dried over MgSO4, filtered, and concentrated under reduced pressure. Purification by column chromatography on silica gel (hexane/ethyl acetate as the eluent) gave the enynol S4 (yields: R^1= Me, 86%; Bu, 80%) (Purpura and Krause 1999).

To the solution of **S4** (≈17 mmol) in 66 mL of dry diethyl ether, 30 g of activated MnO_2 was added, and the mixture was stirred overnight at room temperature. After filtration through Celite, the solution was concentrated under reduced pressure. The crude aldehyde (**S5**) was used in the next step. (Betzer, et al. 1997).

The crude aldehyde (**S5**) was dissolved in 36 mL of anhydrous THF and treated at -78 °C with 1.2 equivalent ethereal solution of R^3MgX (1.6-2.0 M, X stands for iodine in the case of methylation, and bromine for the others) under Ar. At the end of the addition of the Grignard reagent, the mixture was warmed with stirring to -40 °C at nearly 2 h and then, hydrolyzed by the addition of 30 mL of a saturated NH_4Cl solution. After extraction with diethyl ether, the combined organic layers were washed with water, dried over $MgSO_4$, and filtered. The solvent was removed in vacuo, and the crude residue was purified by column chromatography on silica gel (hexane/ethyl acetate, yields: R^1= Bu, R^3= Me, 65%; R^1= Me, R^3=Bu, 80%; R^1= Me, R^3= *i*-Pr, 40%).

(*E*)-4-methylhept-3-en-5-yn-2-yl acetate ((*E*)-**1a**) was synthesized according to a reported method (Purpura and Krause 1999).

The preparation of acetates from the synthesized enynols (**S6**) was performed via a prescribed method (Purpura and Krause 1999). The products were purified by column chromatography on silica gel (hexane/ethyl acetate) (yields: **1a**, 66%; **1b**, 70%.; **1h**, 48%; **1i**, 50%, **1m** 65%).

4.2.2. Synthesis of *Z*-Enyne Acetates 1c-1e

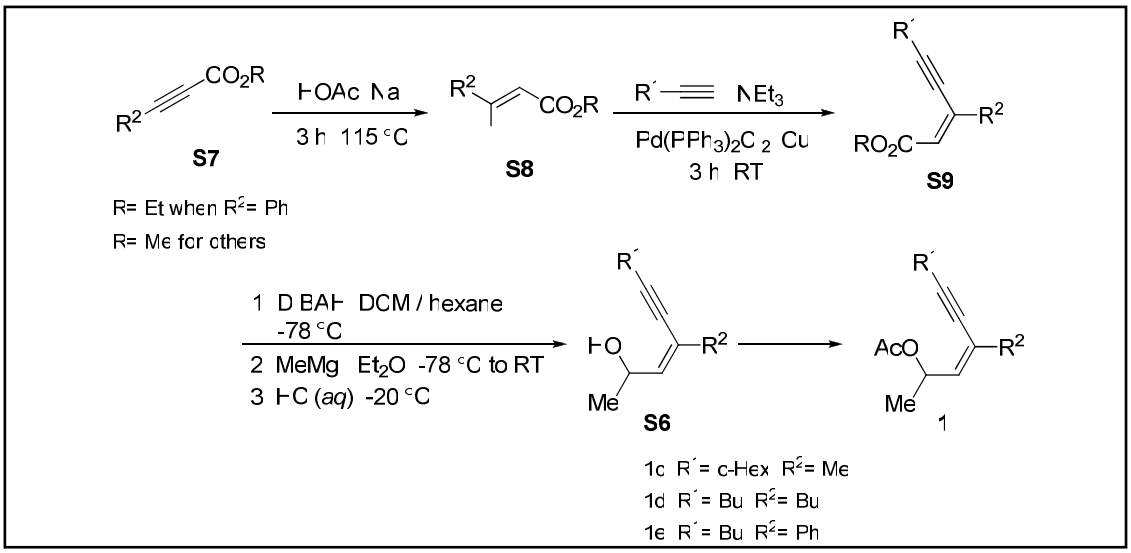

Figure 4.2. Synthesis of Z-Enyne Acetates 1c-1e

To a solution of alkynoic ester (**S7)** (≈40 mmol) and acetic acid (240 mmol, 13.8 mL) (512 mmol, 20.8 mL when (**S7)** is ethyl 3-phenylpropiolate was added sodium iodide (9.6 g, 64 mmol) (19.2 g, 128 mmol when (**S7)** is ethyl 3-phenylpropiolate) and stirred for 3 h at 115 °C. After completion of the reaction, the brown mixture was transferred while hot to a separatory funnel containing water (≈10 mL/mmol of the ester substrate). The reaction flask was washed with a mixture of water (≈5 mL) and diethyl ether (≈30 mL/mmol of the ester substrate). The washings were combined in a separatory funnel. The phases were separated and the aqueous phase was extracted with diethyl ether. The combined organic phases were treated sequentially with saturated aqueous sodium bicarbonate, aqueous sodium thiosulfate (1 M), and brine and then were dried over $MgSO_4$, filtered, and concentrated under reduced pressure. The product was purified by column chromatography on silica gel (hexane/ethyl acetate, yields, (**S8)**: R^2= H, 84%, Me, 87%; Bu, 84%; Ph, 93%) (Piers, et al. 1994).

A mixture of (**S8)** (≈35 mmol), $PdCl_2(PPh_3)_2$ (210.6 mg, 0.3 mmol), and CuI (33 mg, 0.17 mmol), in 140 mL of Et_3N was stirred for 10 min at room temperature under Ar, and then, to this mixture was added a terminal alkyne (38 mmol). The mixture was stirred at room temperature for 3h. At the end of the reaction, water was added to the resulting mixture and then extracted with Et_2O The combined organic layers were dried over $MgSO_4$. The solvent was evaporated in vacuo and the product (**S9**) was purified by column chromatography on silica gel (hexane/ethyl acetate, yields: R^1= Bu, R^2= H, 92%; R^1= Ph, R^2= Me, 93%; R^1= *c*-Hex, R^2= Me, 90%; R^1= *t*-Bu, R^2= Me, 85%; R^1= Bu, R^2= Bu, 92; R^1= Bu, R^2= Ph, 82) (Takeuchi, et al. 2000).

A dry, three-necked, round-bottomed 250-mL flask equipped with an internal thermometer, a rubber septum, and an Ar gas inlet, was charged with ≈31 mmol of (**S9)** and 63 mL of anhydrous dichloromethane. The stirred solution was cooled to -78 °C and 31 mL of a 1 M solution of diisobutylaluminum hydride in hexane was added dropwise with a syringe at such a rate that the temperature would not exceed -75 °C. After stirring for 30 min at -78 °C, 17 mL Et_2O solution of a MeMgI (34 mmol, 2.0 M) was added dropwise at -78 °C with a syringe. The cooling bath was removed and the reaction mixture was allowed to warm to room temperature. The mixture was hydrolyzed at -20 °C by dropwise addition of 63 mL of a 1 M aqueous solution of hydrochloric acid, followed by addition of 81 mL of ether. The organic layer was separated, the aqueous layer was extracted with ether, and the combined extracts were dried over $MgSO_4$. The solvent was evaporated in vacuo. The product was purified by column chromatography on silica gel (hexane/ethyl acetate; yields: R^1= Bu, R^2= H, 65%; R^1= Ph, R^2= Me, 55%; R^1= *c*-Hex, R^2= Me, 48%; R^1= *t*-Bu, R^2= Me, 60%; R^1= Bu, R^2= Bu, 44%; R^1= Bu, R^2= Ph, 40%) (Marek 1998).

The preparation of acetates from the synthesized enynols (**S6**) was performed via a prescribed method (Purpura and Krause 1999). The products were purified by column chromatography on silica gel (hexane/ethyl acetate).(yields: **1c**, 70%; **1d**, 64%.; **1e** 65%).

4.2.3. Synthesis of non-2-en-4-yn-3ylbenzene

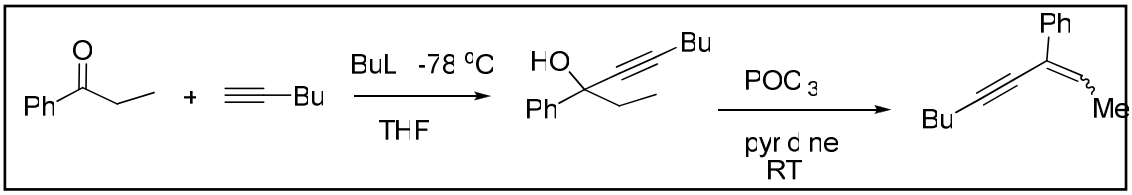

Figure 4.3. Synthesis of non-2-en-4-yn-3ylbenzene

To a stirred solution of 1-hexyne (6.5 mL, 59 mmol) in THF (150 mL) were added 1.6 M hexane solution of n-BuLi (40.5 mL, 64 mmol) at –78 °C. After stirring was continued for 1 h, (4.8 g, 49 mmol) was added dropwise to the reaction mixture at the same temperature, and stirring was continued for 2 h at the same temperature. The reaction mixture was diluted with water and then extracted with AcOEt. The combined extracts were washed with brine. The crude product was used for next step (Dieter, et al. 2005)

To a stirred solution of alkynylalcohol (9.8 g, 49 mmol) in pyridine (200 mL) was added $POCl_3$ (13.8 mL, 148 mmol) at 0 °C, and the stirring was continued for 2 h at rt. The reaction mixture was diluted with water at 0 °C and extracted with AcOEt. The combined extracts were washed with brine, and the residue upon workup was chromatographed on silica gel with only hexane as eluent to give enyne (%55) (Yoshida, et al. 2007).

4.2.4 Synthesis of (*R,Z*)-4-methylhept-3-en-5-yn-2-yl acetate [(*R,Z*)-1a]

Sharpless's kinetic resolution method was employed for the preparation of *(R,Z)*-4-methylhept-3-en-5-yn-2-ol. Accordingly, 22.9 mmol of Ti(O*i*Pr)$_4$, and 27.5 mmol of L-(+)-diisopropyl tartrate, were dissolved in 200 mL of dry DCM and cooled to -20 °C. To this mixture, dry DCM solution of 22.9 mmol of racemic mixture of (*Z*)-4-methylhept-3-en-5-yn-2-ol was added and then stirred for 30 min at -20 °C. Then, 45.8 mmol of *t*-butyl hydroperoxide (4 M in toluene) was added and left in a freezer (-20 °C) for 13.5 h. After completion, a pre-cooled (0 °C) 37 mL aqueous solution of 42.4 mmol $FeSO_4$ and 68.7 mmol tartaric acid mixtures were added to the reaction mixture with

small portions while stirring at -20 °C. The mixture was slowly warmed to room temperature over 1 h, and then extracted with DCM. The DCM solution was concentrated by evaporation and 103 mL of Et_2O was added. The ethereal solution was cooled to 0 °C, and 109 mL of aqueous NaOH was added and stirred at this temperature for 1.5 h. Extraction with ether, drying with MgSO4, and following column chromatography on silica gel using hexane/ethyl acetate eluent yielded the isolated product at 45% (Verhoeven 1979). Enantiomeric purity was determined as 94.5% *ee* by GC method using a Hydodex-beta-3P column (25 m, 0.25 mm ID). $[\alpha]_D^{22}$= -1.9° (*c*= 1.0, $CHCl_3$). Its hydroxyl group was modified to carbonate as described above. $[\alpha]_D^{22}$= -1.2° (*c*= 0.2, in $CHCl_3$). Specific Rotation was determined according to Equation 4.1.

$$[\alpha]_D^T = \frac{\text{Observed Rotation, } (\alpha)}{\text{Path length, l (dm) * Concentration of Sample, c (g/ml)}} \quad (4.1)$$

4.3. Characterization of Reactants

The synthesized reactants were analyzed by GC and GC-MS (HP 6890/5973N) and isolated by column chromatography using a hexane-ethyl acetate eluent. High-resolution mass spectral analyses were performed at the Dortmund University of Technology Mass Spectrometry Laboratory on a Thermo Electron system. NMR spectra were recorded on a Varian VnmrJ 400 spectrometer, a Varian Mercury AS 400, or a Bruker DRX 400 spectrometer. Infrared spectra were obtained using a Perkin–Elmer Spectrum 100 by ATR method with neat samples. Optical rotations were measured on a Rudolph Autopol I polarimeter.

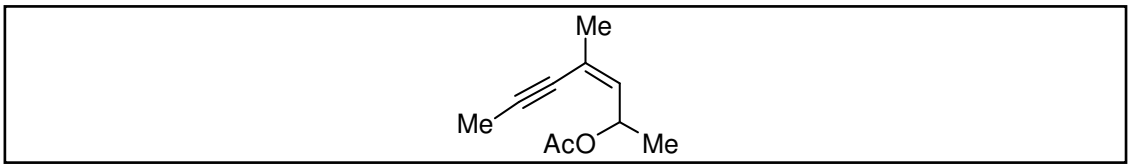

Figure 4.4. (*Z*)-4-methylhept-3-en-5-yn-2-yl acetate

1a: ^{1}H NMR (400 MHz, $CDCl_3$) δ 5.71 (dq, *J*= 8.8, 6.8 Hz, 1H), 5.56 (dq, *J*= 8.8, 1.2 Hz, 1H), 2.01 (s, 3H), 1.97 (s, 3H), 1.81 (d, *J*= 1.2 Hz, 3H), 1.28 (d, *J*= 6.8 Hz, 3H); ^{13}C NMR (101 MHz, $CDCl_3$) δ: 170.4, 134.9, 121.5, 91.7, 77.7, 70.3, 23.5, 21.5, 20.5, 4.5; IR (ν_{max}/cm^{-1}): 2982, 2233, 1730, 1639, 1433, 1235, 1152, 1046; MS (EI, *m/z*): 166 (11, M^+), 151 (37), 137 (4), 123 (100), 109 (92), 91 (98), 79 (33); HRMS (EI, *m/z*, M^+): 166.0988 (calculated), 166.0993 (found).

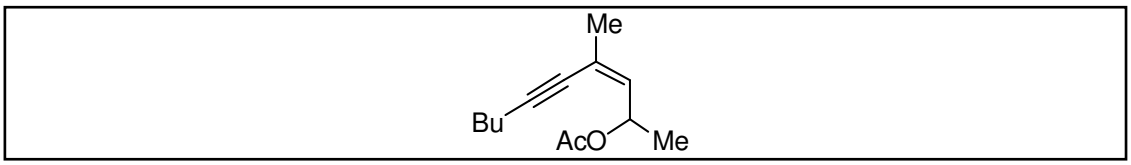

Figure 4.5. (*Z*)-4-methyldec-3-en-5-yn-2-yl acetate

1b: ^{1}H NMR (400 MHz, $CDCl_3$) δ: 5.73 (dq, *J*= 8.4, 6.4 Hz, 1H), 5.56 (dq, *J*= 8.4, 1.4 Hz, 1H), 2.34 (t, *J*= 7.0 Hz, 2H), 2.02 (s, 3H), 1.83 (d, *J*= 1.6 Hz, 3H), 1.38-1.58 (m, 4H), 1.29 (d, *J*= 6.4 Hz, 3H), 0.92 (t, *J*= 7.2 Hz, 3H); ^{13}C NMR (101 MHz, $CDCl_3$)**:** δ: 170.3, 134.9, 121.6, 96.4, 78.6, 70.4, 30.9, 23.6, 22.1, 21.5, 20.4, 19.3, 13.7; IR (ν_{max}/cm^{-1})**:** 2941, 2870, 2223, 1736, 1636, 1371, 1232, 1036; MS (EI, *m/z*): 208 (8, M^+), 193 (8), 179 (4), 165 (100), 151 (24), 137 (14), 123 (49), 109 (88), 91 (82), 79 (47); HRMS (EI, *m/z*, M^+)**:** 208.1458 (calculated), 208.1455 (found).

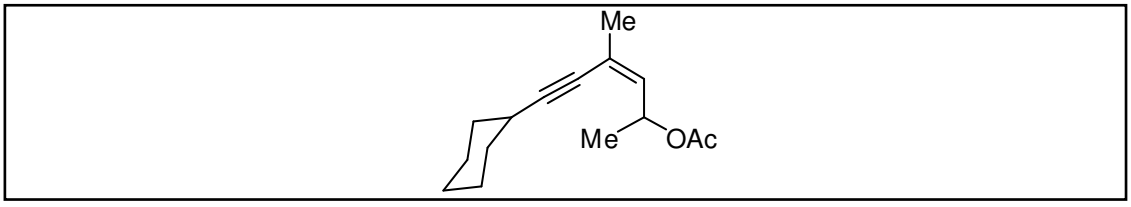

Figure 4.6. (*Z*)-6-cyclohexyl-4-methylhex-3-en-5-yn-2-yl acetate

1c: ^{1}H NMR (400 MHz, $CDCl_3$) δ: 5.78-5.66 (m, 1H), 5.56 (dq, *J*= 8.4, 0.8 Hz, 2H), 2.55-2.48 (m, 1H), 2.01 (s, 3H), 1.82 (d, *J*= 1.2 Hz, 3H), 1.83-1.76 (m, 2H), 1.66-1.74 (m, 2H), 1.43-1.53 (m, 3H), 1.30-1.37 (m, 3H), 1.35 (d, *J*= 5.6 Hz, 3H); ^{13}C NMR (100 MHz, $CDCl_3$) δ: 170.3, 134.8, 128.6, 121.8, 100.5, 78.5, 70.3, 63.4, 32.8, 29.8, 26.0, 24.9, 23.6, 21.5, 20.4; IR (ν_{max}/cm^{-1}): 2971, 2929, 2854, 2212, 1737, 1448, 1368, 1234, 1153, 1041; MS (EI, *m/z*): 234 (10, M^+), 219 (12), 191 (89), 177 (19), 149 (26), 131 (31), 117 (24), 109 (100), 91 (51), 77 (25); HRMS (EI, *m/z*, M^+): 234.1614 (calculated), 234.1616 (found).

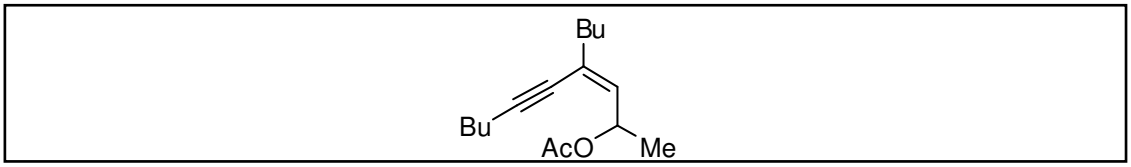

Figure 4.7. (*Z*)-4-butyldec-3-en-5-yn-2-yl acetate

1d: ^{1}H NMR (400 MHz, C_6D_6) δ: 6.25 (dq, *J*= 8.4, 6.4 Hz, 1H), 5.67 (d, *J*= 8.8 Hz, 1H), 2.15 (t, *J*= 6.8 Hz, 2H), 2.11 (t, *J*= 8.0 Hz, 2H), 1.69 (s, 3H), 1.56 (quint, *J*= 7.6 Hz, 2H), 1.42-1.31 (m, 4H), 1.38 (d, *J*= 6.4 Hz, 3H), 1.30-1.20 (m, 2H), 0.85 (t, *J*= 7.2 Hz, 3H), 0.81 (t, *J*= 7.2 Hz, 3H); ^{13}C NMR (101 MHz, C_6D_6) δ: 169.4, 135.1, 126.7, 97.1, 78.5, 70.1, 37.4, 31.1, 30.8, 22.4, 22.2, 21.0, 20.7, 19.4, 14.1, 13.7; IR (ν_{max}/cm^{-1}): 2955, 2932, 2865, 2216, 1742, 1631, 1457, 1369, 1237, 1041; MS (EI, *m/z*): 250 (3, M^+) 235 (10), 221 (3), 207 (80), 190 (28), 161 (33), 151 (68), 133 (48), 119 (51), 105 (100), 91 (98), 77 (34); HRMS (EI, *m/z*, M^+): 250.1927 (calculated), 250.1928 (found).

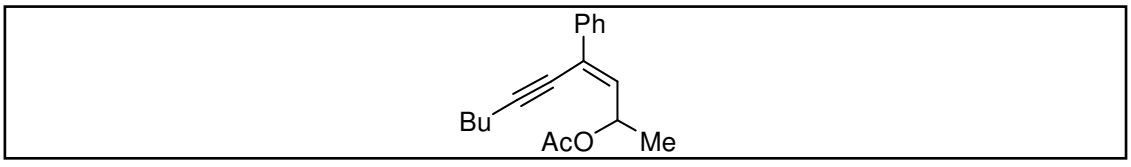

Figure 4.8. (*Z*)-4-phenyldec-3-en-5-yn-2-yl acetate

1e: ^{1}H NMR (400 MHz, C_6D_6) δ: 7.70-7.65 (m, 2H), 7.17-7.04 (m, 3H), 6.42 (dq, J_{AB}= 8.4, 6.4 Hz, 1H), 6.34 (d, J_{AB}= 8.4 Hz, 1H), 2.18 (t, *J*= 6.8 Hz, 2H), 1.70 (s, 3H), 1.44-1.29 (m, 4H), 1.42 (d, *J*= 6.4 Hz, 3H), 0.81 (t, *J*= 7.2 Hz, 3H); ^{13}C NMR (101 MHz, C_6D_6) δ: 169.4, 138.2, 135.3, 128.7, 128.4, 126.7, 126.2, 99.2, 77.4, 70.4, 31.0,

22.3, 20.9, 20.5, 19.5, 13.7; IR (ν_{max}/cm^{-1}): 2960, 2932, 2865, 2233, 1739, 1368, 1234, 1039, 761, 693; MS (EI, *m/z*): 270 (6, M^+) 255 (6), 227 (63), 211 (16), 185 (42), 167 (100), 153 (94), 141 (33), 128 (34), 115 (37), 91 (23), 77 (14); HRMS (EI, *m/z*, M^+): 270.1614 (calculated), 270.1613 (found).

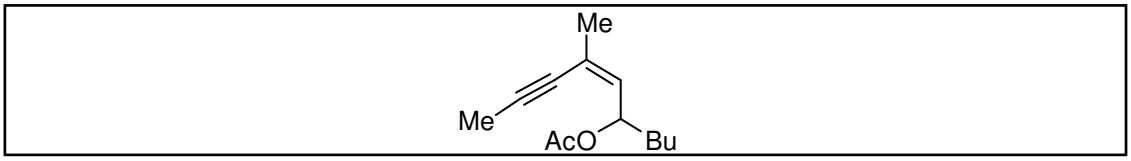

Figure 4.9. (*Z*)-7-methyldec-6-en-8-yn-5-yl acetate

1f: ^{1}H NMR (400 MHz, C_6D_6) δ: 6.12 (dt, *J*= 8.4, 6.8 Hz, 1H), 5.55 (dq, *J*= 8.6 Hz, 1.0 Hz, 1H), 1.83-1.74 (m, 2H), 1.76 (d, *J*= 1.2 Hz, 3H), 1.72 (s, 3H), 1.60 (s, 3H), 1.38-1.25 (m, 4H), 0.84 (t, *J*=7.2 Hz, 3H); ^{13}C NMR (101 MHz, C_6D_6): δ: 169.4, 134.7, 122.6, 91.8, 78.6, 73.3, 34.9, 27.6, 23.6, 22.9, 20.9, 14.2, 4.05; IR (ν_{max}/cm^{-1}): 2958, 2922, 2857, 2232, 1738, 1634, 1363, 1371, 1234, 1018, 953; MS (EI, *m/z*): 208 (5, M^+), 193 (14), 165 (59), 151 (43), 123 (28), 109 (100), 91 (49), 79 (32); HRMS (EI, *m/z*, M^+): 208.1458 (calculated), 208.1456 (found).

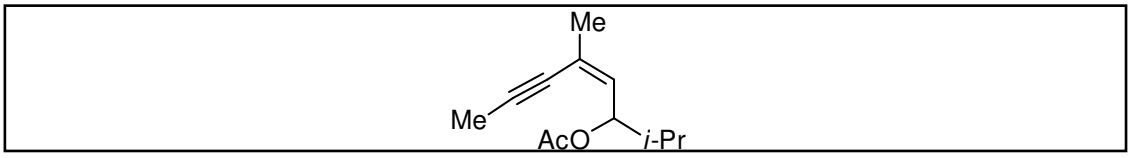

Figure 4.10. (*Z*)-2,5-dimethyloct-4-en-6-yn-3-yl acetate

1g: ^{1}H NMR (400 MHz, C_6D_6) δ: 6.01 (dd, *J*= 8.8, 6.4 Hz, 1H), 5.55 (dq, *J*= 8.8, 0.8 Hz, 1H), 1.98 (octet, *J*= 6.8 Hz, 1H), 1.77 (d, *J*= 1.6 Hz, 3H), 1.72 (s, 3H), 1.60 (s, 3H), 0.98 (d, *J*= 6.8 Hz, 3H), 0.95 (d, *J*= 6.8 Hz, 3H); ^{13}C NMR (101 MHz, C_6D_6) δ: 169.3, 132.7, 123.6, 91.7, 78.8, 77.4, 33.0, 23.8, 20.8, 18.4, 18.1, 4.10; IR (ν_{max}/cm^{-1}): 2963, 2920, 2876, 2240, 1733, 1637, 1435, 1369, 1232, 1017, 972, 606; MS (EI, *m/z*): 194 (4, M^+), 179 (2), 151 (41), 137 (8), 119 (24), 109 (100), 91 (15), 79 (13); HRMS (EI, *m/z*, M^+): 194.1301 (calculated), 194.1307 (found).

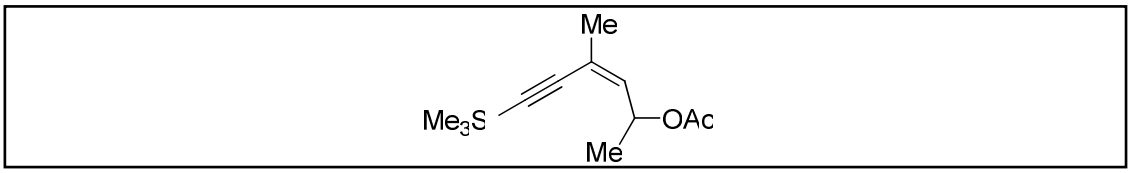

Figure 4.11. (*Z*)-4-methyl-6-(trimethylsilyl)hex-3-en-5-yn-2-yl acetate

1h ^{1}H-NMR (400 MHz C_6D_6) δ 6.17(dq, *J*=14.8, 6.4Hz, 1H), 5.58(dd, *J*=8.2, 0.7Hz, 1H), 1.68-1.67(m, 6H), 1.27(d, *J*=6.4Hz, 3H), 0.20(s, 9H) ^{13}C-NMR (100 MHz, C_6D_6): δ: 169.2, 138.4, 132.5, 121.3, 103.6, 100.5, 69.6, 63.0, 22.8, 20.9, 20.3, 0.04 IR (ν_{max}/cm^{-1}): 3655, 3455, 2981, 2898, 2793, 2147, 1735, 1628, 1369, 1234, 1145, 1045, 952, 914, 880,839, 759, 700, 634, 610, 508 MS (EI, m/z): 224 (33, M^+), 209 (24), 195 (27), 181 (89), 165 (17), 149 (47), 135 (6), 117 (46), 109 (92), 91 (19), 73 (100) HRMS (EI, m/z, $[M]^+$): 224.1227 (calculated), 224.1221 (found).

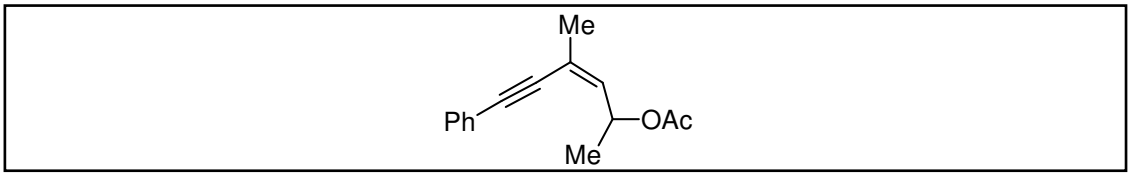

Figure 4.12. (*Z*)-4-methyl-6-phenylhex-3-en-5-yn-2-yl acetate

1i: ^{1}H-NMR (400 MHz C_6D_6) δ 7.53(dt, *J*=6.0, 1.6Hz, 2H), 6.99-6.93(m, 3H), 6.28(dt, *J*=15.4, 6.4Hz, 1H), 5.62(dd, *J*=8.6, 1.4Hz, 1H), 1.77(d, *J*=1.6Hz, 3H), 1.69(s, 3H), 1.30(d, *J*=6.4Hz, 3H) ^{13}C-NMR (100 MHz, C_6D_6): δ: 169.4, 137.2, 132.0, 128.7, 128.6, 123.6, 121.4, 95.7, 87.8, 69.7, 23.0, 20.9, 20.5 IR (ν_{max}/cm^{-1}): 3652, 3451, 3060, 2976, 2464, 2200, 1952, 1734, 1596, 1567, 1490, 1443, 1309, 1235, 1185, 1138, 1042, 1016, 950, 913, 849, 755, 690, 609 MS (EI, m/z): 228 (9, M^+), 213 (25), 185 (100), 171 (37), 167 (92), 152 (82), 141 (27), 128 (39), 115 (33), 102 (13), 91 (15), 77 (15), 63 (8), 51 (8) HRMS (EI, m/z, $[M]^+$): 228.11448 (calculated), 228.11355 (found).

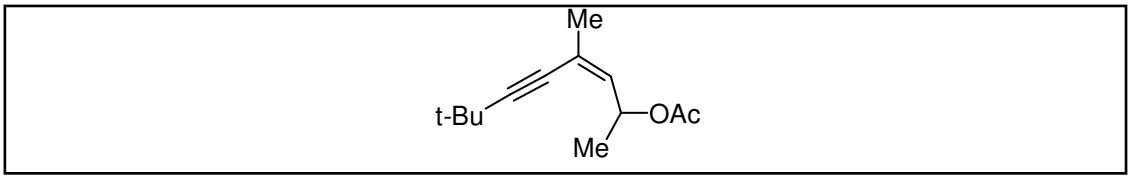

Figure 4.13. (*Z*)-4,7,7-trimethyloct-3-en-5-yn-2-yl acetate

1j: ^{1}H-NMR (400 MHz C_6D_6) δ 6.2(dt, *J*=14.7, 6.5Hz, 1H), 5.55(dd, *J*=8.0, 1.4Hz, 1H), 1.73(d, *J*=1.6Hz, 3H), 1.69(s, 3H), 1.32(d, *J*=6.4Hz, 3H), 1.23(s, 9H) ^{13}C-NMR (100 MHz, C_6D_6): δ: 169.3, 135.7, 122.0, 104.6, 77.8, 69.8, 31.0, 28.3 23.4, 20.9, 20.5 IR (ν_{max}/cm^{-1}): 3451, 2971, 2870, 2221, 1741, 1630, 1451, 1370, 1306, 1239, 1201, 1147, 1046, 942, 853 MS (EI, m/z): 208(46% M^+), 193 (20), 165 (49), 151 (46), 133 (60), 123 (24), 109 (100), 105 (56), 95 (11), 91 (57), 81 (12), 77 (27), 65 (13) HRMS (EI, m/z, $[M]^+$): 208.14578 (calculated), 208.14506 (found).

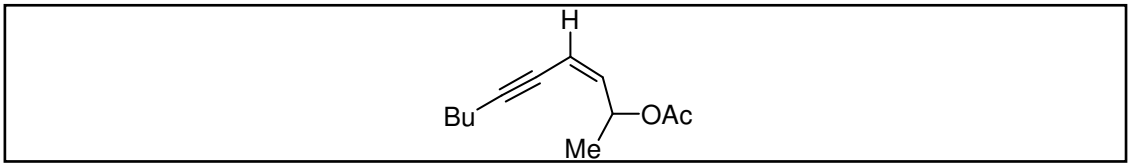

Figure 4.14. (*Z*)-dec-3-en-5-yn-2-yl acetate

1k: ^{1}H-NMR (400 MHz C_6D_6) δ 6.18(quintet, *J*=6.8Hz, 1H), 5.68(dd, *J*=10.8, 8.0Hz, 1H), 5.47(dd, *J*=10.8, 0.8Hz, 1H), 2.10(td, *J*=6.7, 2.0Hz, 2H), 1.60(s, 3H), 1.38-1.24(m, 4H), 1.30(d, *J*=6.4Hz, 3H), 0.78(t, *J*=7.2Hz, 3H) ^{13}C-NMR (100 MHz, C_6D_6): δ: 169.3, 140.9, 111.7, 97.6, 76.7, 69.2, 31.0, 22.2, 20.8, 20.3, 19.4, 13.7 IR (ν_{max}/cm^{-1}): 3451, 3029, 2959, 2933, 2873, 2211, 1737, 1617, 1454, 1425, 1368, 1326, 1296, 1232, 1154, 1116, 1094, 1039, 1013, 948, 897, 854, 739, 607, 562 MS (EI, m/z): 194 (5, M^+), 179 (9), 165 (5), 151 (100), 137 (21), 123 (22), 109 (67), 95 (92), 91 (95), 81 (33), 77 (35), 65 (23) HRMS (EI, m/z, $[M]^+$): 194.13013(calculated), 194.13094 (found).

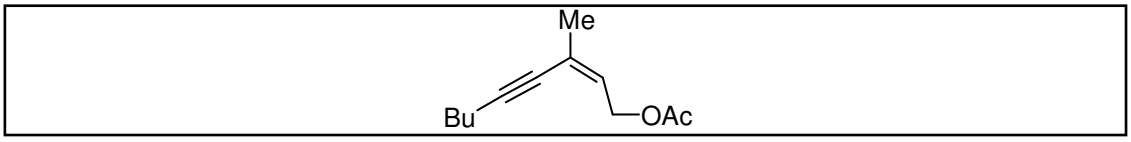

Figure 4.15. (*Z*)-3-methylnon-2-en-4-ynyl acetate

1l: ^{1}H-NMR (400 MHz C_6D_6) δ 5.68 (dt, *J*=7.0, 1.2Hz, 1H), 4.96(d, *J*=6.8Hz, 2H), 2.09(t, *J*=6.8Hz, 2H), 1.74(d, *J*=1.2Hz, 3H), 1.66(s, 3H), 1.36-1.22(m, 4H), 0.77(t, *J*=7.2Hz, 3H) ^{13}C-NMR (100 MHz, C_6D_6): δ: 170.1, 129.7, 124.2, 96.7, 79.1, 63.3.0, 31.0, 23.6, 20.7, 22.2, 19.3, 13.7 IR (ν_{max}/cm^{-1}): 3651, 3461, 2950, 2933, 2870, 2216,

1740, 1636, 1433, 1377, 1228, 1103, 1024, 962, 890, 813, 605 MS (EI, m/z): 194 (17, M^+), 179 (9), 165 (8), 151 (68), 135 (10), 123 (16), 110 (44), 95 (100), 91 (71), 81 (41), 77 (34), 65 (17) HRMS (EI, m/z, $[M]^+$): 194.13013(calculated), 194.12958 (found).

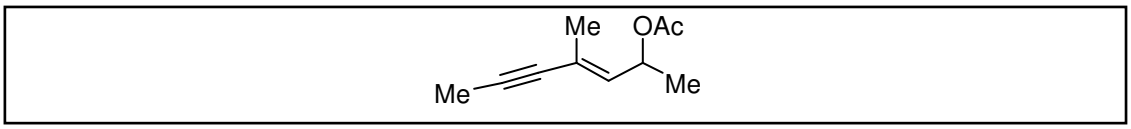

Figure 4.16. (*E*)-4-methylhept-3-en-5-yn-2-yl acetate

(*E*)**-1a:** ^{1}H-NMR (400 MHz $CDCl_3$) δ 5.65(d, *J*=9.2, 1H), 5.54-5.61(m, 1H), 2.01(s, 3H), 1.93(s, 3H), 1.85(d, *J*=0.8 Hz, 3H), 1.27 (d, *J*=6.4 Hz, 3H) ^{13}C-NMR (100 MHz, $CDCl_3$): δ: 170.4, 134.8, 121.8, 84.7, 81.8, 67.5, 21.4, 20.4, 18.2, 4.3 FTIR (ν_{max}/cm^{-1}): 2980, 2918, 2228, 1731, 1638, 1443, 1154, 1040, 1015, 943, 864, 610; MS (EI, *m/z*): 166 (13, M^+), 151 (30), 123 (100), 109 (79), 91 (87), 79 (26),

4.4. General Procedure for Arylation Reactions

To an oven-dried flask containing (Z)-2-en-4-yne acetate (0.3 mmol) and arylboronic acid (0.9 mmol, 3 equiv) was added CsF (0.45 mmol, 1.5 equiv), $[RhOH(cod)]_2$ (6 mol % Rh), degassed water (0.1 mL), and dry THF (2.0 mL), successively, under Ar. The reaction mixture was stirred magnetically at room temperature for 16 h. The solvent was removed under reduced pressure and the residue was purified by column chromatography using hexane-ethyl acetate as eluent to give vinyl allene.

4.5. Characterization of Products

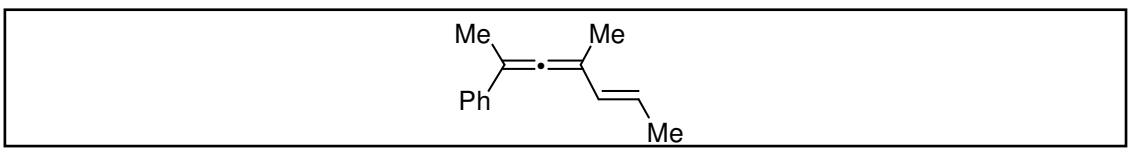

Figure 4.17. (*E*)- 2-phenyl-4-methylhepta-2,3,5-triene

3aa: ^{1}H NMR (400 MHz, $CDCl_3$) δ**:** 7.34-7.38 (m, 2H), 7.28-7.33 (m, 2H), 7.14-7.21 (m, 1H), 6.06 (dq, *J*= 15.6, 1.6 Hz, 1H), 5.64 (dq, *J*= 16.0, 6.8 Hz, 1 H), 2.09 (s, 3H), 1.90 (s, 3H), 1.80 (dd, *J*= 6.8, 1.6 Hz, 3H); ^{13}C NMR (100 MHz, $CDCl_3$) δ: 207.0, 137.8, 129.2, 128.3, 126.4, 125.8, 124.5, 101.8, 99.6, 18.3, 17.1, 15.5; FTIR (ν_{max}/cm^{-1})**:** 3029, 2981, 2911, 1933, 1598, 1491, 1444, 1367, 1065, 1026, 961, 757, 690, 603, 594; MS (EI, *m/z*): 184 (100, M^+), 169 (98), 154 (86), 141 (70), 128 (51), 115 (36), 105 (19), 91 (30), 77 (15); HRMS (ESI, *m/z*, $(M+H)^+$)**:** 185.1325 (calculated), 185.1324 (found).

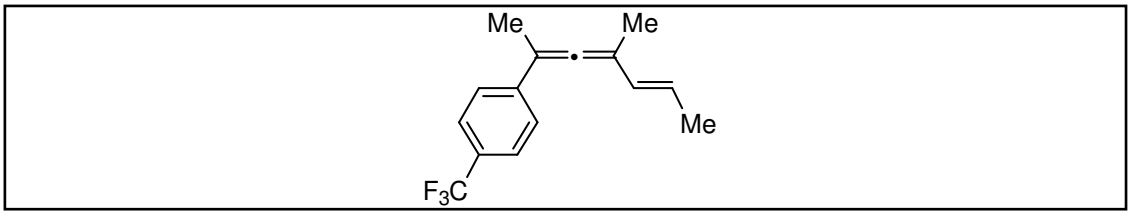

Figure 4.18. ((*E*)-2-(4-(trifluoromethyl)-phenyl)-4-methylhepta-2,3,5-triene

3ab: ^{1}H NMR (400 MHz, $CDCl_3$) δ**:** 7.54 (d, J_{AB}= 8.0 Hz, 2H), 7.44 (d, J_{AB}= 8.0 Hz, 2H), 6.05 (dq, *J*= 16.0, 2.0 Hz, 1H), 5.64 (dq, *J*=15.6, 6.8 Hz, 1H), 2.1 (s, 3H), 1.91 (s, 3H), 1.79 (dd, *J*= 6.8, 1.6 Hz, 3H); ^{13}C NMR (100 MHz, $CDCl_3$) δ: 207.8, 141.7, 128.5, 128.3 (q, *J*=32 Hz) 125.9, 125.4, 125.1 (q, *J*= 3.9 Hz), 124.4 (q, *J*= 270 Hz) 102.5, 99.0, 18.3, 17.0, 15.3; FTIR (ν_{max}/cm^{-1}): 2987, 2928, 2855, 1933, 1616, 1323, 1164, 1114, 1074, 1014, 840, 607; MS (EI, *m/z*): 252 (100, M^+), 237 (82), 222 (21), 209 (43), 197 (64), 183 (26), 168 (36), 153 (39), 141 (17), 128 (14), 115 (13), 91 (16); HRMS (EI, *m/z*, M^+)**:** 252.1120 (calculated), 252.1119 (found).

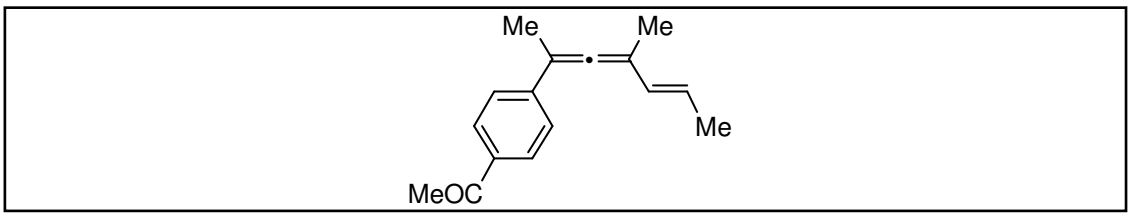

Figure 4.19. (*E*)-2-(4-acetylphenyl)-4-methylhepta-2,3,5-triene

3ac: ^{1}H NMR (400 MHz, $CDCl_3$) δ**:** 7.89 (d, *J*= 8.4 Hz, 2H), 7.43 (d, J_{AB}= 8.0 Hz, 2H), 6.04 (dq, J_{AB}= 15.6, 1.6 Hz, 1H), 5.68 (dq, *J*= 15.2, 6.8 Hz, 1H), 2.57 (s, 3H),

2.1 (s, 3H), 1.9 (s, 3H), 1.80 (dd, *J*= 6.4, 1.2 Hz, 3H); ^{13}C NMR (100 MHz, $CDCl_3$) δ: 208.3, 197.7, 143.0, 135.0, 128.43, 128.39, 125.8, 125.4, 102.4, 99.4, 26.6, 18.4, 17.0, 15.3; FTIR (ν_{max}/cm^{-1}): 2925, 2850, 1930, 1681, 1601, 1357, 1266, 959, 838, 646, 602; MS (EI, *m/z*): 226 (100, M^+), 211 (57), 183 (37), 168 (43), 153 (39), 141 (24), 128 (19), 115 (21), 91 (11); HRMS (ESI, *m/z*, $(M+H)^+$)**:** 227.1430 (calculated), 227.1429 (found).

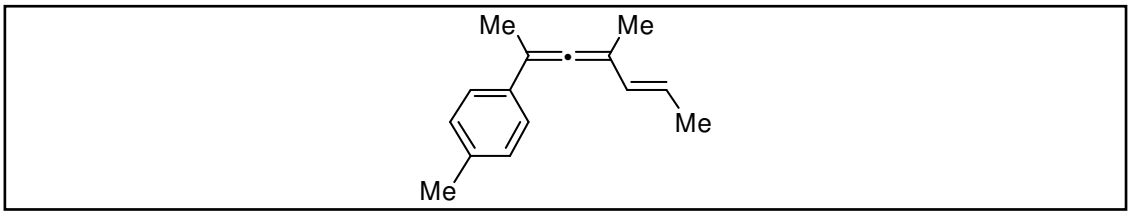

Figure 4.20. (*E*)-2-(4-meyhylphenyl)-4-methylhepta-2,3,5-triene

3ad: ^{1}H NMR (400 MHz, $CDCl_3$) δ**:** 7.24 (d, J_{AB}= 8.0, 2H), 7.11 (d, J_{AB}= 8.0 Hz, 2H), 6.06 (dq, *J*= 16.0, 2.0 Hz, 1H), 5.64 (dq, *J*= 15.6, 6.4 Hz, 1H), 2.32 (s, 3H), 2.07 (s, 3H), 1.80 (s, 3H), 1.79 (dd, *J*= 6.8, 1.6 Hz, 3H); ^{13}C NMR (100 MHz, $CDCl_3$) δ**:** 206.7, 136.1, 134.8, 129.5, 129.0, 125.7, 124.3, 101.7, 99.5, 21.1, 18.3, 17.2, 15.5; FTIR (ν_{max}/cm^{-1}): 3038; 2982, 2921, 2850, 1510, 1444, 1370, 1025, 963, 816, 590; MS (EI, *m/z*): 198 (100, M^+), 183 (93), 168 (82), 153 (48), 141 (36), 128 (33), 115 (35), 105 (18), 91 (30), 77 (19); HRMS (ESI, *m/z*, $(M+H)^+$)**:** 199.1481 (calculated), 199.1481 (found).

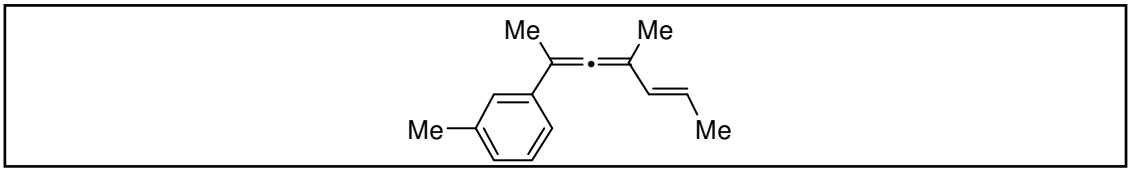

Figure 4.21. (*E*)-2-(3-meyhylphenyl)-4-methylhepta-2,3,5-triene

3ae: ^{1}H NMR (400 MHz, $CDCl_3$) δ: 7.20-7.41 (m, 3H), 7.02-7.05 (m, 1H), 6.10 (dq, *J*= 15.2, 1.6 Hz, 1H), 5.67 (dq, *J*= 15.2, 6.4 Hz, 1H), 2.37 (s, 3H), 2.11 (s, 3H), 1.93 (s, 3H), 1.83 (dd, *J*= 6.8, 1.6 Hz, 3 H); ^{13}C NMR (100 MHz, $CDCl_3$) δ: 207.0, 138.79, 137.8, 129.4, 128.2, 127.3, 126.6, 124.3, 123.0, 101.6, 99.6, 21.6, 18.3, 17.3, 15.5; FTIR (ν_{max}/cm^{-1}): 3013, 2918, 2855, 1933, 1604, 1488, 1444, 1376, 1028, 962, 781, 696; MS (EI, *m/z*): 198 (100, M^+), 183 (87), 168 (78), 153 (47), 141 (37), 128 (32),

115 (34), 105 (17), 91 (32); HRMS (ESI, *m/z*, $(M+H)^+$)**:** 199.1481 (calculated), 199.1481 (found).

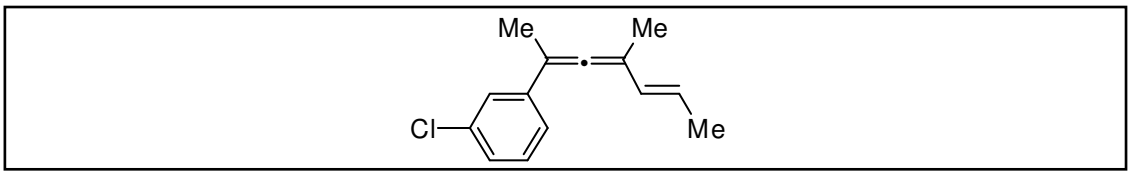

Figure 4.22. (*E*)-2-(3-chlorophenyl)-4-methylhepta-2,3,5-triene

3af: ^{1}H NMR (400 MHz, CD_3Cl) δ: 7.31-7.32 (m, 1H), 7.21-7.23 (m, 2H), 7.13-7.17 (m, 1H), 6.04 (dq, *J*= 15.6, 1.6 Hz, 1H), 5.67 (dq, *J*= 6.8, 15.6 Hz, 1H), 2.07 (s, 3H), 1.89 (s, 3H), 1.81 (dd, *J*= 6.8, 1.6 Hz, 3H); ^{13}C NMR (100 MHz, $CDCl_3$) δ: 207.3, 140.1, 134.4, 129.5, 128.9, 126.5, 126.0, 125.3, 124.1, 102.5, 99.0, 18.5, 17.3, 15.6; FTIR (ν_{max}/cm^{-1}): 3034, 2982, 2916, 2855, 1933, 1592, 1566, 1475, 1443, 1417, 1368, 1106, 1080, 1067, 1027, 961, 776, 748, 687, 609; MS (EI, *m/z*): 218 (97, M^+), 203 (70), 183 (33), 175 (19), 168 (100), 153 (77), 141 (45), 128 (31), 115 (33), 102 (12), 91 (21), 77 (20); HRMS (ESI, *m/z*, $(M+H)^+$): 219.0935 (calculated), 219.0936 (found).

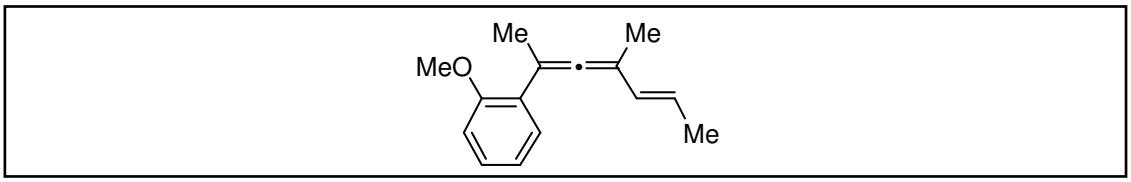

Figure 4.23. (*E*)-2-(2-methoxyhenyl)-4-methylhepta-2,3,5-triene

3ag: ^{1}H NMR (400 MHz, $CDCl_3$) δ: 7.20-7.41 (m, 2H), 6.84–6.93 (m, 2H), 6.10 (dq, *J*= 15.6, 1.6 Hz, 1H), 5.54 (dq, *J*= 16.0, 6.8 Hz, 1H), 3.81 (s, 3H), 2.07 (s, 3H), 1.84 (s, 3H), 1.78 (dd, *J*= 6.4, 1.6 Hz, 3H, ^{13}C NMR (100 MHz, $CDCl_3$) δ: 207.5, 157.0, 130.1, 129.2, 128.1, 127.9, 123.4, 120.5, 111.4, 98.5, 97.2, 55.7, 19.6, 18.3, 15.7; FTIR (ν_{max}/cm^{-1}): 2924, 1596, 1578, 1491, 1434, 1245, 1029, 962, 749, 603; MS (EI, *m/z*): 214 (23, M+), 199 (100), 184 (38), 165 (34), 152 (25), 141 (25), 135 (78), 128 (29), 115 (34), 91 (30), 77 (28); HRMS (ESI, *m/z*, $(M+H)^+$)**:** 215.1430 (calculated), 215.1430 (found).

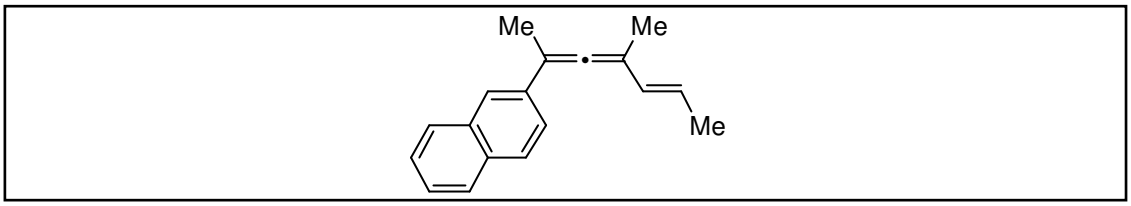

Figure 4.24. (*E*)- 2-(2-naphthyl)-4-methylhepta-2,3,5-triene

3ah: ^{1}H NMR (500 MHz, $CDCl_3$) δ: 7.78-7.87 (m, 2H), 7.70-7.77 (m, 2H), 7.54-7.59 (m, 1H), 7.40-7.52 (m, 2H), 6.14 (dq, *J*= 16.0, 1.0 Hz, 1H), 5.72 (dq, *J*= 15.5, 6.5 Hz, 1H), 2.25 (s, 3H), 1.97 (s, 3H), 1.85 (d, *J*= 5.5 Hz, 3H); ^{13}C NMR (126 MHz, $CDCl_3$) δ: 208.0, 135.4, 133.8, 132.5, 129.3, 128.1, 127.71, 127.68, 126.2, 125.6, 125.5, 124.8, 123.5, 102.2, 100.1, 18.5, 17.4, 15.7; FTIR (ν_{max}/cm^{-1}): 3053, 2982, 2915, 1929, 1629, 1597, 1505, 1371, 1025, 961, 854, 817, 783, 745; MS (EI, *m/z*): 234 (100, M^+), 219 (88), 204 (81), 189 (27), 178 (43), 165 (25), 152 (20), 141 (15); HRMS (ESI, *m/z*, $(M+H)^+$)**:** 235.1481 (calculated), 235.1481 (found).

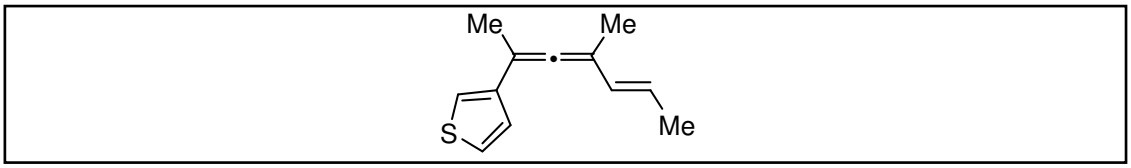

Figure 4.25. (*E*)- 2-(3-thienyl)-4-methylhepta-2,3,5-triene

3ai: ^{1}H NMR (400 MHz, $CDCl_3$) δ: 7.20-7.23 (m, 1H), 7.01-7.05 (m, 2H), 6.27 (dq, *J*= 15.6, 1.6 Hz, 1H), 5.96 (dq, *J*= 15.6, 6.4 Hz, 1H), 2.06 (s, 3H), 1.87 (s, 3H), 1.79 (dd, *J*= 6.8, 1.2 Hz, 3H); ^{13}C NMR (100 MHz, $CDCl_3$) δ: 206.8, 140.1, 129.3, 126.9, 125.2, 124.5, 118.7, 103.3, 99.1, 18.3, 17.7, 15.6; FTIR (ν_{max}/cm^{-1}): 3103, 2987, 2922, 2855, 1929, 1442, 1368, 1247, 1183, 1026, 962, 864, 775, 644; MS (EI, *m/z*): 190 (95, M^+), 175 (100), 160 (45), 147 (32), 142 (59), 134 (23), 129 (17), 115 (25); HRMS (ESI, *m/*z, $(M+H)^+$)**:** 191.0889 (calculated), 191.0889 (found).

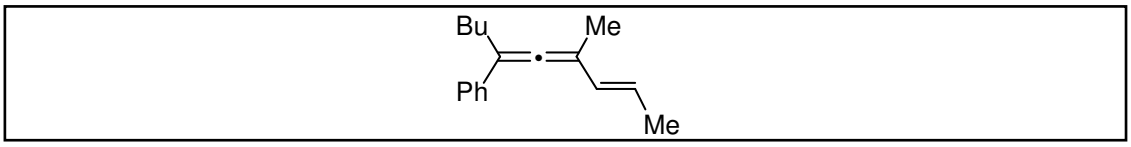

Figure 4.26. (*E*)- 6-phenyl-4-methyldeca-2,4,5-triene

3ba: ^{1}H NMR (400 MHz, $CDCl_3$) δ: 7.37-7.41 (m, 2H), 7.28-7.34 (m, 2 H), 7.17-7.23 (m, 1H), 6.10 (dq, *J*= 15.6, 1.6 Hz, 1H), 5.67 (dq, *J*= 15.6, 6.6 Hz, 1H), 2.47 (t, *J*= 7.6, 2H), 1.93 (s, 3H), 1.83 (dd, *J*= 6.6, 2.0 Hz, 3H), 1.53 (quint, *J*= 7.2 Hz, 2H), 1.44 (sext, *J*= 7.6 Hz, 2H), 0.95 (t, *J*=7.4 Hz, 3H); ^{13}C NMR (100 MHz, $CDCl_3$) δ: 207.0, 137.8, 129.6, 128.4, 126.5, 126.3, 124.4, 105.1, 103.2, 30.3, 30.2, 22.6, 18.5, 15.7, 14.1; FTIR (ν_{max}/cm^{-1})**:** 3025, 2957, 2928, 2859, 1931, 1599, 1492, 1446, 1376, 961, 757, 693; MS (EI, *m/z*): 226 (13, M^+), 211 (7), 197 (13), 184 (50), 169 (100), 155 (37), 141 (31), 128 (23), 115 (21), 91 (25), 77 (8); HRMS (EI, *m/z*, M^+)**:** 226.1716 (calculated), 226.1712 (found).

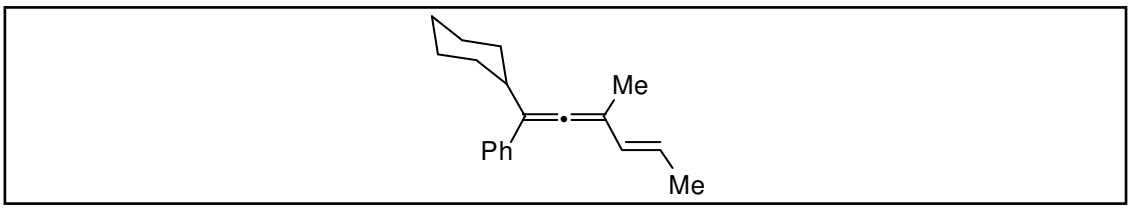

Figure 4.27. (*E*) 1-cyclohexyl-1-phenyl-3-methyl-hexa-1,2,4-triene

3ca: ^{1}H NMR (400 MHz, C_6D_6) δ: 7.44-7.57 (m, 2H), 7.17-7.21 (m, 2H), 7.02-7.09 (m, 1H), 6.19 (dq, *J*= 15.6, 1.6 Hz, 1H), 5.54 (dq, *J*= 15.6, 6.8 Hz, 1H), 2.44-2.52 (m, 1H), 1.95-2.03 (m, 2H), 1.87 (s, 3H), 1.65 (dd, *J*= 6.8, 1.6 Hz, 3H), 1.59-1.73 (m, 3H), 1.24-1.32 (m, 4H), 1.11-1.19 (m, 1H); ^{13}C NMR (101 MHz, C_6D_6) δ: 207.1, 137.8, 130.2, 128.7, 127.2, 126.8, 124.2, 112.2, 104.3, 38.6, 33.3, 33.5, 27.0, 26.8, 18.4, 15.9; FTIR (ν_{max}/cm^{-1}): 3021, 2924, 2851, 1928, 1598, 1493, 1446, 961, 764, 693; MS (EI, *m/z*): 252 (18, M^+), 237 (18), 223 (31), 195 (26), 183 (100), 169 (50), 155 (48), 141 (30), 128 (29), 115 (25), 91 (36), 77 (12); HRMS (EI, *m/z*, M^+): 252.1873 (calculated), 252.1871 (found).

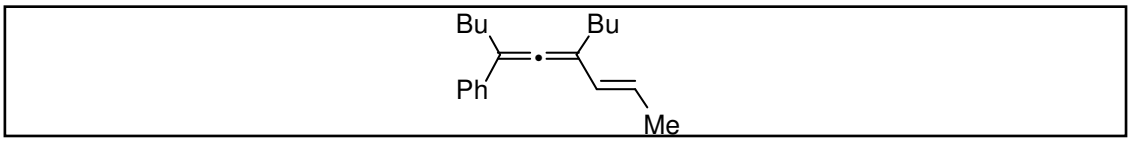

Figure 4.28. (*E*)-5-phenyl-7-(prop-1-enyl)undeca-5,6-diene

3da: ^{1}H NMR (400 MHz, C_6D_6) δ: 7.46-7.53 (m, 2H), 7.16-7.23 (m, 2H), 7.03-7.09 (m, 1H), 6.14 (dd, *J*= 15.7, 1.6 Hz, 1H), 5.65 (dq, *J*= 15.7, 6.7 Hz, 1H), 2.46 (t, *J*= 8.0 Hz, 2H), 2.26 (t, *J*= 7.6 Hz, 2H), 1.66 (dd, *J*= 6.8, 1.5 Hz, 3H), 1.54-1.64 (m, 4H), 1.30-1.41 (m, 4H), 0.88 (t, *J*= 7.2 Hz, 3H), 0.85 (t, *J*= 7.2 Hz, 3H); ^{13}C NMR (101 MHz, C_6D_6) δ: 206.8, 138.0, 129.4, 128.7, 126.9, 126.5, 124.1, 108.7, 107.3, 30.8, 30.61, 30.60, 29.6, 23.2, 23.0, 18.6, 14.3, 14.2; FTIR (ν_{max}/cm^{-1}): 3023, 2956, 2927, 2858, 1597, 1493, 1448, 1377, 961, 757, 692; MS (EI, *m/z*): 268 (2, M^+), 239 (4), 226 (3), 211 (39), 183 (33), 169 (100), 155 (38), 141 (48), 128 (14), 115 (17), 91 (28), 77 (8); HRMS (EI, *m/z*, M^+)**:** 242.1485 (calculated), 242.1485 (found).

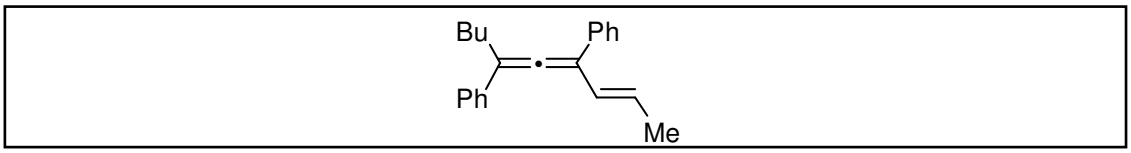

Figure 4.29. (*E*)-4,6-diphenyl-deca-2,4,5-triene

3ea: ^{1}H NMR (400 MHz, C_6D_6) δ: 7.50-7.57 (m, 4H), 7.12-7.20 (m, 4H), 7.02-7.09 (m, 2H), 6.27 (dq, *J*= 15.6, 2.0 Hz, 1H), 5.96 (dq, *J*= 15.6, 6.8 Hz, 1H), 2.47 (dt, *J*= 7.6, 1H), 2.46 (t, *J*=7.6 Hz, 1H), 1.62 (dd, *J*= 6.8, 1.6 Hz, 3H), 1.54-1.65 (m, 2H), 1.31 (sext, *J*= 15.6, 2H), 0.82 (t, *J*= 15.6 Hz, 3H); ^{13}C NMR (101 MHz, C_6D_6) δ: 207.7, 137.3, 137.1, 128.9, 128.8, 128.7, 127.9, 127.4, 127.2, 127.0, 126.5, 111.3, 109.1, 30.6, 30.5, 23.0, 18.5, 14.2; FTIR (ν_{max}/cm^{-1}): 3026, 2956, 2929, 2858, 1597, 1492, 1445, 960, 756, 692; MS (EI, *m/z*): 288 (8, M^+), 259 (19), 246 (168), 231 (100), 215 (77), 202 (28), 165 (16), 155 (20), 128 (21), 115 (28), 91 (26), 77 (13); HRMS (EI, *m/z*, M^+)**:** 288.1873 (calculated), 288.1876 (found).

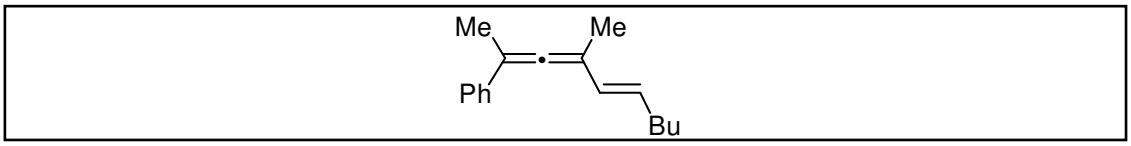

Figure 4.30. (*E*)-4-methyl-2-phenyl-deca-2,3,5-triene

3fa: ^{1}H NMR (400 MHz, CD_3Cl) δ: 7.37-7.43 (m, 2H), 7.31-7.36 (m, 2H), 7.21-7.24 (m, 1H), 6.08 (dt, *J*= 19.6, 1.6 Hz, 1H), 5.66 (dt, *J*= 15.6, 7.2 Hz, 1H), 2.13-2.20 (m, 2H), 2.13 (s, 3H), 1.93 (s, 3H), 1.32-1.48 (m, 4H), 0.94 (t, *J*= 7.6 Hz, 3H); ^{13}C NMR (101 MHz, CD_3Cl) δ: 207.2, 137.8, 130.08, 128.3, 127.9, 126.4, 125.9, 101.9, 99.6, 32.7, 31.8, 22.3, 17.1, 15.5, 14.0; FTIR (ν_{max}/cm^{-1}): 3027, 2956, 2925, 2863, 1933, 1492, 1444, 1367, 1027, 963, 758, 692, 604, 596; MS (EI, *m/z*): 226 (38, M^+), 211 (21), 197 (9), 183 (100), 168 (52), 155 (83), 141 (55), 128 (40), 115 (37), 105 (28), 91 (33), 77 (21); HRMS (ESI, *m/z*, $(M+H)^+$): 227.1794 (calculated), 227.1795 (found).

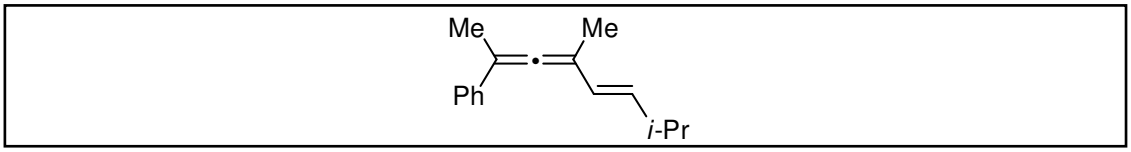

Figure 4.31. (*E*)-4,7-dimethyl-2-phenyl-octa-2,3,5-triene

3ga: ^{1}H NMR (400 MHz, C_6D_6) δ: 7.32-7.50 (m, 2H), 7.10-7.20 (m, 2H), 7.00-7.08 (m, 1H), 6.20 (dd, *J*= 15.8, 1.4 Hz, 1H), 5.59 (dd, *J*= 15.6, 7.0 Hz, 1H), 2.21-2.32 (m, 1H), 2.03 (s, 3H), 1.89 (s, 3H), 0.956 (d, *J*=7.2 Hz, 3H), 0.953 (d, *J*=7.2 Hz, 3H); ^{13}C NMR (101 MHz, C_6D_6) δ: 207.9, 138.2, 137.0, 128.7, 126.9, 126.4, 125.9, 102.3, 100.4, 31.9, 22.7, 17.3, 15.7 ppm; FTIR (ν_{max}/cm^{-1}): 3027, 2958, 2867, 1933, 1597, 1492, 1465, 1444, 1366, 1066, 1029, 964, 758, 692, 603; MS (EI, *m/z*): 212 (47, M^+), 197 (100), 182 (32), 169 (31), 165 (29), 155 (48), 141 (36), 128 (35), 115 (29), 91 (24), 77 (15); HRMS (EI, *m/z*, M^+)**:** 212.1560 (calculated), 212.1551 (found).

4.6. Computational Details

The geometry optimizations were performed by using the density functional theory (DFT) with Becke Three Parameter Lee, Yang, and Parr, (B3LYP) functional and LANL2DZ basis set implemented in Gaussian 09 software (Becke 1993). The imaginary frequencies have been checked with the frequencies for these structures. The geometry analysis is shown in Supplementary Information for some selected geometrical parameters. The natural Bond Orbital (NBO) and Mulliken charges were used for the charge analysis.

CHAPTER 5

RESULTS AND DISCUSSION

The reaction of a (*Z*)-configured enyne acetate **1a** with 3 equivalents of phenylboronic acid proceeded in THF solvent, at room temperature, and in the presence of $[RhCl(cod)]_2$ (6% Rh), 3 equivalents of KOH, and 0.1 mL of water to yield the desired phenyl-substituted vinylallene **3aa** product, which, however, was accompanied by significant amounts of nonseparable intricate isomers of the vinylallene with unassigned structures (Table 5.1, entry 1).

Yet, the reaction halted after a period of time and the conversion was incomplete even with the load of higher proportions of Rh at the beginning of the reaction, indicating that a change in the composition of reaction medium (possibly due to an increased concentration of the acetate dispelled from the enyne substrate) lowered the activity of the rhodium significantly.

The complete conversion of **1a** could be attained by substituting the base with CsF (entry 2) in the presence of $[RhOH(cod)]_2$ complex. The formation of isomeric byproducts could be minimized and thereby high yields of **3aa** product could be achieved by decreasing the CsF addition to 1.5 equivalent amounts (entries 2-5). The fine adjustment of the amount of added water seemed highly critical for the effectiveness of the process; the arylative substitution reaction did not proceed to completion when the reaction medium contained less or higher than 0.1 mL of water (entries 6-8). KF salt could not be an alternative flouride source (entry 9) and the use of other Cs compounds instead were useless (entries 10 and 11). A number of bases, such as NEt_3, NaOAc, K_2CO_3, NaOH, K_3PO_4, $NaHCO_3$, was also tested. However, the reactions resulted in incomplete conversion of the *Z*-enyne **1a** and accompanied by the formation of byproducts when using any of these bases.

Table 5.1. Effect of Base and Water Additives on the Rh(I)-Catalyzed Reaction of Z-Enyne Acetate 1a with Phenylboronic Acid.

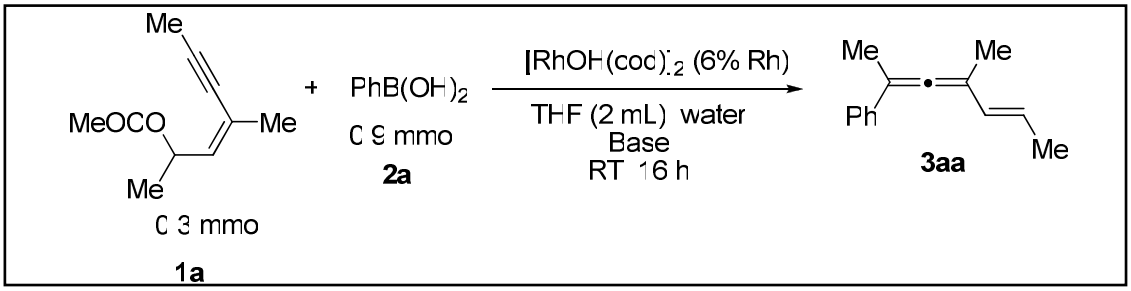

entry	base (equiv)	water (mL)	conversion (%)[a]	yield, **3ba** (%)[a]
1[b]	KOH (3)	0.1	78	58
2	CsF (3)	0.1	100	55
3	CsF (2)	0.1	100	75
4	CsF (1.5)	0.1	100	85
5	CsF (1.1)	0.1	95	75
6	CsF (1.5)	-	25	20
7	CsF (1.5)	0.05	77	67
8	CsF (1.5)	0.2	55	42
9	KF (3)	0.1	40	38
10	CsOH (1.5)	0.1	100	50
11	Cs_2CO_3 (1.5)	0.1	82	40

[a] Determined by ^{1}H NMR using benzaldehyde as internal standard.

[b] Rhodium complex charged was $[RhCl(cod)]_2$.

Having established the effective conditions, an array of substituted boronic acids was then subjected to the reactions with the enyne acetate **1a** (Table 5.2). The reaction tolerated both electron-withdrawing and -donating groups on the *m*- and *p*-positions, giving rise to high yields of the corresponding arylated vinylallene products **3aa–3af** (entries 1-6). A sterically congested organoboronic acid, 2-naphthylboronic acid, and 3-thienylboronic acid, were also suitable components for the reaction, yielding related products **3ag–3ai** with isolated yields in the range of 76–83% (entries 7–9). No

successful results could be obtained by the use of 1-naphthyl-, 3-pyridyl-, and 1-pentenylboronic acids.

Table 5.2. Rh(I)-Catalyzed Reaction of the *Z*-Enyne Acetate 1a with Organoboronic Acids

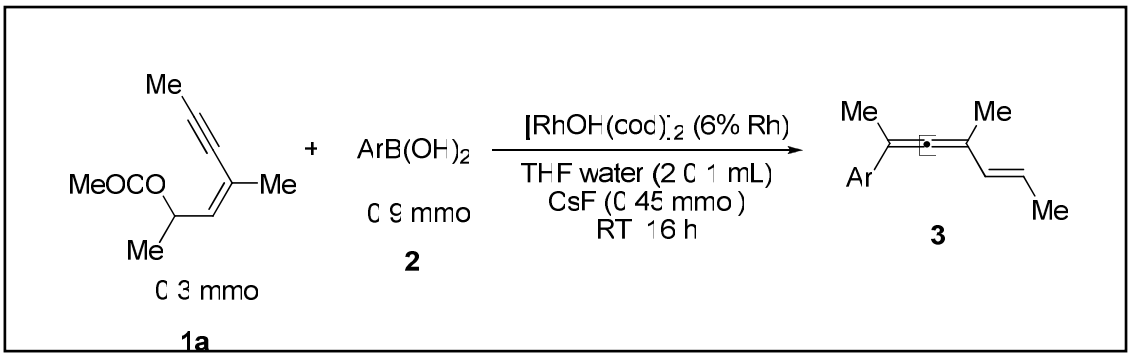

entry	Ar	product	isolated yield (%)
1	**2a** Ph	**3aa**	82
2	**2b** 4-$CF_3C_6H_4$	**3ab**	76
3	**2c** 4-$MeCOC_6H_4$	**3ac**	77
4	**2d** 4-MeC_6H_4	**3ad**	83
5	**2e** 3-MeC_6H_4	**3ae**	86
6	**2f** 3-ClC_6H_4	**3af**	77
7	**2g** 2-$MeOC_6H_4$	**3ag**	83
8	**2h** 2-naphthyl	**3ah**	76
9	**2i** 3-thienyl	**3ai**	81

The scope of the arylation method was also surveyed for a range of acetates of secondary *Z*-enynols. The method appeared suitable for the enyne acetates bearing butyl (**1b**) or cyclohexyl (**1c**) groups on the alkynyl moiety (R^1, Table 5.3, entries 1 and 2), butyl (**1d**) or phenyl (**1e**) groups in the R^2 position (entries 3 and 4), and butyl (**1f**) or isopropyl (**1g**) groups on the allylic carbon (R^3, entries 5 and 6), affording the corresponding vinylallenes in good yields when reacted with phenylboronic acid (70-79%). The reactions of enynes with substituents; *tert*-butyl (**1j**), $SiMe_3$ (**1h**), or Ph (**1i**),

substituents on the R^1 position (R^2= R^3= Me) and that acetate (**1l**) of a primary enyne alcohol (R^1= R^2= Me, R^3= H) were highly sluggish and afforded the related vinylallene products in very low yields, usually <20% (entries 7,8,9 and 10).

Table 5.3. Rh(I)-Catalyzed Reaction of *Z*-Enyne Acetates with Phenylboronic Acid

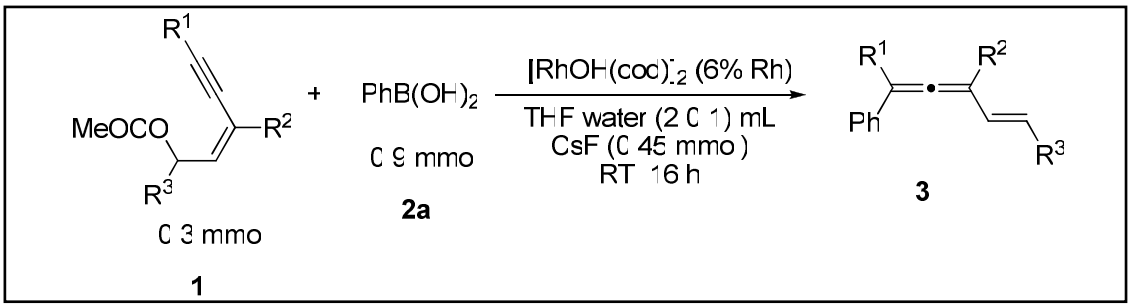

entry	substrate	R^1	R^2	R^3	product	isolated yield (%)
1	**1b**	Bu	Me	Me	**3ba**	72
2	**1c**	Cy	Me	Me	**3ca**	70
3	**1d**	Bu	Bu	Me	**3da**	75
4	**1e**	Bu	Ph	Me	**3ea**	73
5	**1f**	Me	Me	Bu	**3fa**	79
6	**1g**	Me	Me	*i*-Pr	**3ga**	77
7	**1h**	$SiMe_3$	Me	Me	**-**	<20
8	**1i**	Ph	Me	Me	**-**	<20
9	**1j**	*tert*-Bu	Me	Me	**-**	<20
10	**1k**	Bu	Me	H	**-**	<20

The Rh(I)-catalyzed reaction of the acetate of an enantiomerically enriched enynol reagent, (*R*,*Z*)-**1a** (94.5% *ee*) with phenylboronic acid under the optimal conditions proceeded with partial racemization, and yielded (*S*)-(+)-vinylallene as the major enantiomer (82% isolated yield, 40% *ee*, $[\alpha]_D^{25}$= +0.33 (c= 0.29, $CHCl_3$)) (Figure 5.2). (Lowe 1965; Ogasawara, et al. 2006; Ogasawara, et al. 2007)

The reaction should involve the regioselective *cis*-1,2-addition of the *in-situ* generated phenylrhodium(I) species across the carbon-carbon triple bond, which should be directed through the dual coordinative interaction of rhodium with alkynyl and acetate moieties (**I**), to afford the alkenylrhodium(I) intermediate (**II**) (Figure 5.2). It should be noted that the application of the rhodium-mediated protocol on the following conjugated enynes (**4** and **5**) which lack a leaving group at the allylic carbon resulted in complex mixtures of various isomers of mono- and dialkylated products:

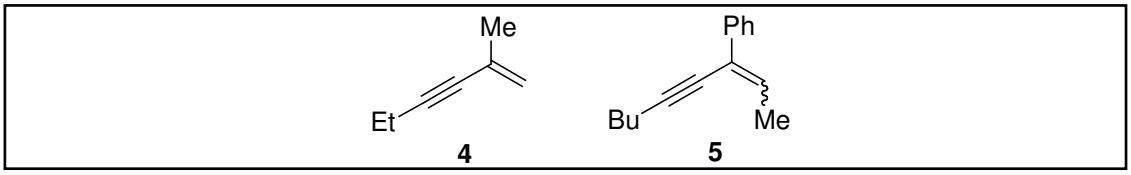

Figure 5.1. Conjugated enynes without leaving group

The subsequent δ-elimination of [Rh]-OAc and double bond migration may take place concurrently via both *anti*- and *syn*-modes, *syn*-deacetylation being the major path, to produce the enantiomers of arylated vinylallene products and regenerating the active Rh(I) catalyst for the next cycle. Alternatively, the formation of a benzylidene-π-allyrhodium intermediate (**III**) may precede the deacetylation step.

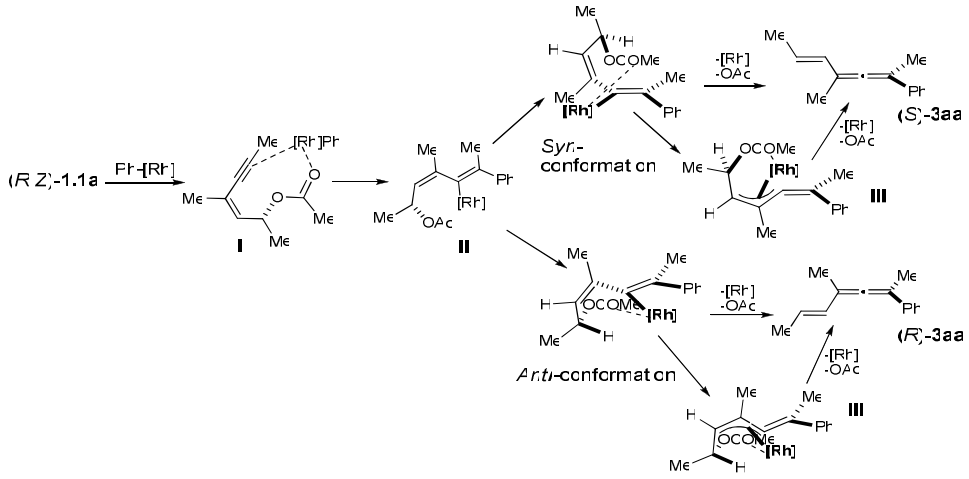

Figure 5.2. Stereochemistry of Rh(I)-Catalyzed Arylation of (R,Z)-2-En-4-Yne Acetate.

However, in both instances, the elimination step should be activated via the coordination of the rhodium and the oxygen functionality (Miura, et al. 2010). Indeed, we found that the Rh-mediated protocol is not applicable to *E*-configured enyne acetates; an analogous reaction with (*E*)-**1a** furnished a dienyl acetate structure (**6**) as the major product (62% NMR yield) and consequently formation of the desired vinylallene product was less than 10% (Figure 5.3). This result indicates that the alkenylrhodium intermediate **II'** which is arised through rhodoarylation of (*E*)-**1a** could not undergo the δ-elimination of [Rh]-OAc, instead, however, underwent demetallation to yield a hydroarylated product **6** and that could be ascribed to the fact that the intermediate **II'** can not maintain a suitable geometry for an effective Rh(I)-OAc interaction which seems necessary for the elimination step.

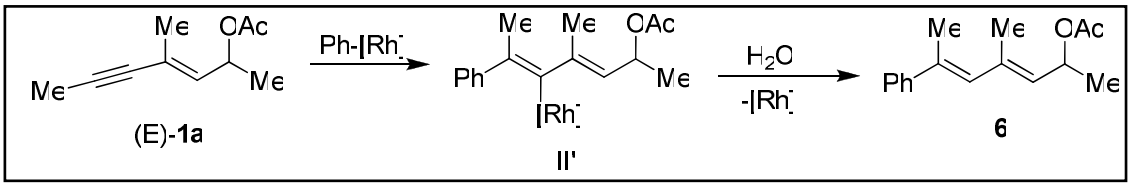

Figure 5.3. Rh(I)-Catalyzed Arylation of (*E*)- 4-methylhept-3-en-5-yn-2-yl acetate

For better rationalization of the observed enantiospecific outcome of the rhodium-mediated reaction of (*R*,*Z*)-**1.1a** with phenylboronic acid, we performed conformational analyses by using the density functional theory (dft) calculations for the intermediate **II**. The conformations were searched by different combination of rotations about four different single carbon-carbon bonds (Q1-Q4), as depicted in Figure 5.4., and 81 conformers were obtained. Then, more rotations were performed so as to achieve conformers which include the rhodium and the acetate group in a sufficient vicinity for effective coordination (typically 2.2706-2.2862 Å), which is necessary for the next Rh-OAc elimination step to form **3**.

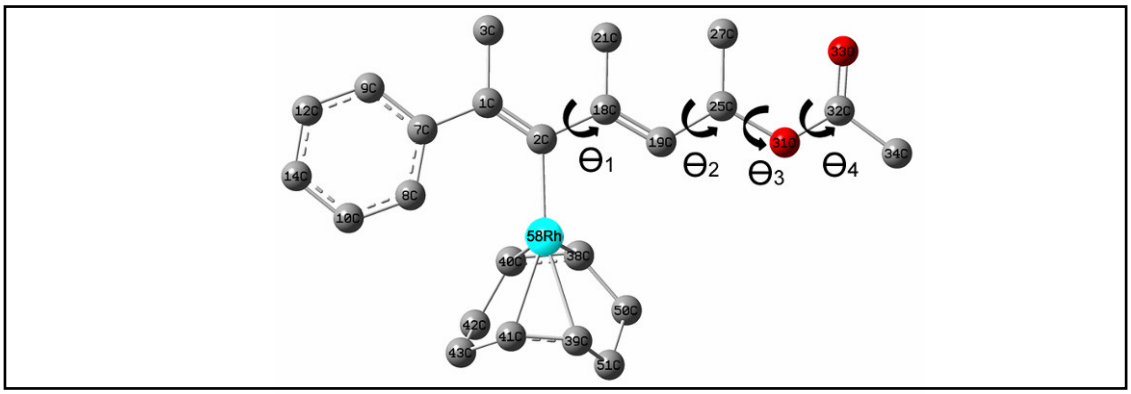

Figure 5.4. The structure of intermediate II which was subjected to dft calculations (hydrogens atoms are omitted for clarity)

As a result, the overall conformational analysis study yielded a minimum energy that is associated with the conformer **ES** as shown in Figure 5.5.. Interestingly this conformer could potentially follow a [Rh]-OAc elimination path leading to the product (*S*)-**3aa**. The other structures which are assigned as **ER**, **ZS**, and **ZR** (Figure 6.5.) represent the conformers of local minimum energies and potentially lead to the products (*E*,*R*), (*Z*,*S*), and (*Z*,*R*)-**3aa**, respectively. The fact that the conformer **ER** had a potential energy that is 3.83 kcal/mol higher than that of the conformer **ES** may account for the resulting enantiomeric ratio of the **3aa** products. The relative energies of the **ZR** and **ZS** as compared to **ES** are about 6.94 and 8.85 kcal/mol higher, respectively. It should be noted that no *Z*-configured vinylallene production was observed in the course of this study.

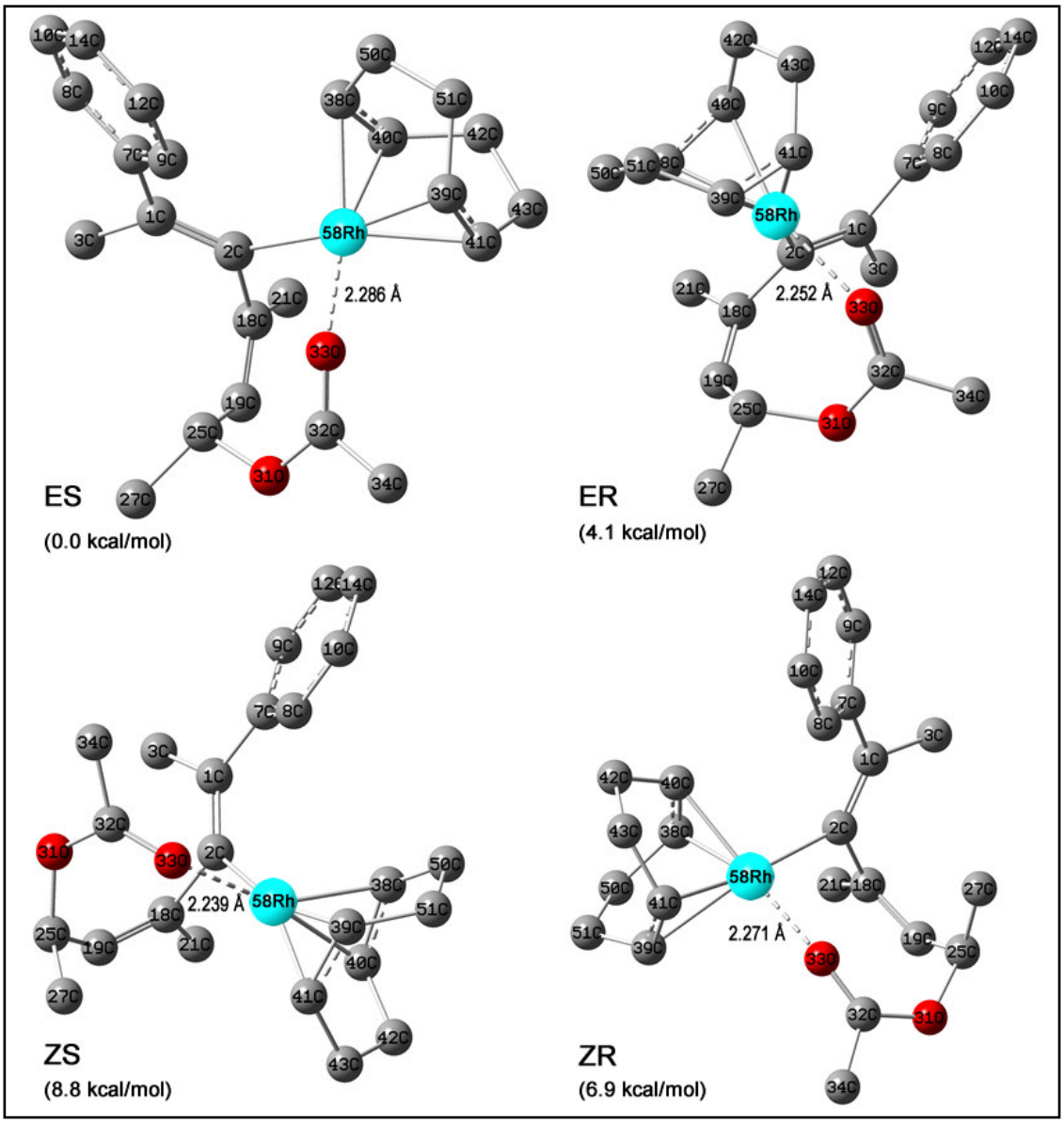

Figure 5.5. Optimized conformers for the intermediate II (hydrogen atoms are omitted for clarity and the energy values are relative energies)

CHAPTER 6

CONCLUSION

As a consequence, in this study new method was developed for the synthesis of *E*-configured vinyl allenes with an aryl moiety via the reaction of *Z*-2,4-enyne acetate with arylboronic acids in the presence of a Rh catalyst. $[RhOH(cod)]_2$ was found as the most effective complex in catalyzing the reaction.

Rh(I)-catalyzed reactions proceeded via typically S_N2'' type substitution of (*Z*)-2-en-4-yne acetates, which is triggered by *cis*-addition of *in-situ* formed nucleophilic arylrhodium(I) species with coordinating of alkynyl and acetate moieties. Deacetylation took place in both *syn*- and *anti*-modes; nevertheless, *syn*-elimination was the dominating route. The geometry of the (*E*)-2-en-4-yne acetate wouldn't allow the coordinative interaction of arylrhodium(I) species with both triple bond and oxygen of acetate moiety to produce vinylallene. Interestingly, *E*-enyne acetate underwent 4,5-arylative nucleophilic addition reaction with the same conditions as *Z*-enyne acetae to produce dienyl acetate product.

REFERENCES

Akpinar, G. E., et al. 2011 Palladium-Catalyzed Alkoxycarbonylation of (Z)-2-En-4-yn Carbonates Leading to 2,3,5-Trienoates. Organic Letters 13(4):748-751.

Arao, T., K. Kondo, and T. Aoyama 2007 Nickel-catalyzed 1,2-addition of arylboroxines to aromatic aldehydes. Tetrahedron Letters 48(23):4115-4117.

Arcadi, A., et al. 2008 Pd-catalyzed regioselective hydroarylation of alpha-(2-aminoaryl)-alpha,beta-ynones with organoboron derivatives as a tool for the synthesis of quinolines: experimental evidence and quantum-chemical calculations. Tetrahedron 64(22):5354-5361.

Becke, Axel D. 1993 Density-functional thermochemistry. III. The role of exact exchange. The Journal of Chemical Physics 98(7):5648-5652.

Betzer, Jean-François, et al. 1997 Radical Hydrostannylation, Pd(0)-Catalyzed Hydrostannylation, Stannylcupration of Propargyl Alcohols and Enynols: Regio- and Stereoselectivities. The Journal of Organic Chemistry 62(22):7768-7780.

Cho, C. S., et al. 1995 A New Catalytic Aactivity of Antimony(III) Chloride in Palladium(0)-Catalyzed Conjugate Addition of Aromatics to Alpha,Beta-Unsaturated Ketones and Aldehydes with Sodium Tetraphenylborate and Arylboronic Acids. Journal of Organic Chemistry 60(4):883-888.

Fagnou, K., and M. Lautens 2003 Rhodium-catalyzed carbon-carbon bond forming reactions of organometallic compounds. Chemical Reviews 103(1):169-196.

Giordano, G., et al. 2007 Di-μ-Chloro-Bis(η4-1,5-Cyclooctadiene)-Dirhodium(I): John Wiley & Sons, Inc.

Gore, J., and J. P. Dulcere 1972 New Synthesis of Vinylallenes. Journal of the Chemical Society-Chemical Communications (15):866

Hayashi, T., et al. 2001 Rhodium-catalyzed hydroarylation of alkynes with arylboronic acids: 1,4-shift of rhodium from 2-aryl-1-alkenylrhodium to 2-alkenylarylrhodium intermediate. Journal of the American Chemical Society 123(40):9918-9919.

Hayashi, T., and K. Yamasaki 2003 Rhodium-catalyzed asymmetric 1,4-addition and its related asymmetric reactions. Chemical Reviews 103(8):2829-2844.

Hoffmann-Roder, A., and N. Krause 2004 Synthesis and properties of allenic natural products and pharmaceuticals. Angewandte Chemie-International Edition 43(10):1196-1216.

I. Marek, C. Meyer, J. F. Normant 1998 A Simpe and Convenient Method for the preparation of (Z)-β-iodocrolein and of (Z)- or (E)-γ-iodo allylic alcohols: (Z)- and (E)-1-iodohept-1-en-3-ol Organic Syntheses 9:510.

Konno, Tsutomu, et al. 2008 A first high enantiocontrol of an asymmetric tertiary carbon center attached with a fluoroalkyl group via Rh(I)-catalyzed conjugate addition reaction. Tetrahedron Letters 49(13):2106-2110.

Lautens, M., and C. Dockendorff 2003 Palladium(II) catalyst systems for the addition of boronic acids to bicyclic alkenes: New scope and reactivity. Organic Letters 5(20):3695-3698.

Lautens, M., et al. 2001 Rhodium-catalyzed coupling reactions of arylboronic acids to olefins in aqueous media. Journal of the American Chemical Society 123(22):5358-5359.

Lin, S. H., and X. Y. Lu 2006 Palladium-bipyridine catalyzed conjugate addition of arylboronic acids to alpha,beta-unsaturated carbonyl compounds in aqueous media. Tetrahedron Letters 47(40):7167-7170.

Lowe, G. 1965 The abosolute configuration of allenes. Chemical Communications (London) (17):411-413.

Miura, T., et al. 2009 Stereoselective Synthesis of syn-Configured alpha-Allenols by Rhodium-Catalyzed Reaction of Alkynyl Oxiranes with Arylboronic Acids. Journal of Organic Chemistry 74(16):6050-6054.

Miura, T., et al. 2007 Stereoselective synthesis of alpha-allenols by rhodium-catalyzed reaction of alkynyl oxiranes with arylboronic acids. Angewandte Chemie-International Edition 46(37):7101-7103.

Miura, T., Y. Takahashi, and M. Murakami 2007 Rhodium-catalysed addition reaction of aryl- and alkenylboronic acids to isocyanates. Chemical Communications (34):3577-3579.

Miura, Tomoya, et al. 2010 Stereoselective synthesis of vinyl-substituted (Z)-stilbenes by rhodium-catalysed addition of arylboronic acids to allenic alcohols. Organic & Biomolecular Chemistry 8(18):4074-4076.

Moreau, C., et al. 2001 Rhodium-catalysed aryl transfer to aldehydes: counterion effects with nitrogen containing ligands. Tetrahedron Letters 42(39):6957-6960.

Murakami, Masahiro, and Hideyuki Igawa 2002 A Study of the Stereochemical Course of β-Oxygen Elimination with a Rhodium(I) Complex. Helvetica Chimica Acta 85(12):4182-4188.

Nishimura, T., et al. 2010 Rhodium-Catalyzed Enantioselective 1,6-Addition of Arylboronic Acids to Enynamides: Asymmetric Synthesis of Axially Chiral Allenylsilanes. Journal of the American Chemical Society 132(37):12865-12867.

Ogasawara, Masamichi, et al. 2006 Palladium-Catalyzed Preparation of Vinylallenes from 2-Bromo-1,3,5-trienes via an Alkylidene-π-allylpalladium-Mediated Formal SN2‘□‘ Pathway. Organic Letters 8(23):5409-5412.

Ogasawara, Masamichi, et al. 2007 Synthesis, Structure, and Reactivity of (1,2,3-η3-Butadien-3-yl)palladium Complexes. Organometallics 26(20):5025-5029.

Oguma, K., et al. 2000 Merry-go-round multiple alkylation on aromatic rings via rhodium catalysis. Journal of the American Chemical Society 122(42):10464-10465.

Oh, C. H., et al. 2003 The palladium-catalyzed addition of organoboronic acids to alkynes. Angewandte Chemie-International Edition 42(7):805-808.

Özdemir, Ismail, Serpil Demir, and Bekir Çetinkaya 2004 Synthesis of novel rhodium-carbene complexes as efficient catalysts for addition of phenylboronic acid to aldehydes. Journal of Molecular Catalysis A: Chemical 215(1-2):45-48.

Petasis, N. A. 2007 Expanding roles for organoboron compounds - Versatile and valuable molecules for synthetic, biological, and medicinal chemistry. Australian Journal of Chemistry 60(11):795-798.

Piers, E., et al. 1994 A Convenient procedure for the efficient preparation of alkyl (Z)-3-iodo-2-alkenoates. Canadian Journal of Chemistry-Revue Canadienne De Chimie 72(8):1816-1819.

Purpura, M., and N. Krause 1999 Regio- and stereoselective synthesis of vinylallenes by 1,5-(S-N-")-substitution of enyne acetates and oxiranes with organocuprates. European Journal of Organic Chemistry (1):267-275.

Sakai, M., H. Hayashi, and N. Miyaura 1997 Rhodium-catalyzed conjugate addition of aryl- or 1-alkenylboronic acids to enones. Organometallics 16(20):4229-4231.

Sakai, M., M. Ueda, and N. Miyaura 1998 Rhodium-catalyzed addition of organoboronic acids to aldehydes. Angewandte Chemie-International Edition 37(23):3279-3281.

Sakuma, S., et al. 2000 Asymmetric conjugate 1,4-addition of arylboronic acids to alpha,beta-unsaturated esters catalyzed by rhodium(I)/(S)-binap. Journal of Organic Chemistry 65(19):5951-5955.

Shintani, R., K. Okamoto, and T. Hayashi 2005 Rhodium-catalyzed synthesis of indenols by regioselective coupling of alkynes with ortho-carbonylated arylboronic acids. Chemistry Letters 34(9):1294-1295.

Takaya, Y., et al. 1998 Rhodium-catalyzed asymmetric 1,4-addition of aryl- and alkenylboronic acids to enones. Journal of the American Chemical Society 120(22):5579-5580.

Takeuchi, R., K. Tanabe, and S. Tanaka 2000 Stereodivergent synthesis of (E)- and (Z)-2-Alken-4-yn-1-ols from 2-propynoic acid: A practical route via 2-alken-4-ynoates. Journal of Organic Chemistry 65(5):1558-1561.

Uson, R., et al. 2007 Dinuclear Methoxy, Cyclooctadiene, and Barrelene Complexes of Rhodium(I) and Iridium(I): John Wiley & Sons, Inc.

Verhoeven, K. Barry Sharpless and Thomas R. 1979 Metal-Catalyzed,Highly Selective Oxygenations of Olefins and Acetylenes with *tert*-Butyl Hydroperoxide. Practical Considerations and Mechanism. Aldrichimica Acta 12(4):63-77.

Zemlicka, J. 1997 Antiviral nucleoside analogues with axial chirality. Nucleosides & Nucleotides 16(7-9):1003-1012.

APPENDIX A

^{1}H NMR AND ^{13}CNMR SPECTRUMS OF REACTANTS

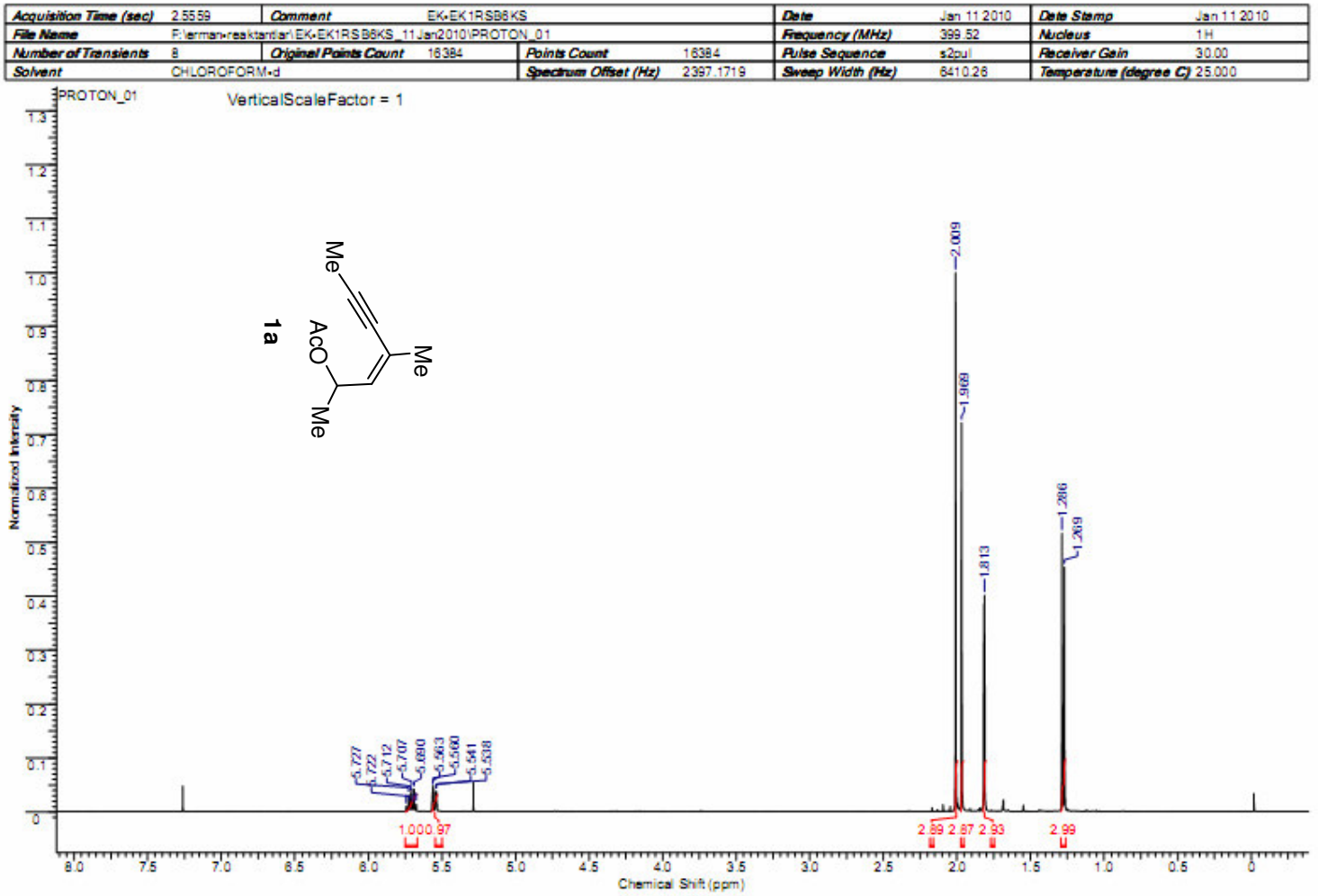

Figure A.1. [1] H NMR of (*Z*)-4-methylhept-3-en-5-yn-2-yl acetate

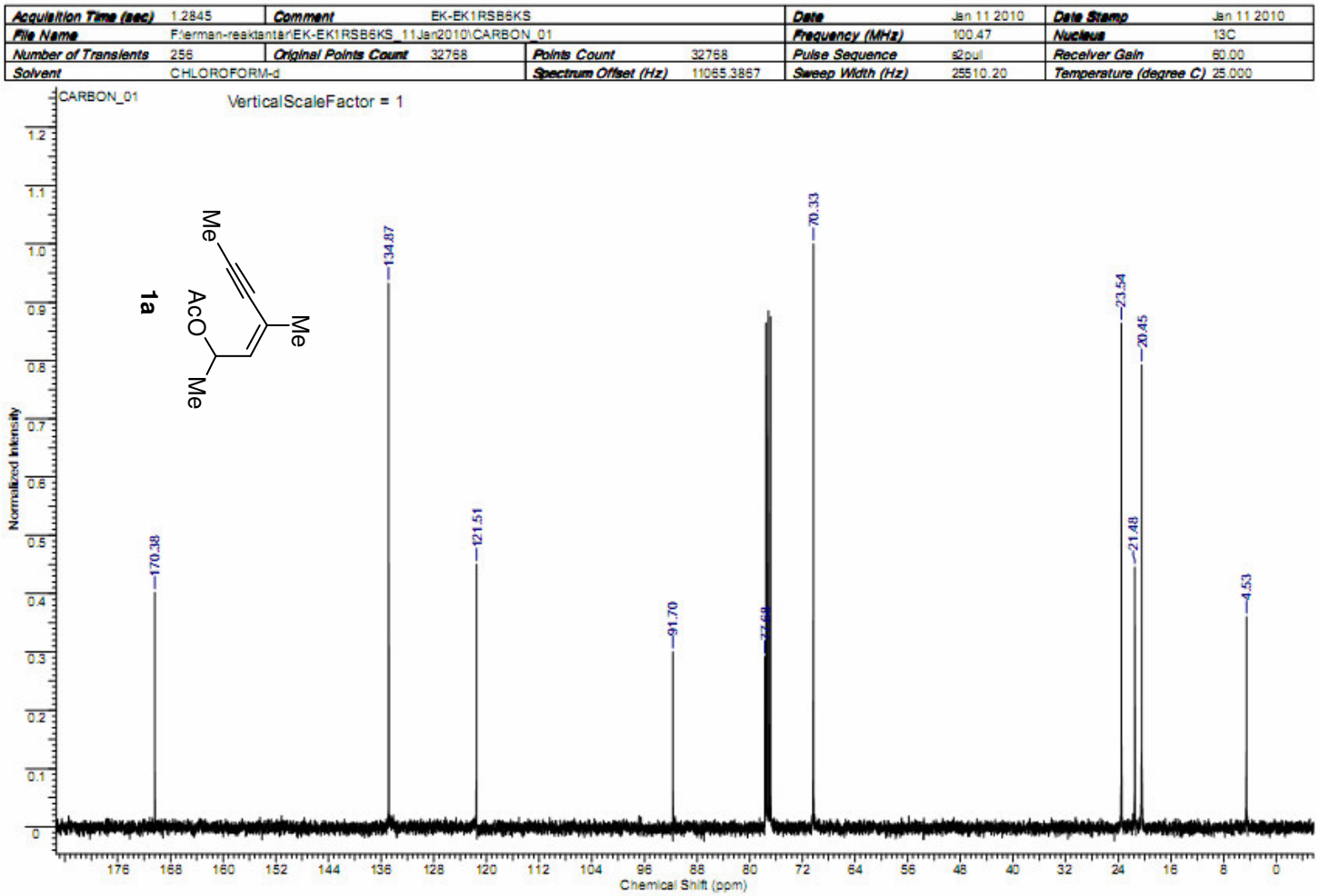

Figure A.2. ^{13}C NMR of (*Z*)-4-methylhept-3-en-5-yn-2-yl acetate

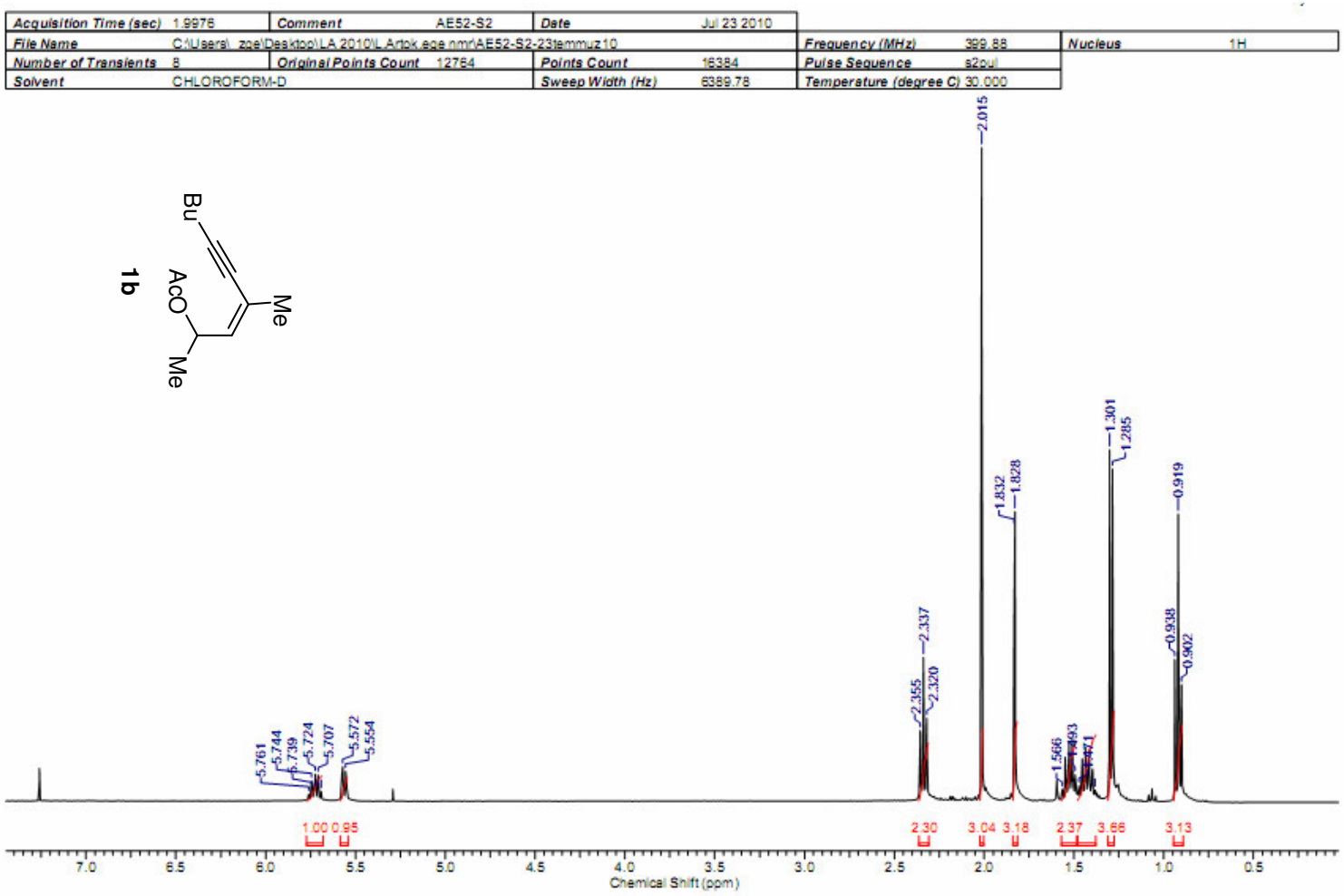

Figure A.3. ^{1}H NMR of (Z)-4-methyldec-3-en-5-yn-2-yl acetate

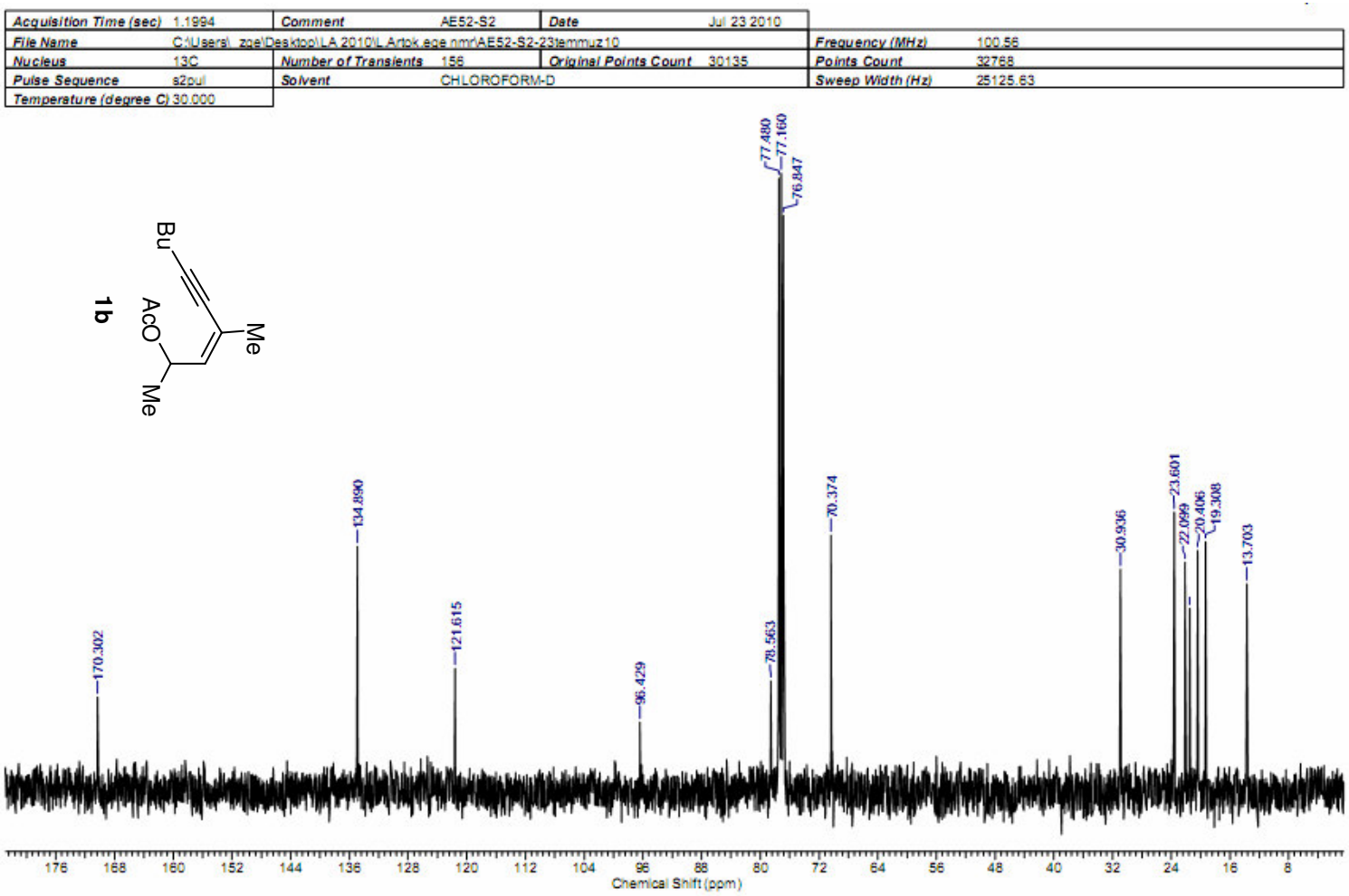

Figure A.4. ^{13}C NMR of (Z)-4-methyldec-3-en-5-yn-2-yl acetate

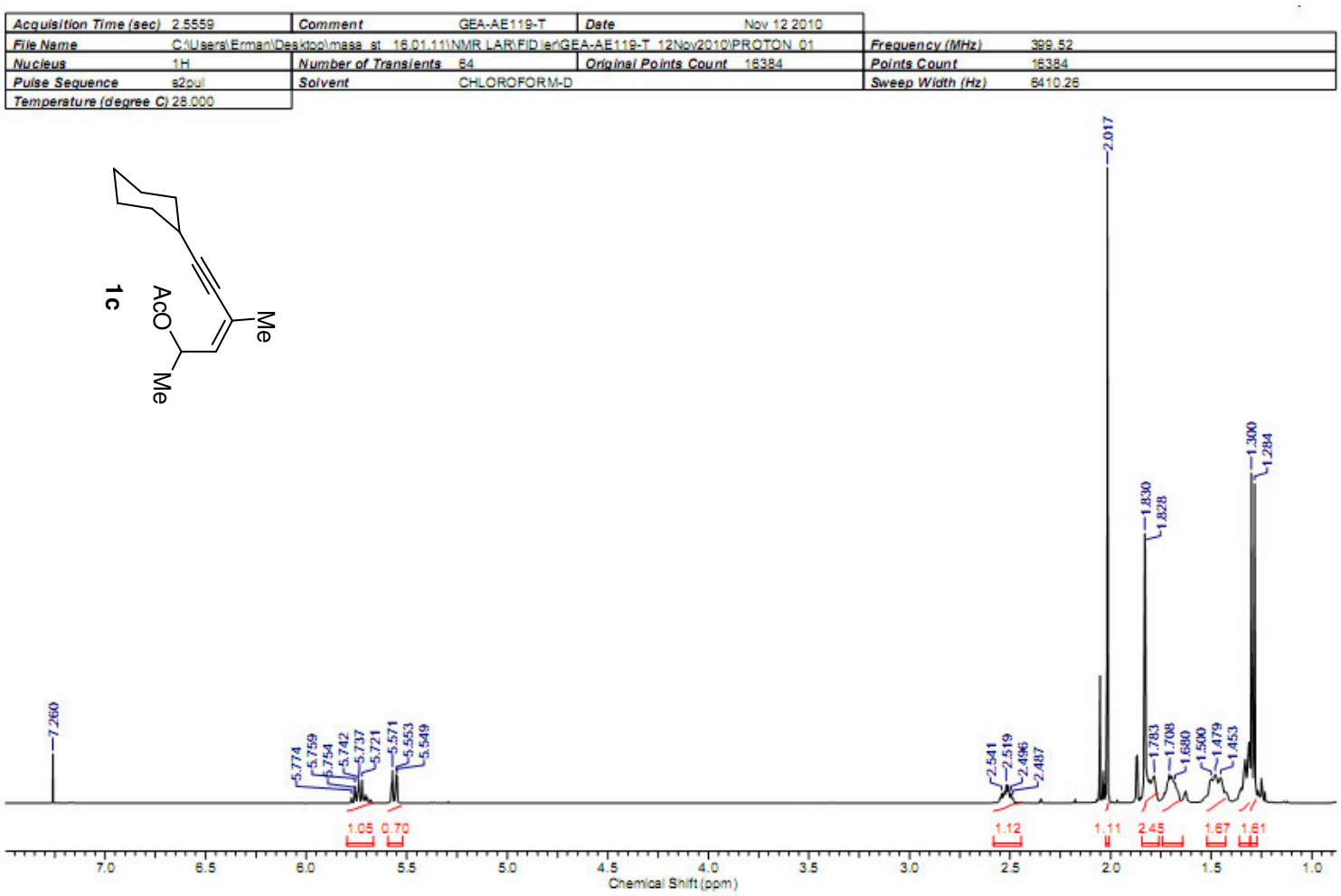

Figure A.5. ^{1}H NMR of (Z)-6-cyclohexyl-4-methylhex-3-en-5-yn-2-yl acetate

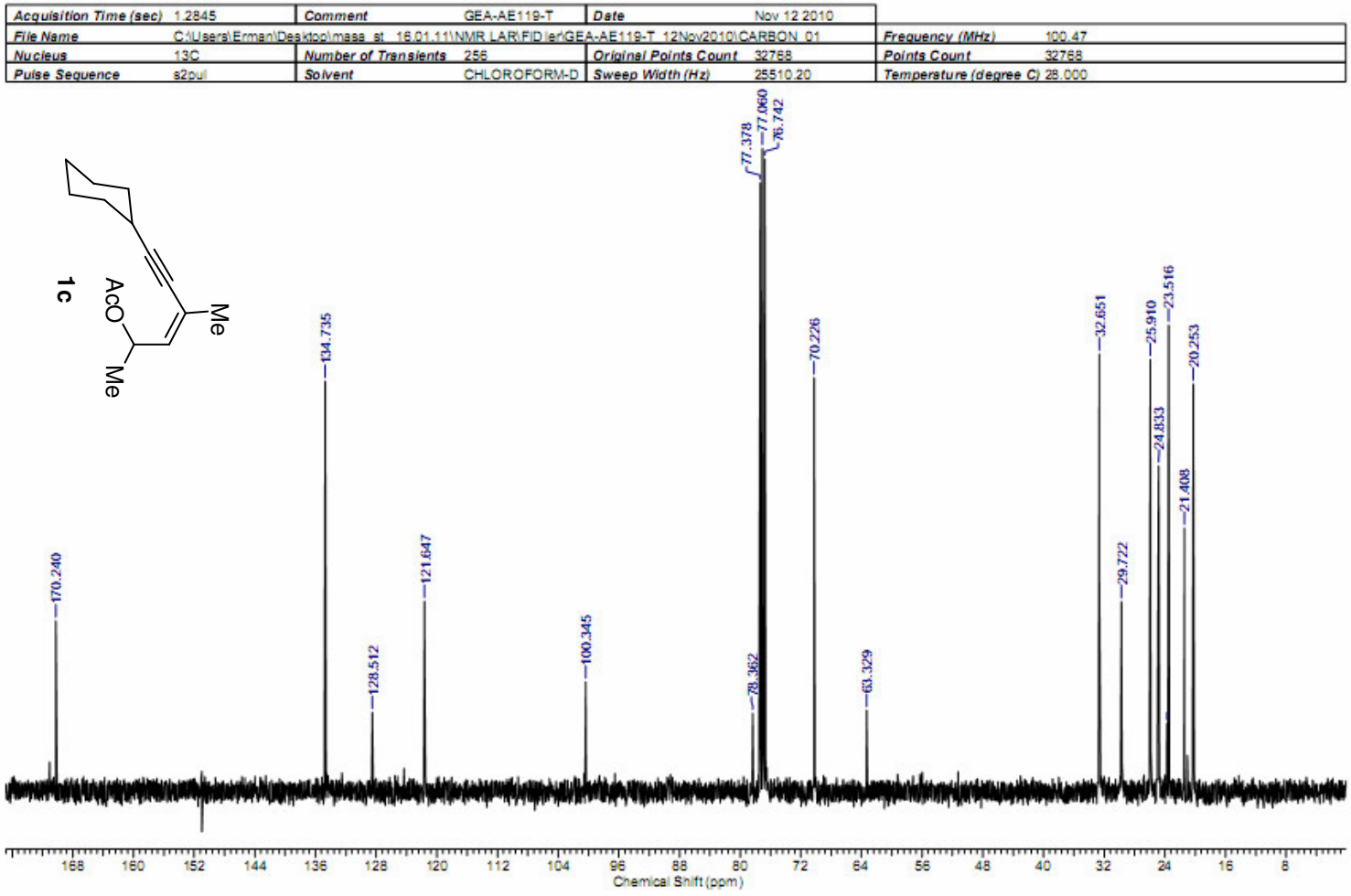

Figure A.6. ^{13}C NMR of (Z)-6-cyclohexyl-4-methylhex-3-en-5-yn-2-yl acetate

Acquisition Time (sec)	3.9846	Comment	5 mm Multinuclear			Date	24 Aug 2010 14:32:32
Date Stamp	24 Aug 2010 14:32:32						
File Name	C:\Users\özge\Desktop\LA 2010\LA NMR FID VE COZUMLERI AGUSTOS 2010\REACTANT\OAAE78\OAAE78_010000\fid						
Frequency (MHz)	400.13	Nucleus	1H	Number of Transients	16	Origin	spect
Original Points Count	32768	Owner	guest	Points Count	32768	Pulse Sequence	zg30
Receiver Gain	143.70	SW(cyclical) (Hz)	8223.68	Solvent	BENZENE-d6	Spectrum Offset (Hz)	2426.1328
Sweep Width (Hz)	8223.43	Temperature (degree C)	27.000				

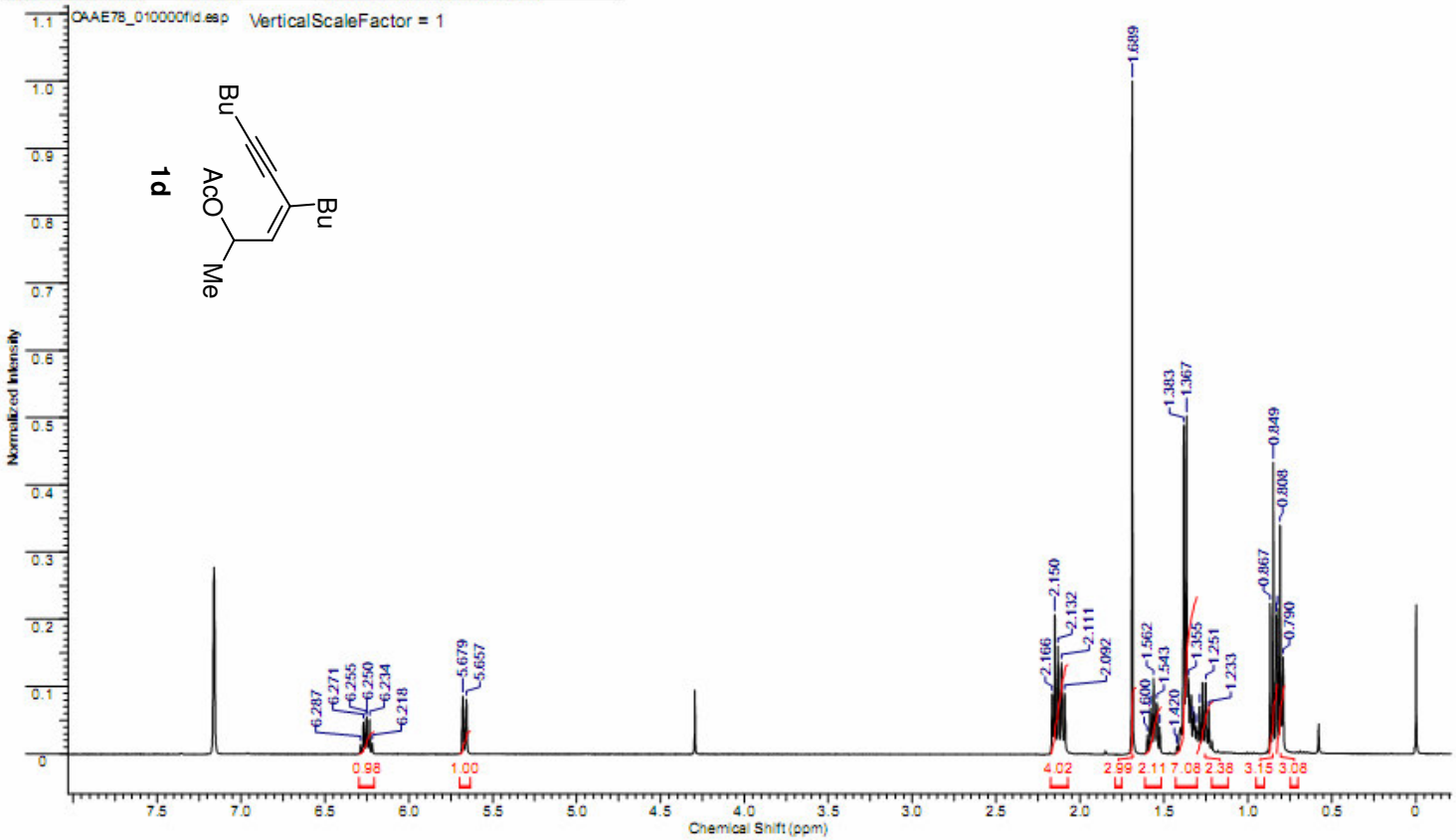

Figure A.7. ^{1}H NMR of (Z)-4-butyldec-3-en-5-yn-2-yl acetate

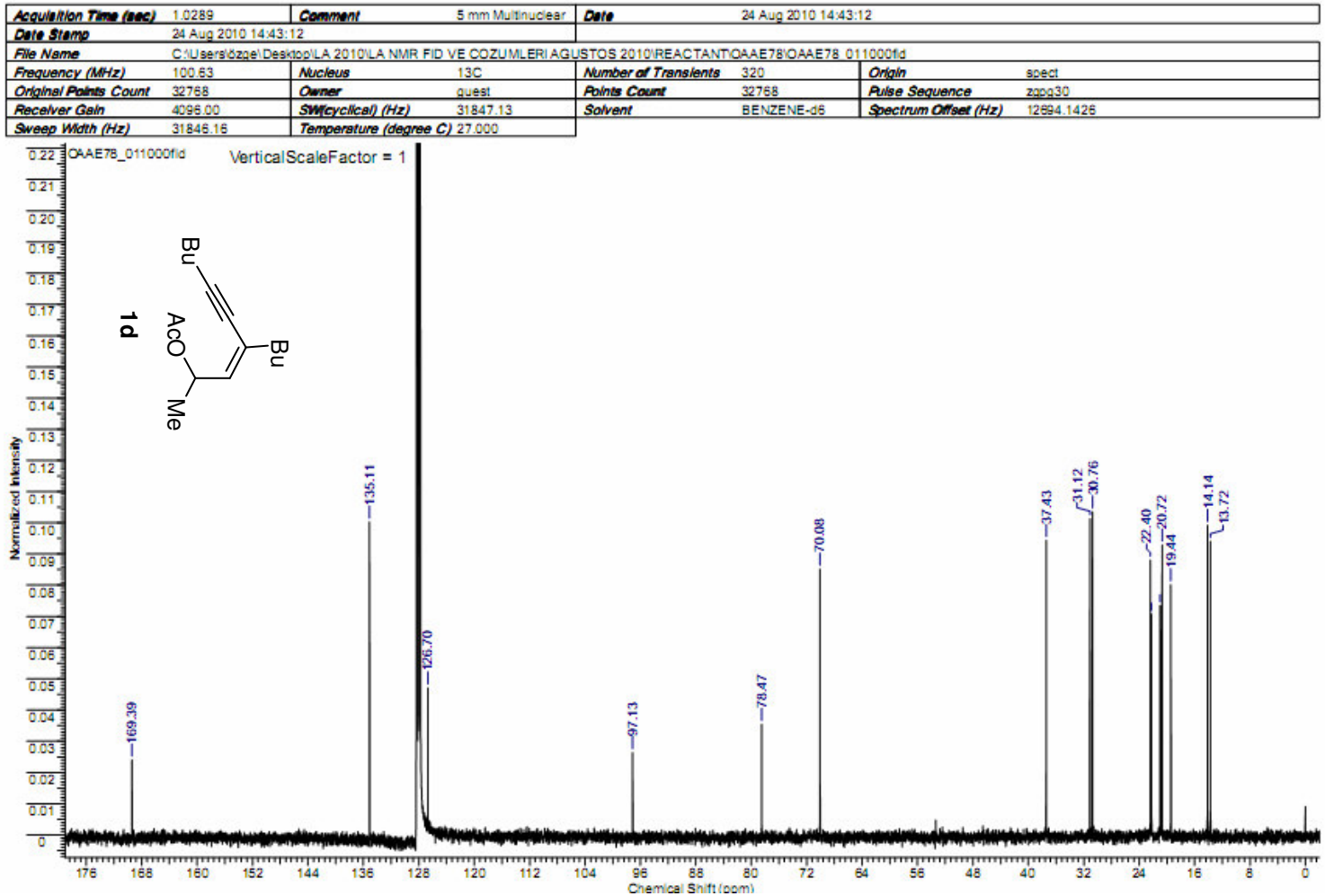

Figure A.8. ^{13}C NMR of (Z)-4-butyldec-3-en-5-yn-2-yl acetate

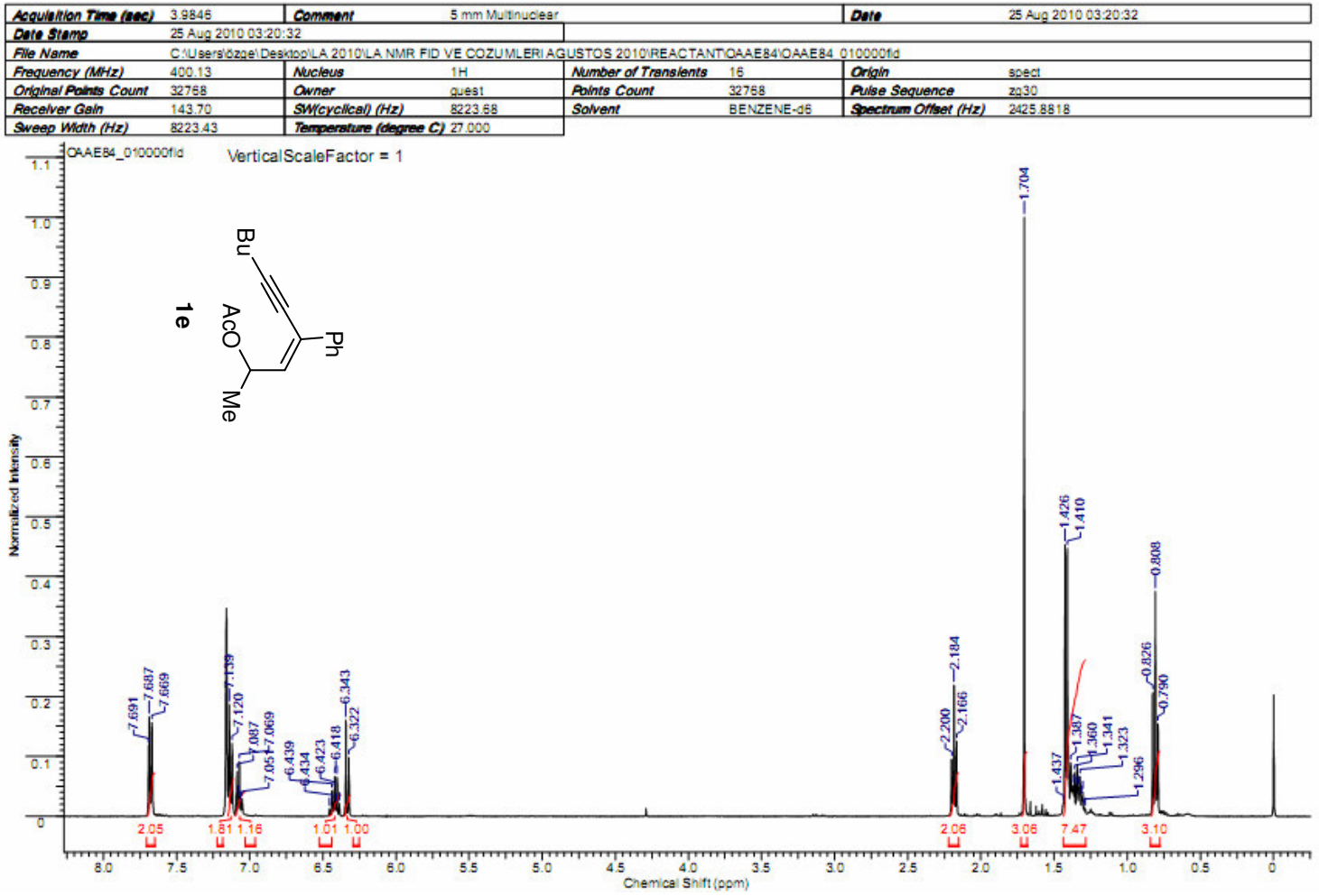

Figure A.9. ^{1}H NMR of (Z)-4-phenyldec-3-en-5-yn-2-yl acetate

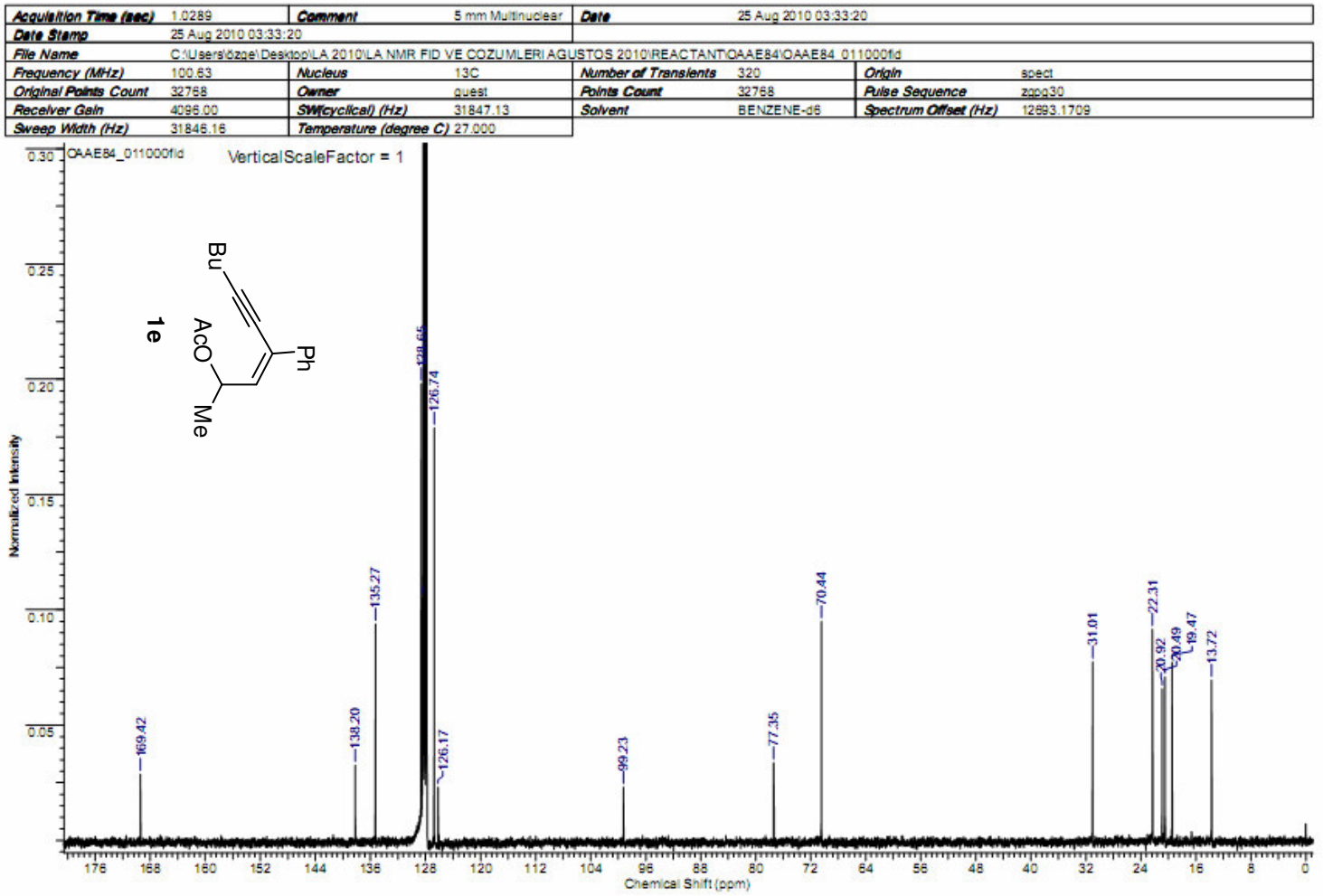

Figure A.10. ^{1}H NMR of (Z)-4-phenyldec-3-en-5-yn-2-yl acetate

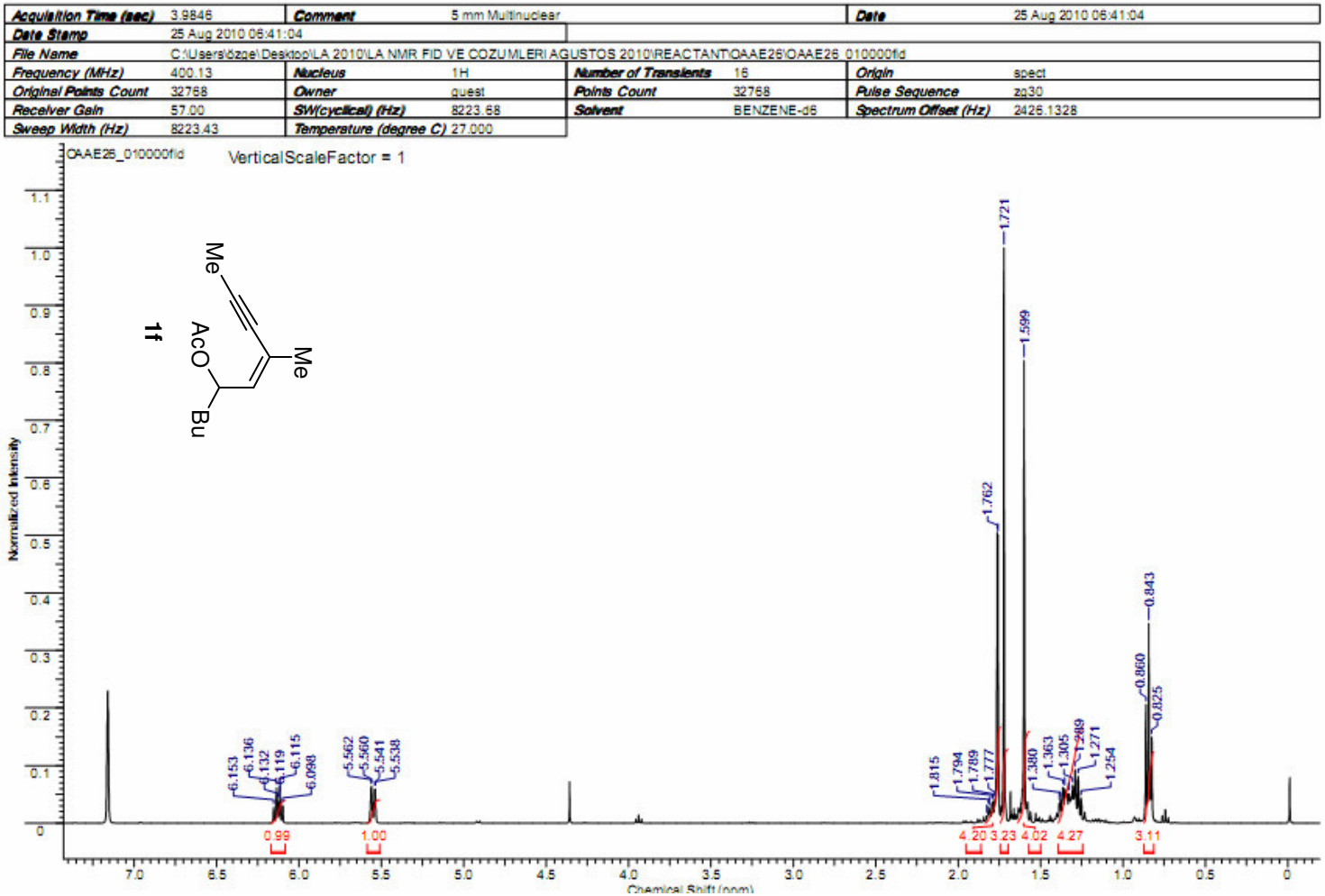

Figure A.11. ^{1}H NMR of (*Z*)-7-methyldec-6-en-8-yn-5-yl acetate

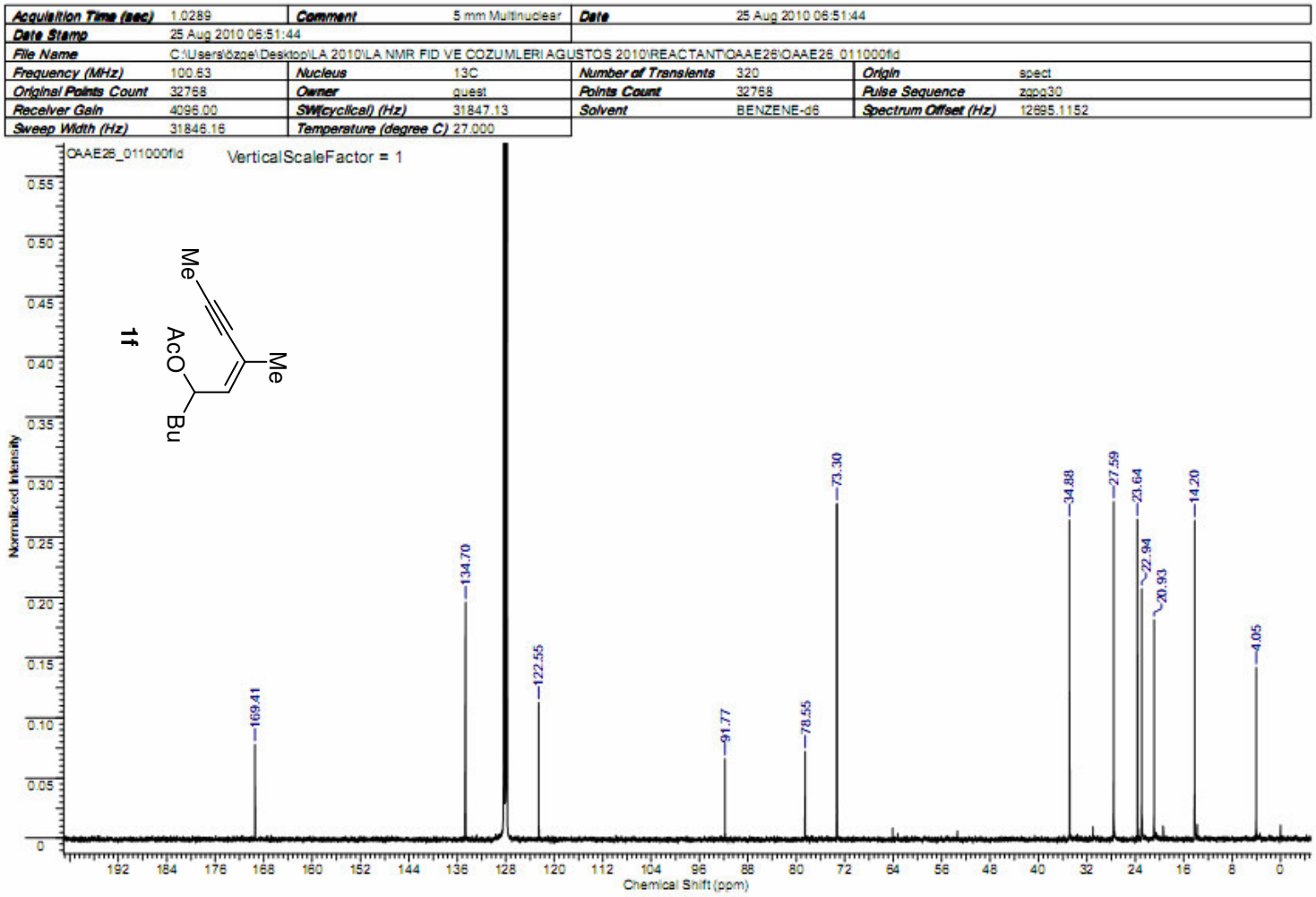

Figure A.12. ^{13}C NMR of (*Z*)-7-methyldec-6-en-8-yn-5-yl acetate

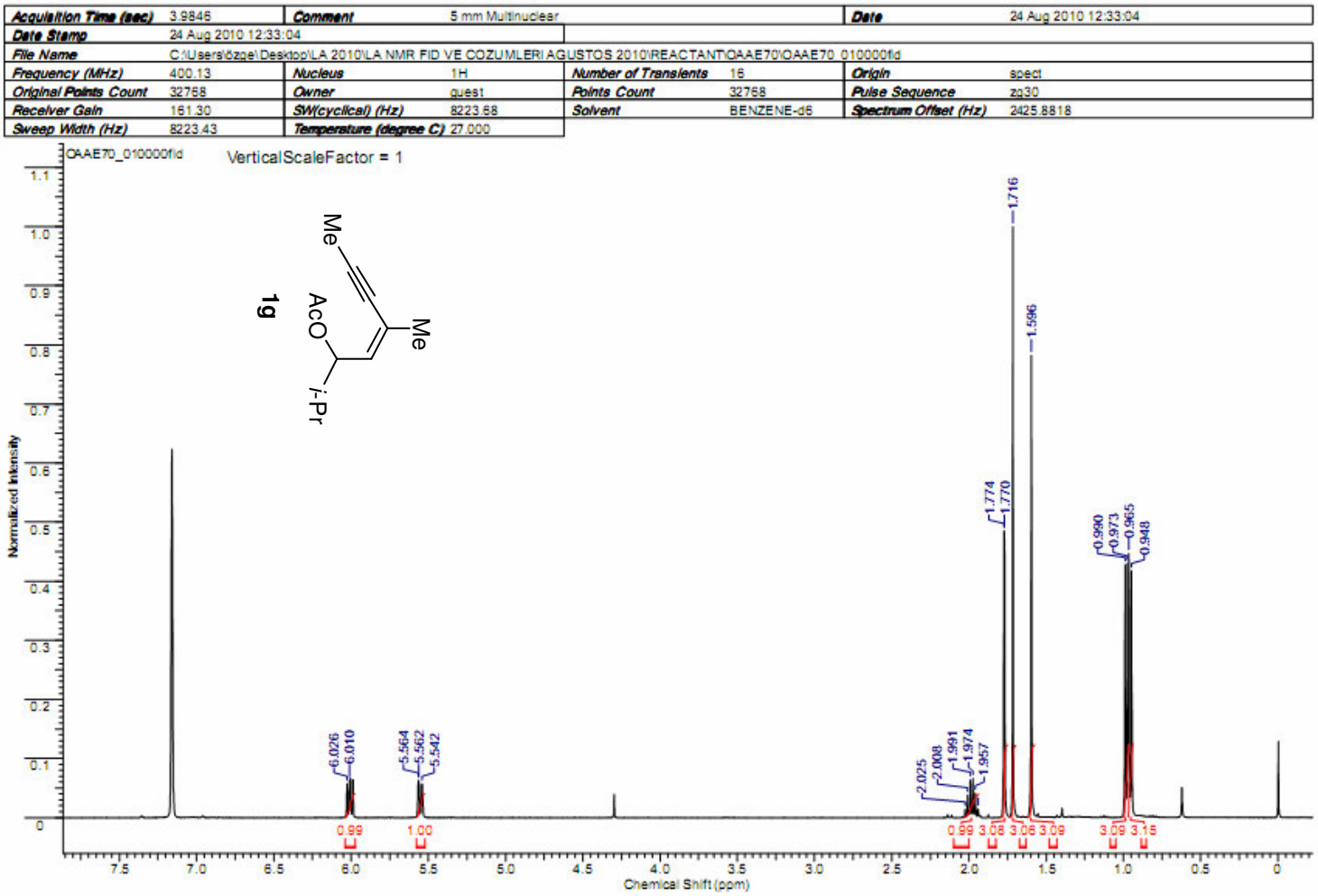

Figure A.13. ^{1}H NMR of (*Z*)-2,5-dimethyloct-4-en-6-yn-3-yl acetate

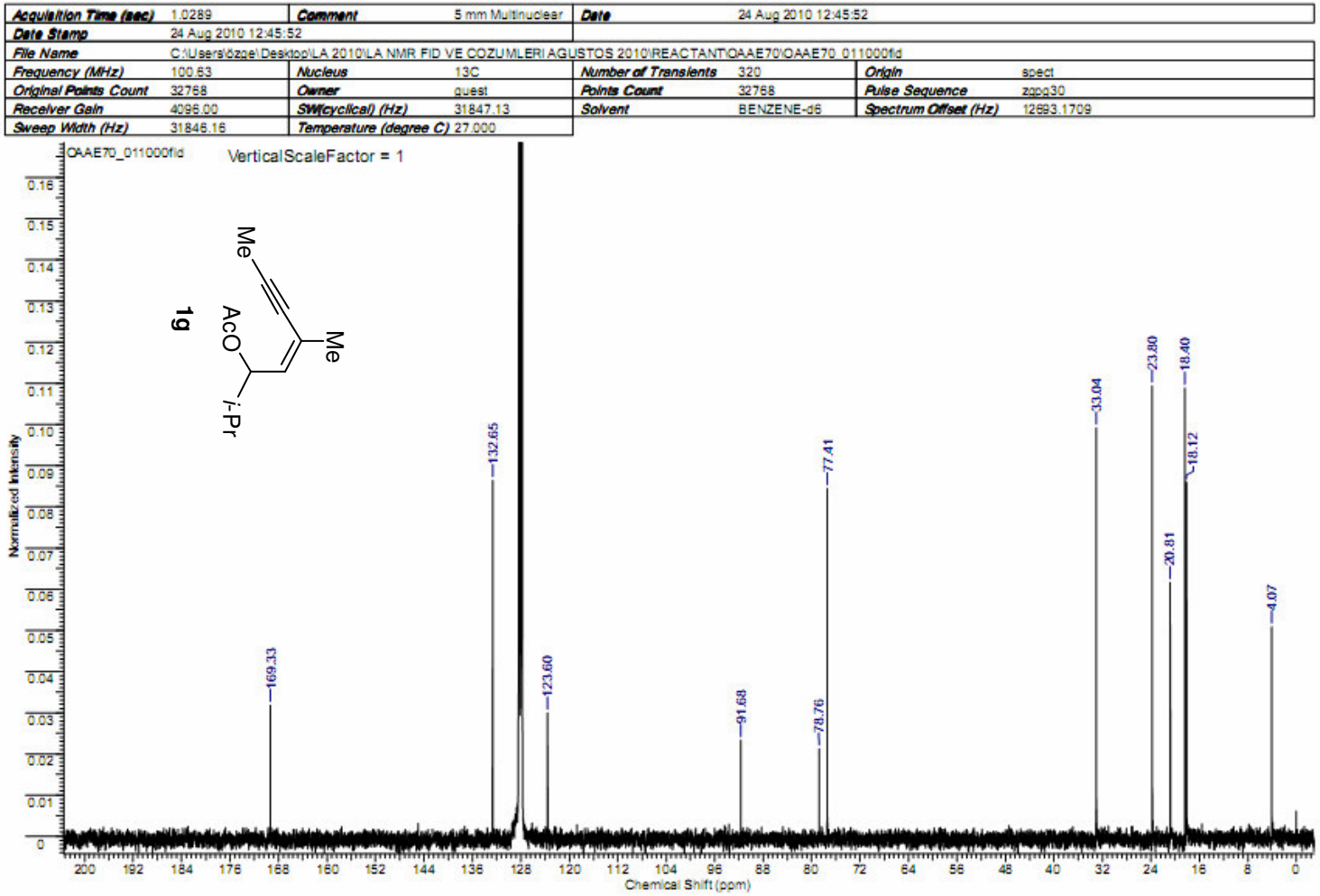

Figure A.14. ^{13}C NMR of (*Z*)-2,5-dimethyloct-4-en-6-yn-3-yl acetate

Acquisition Time (sec)	3.9846	Comment	5 mm Multinuclear			Date	25 Aug 2010 07:00:16
Date Stamp	25 Aug 2010 07:00:16						
File Name	C:\Users\özge\Desktop\LA 2010\LA NMR FID VE COZUMLERI AGUSTOS 2010\REACTANT\OAAE28\OAAE28_010000fid						
Frequency (MHz)	400.13	Nucleus	1H	Number of Transients	16	Origin	spect
Original Points Count	32768	Owner	guest	Points Count	32768	Pulse Sequence	zg30
Receiver Gain	80.60	SW(cyclical) (Hz)	8223.68	Solvent	BENZENE-d6	Spectrum Offset (Hz)	2426.1328
Sweep Width (Hz)	8223.43	Temperature (degree C)	27.000				

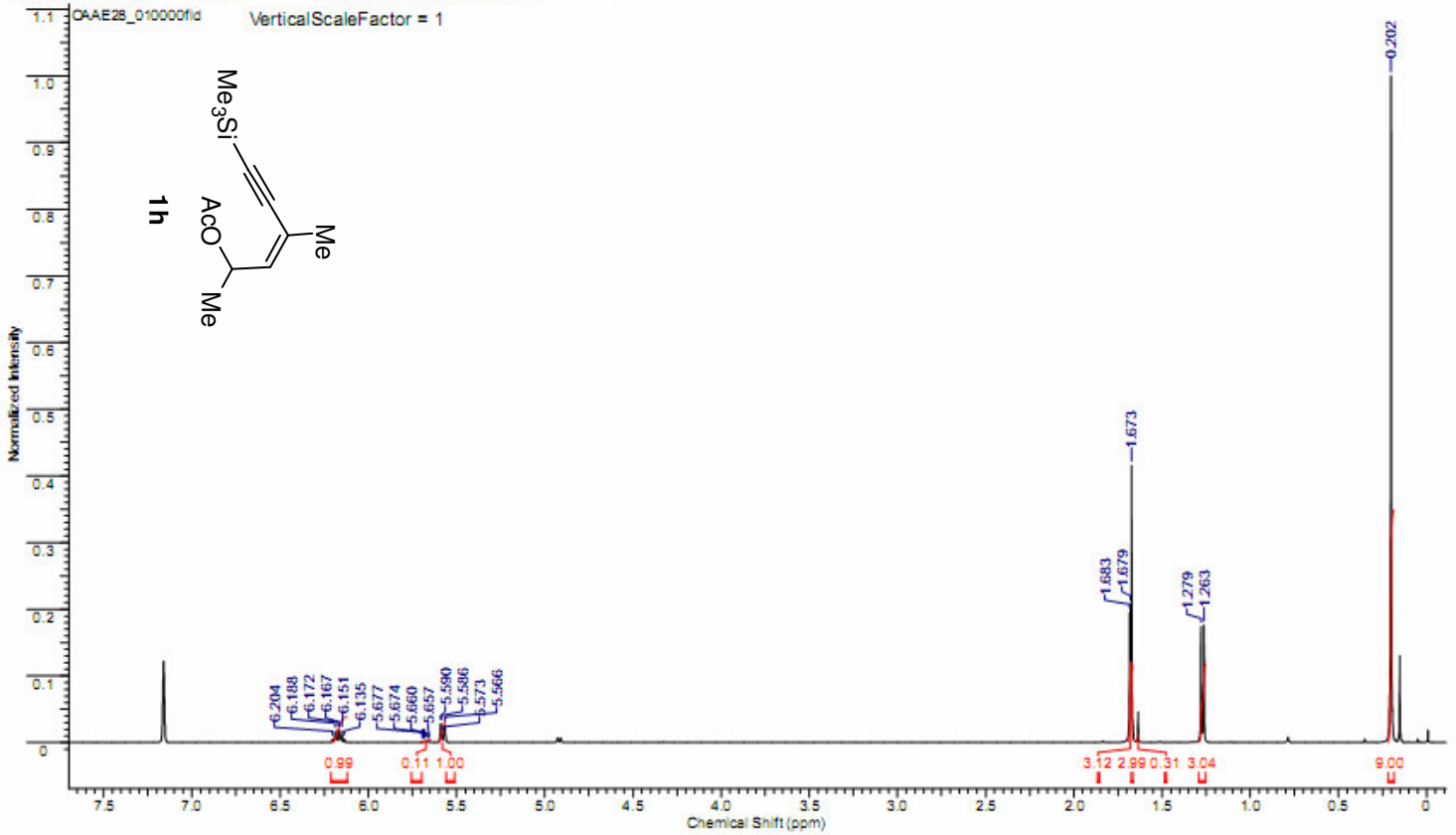

Figure A.15. ^{1}H NMR of (Z)-4-methyl-6-(trimethylsilyl)hex-3-en-5-yn-2-yl acetate

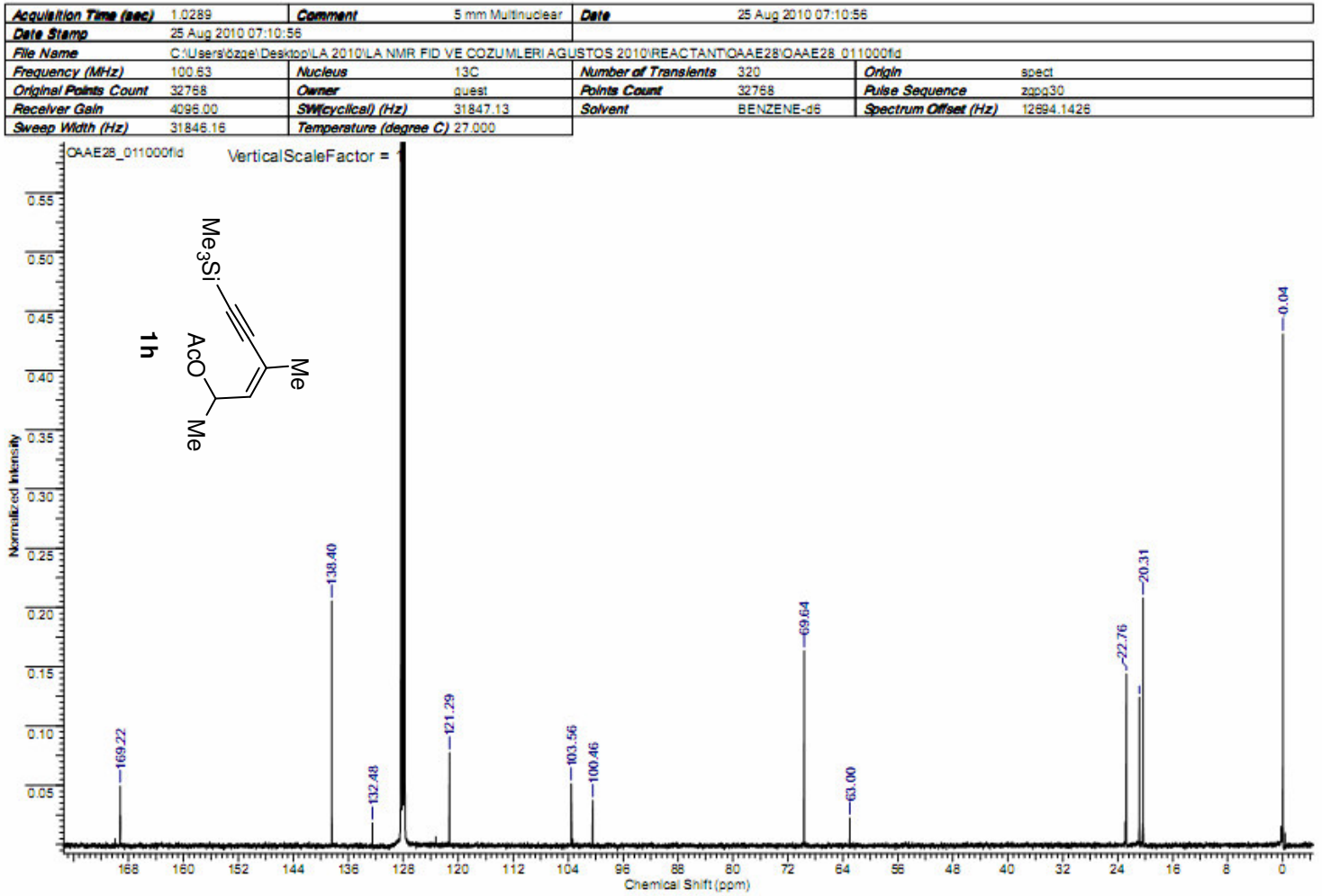

Figure A.16. ^{13}C NMR of (Z)-4-methyl-6-(trimethylsilyl)hex-3-en-5-yn-2-yl acetate

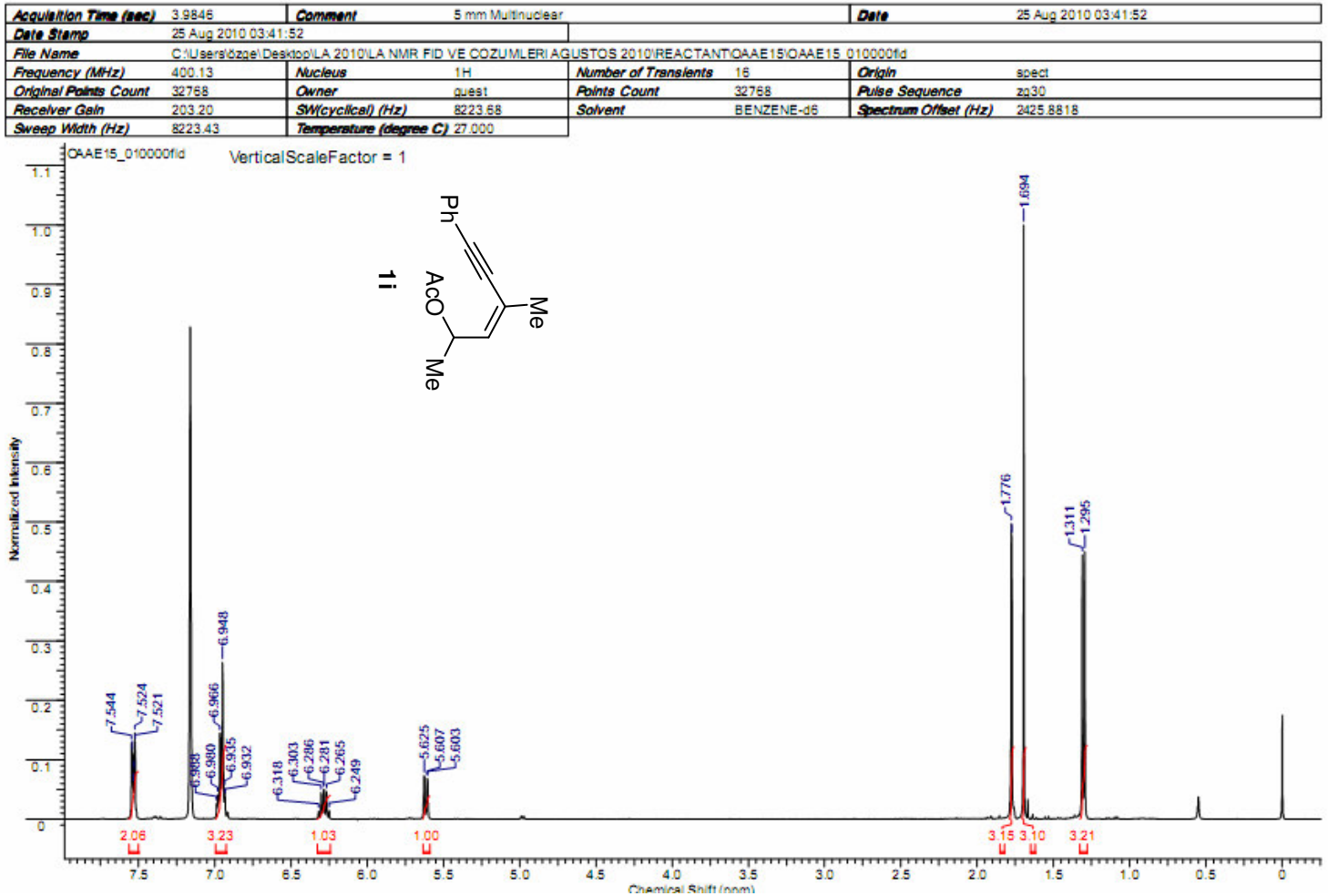

Figure A.17. ^{1}H NMR of (Z)-4-methyl-6-phenylhex-3-en-5-yn-2-yl acetate

Acquisition Time (sec)	1.0289	Comment	5 mm Multinuclear	Date	25 Aug 2010 03:52:32		
Date Stamp	25 Aug 2010 03:52:32						
File Name	C:\Users\özge\Desktop\LA 2010\LA NMR FID VE COZUMLERI AGUSTOS 2010\REACTANT\OAAE15\OAAE15_011000fid						
Frequency (MHz)	100.63	Nucleus	13C	Number of Transients	320	Origin	spect
Original Points Count	32768	Owner	guest	Points Count	32768	Pulse Sequence	zgpg30
Receiver Gain	4096.00	SW(cyclical) (Hz)	31847.13	Solvent	BENZENE-d6	Spectrum Offset (Hz)	12693.1709
Sweep Width (Hz)	31846.16	Temperature (degree C)	27.000				

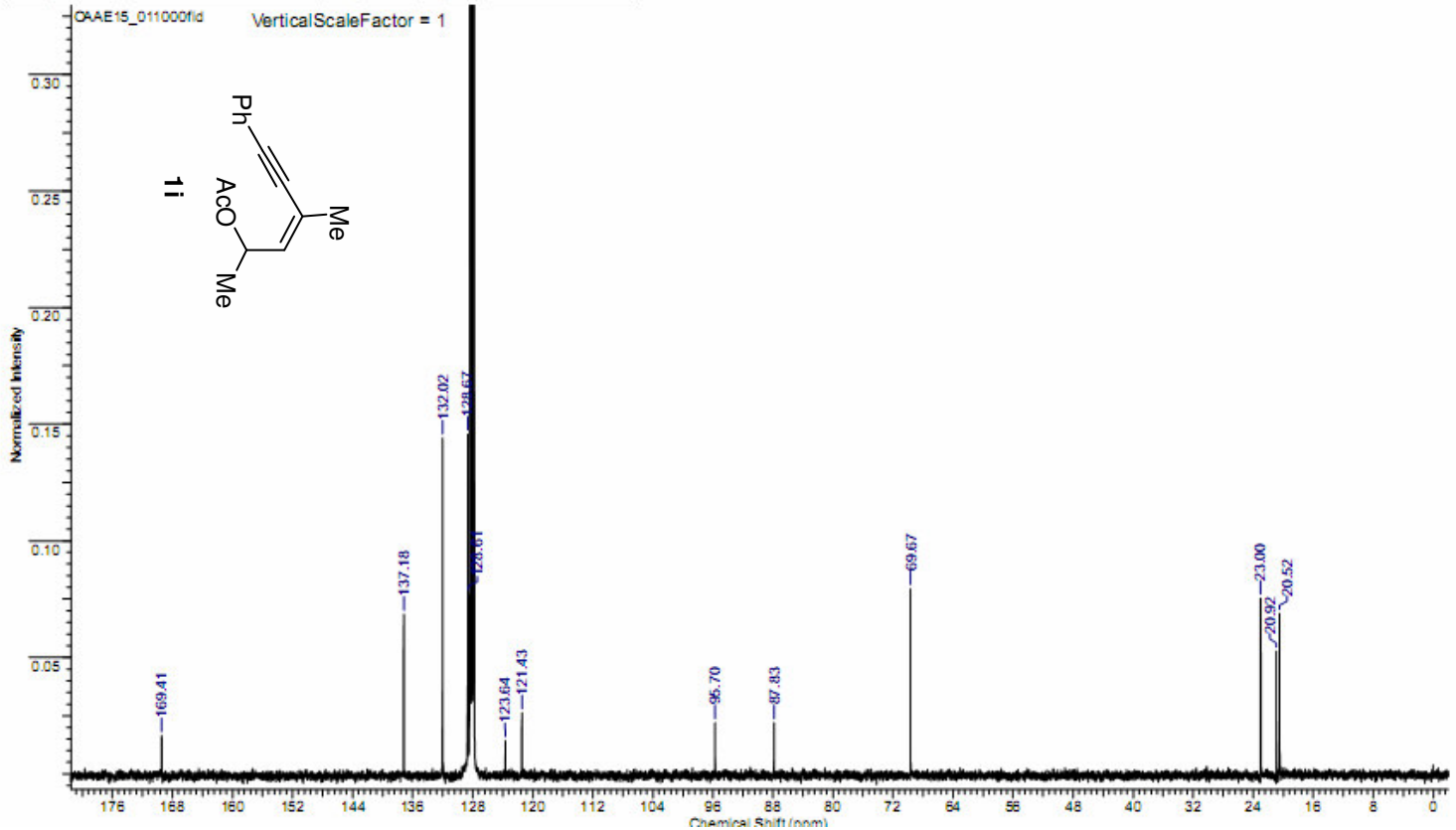

Figure A.18. ^{13}C NMR of (Z)-4-methyl-6-phenylhex-3-en-5-yn-2-yl acetate

Acquisition Time (sec)	3.9846	Comment	5 mm Multinuclear			Date	24 Aug 2010 12:52:16
Date Stamp	24 Aug 2010 12:52:16						
File Name	C:\Users\özge\Desktop\LA 2010\LA NMR FID VE COZUMLERI AGUSTOS 2010\REACTANT\OAAE72\OAAE72_010000fid						
Frequency (MHz)	400.13	Nucleus	1H	Number of Transients	16	Origin	spect
Original Points Count	32768	Owner	guest	Points Count	32768	Pulse Sequence	zg30
Receiver Gain	228.10	SW(cyclical) (Hz)	8223.68	Solvent	BENZENE-d6	Spectrum Offset (Hz)	2425.8818
Sweep Width (Hz)	8223.43	Temperature (degree C)	27.000				

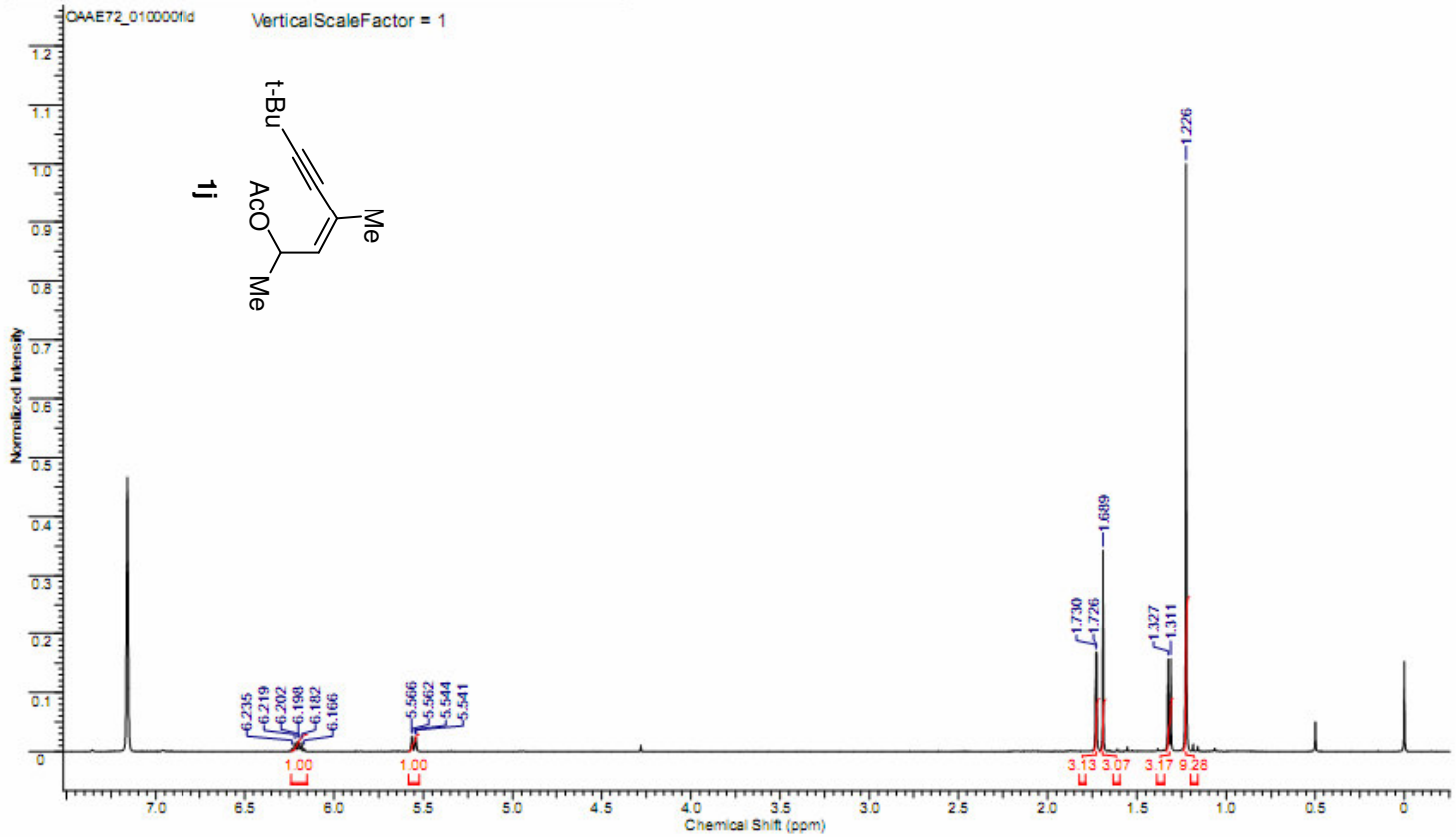

Figure A.19. ^{1}H NMR of (Z)-4,7,7-trimethyloct-3-en-5-yn-2-yl acetate

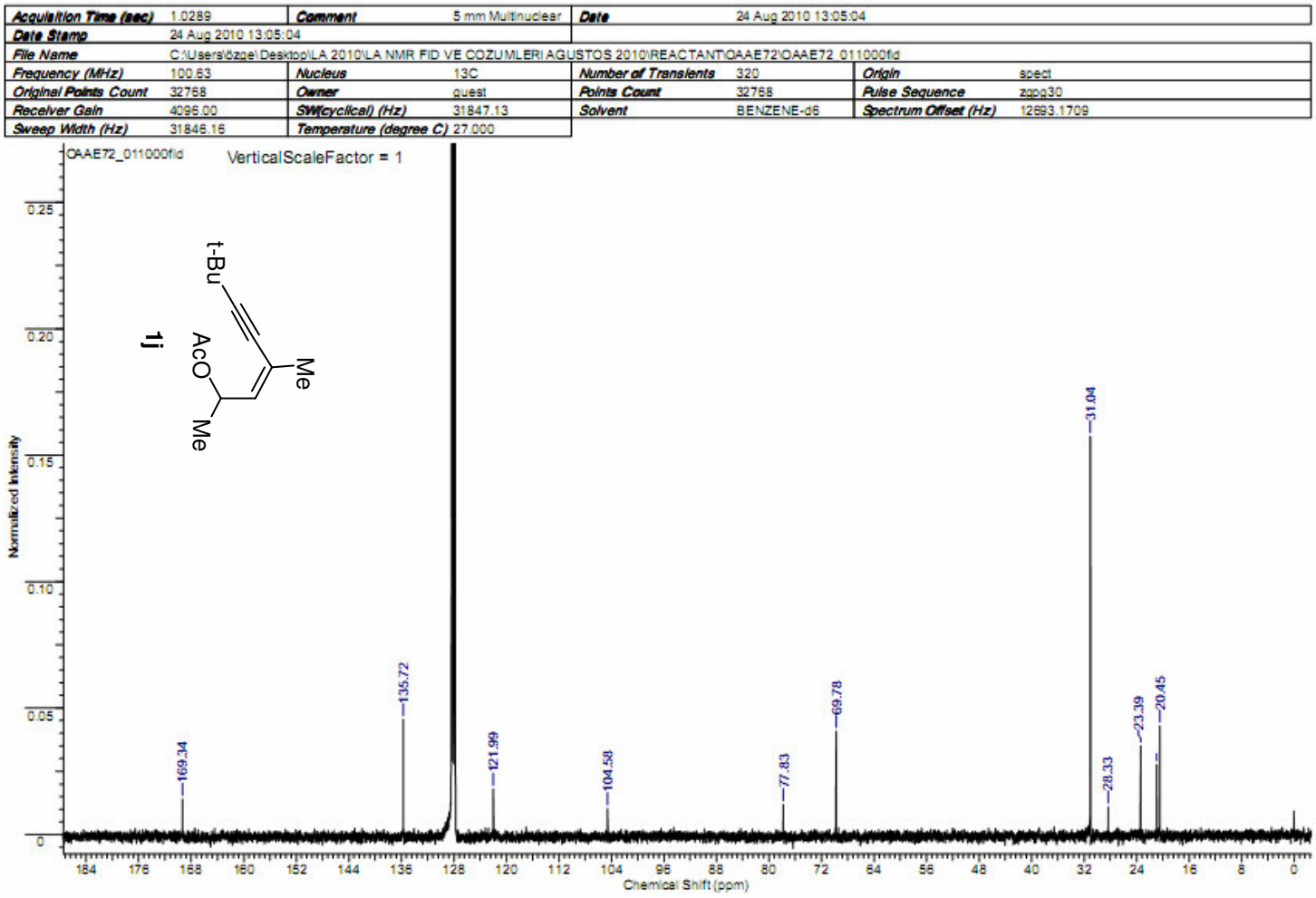

Figure A.20. ^{13}C NMR of (Z)-4,7,7-trimethyloct-3-en-5-yn-2-yl acetate

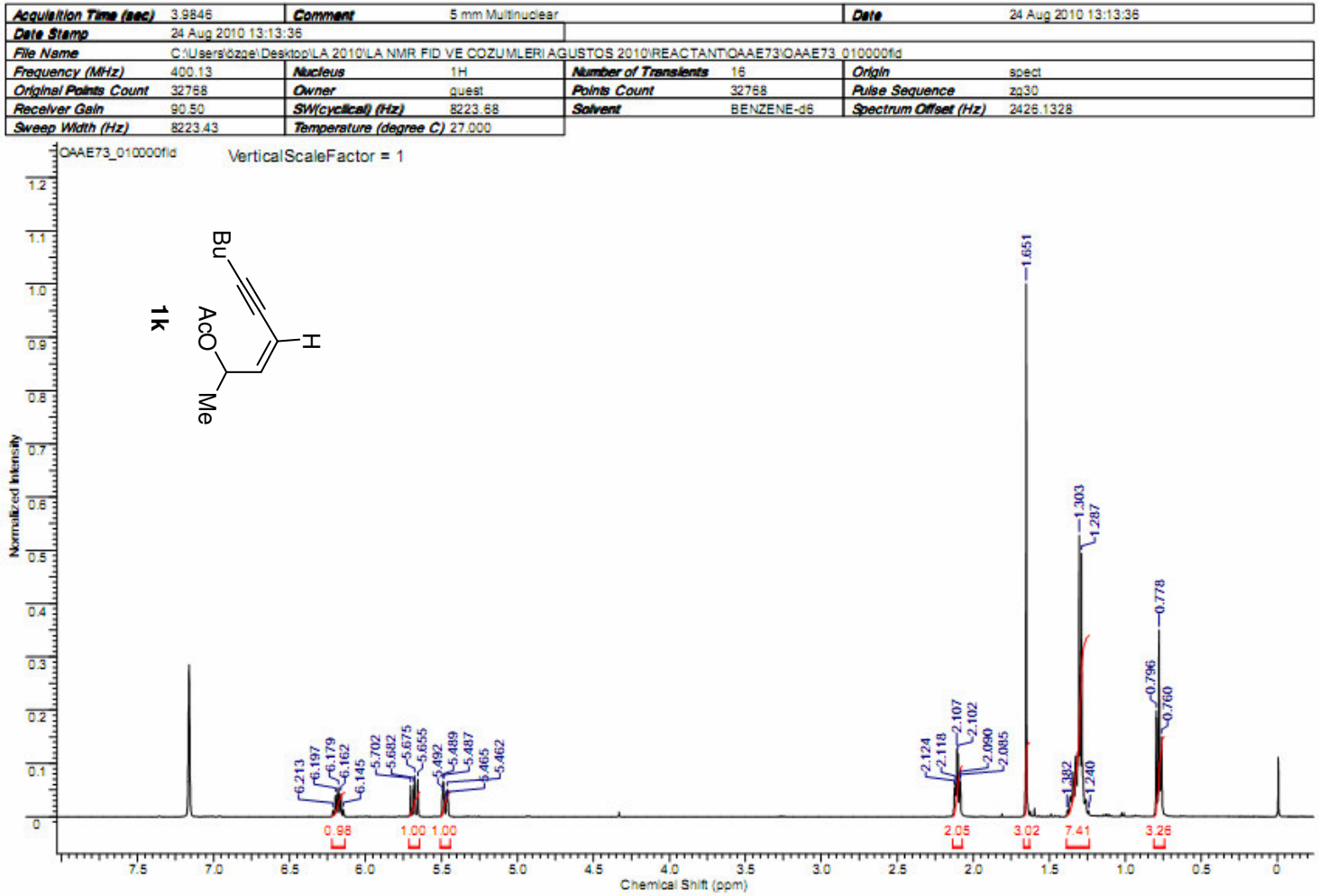

Figure A.21. ^{1}H NMR of (Z)-dec-3-en-5-yn-2-yl acetate

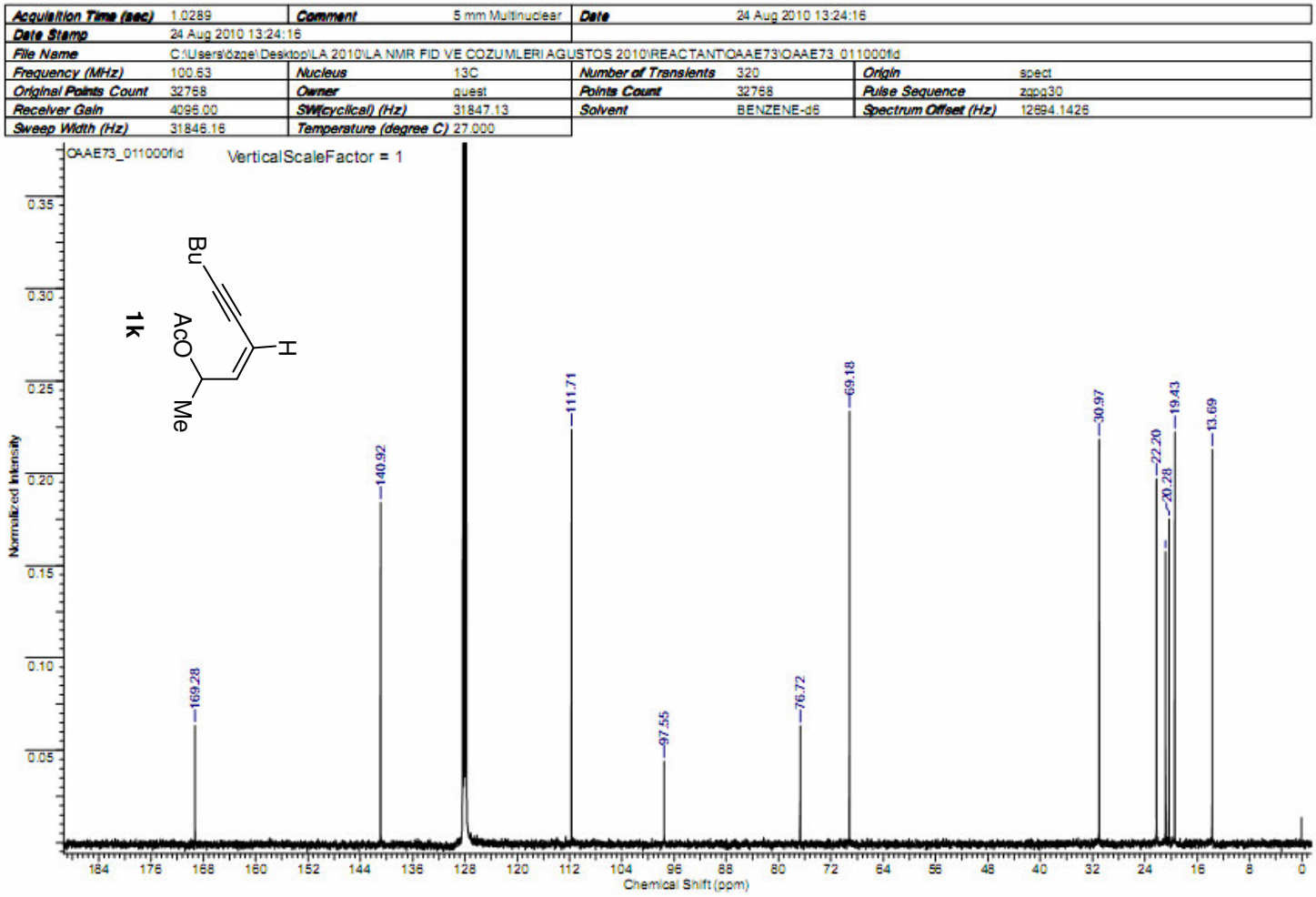

Figure A.22. ^{13}C NMR of (Z)-dec-3-en-5-yn-2-yl acetate

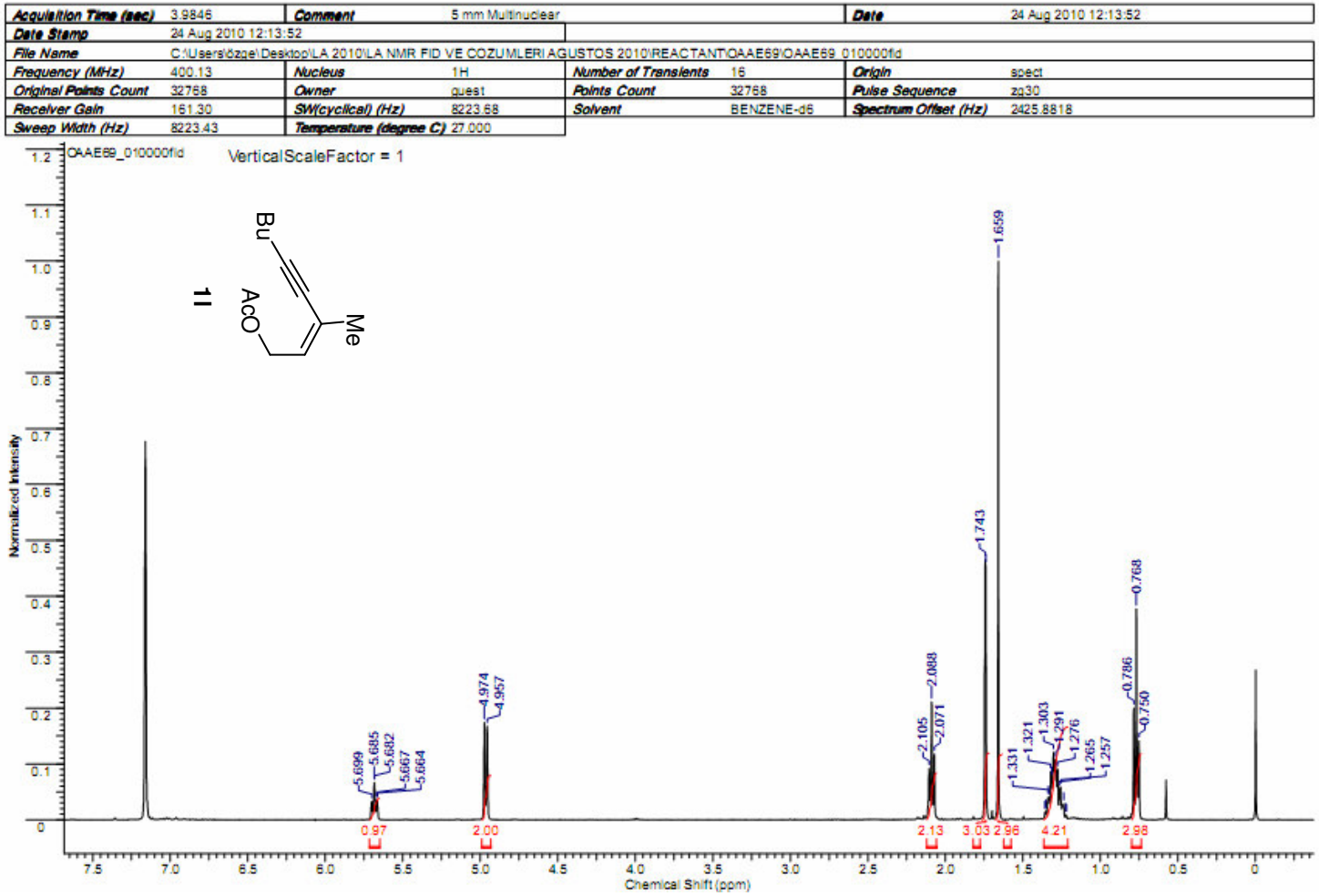

Figure A.23. ^{1}H NMR of (Z)-3-methylnon-2-en-4-ynyl acetate

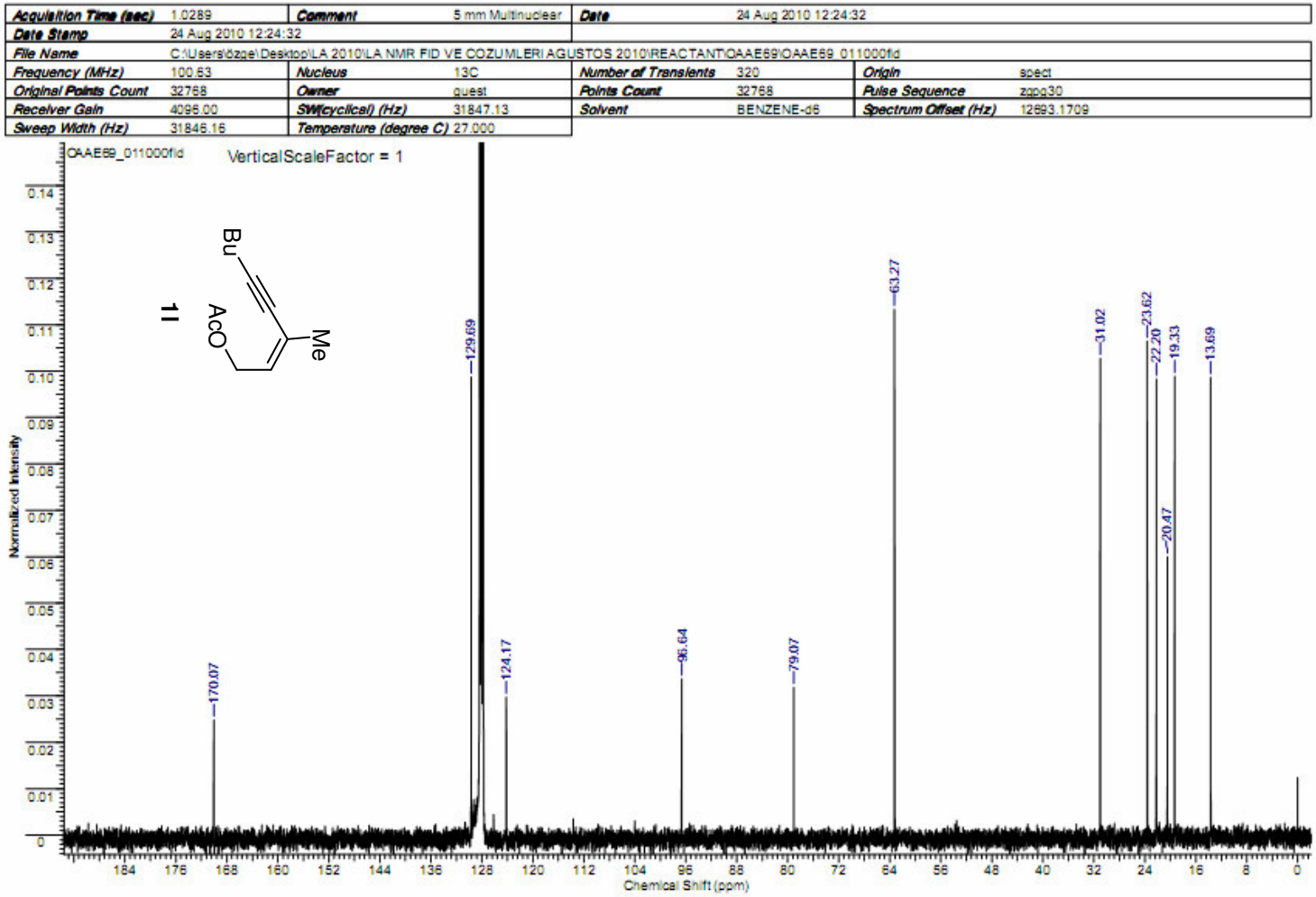

Figure A.24. ^{13}C NMR of (Z)-3-methylnon-2-en-4-ynyl acetate

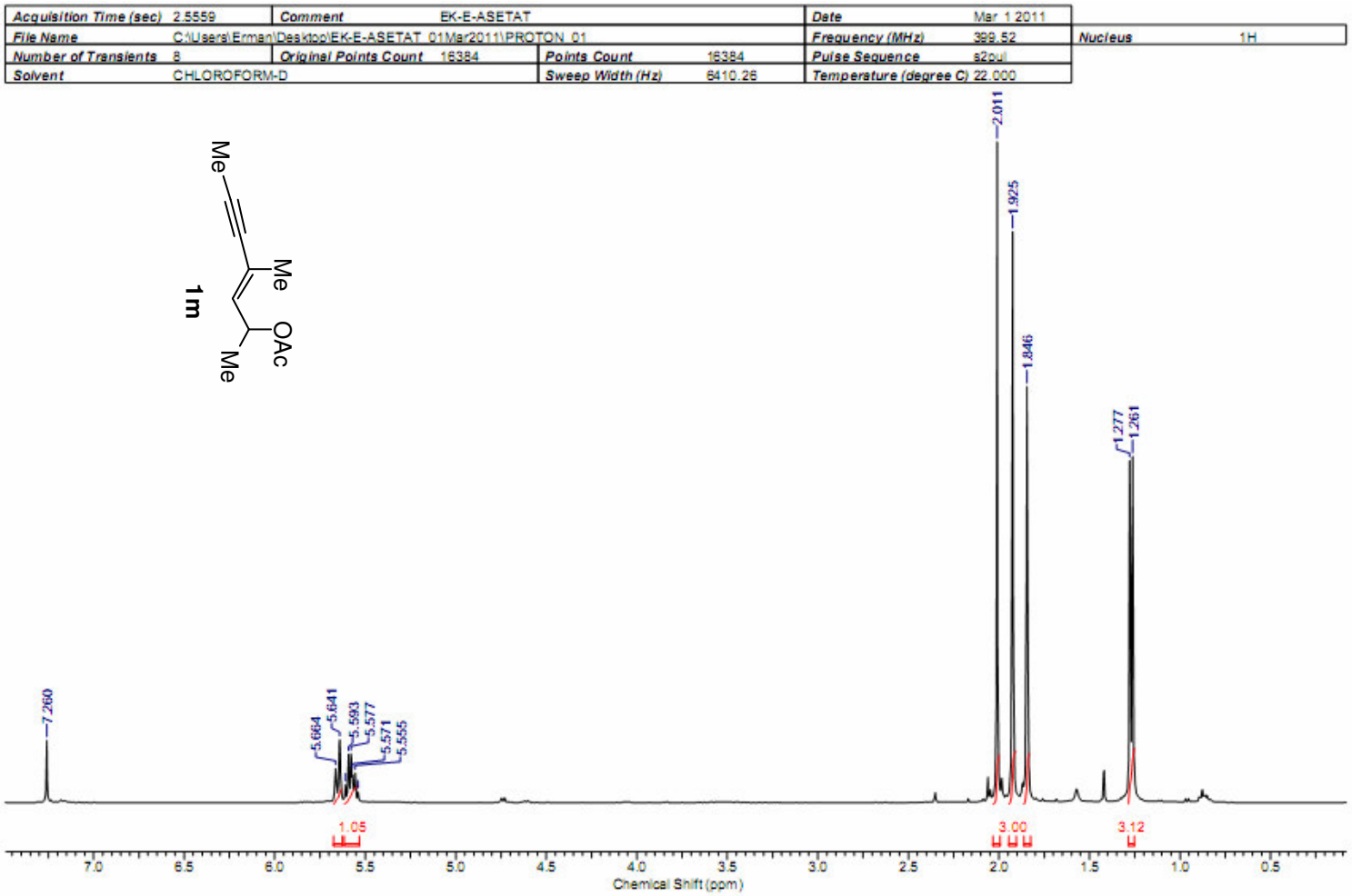

Figure A.25. ^{1}H NMR of (*E*)-4-methylhept-3-en-5-yn-2-yl acetate

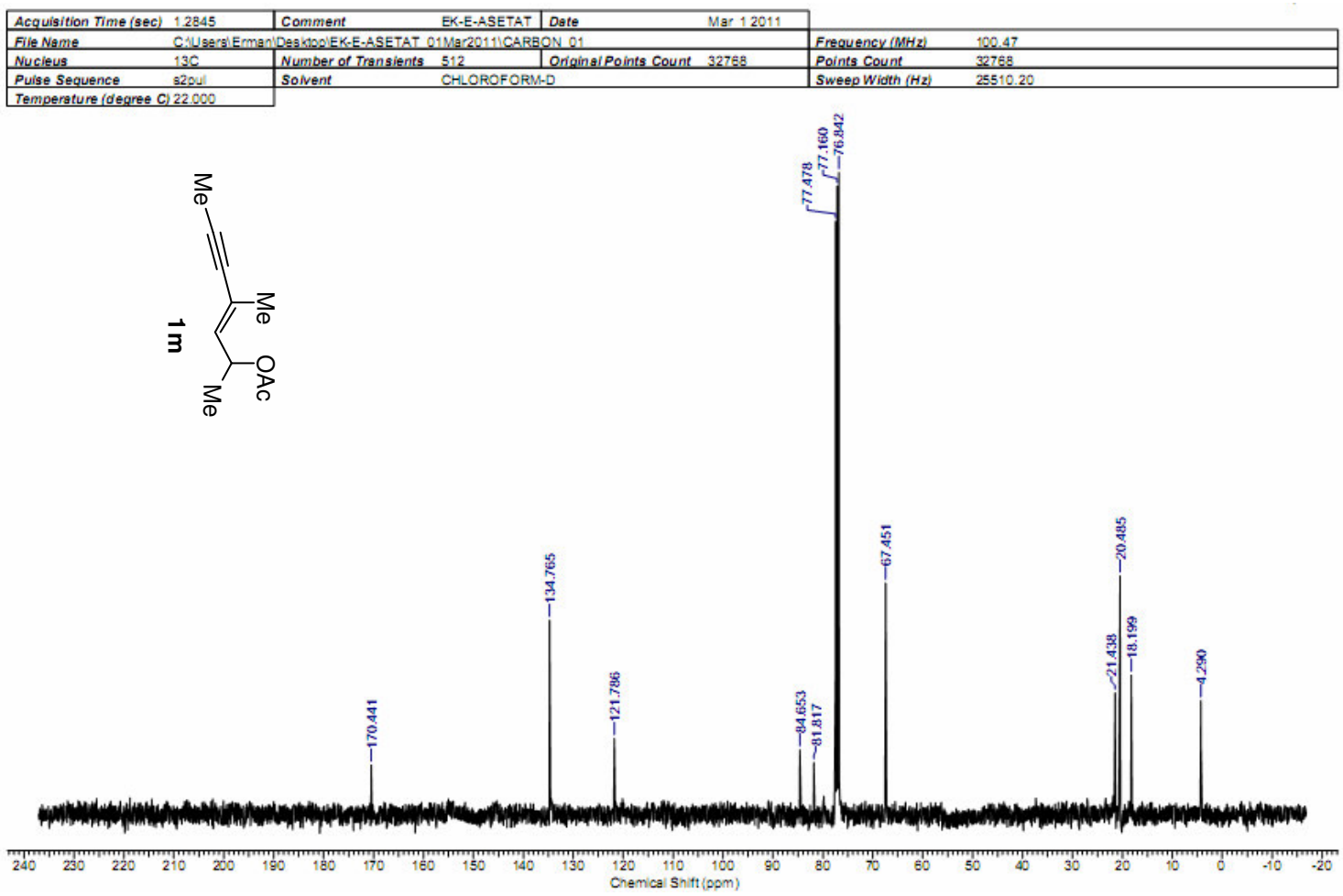

Figure A.26. ^{13}C NMR of (*E*)-4-methylhept-3-en-5-yn-2-yl acetate

APPENDIX B

MASS SPECTRUMS OF REACTANTS

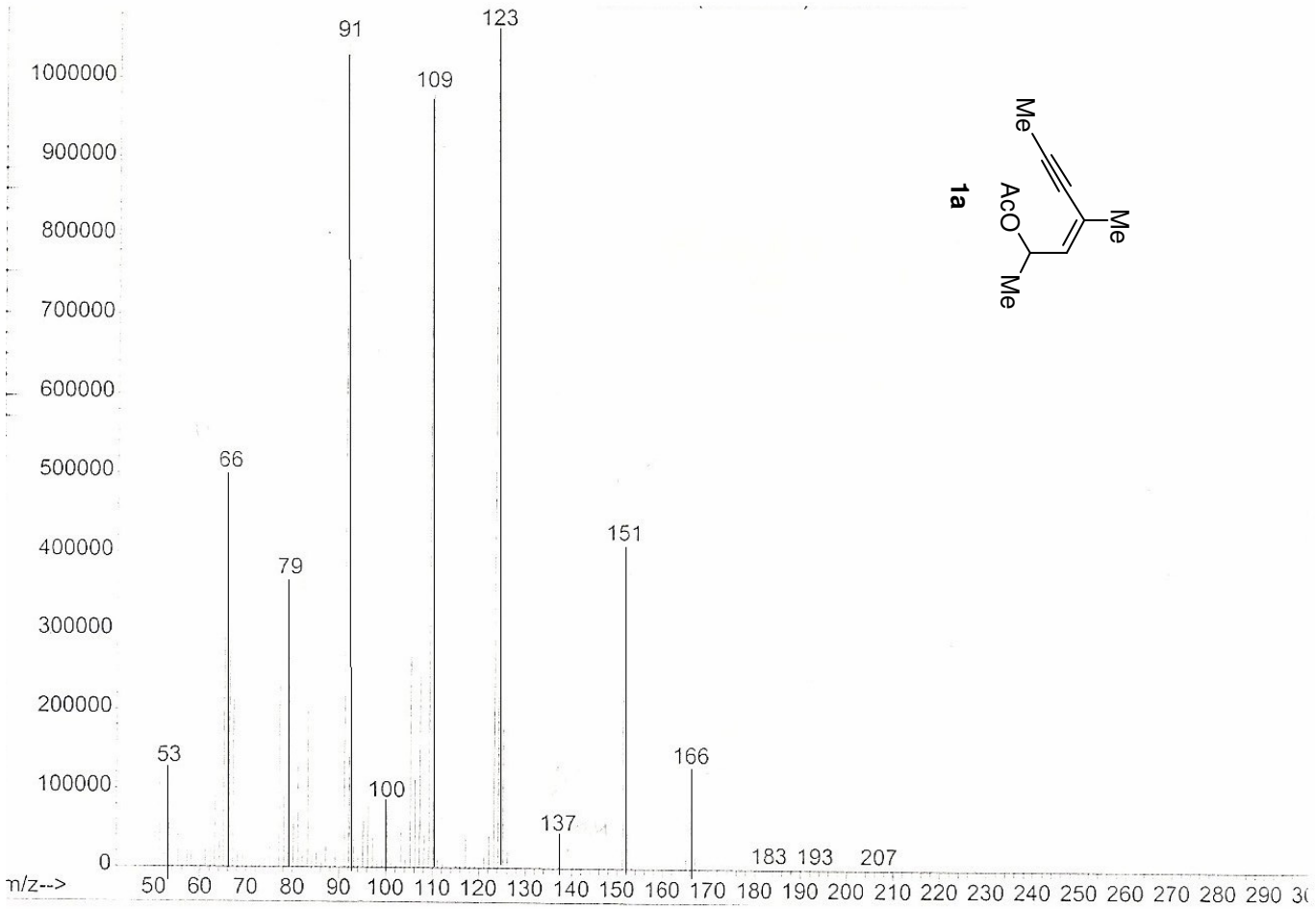

Figure B.1. Mass Spectrum of (*Z*)-4-methylhept-3-en-5-yn-2-yl acetate

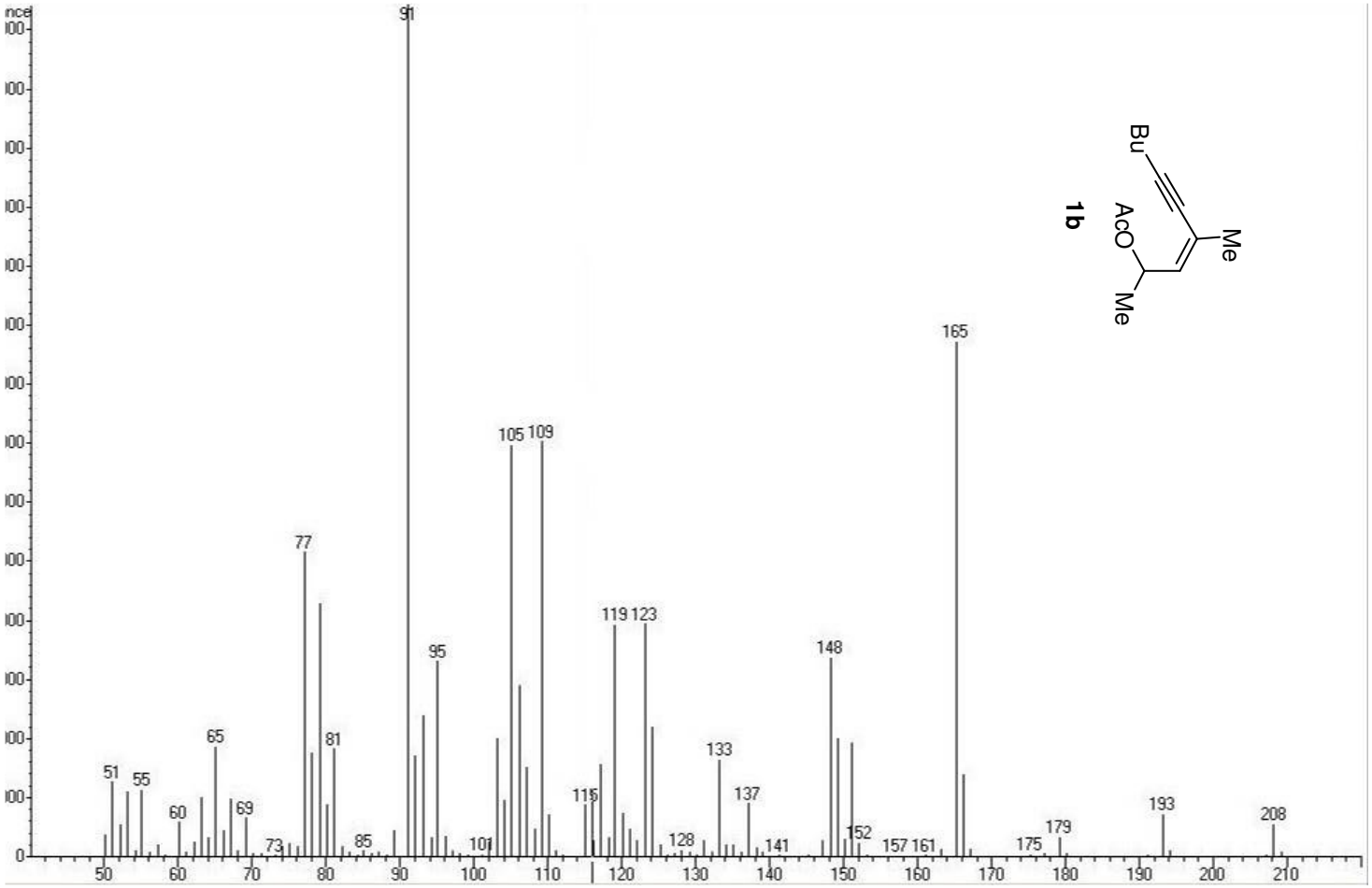

Figure B.2. Mass Spectrum of (Z)-4-methyldec-3-en-5-yn-2-yl acetate

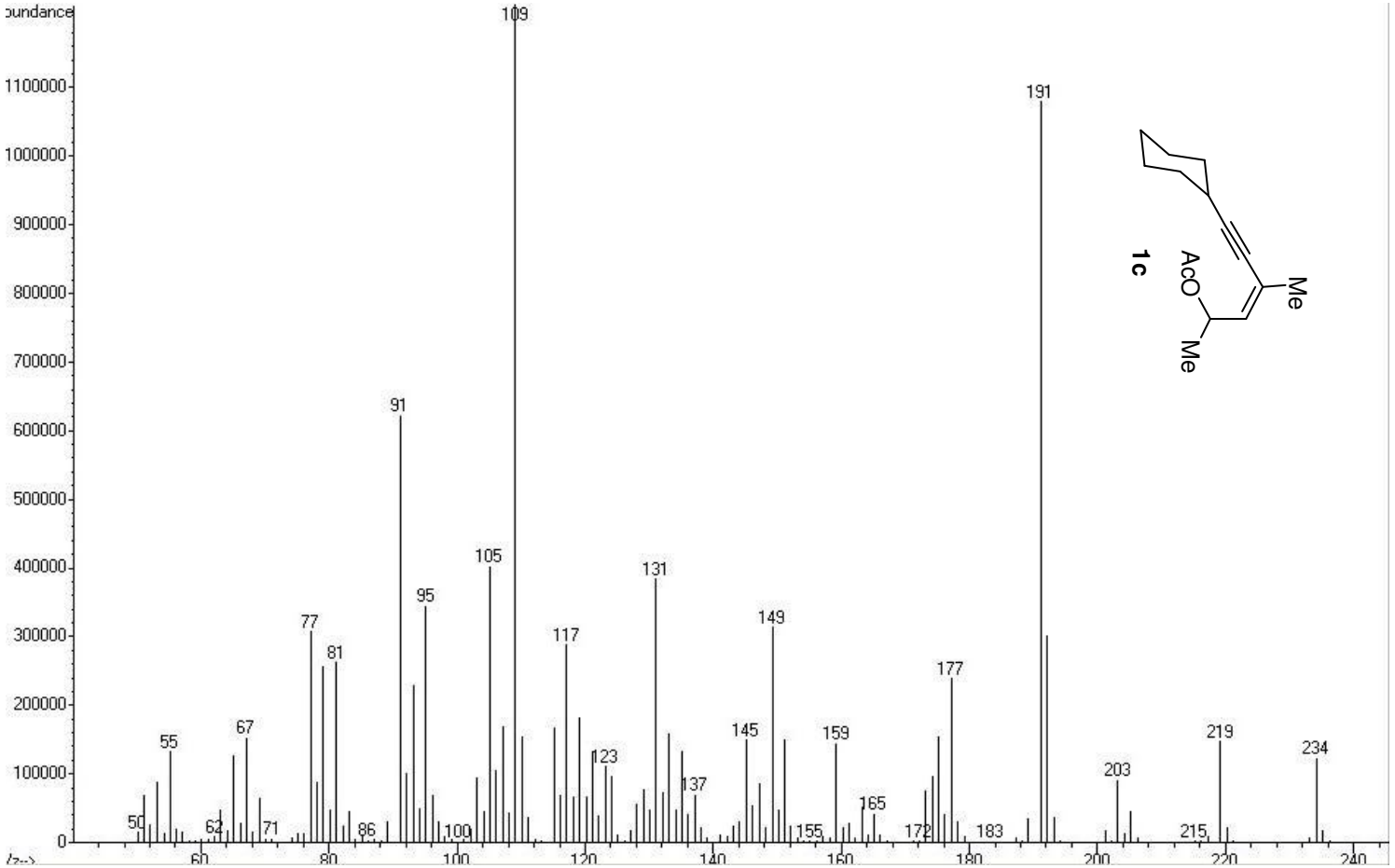

Figure B.3. Mass Spectrum of (Z)-6-cyclohexyl-4-methylhex-3-en-5-yn-2-yl acetate

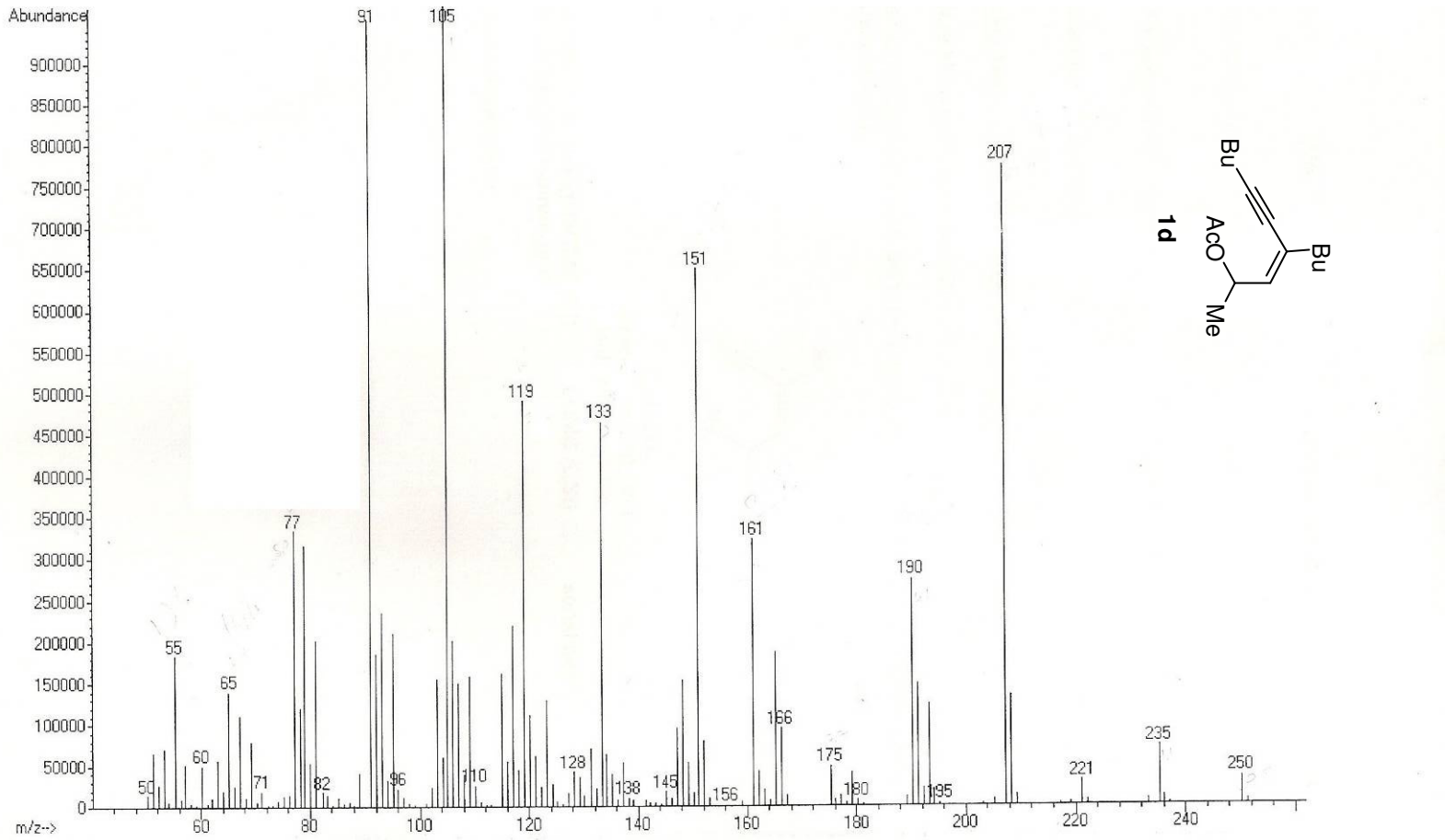

Figure B.4. Mass Spectrum of (Z)-4-butyldec-3-en-5-yn-2-yl acetate

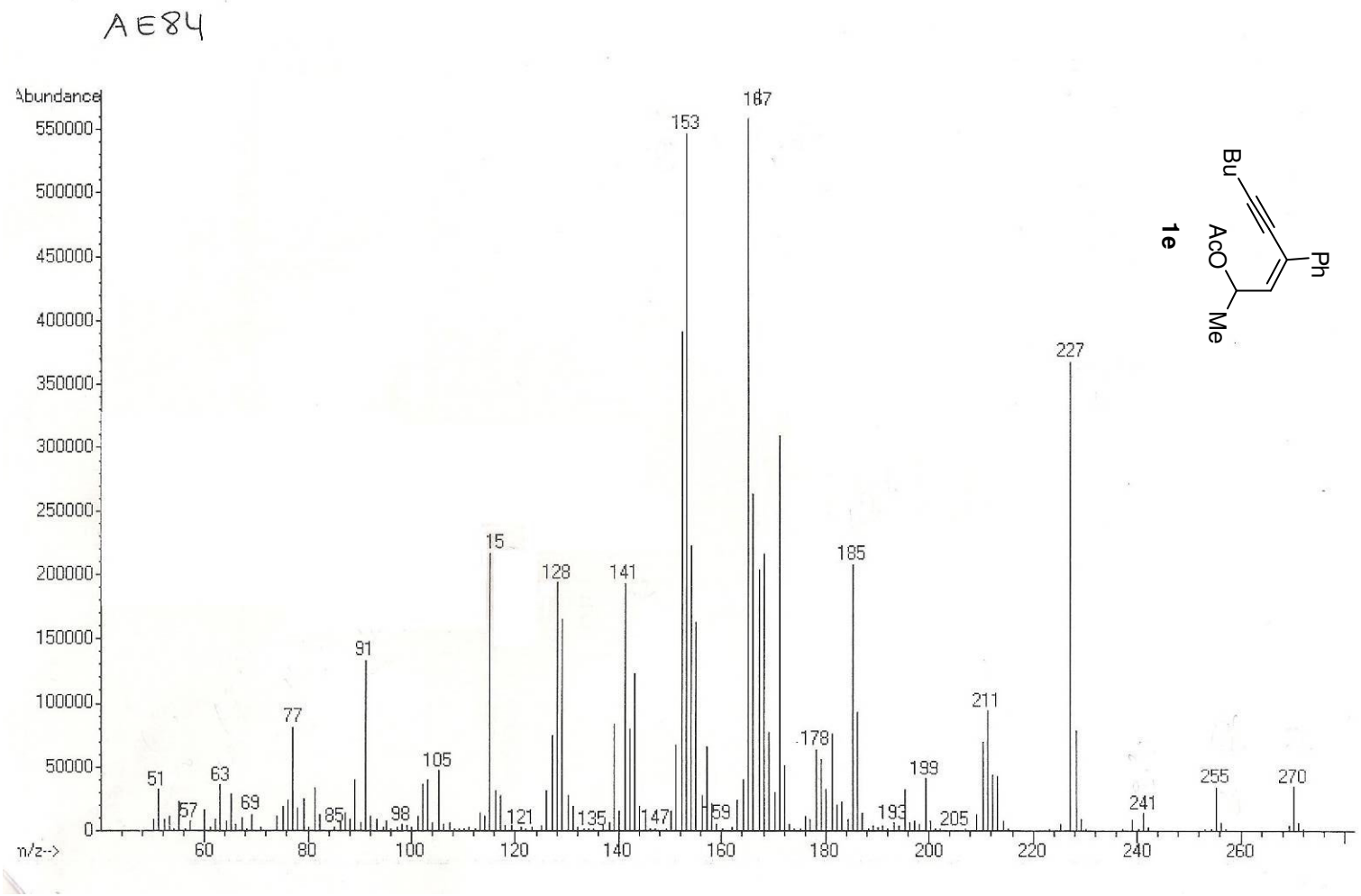

Figure B.5. Mass Spectrum of (Z)-4-phenyldec-3-en-5-yn-2-yl acetate

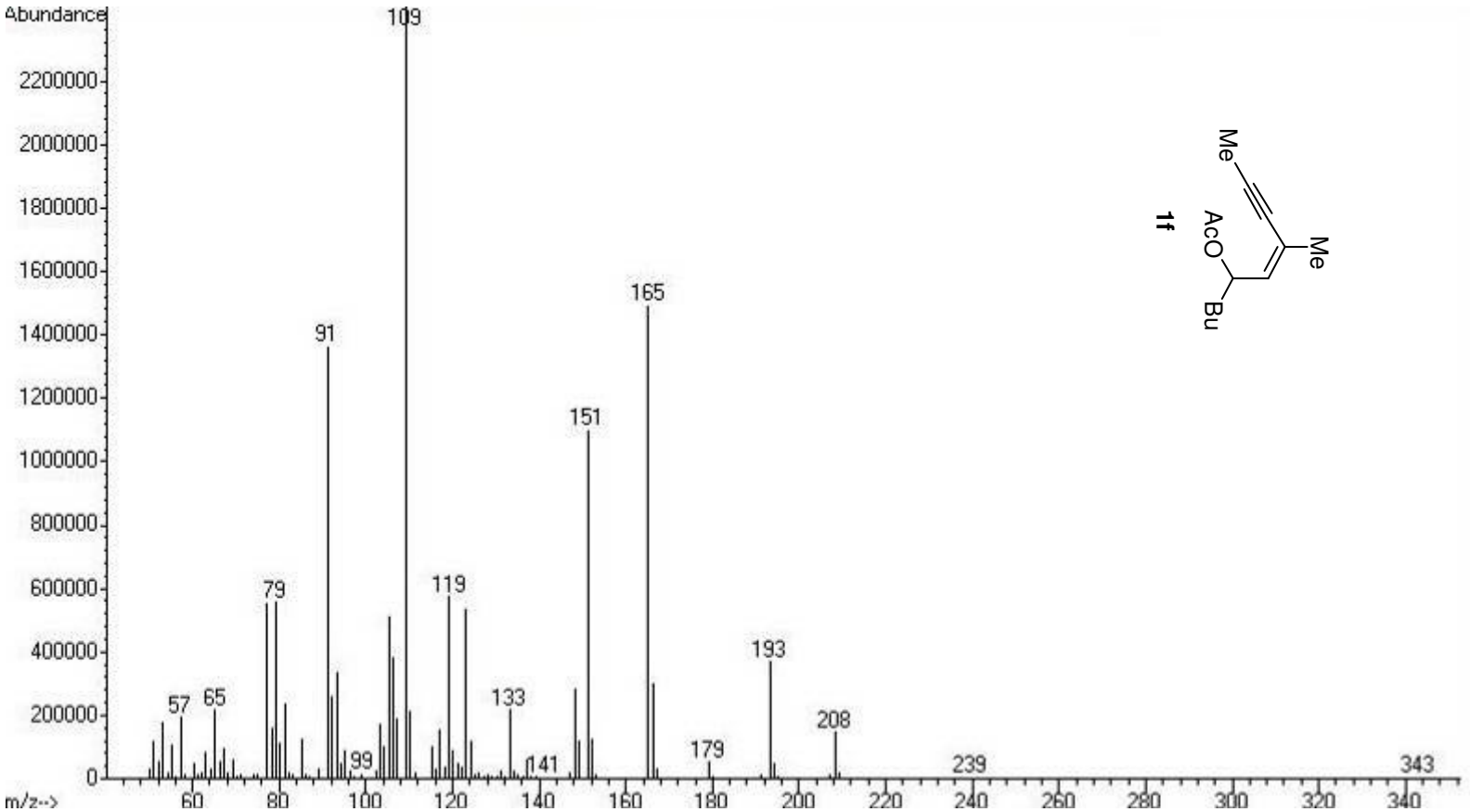

Figure B.6. Mass Spectrum of (*Z*)-7-methyldec-6-en-8-yn-5-yl acetate

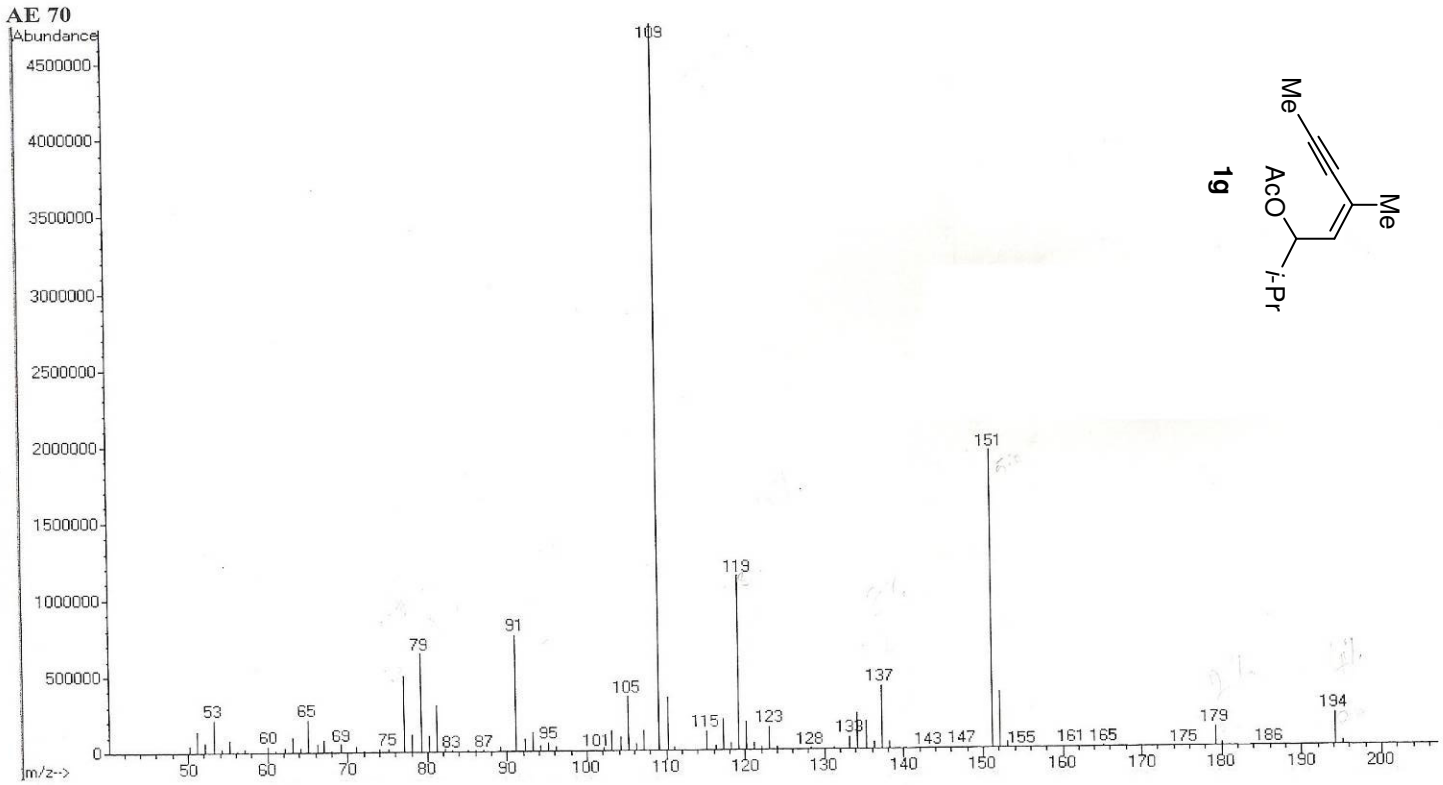

Figure B.7. Mass Spectrum of (*Z*)-2,5-dimethyloct-4-en-6-yn-3-yl acetate

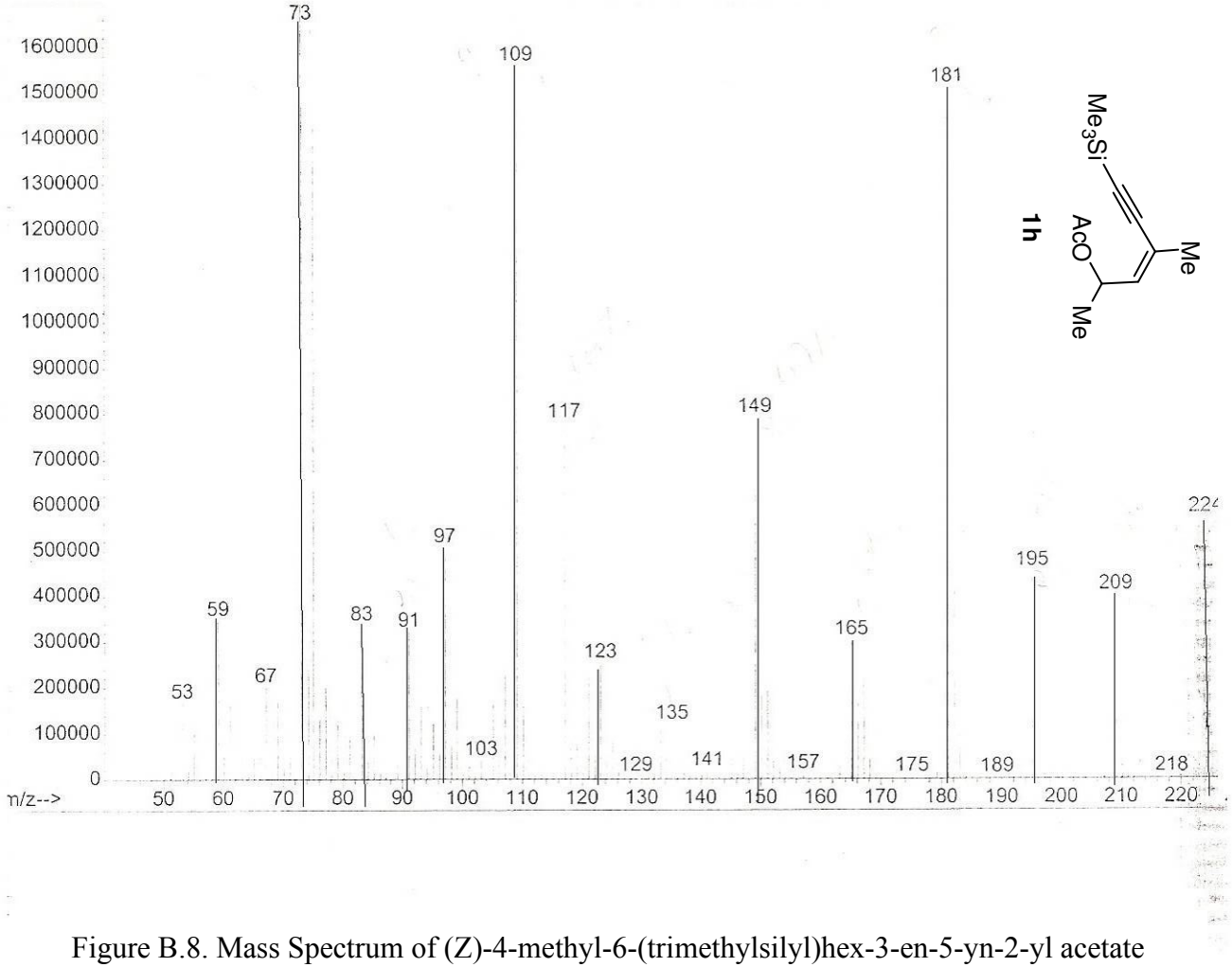

Figure B.8. Mass Spectrum of (Z)-4-methyl-6-(trimethylsilyl)hex-3-en-5-yn-2-yl acetate

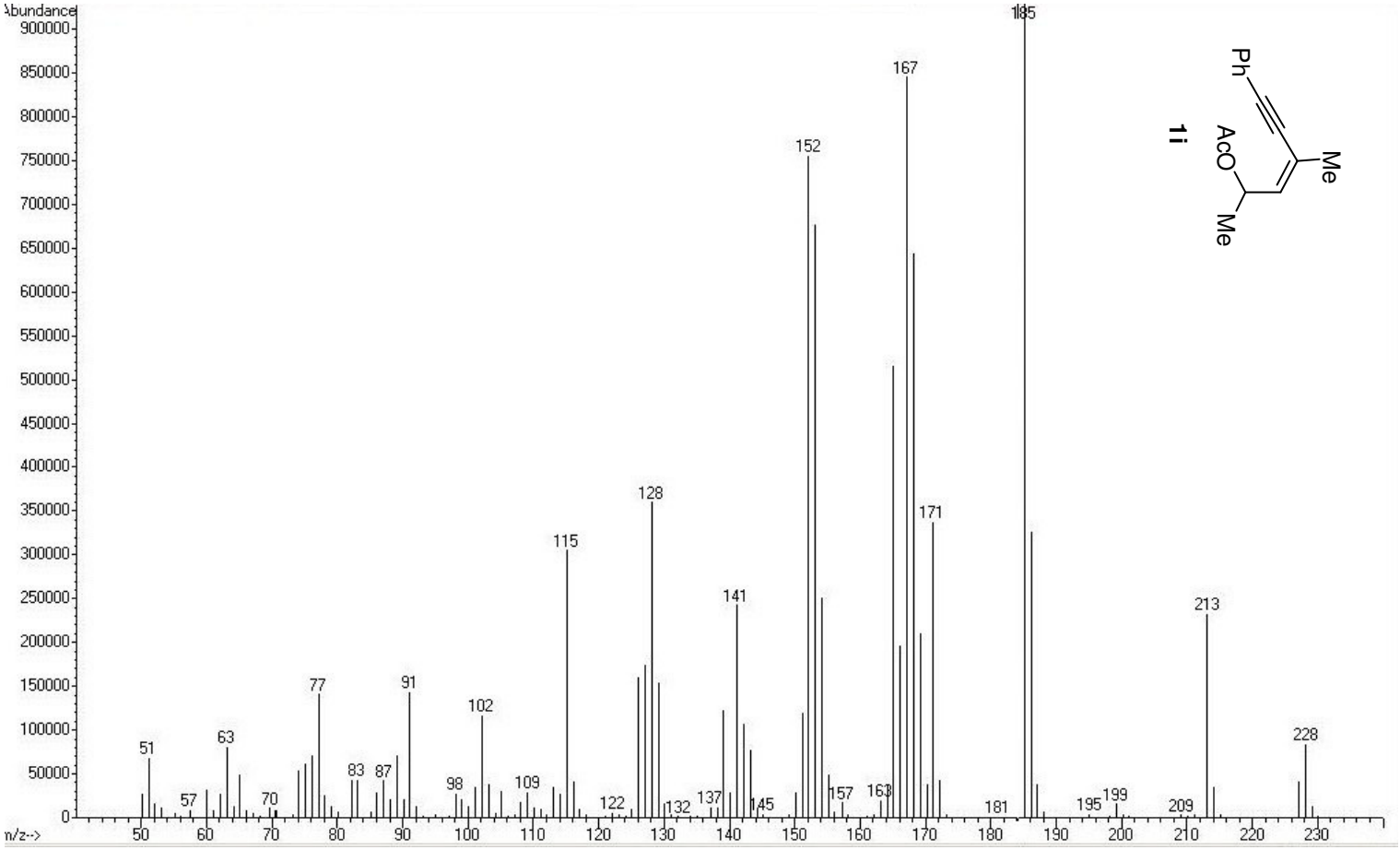

Figure B.9. Mass Spectrum of (Z)-4-methyl-6-phenylhex-3-en-5-yn-2-yl acetate

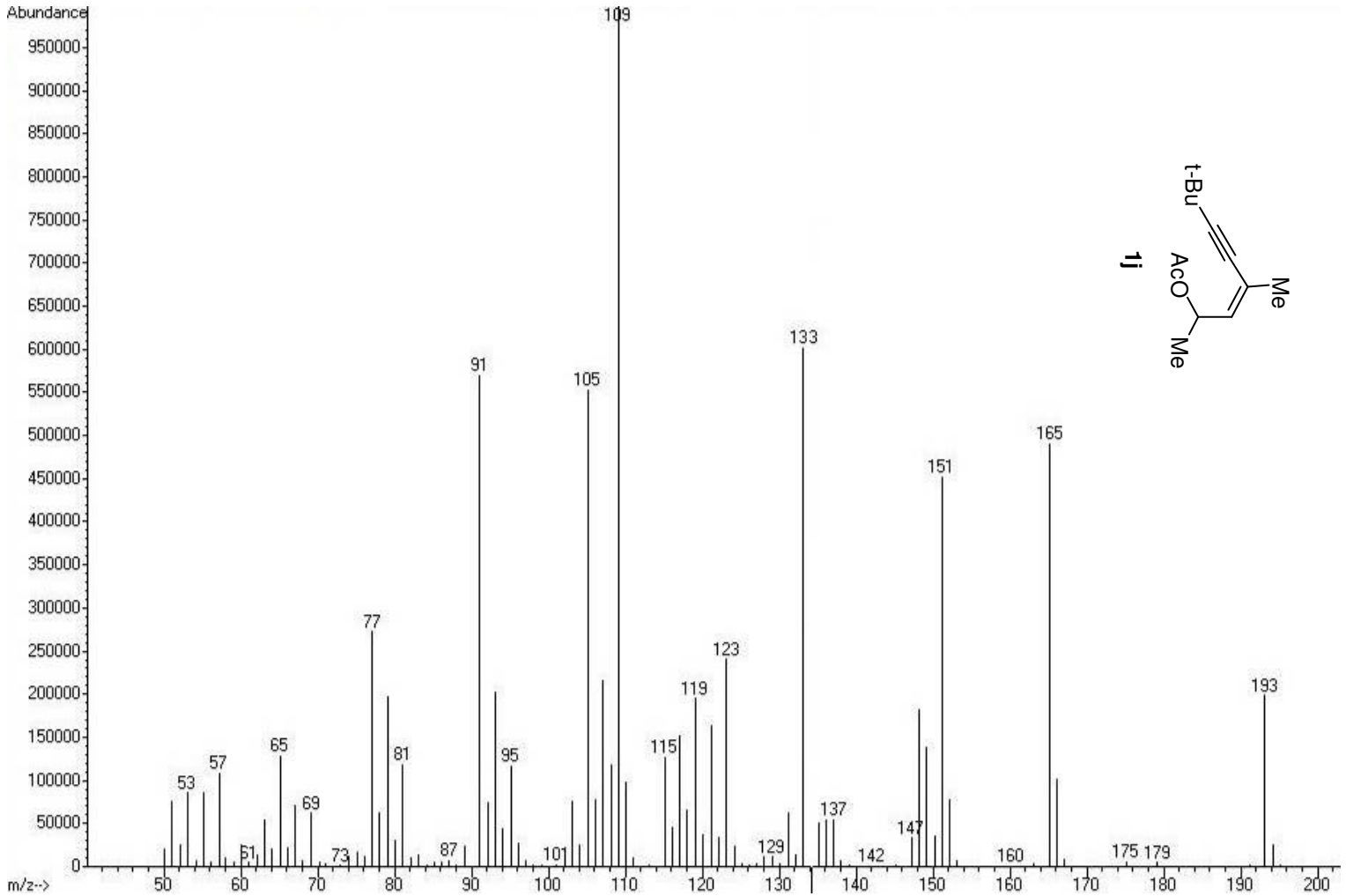

Figure B.10. Mass Spectrum of (Z)-4,7,7-trimethyloct-3-en-5-yn-2-yl acetate

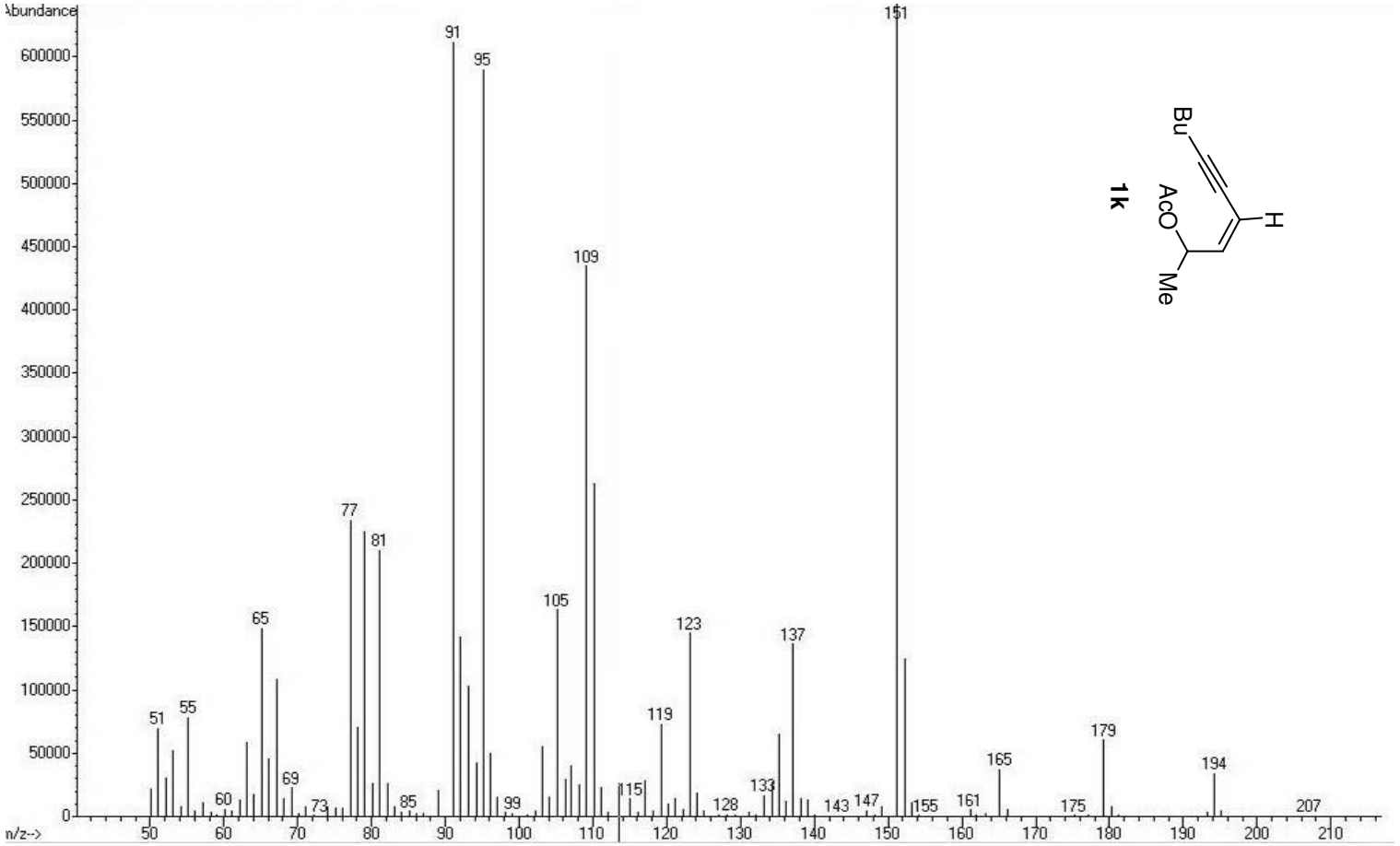

Figure B.11. Mass Spectrum of (Z)-dec-3-en-5-yn-2-yl acetate

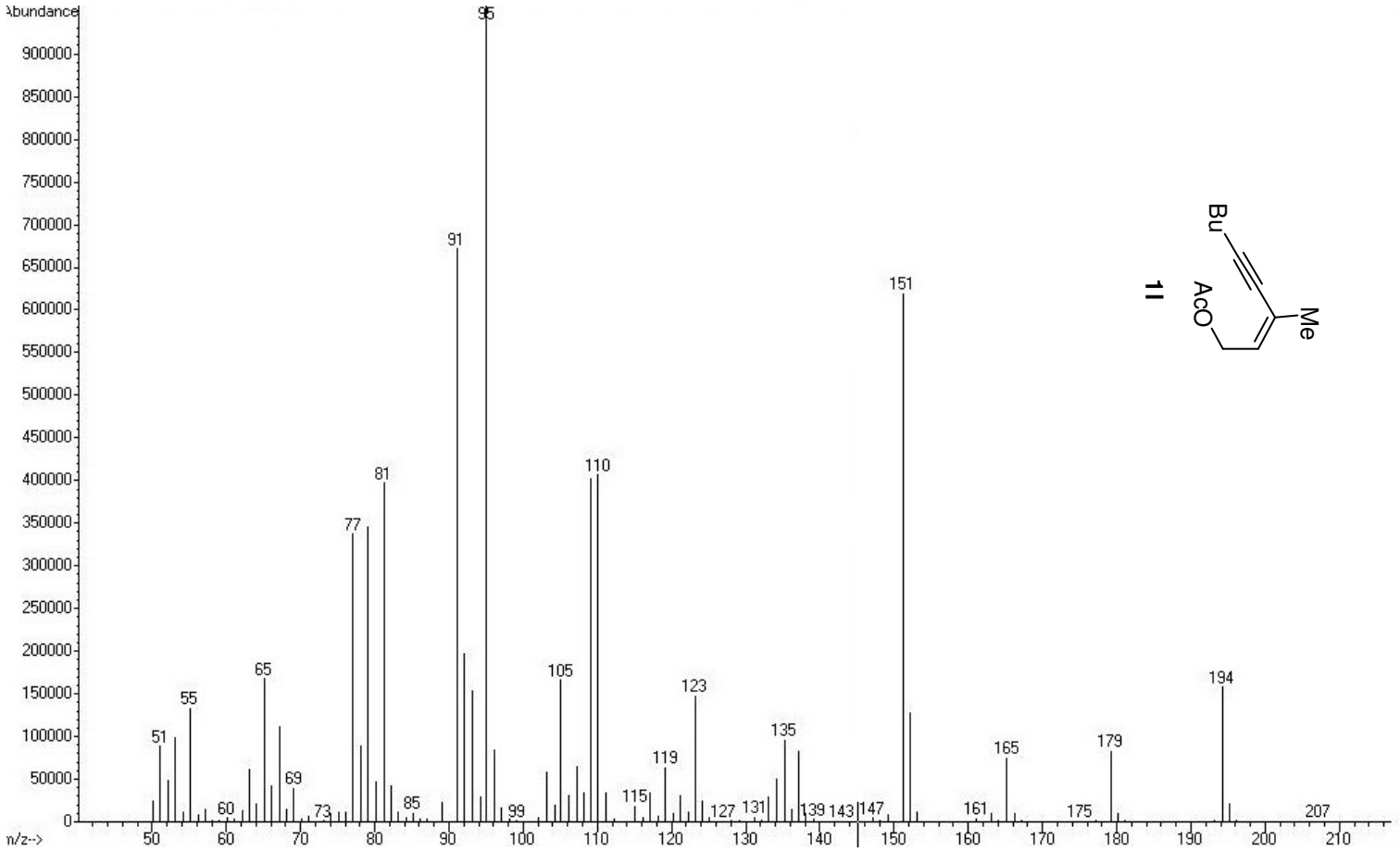

Figure B.12. Mass Spectrum of (Z)-3-methylnon-2-en-4-ynyl acetate

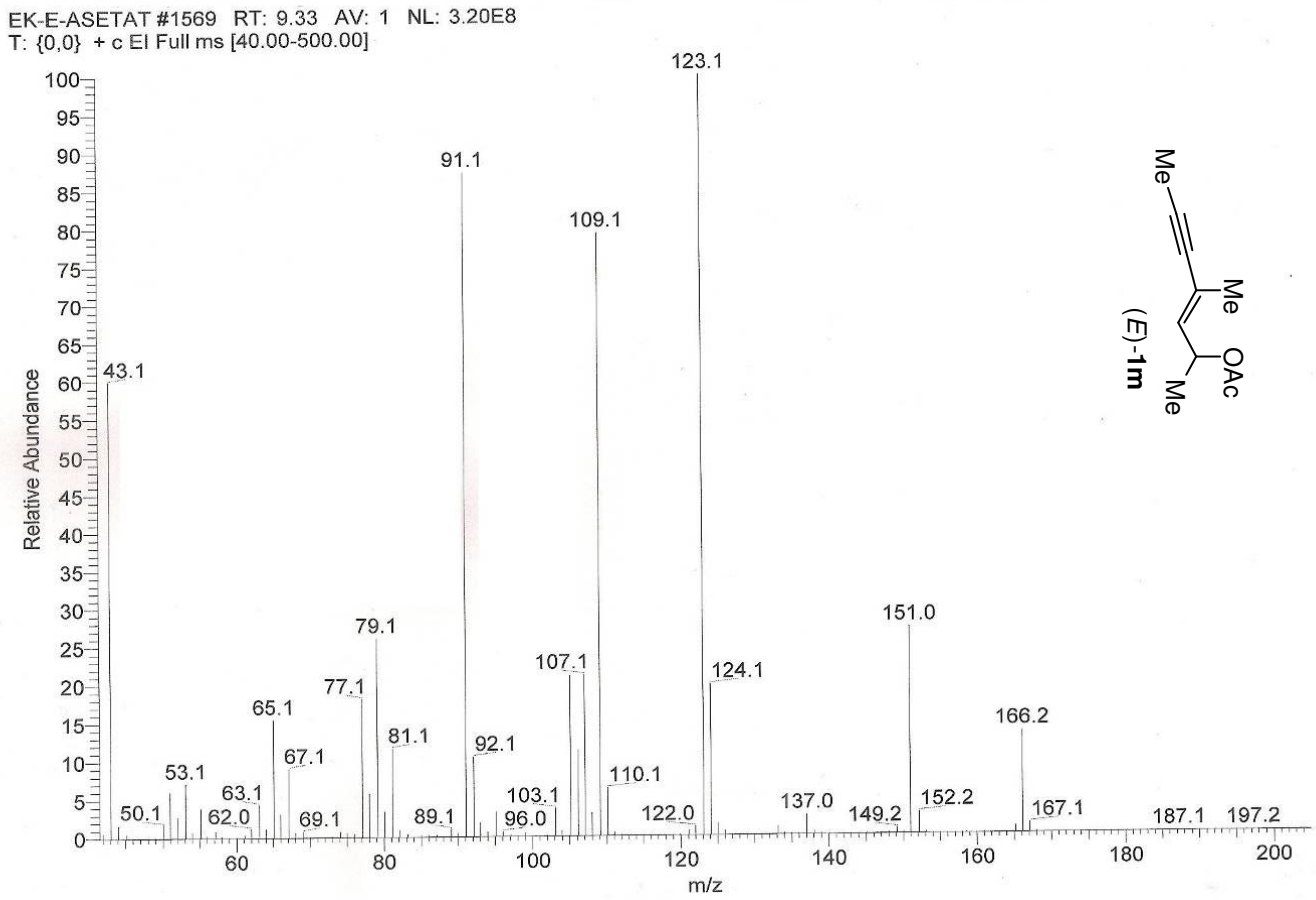

Figure B.13. Mass Spectrum of (*E*)-4-methylhept-3-en-5-yn-2-yl acetate

APPENDIX C

FTIR SPECTRUMS OF REACTANTS

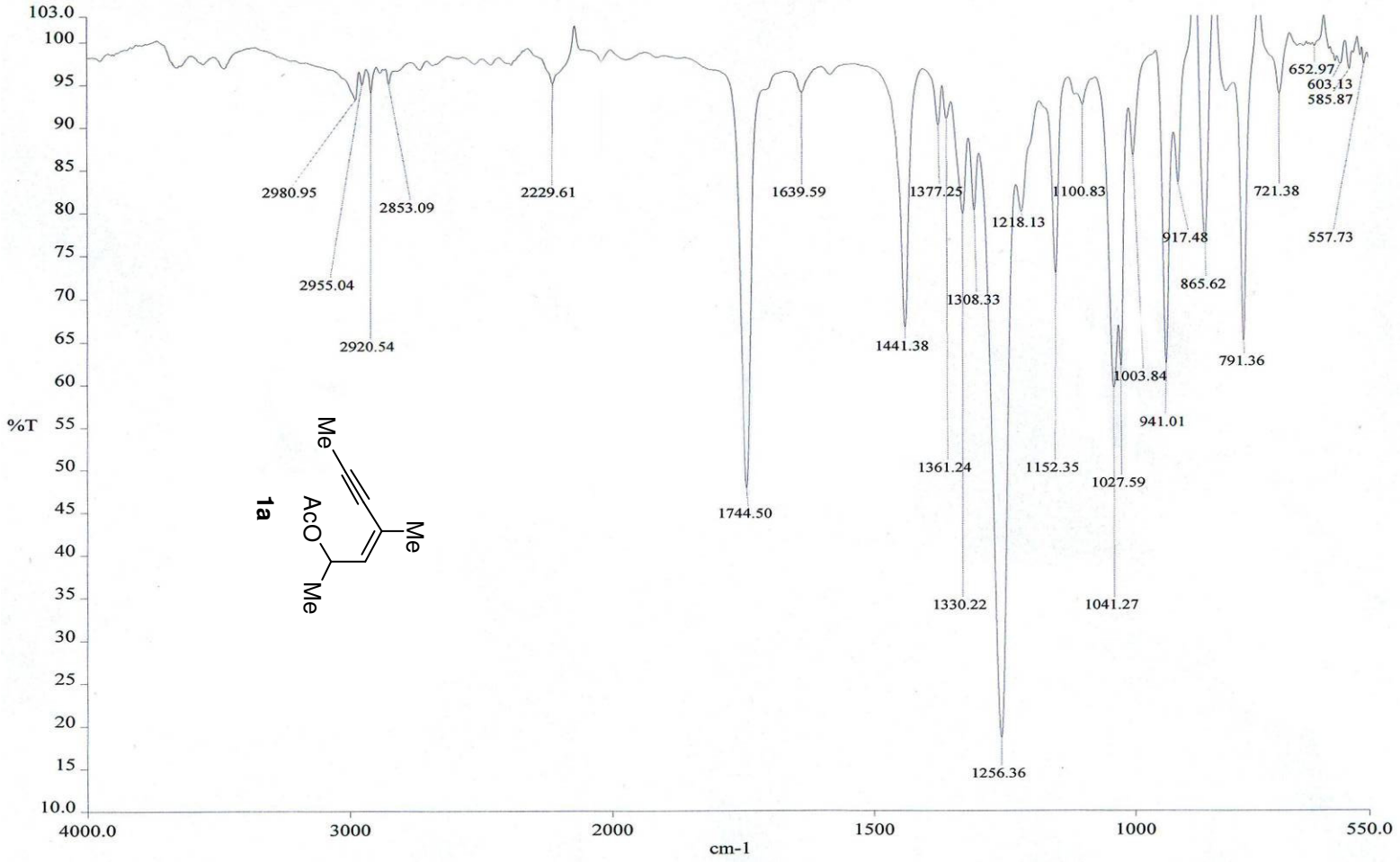

Figure C.1. FTIR Spectrum of (*Z*)-4-methylhept-3-en-5-yn-2-yl acetate

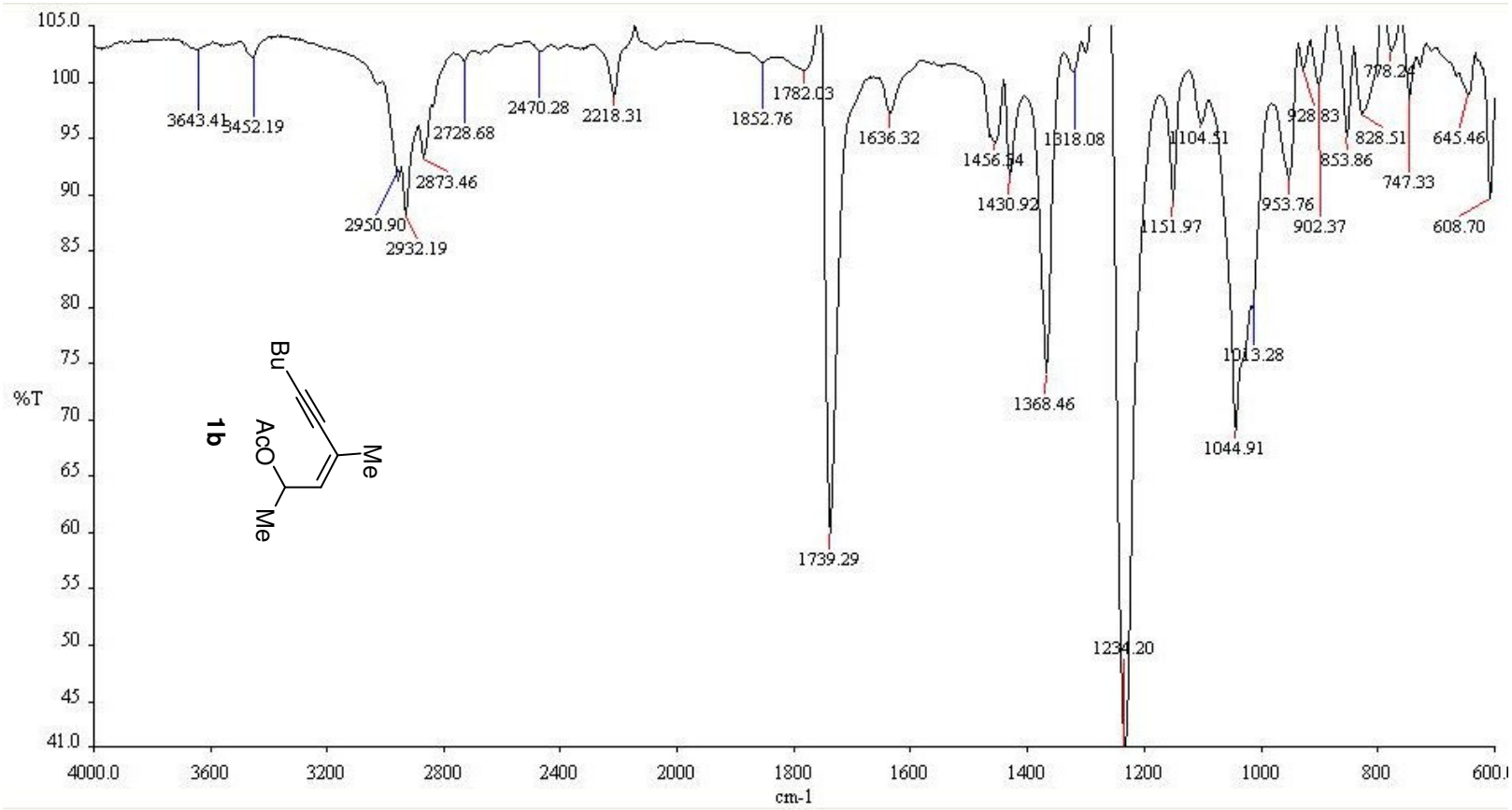

Figure C.2. FTIR Spectrum of (Z)-4-methyldec-3-en-5-yn-2-yl acetate

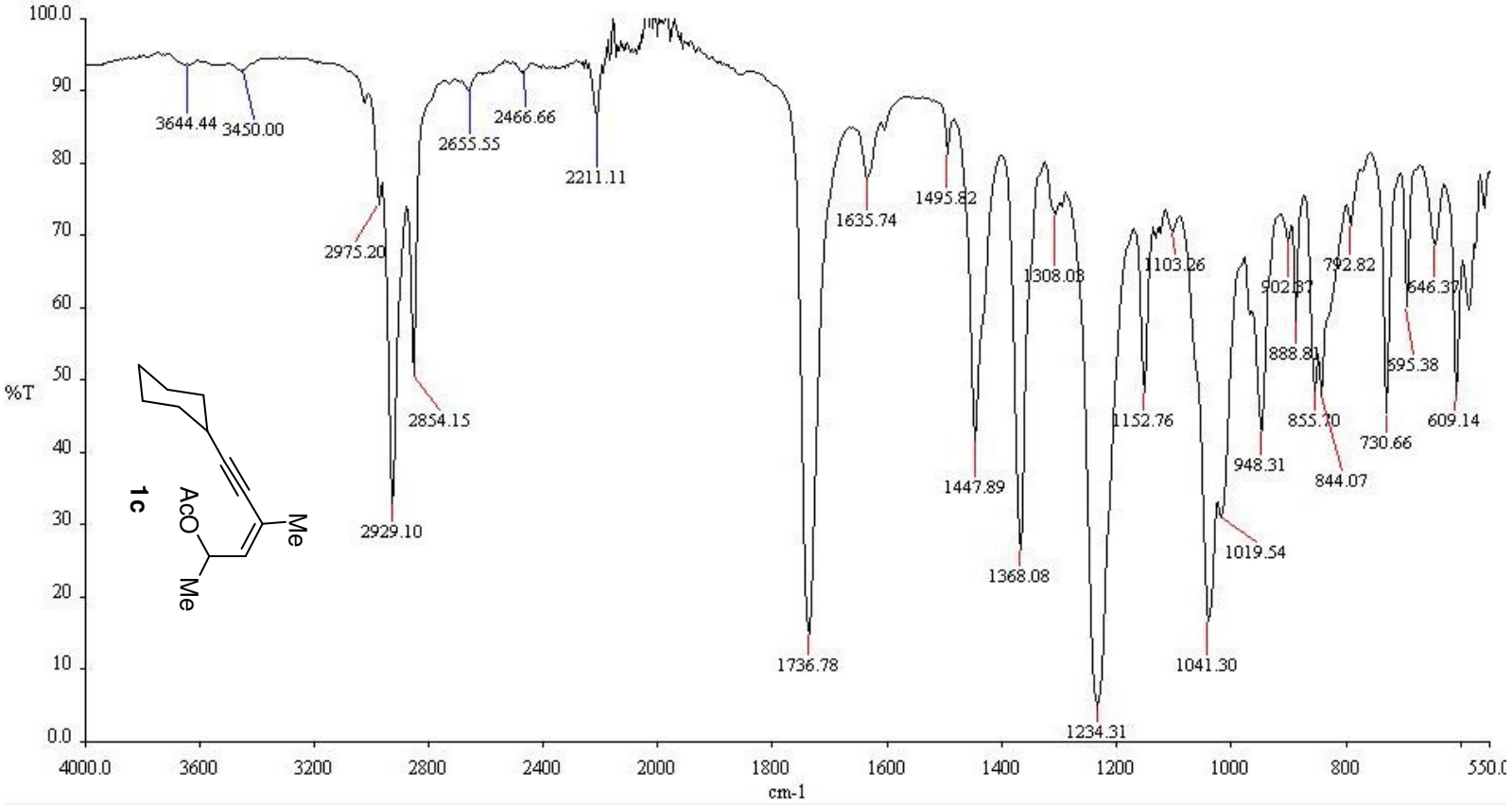

Figure C.3. FTIR Spectrum of (Z)-6-cyclohexyl-4-methylhex-3-en-5-yn-2-yl acetate

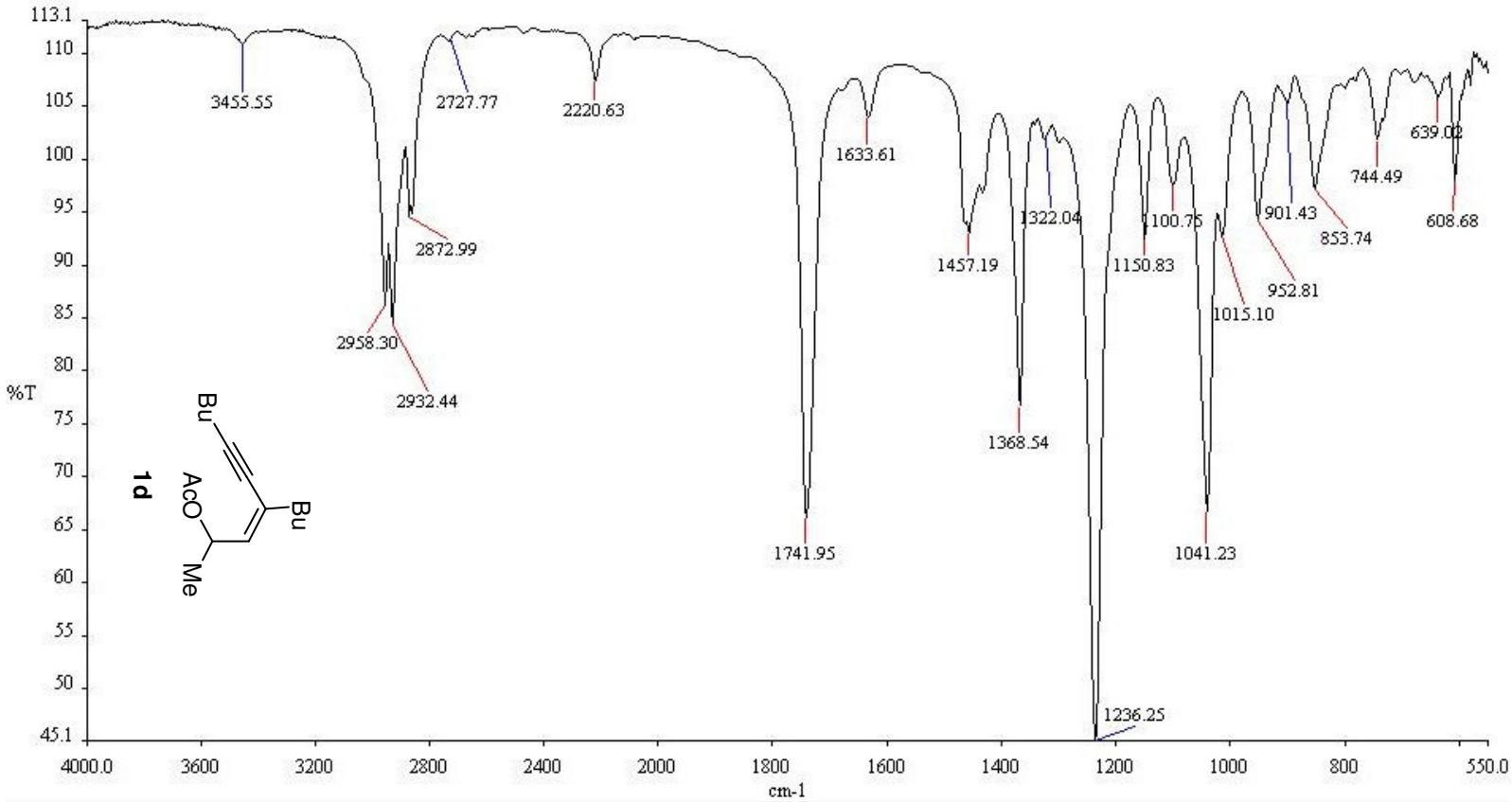

Figure C.4. FTIR Spectrum of (Z)-4-butyldec-3-en-5-yn-2-yl acetate

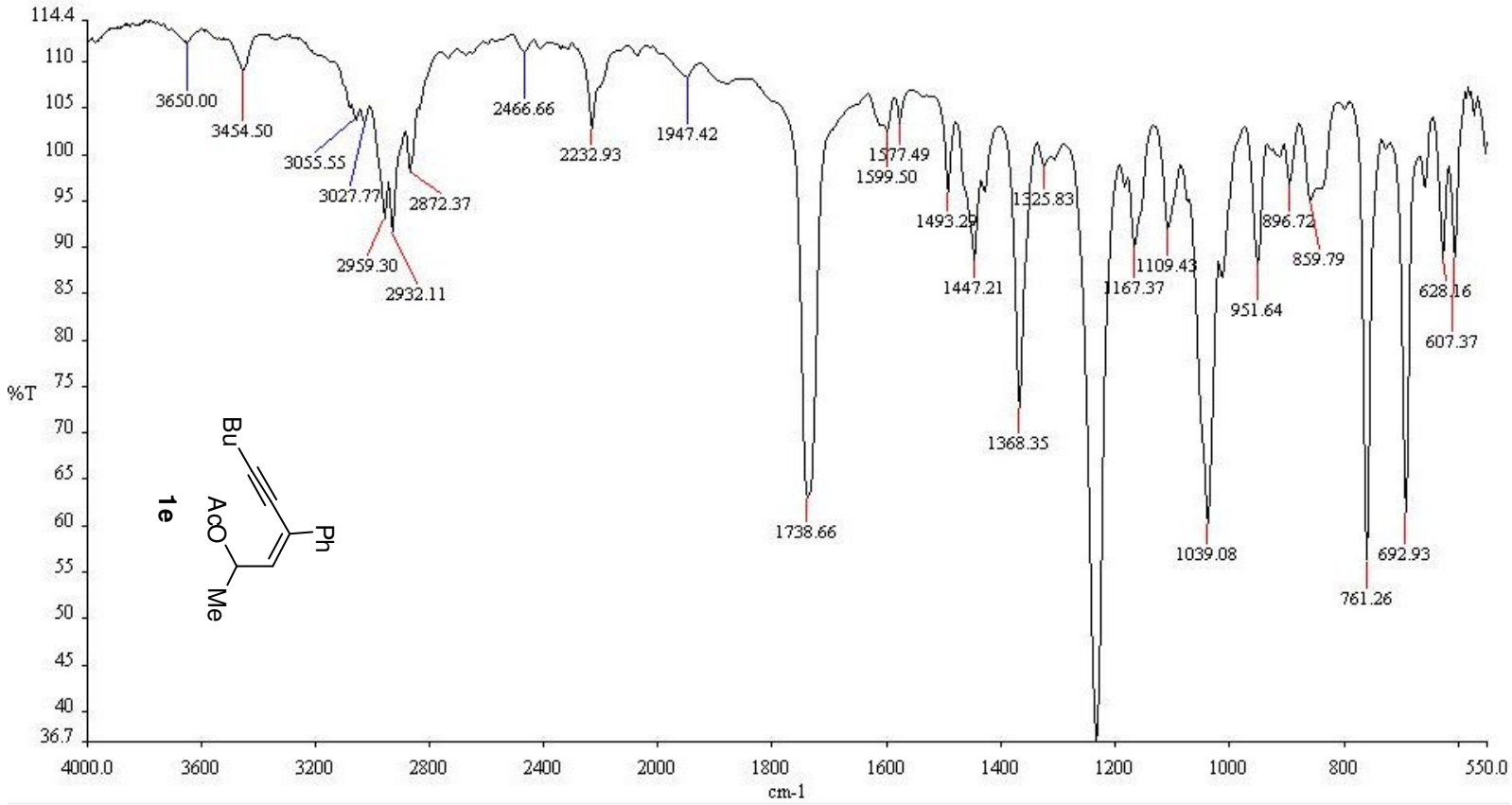

Figure C.5. FTIR Spectrum of (Z)-4-phenyldec-3-en-5-yn-2-yl acetate

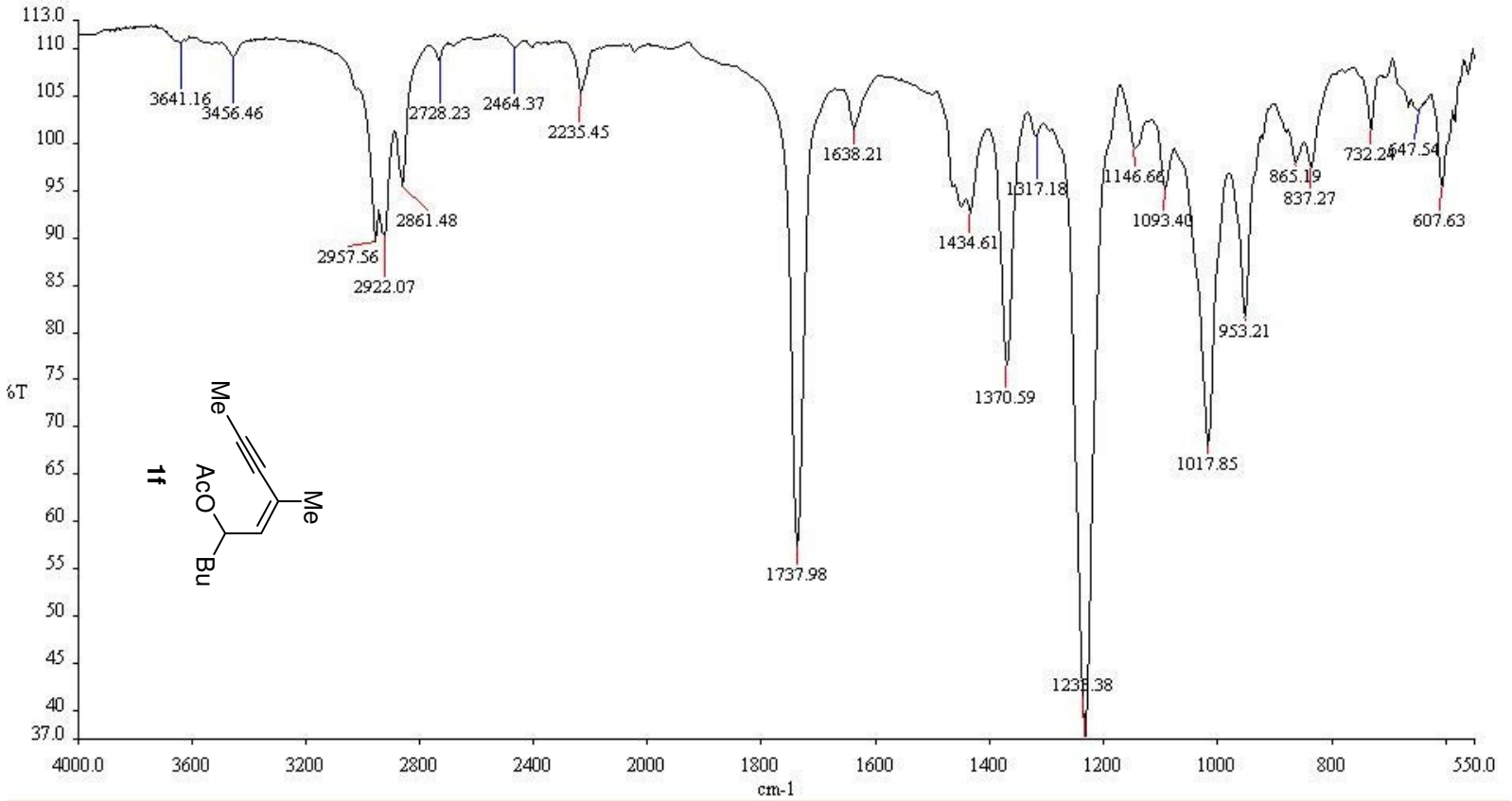

Figure C.6. Mass Spectrum of (*Z*)-7-methyldec-6-en-8-yn-5-yl acetate

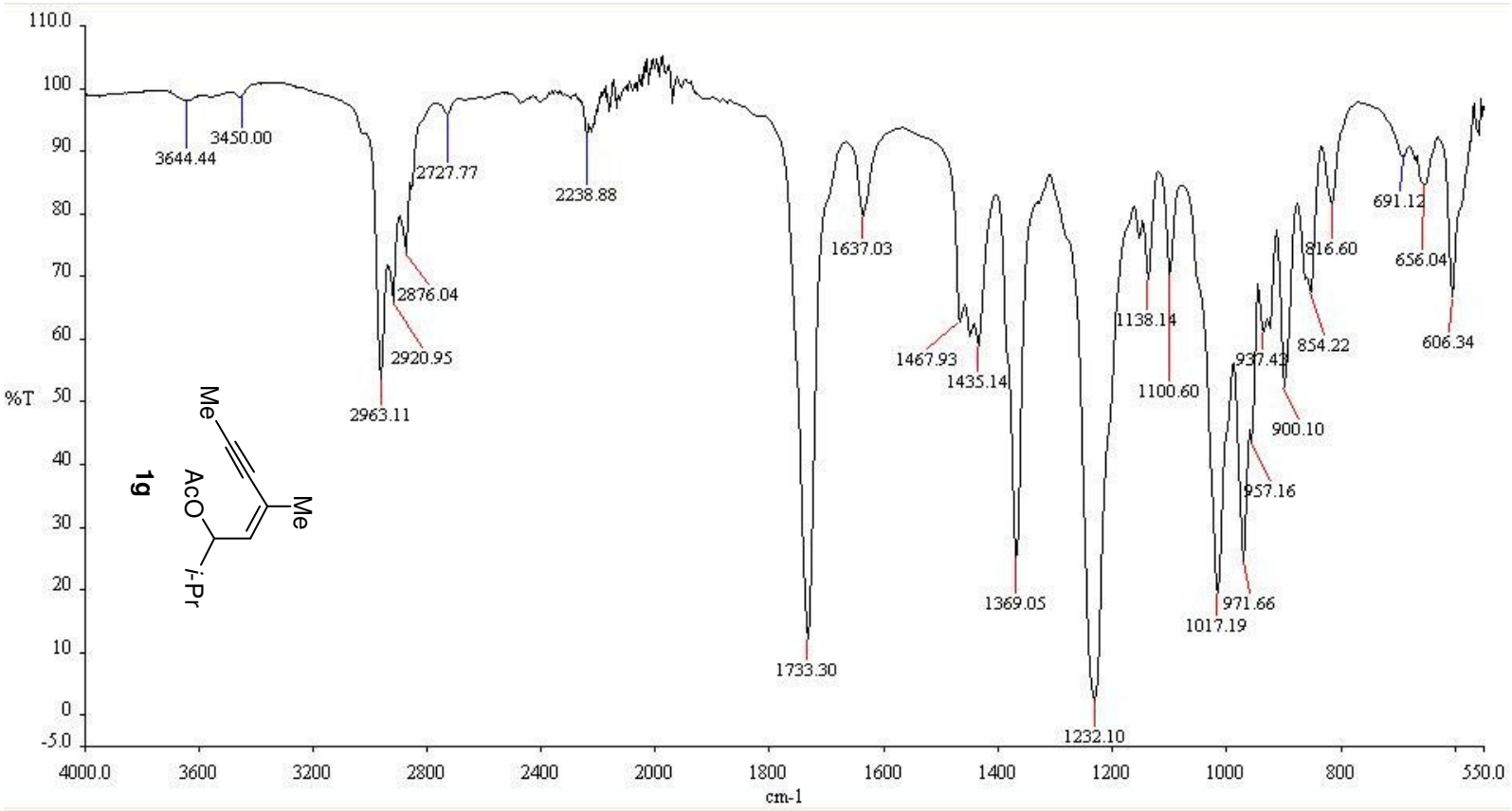

Figure C.7. Mass Spectrum of (*Z*)-2,5-dimethyloct-4-en-6-yn-3-yl acetate

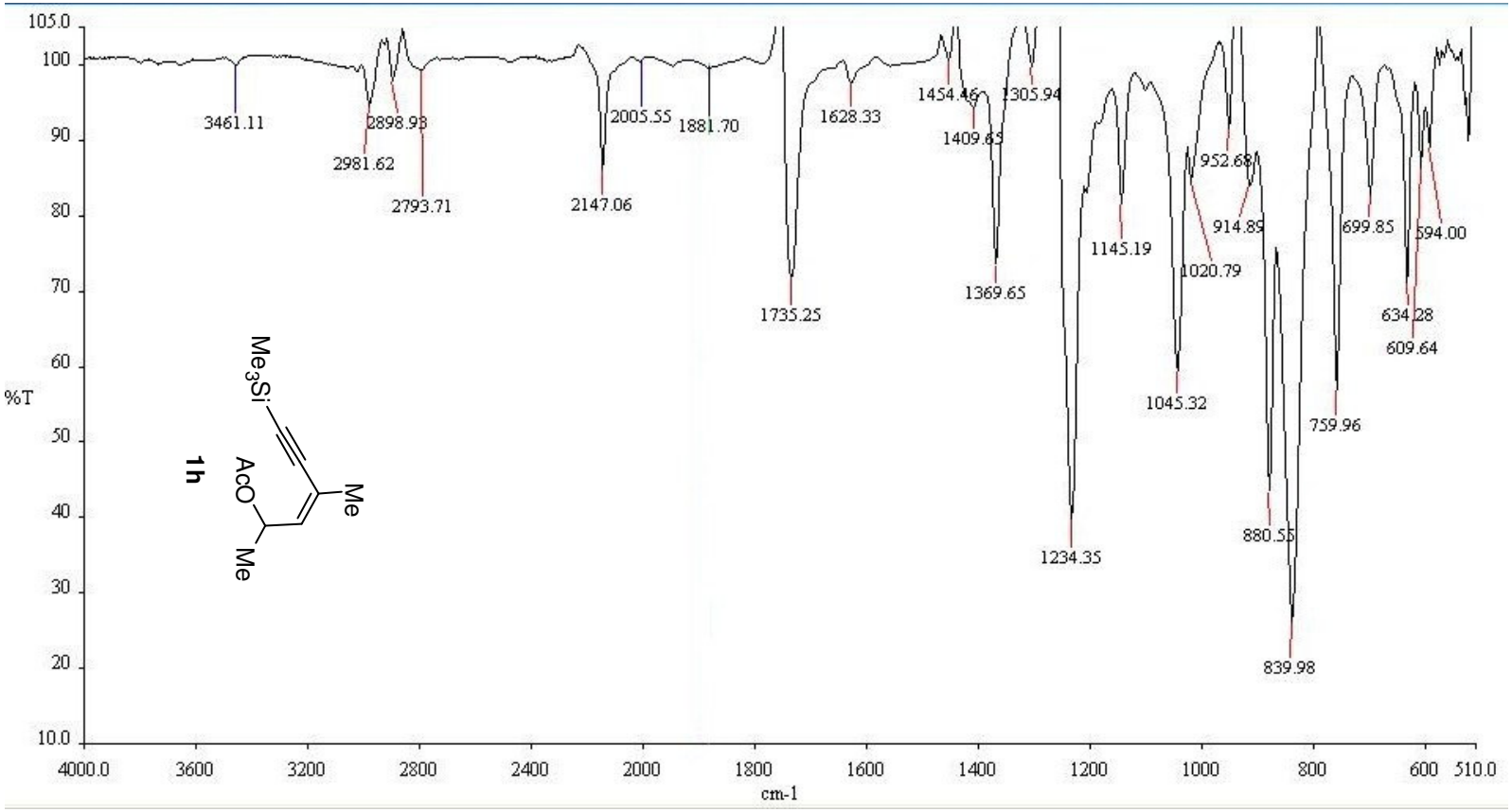

Figure C.8. Mass Spectrum of (Z)-4-methyl-6-(trimethylsilyl)hex-3-en-5-yn-2-yl acetate

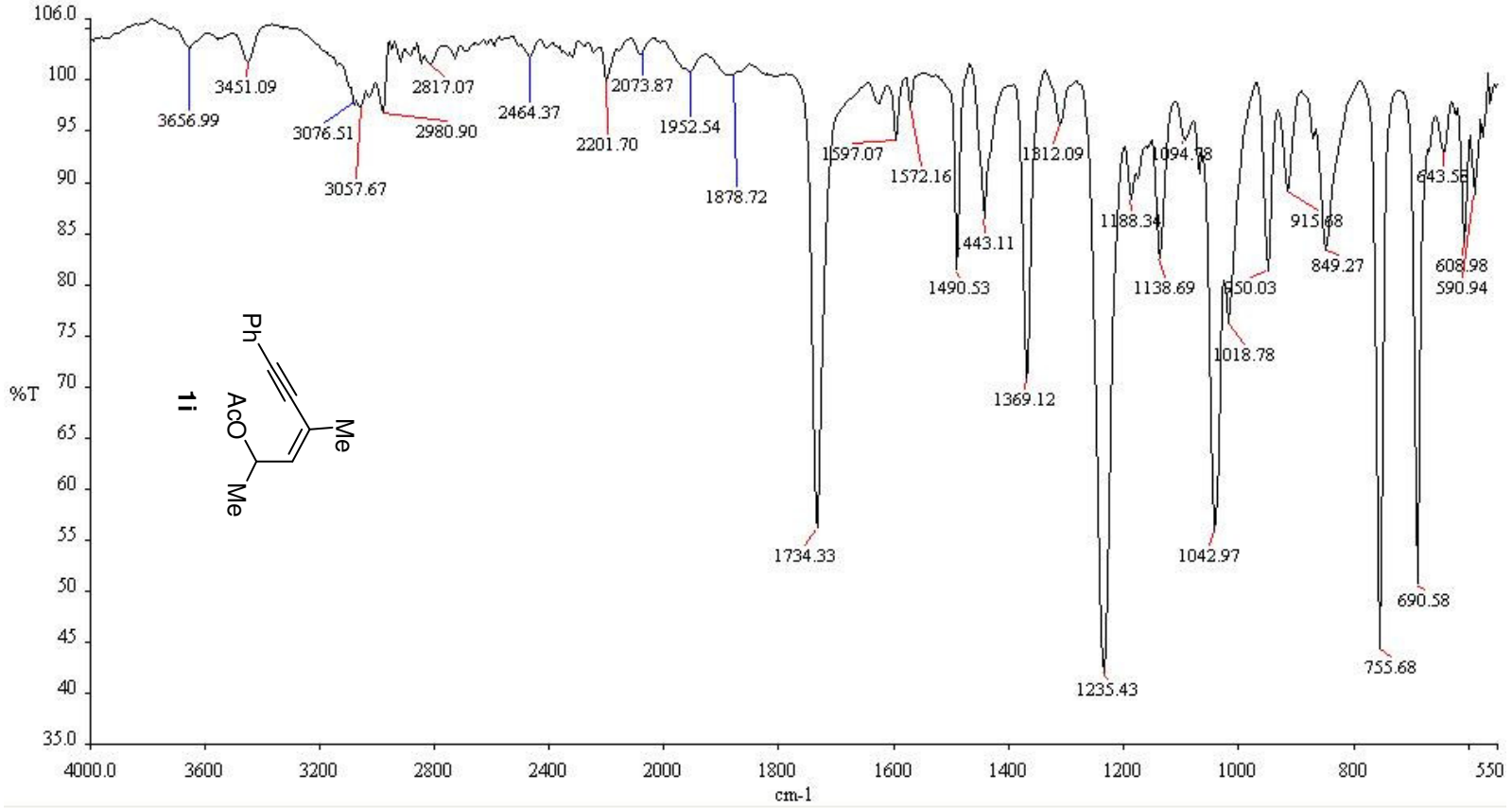

Figure C.9. FTIR Spectrum of (Z)-4-methyl-6-phenylhex-3-en-5-yn-2-yl acetate

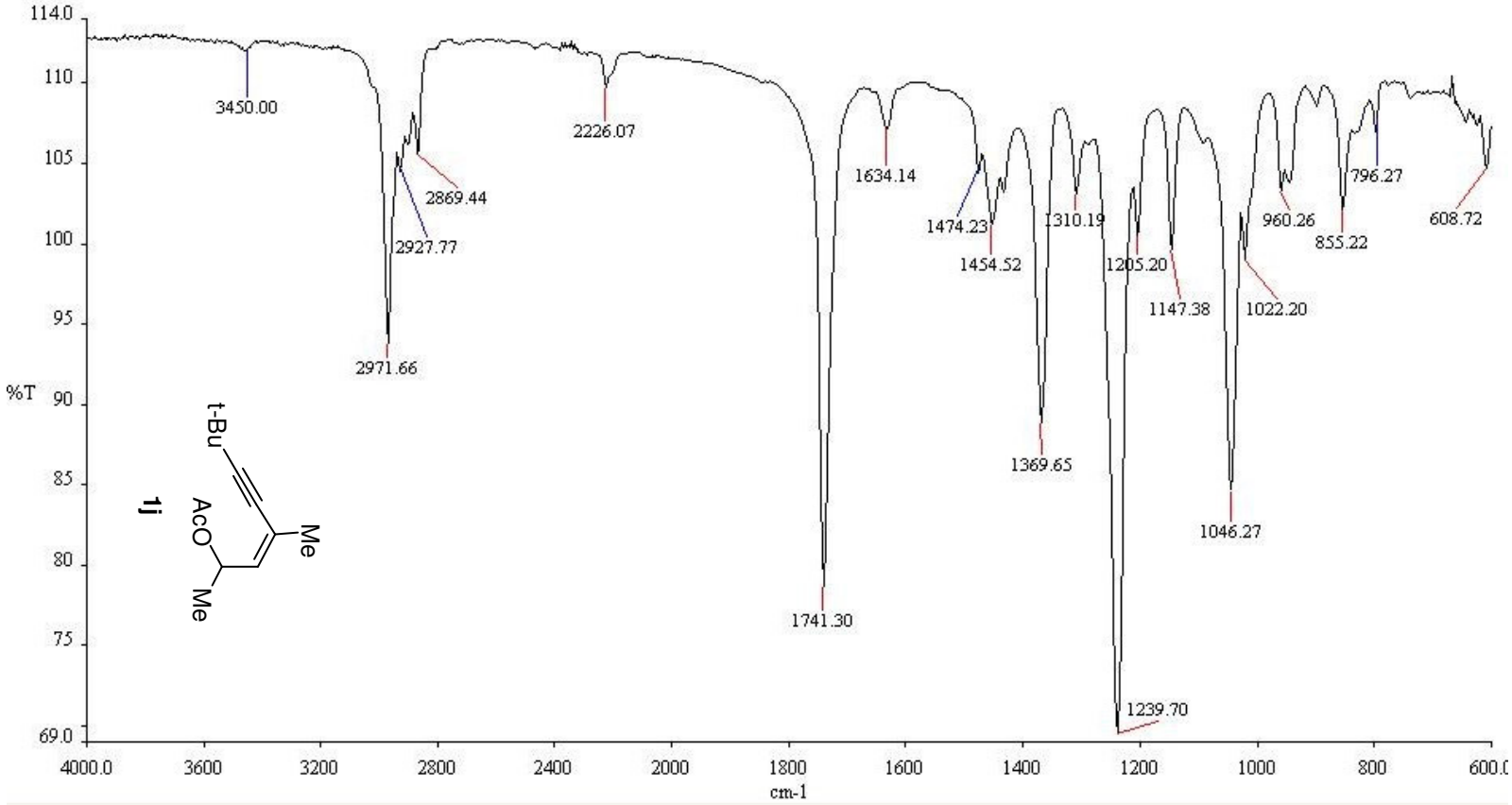

Figure C.10. FTIR Spectrum of (Z)-4,7,7-trimethyloct-3-en-5-yn-2-yl acetate

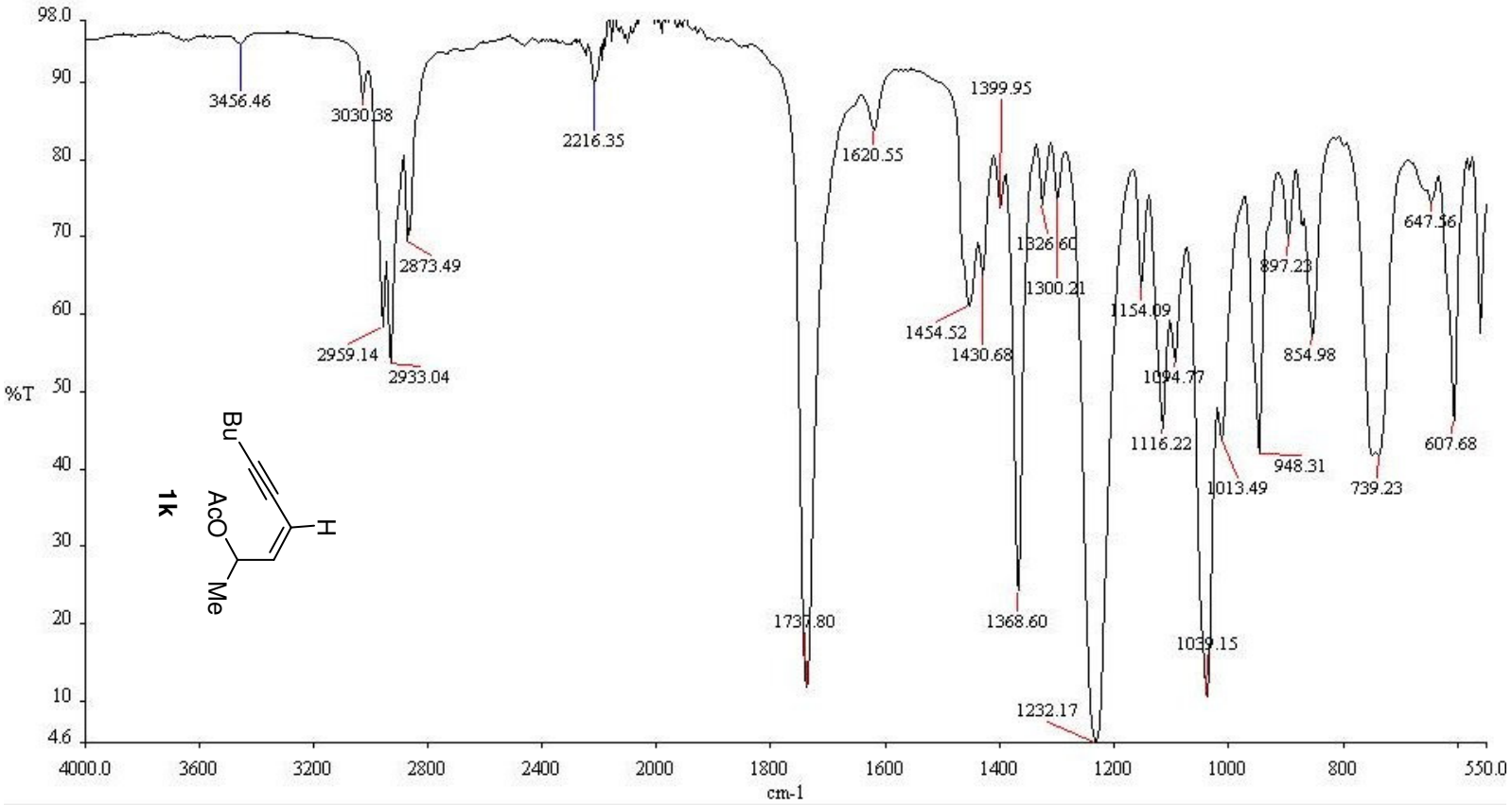

Figure C.11. FTIR Spectrum of (Z)-dec-3-en-5-yn-2-yl acetate

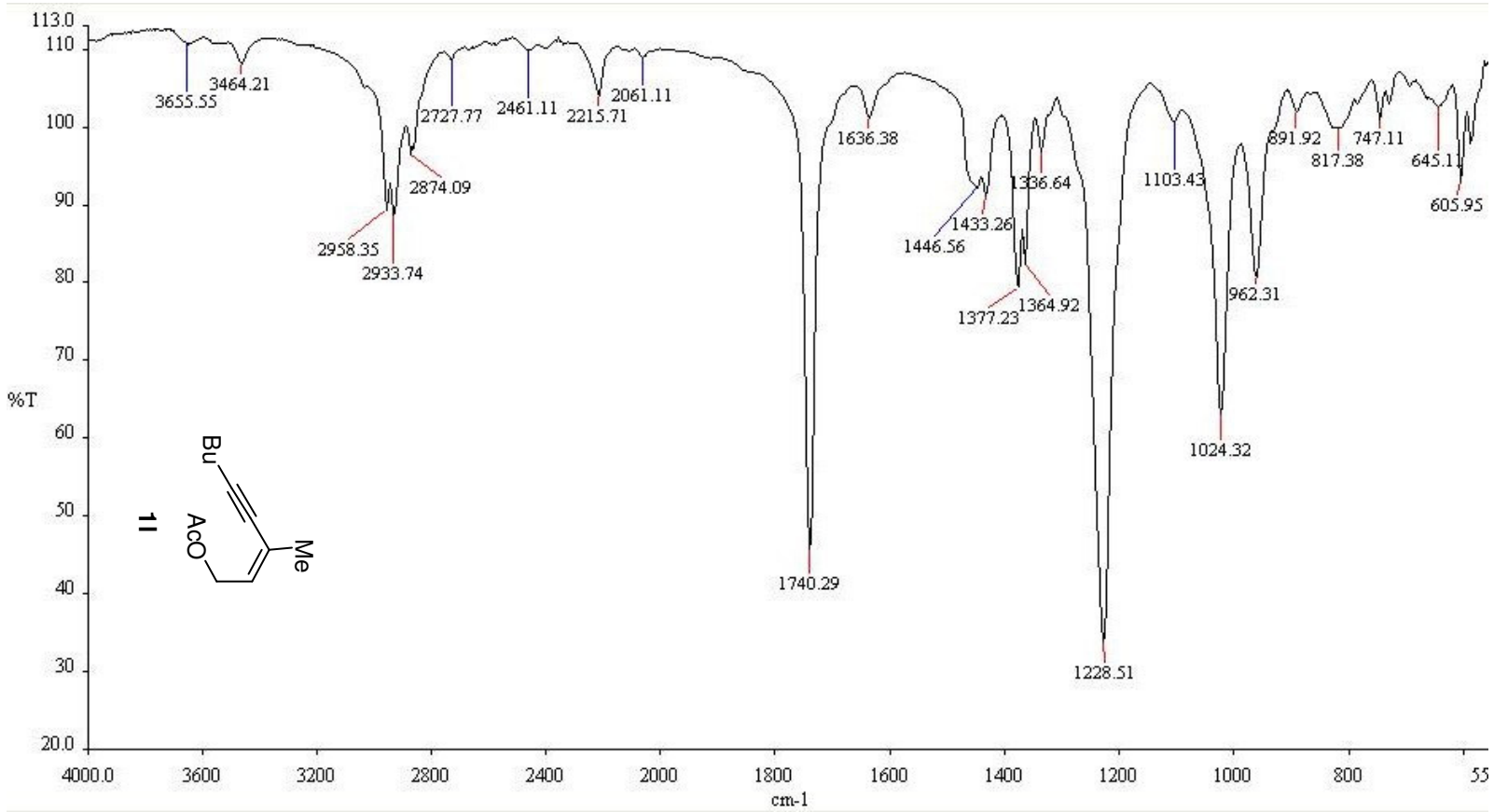

Figure C.12. FTIR Spectrum of (Z)-3-methylnon-2-en-4-ynyl acetate

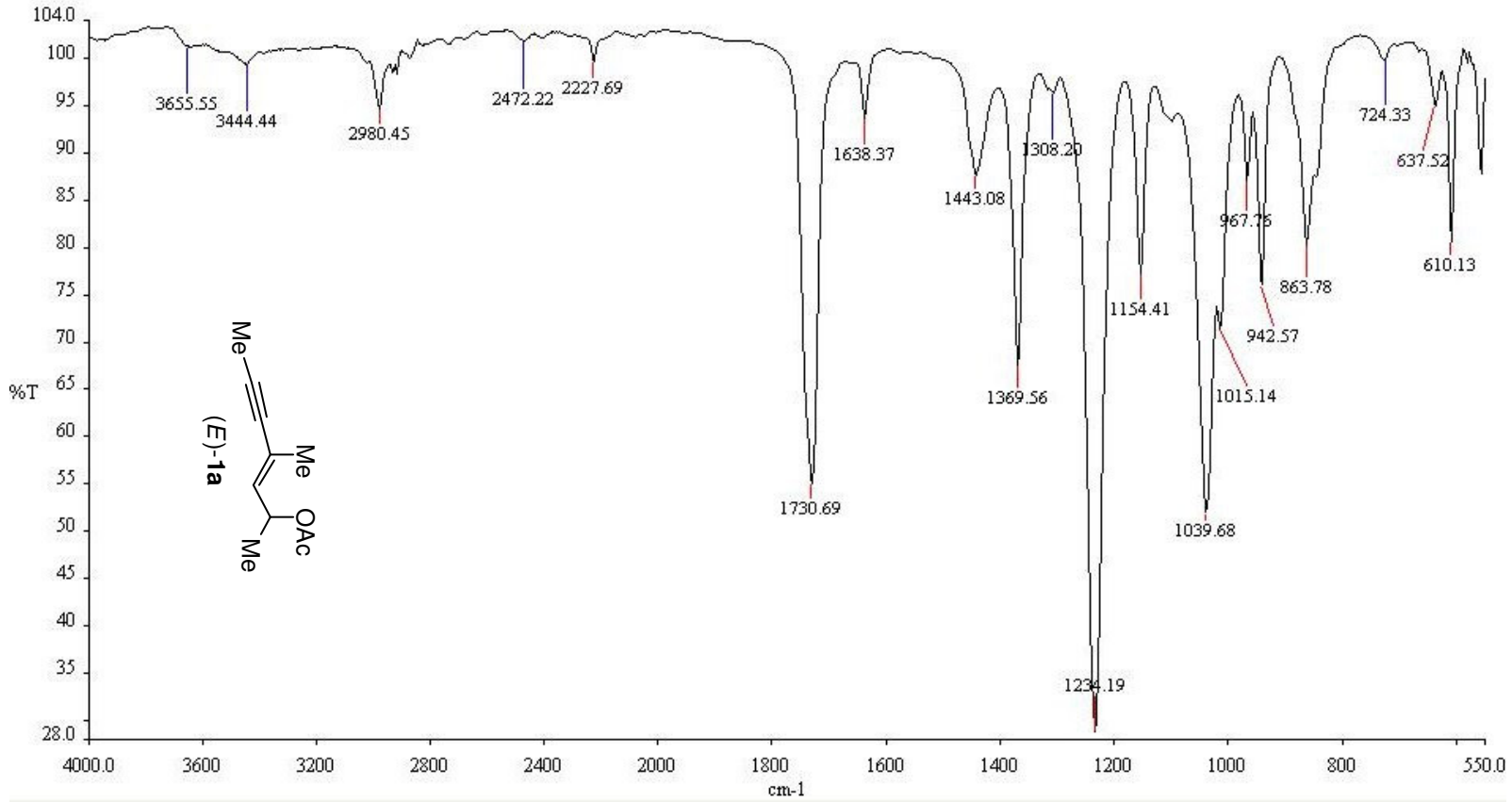

Figure C.13. FTIR Spectrum of (*E*)-4-methylhept-3-en-5-yn-2-yl acetate

APPENDIX D

^{1}H NMR AND ^{13}CNMR SPECTRUMS OF PRODUCTS

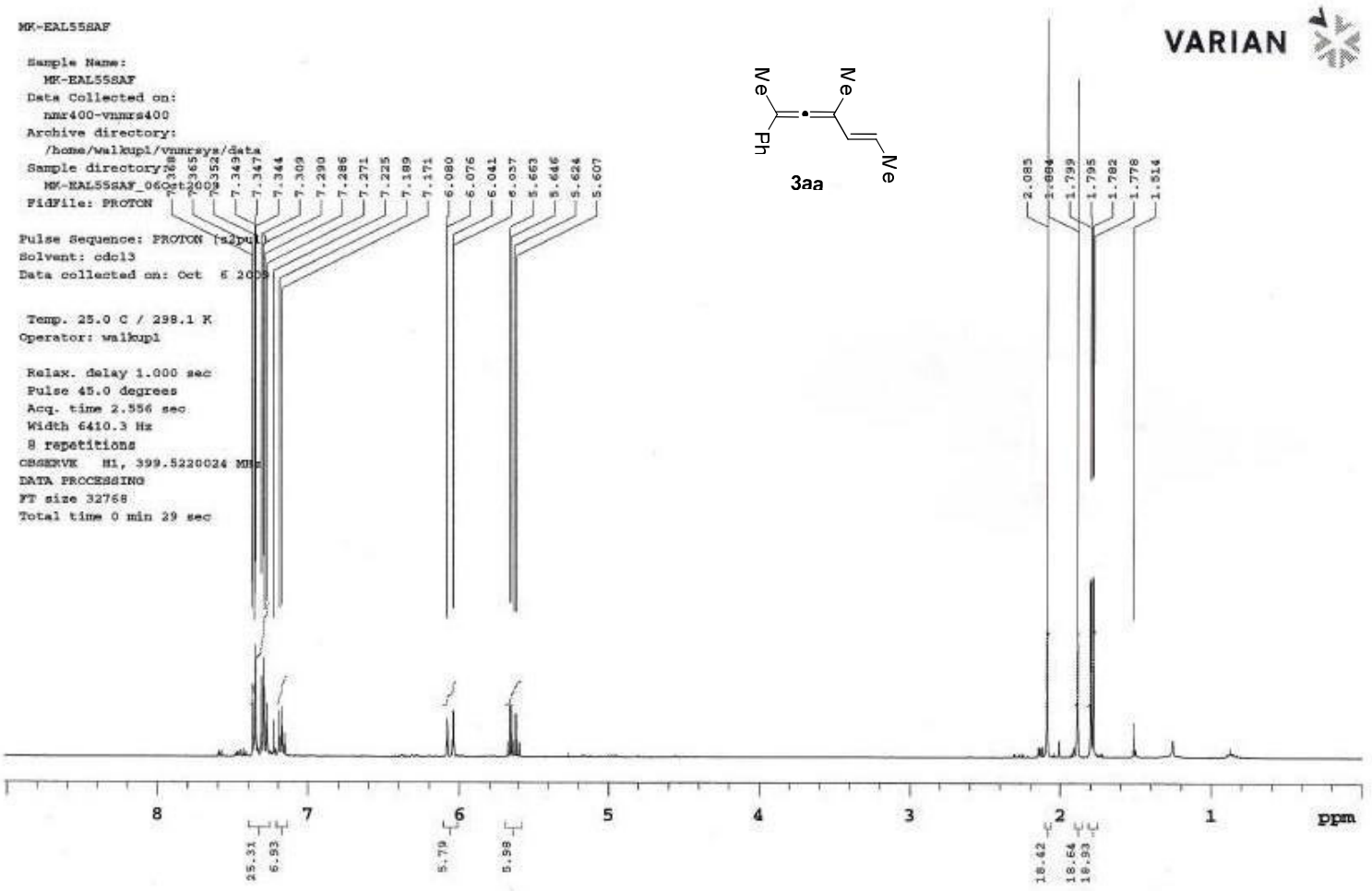

Figure D.1. [1] H NMR of (*E*)- 2-phenyl-4-methylhepta-2,3,5-triene

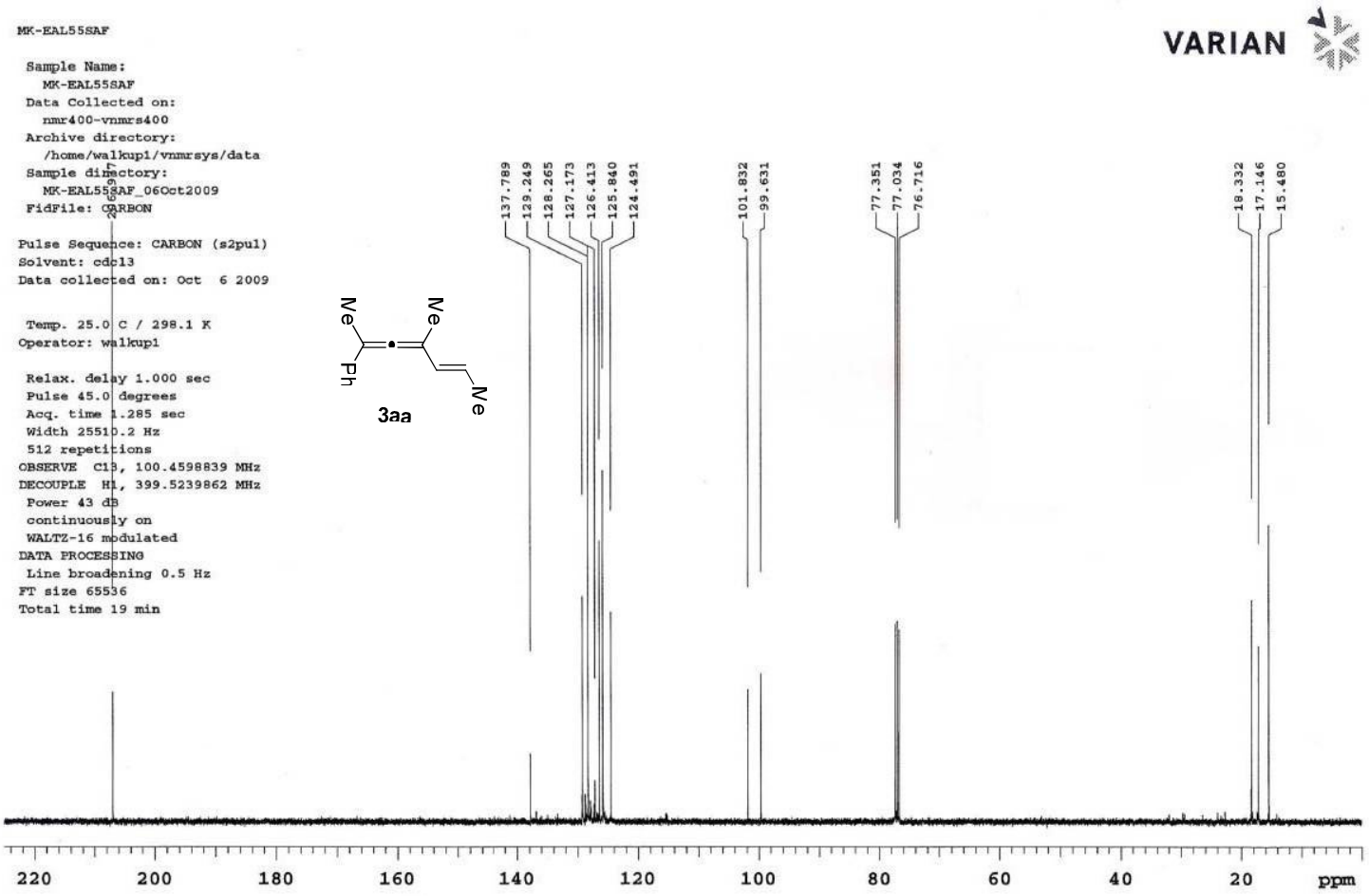

Figure D.2. ^{13} C NMR of (*E*)- 2-phenyl-4-methylhepta-2,3,5-triene

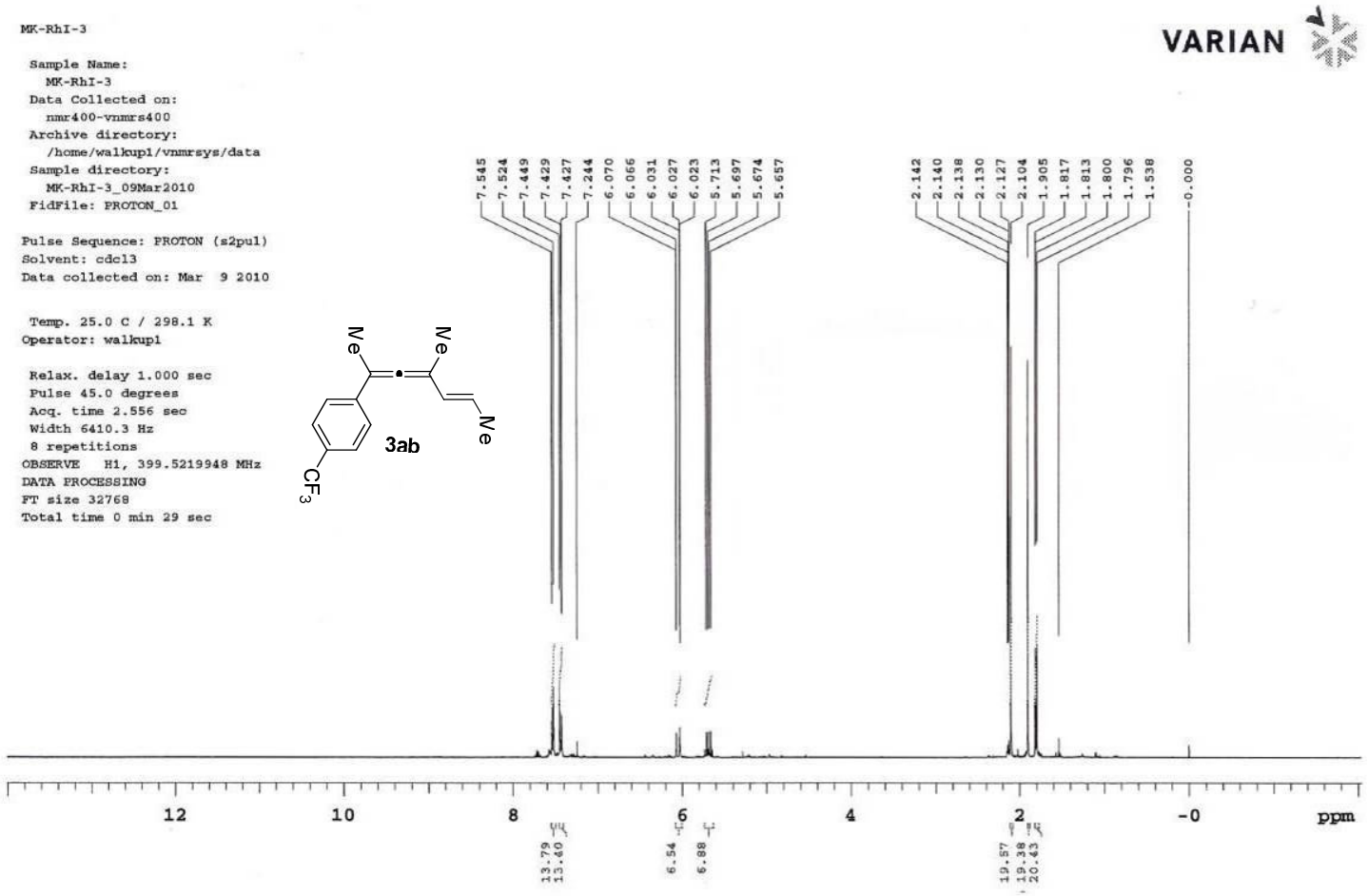

Figure D.3. [1] H NMR of ((*E*)-2-(4-(trifluoromethyl)-phenyl)-4-methylhepta-2,3,5-triene

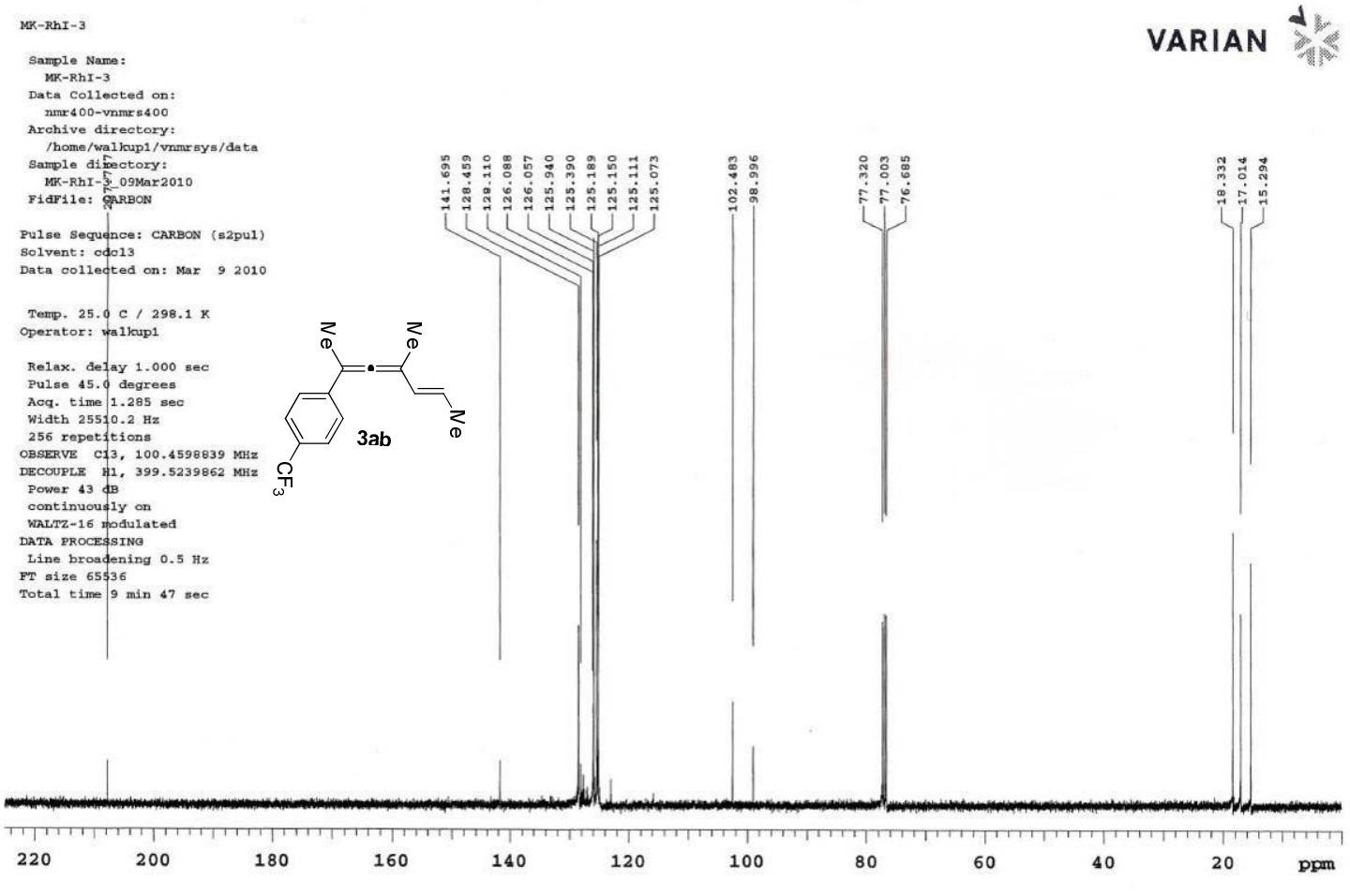

Figure D.4. ^{13} C NMR of ((*E*)-2-(4-(trifluoromethyl)-phenyl)-4-methylhepta-2,3,5-triene

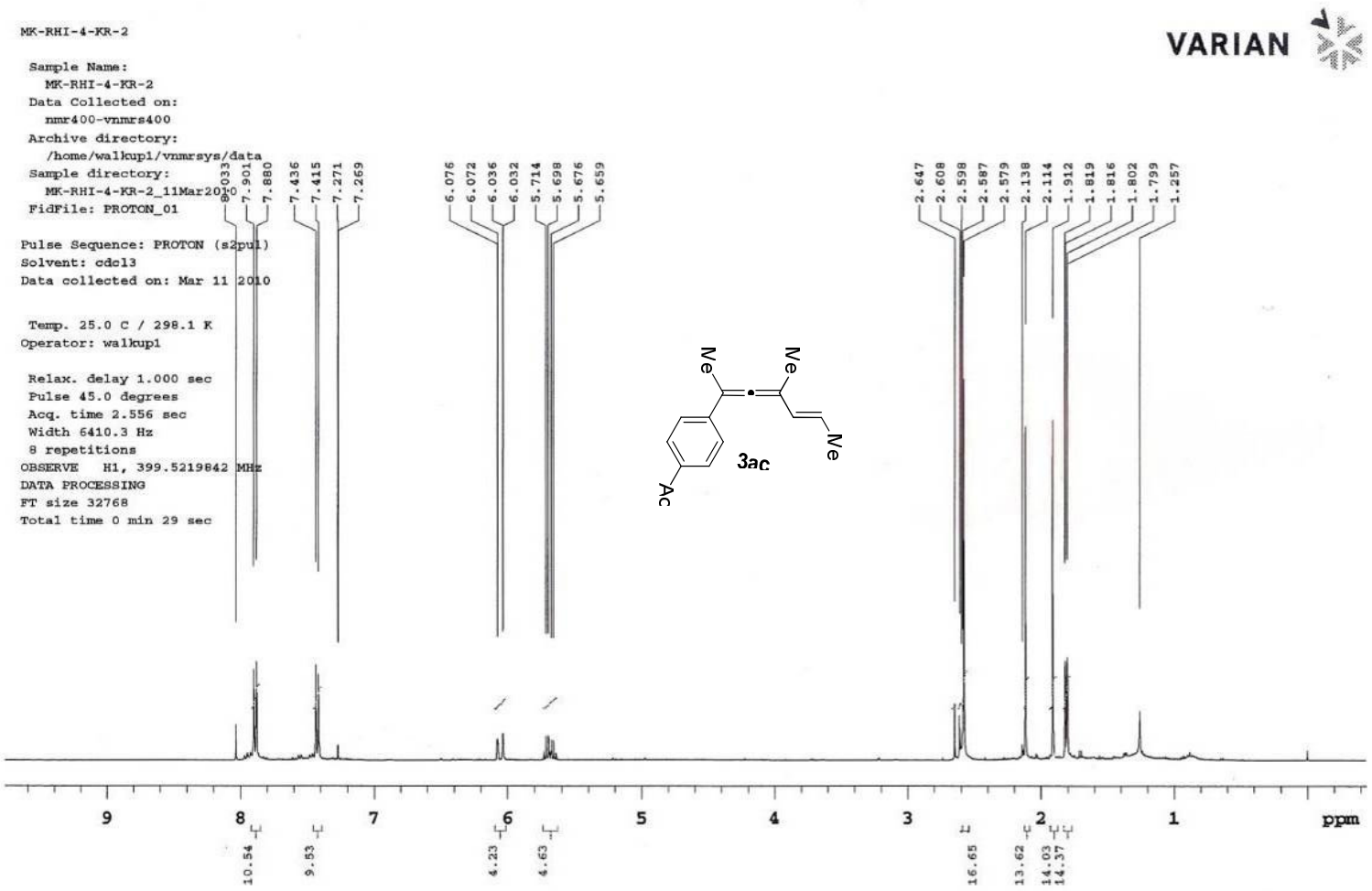

Figure D.5. [1] H NMR of (*E*)-2-(4-acetylphenyl)-4-methylhepta-2,3,5-triene

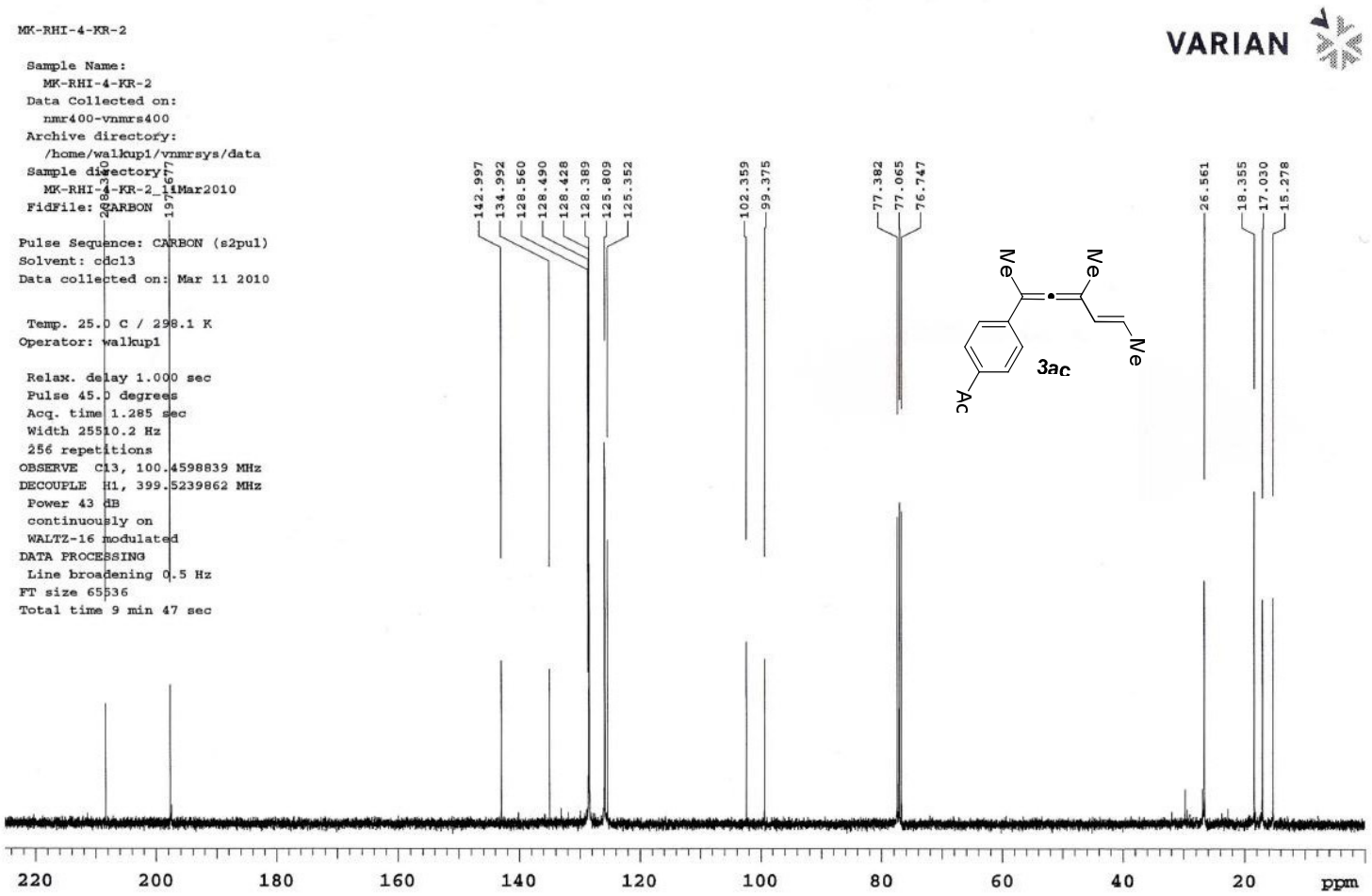

Figure D.6. ^{13} C NMR of (*E*)-2-(4-acetylphenyl)-4-methylhepta-2,3,5-triene

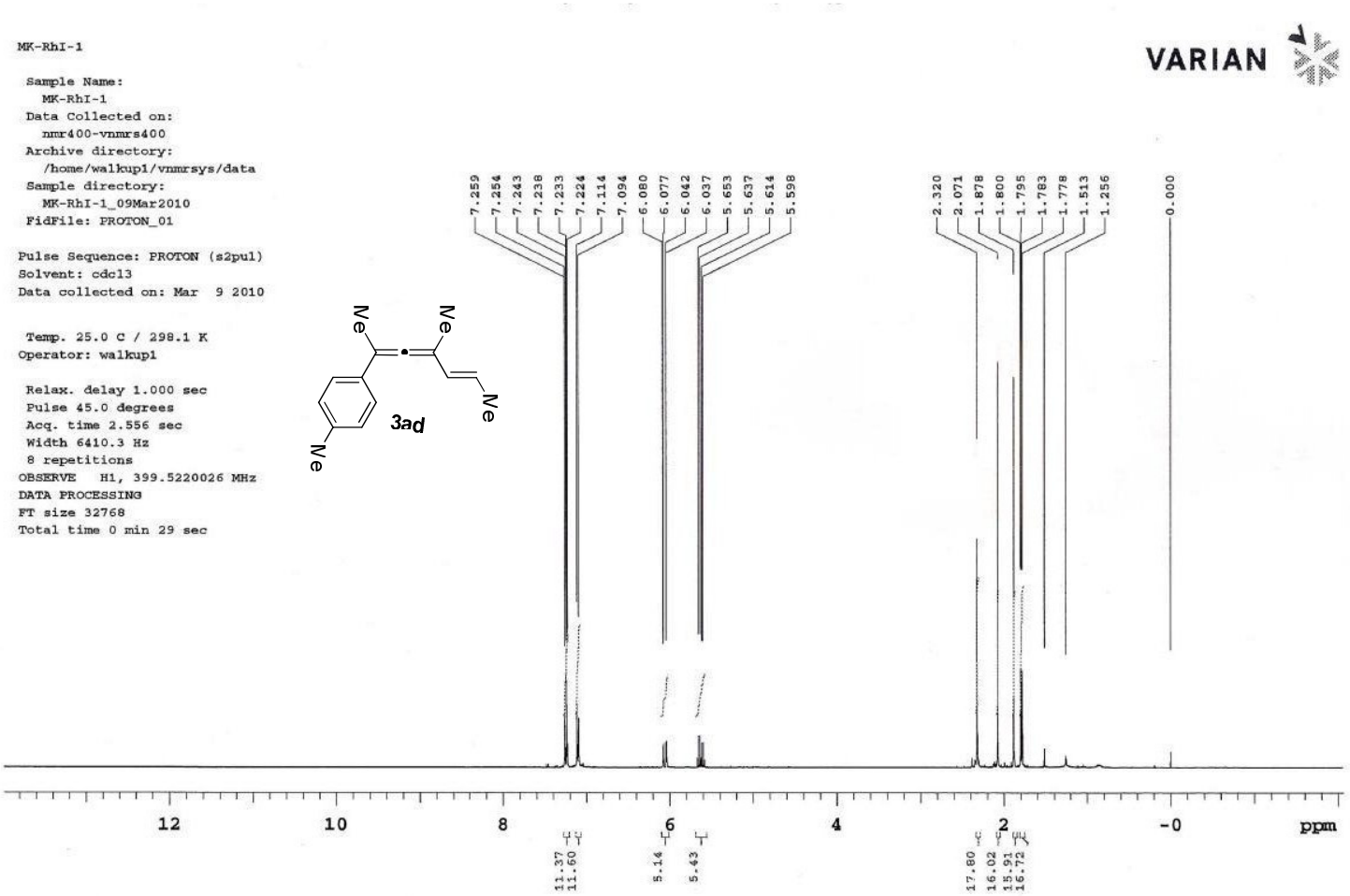

Figure D.7. [1] H NMR of (*E*)-2-(4-meyhylphenyl)-4-methylhepta-2,3,5-triene

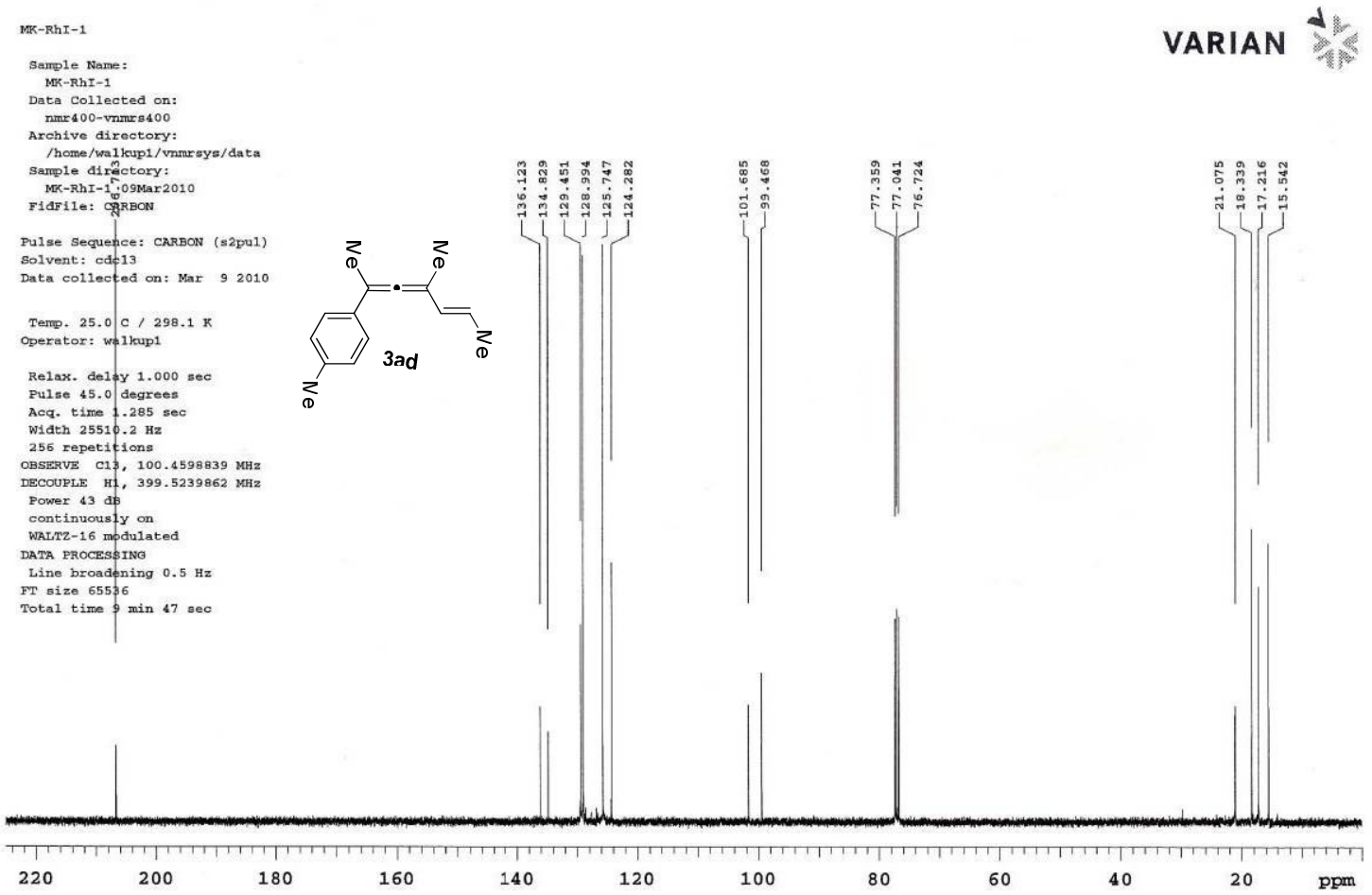

Figure D.8. ^{13} C NMR of (*E*)-2-(4-meyhylphenyl)-4-methylhepta-2,3,5-triene

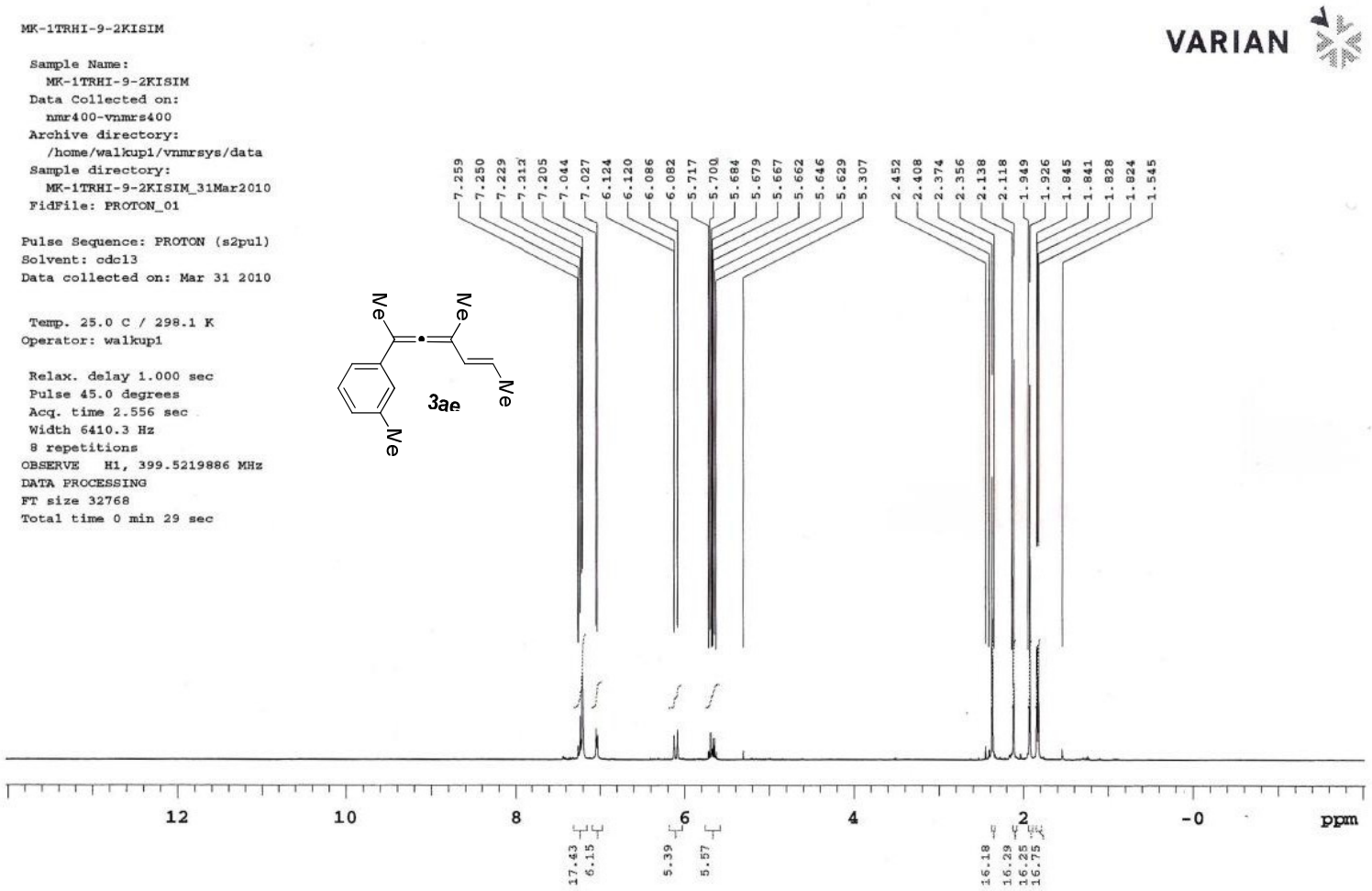

Figure D.9. [1] H NMR of (*E*)-2-(3-meyhylphenyl)-4-methylhepta-2,3,5-triene

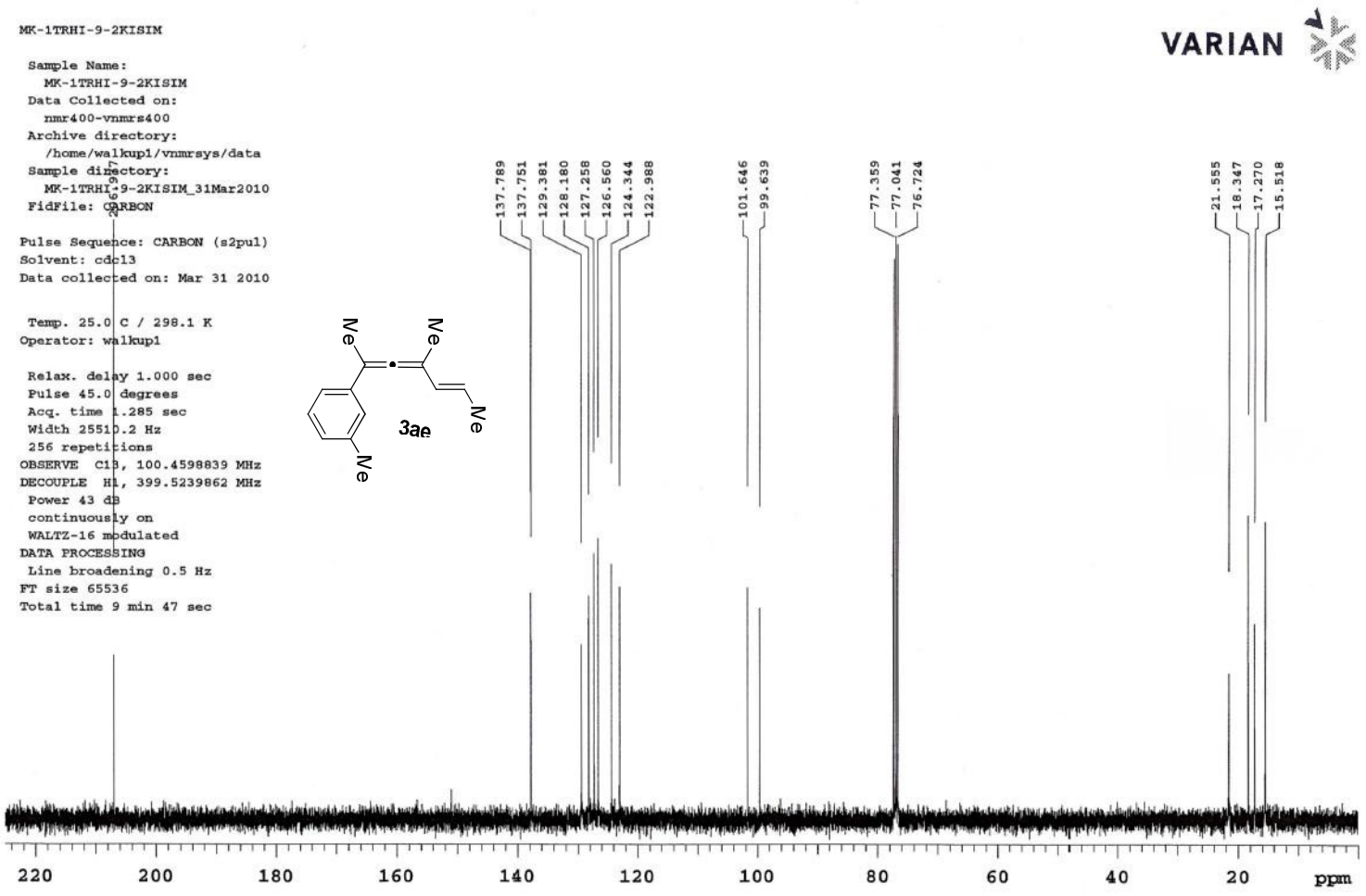

Figure D.10. [13] C NMR of (*E*)-2-(3-meyhylphenyl)-4-methylhepta-2,3,5-triene

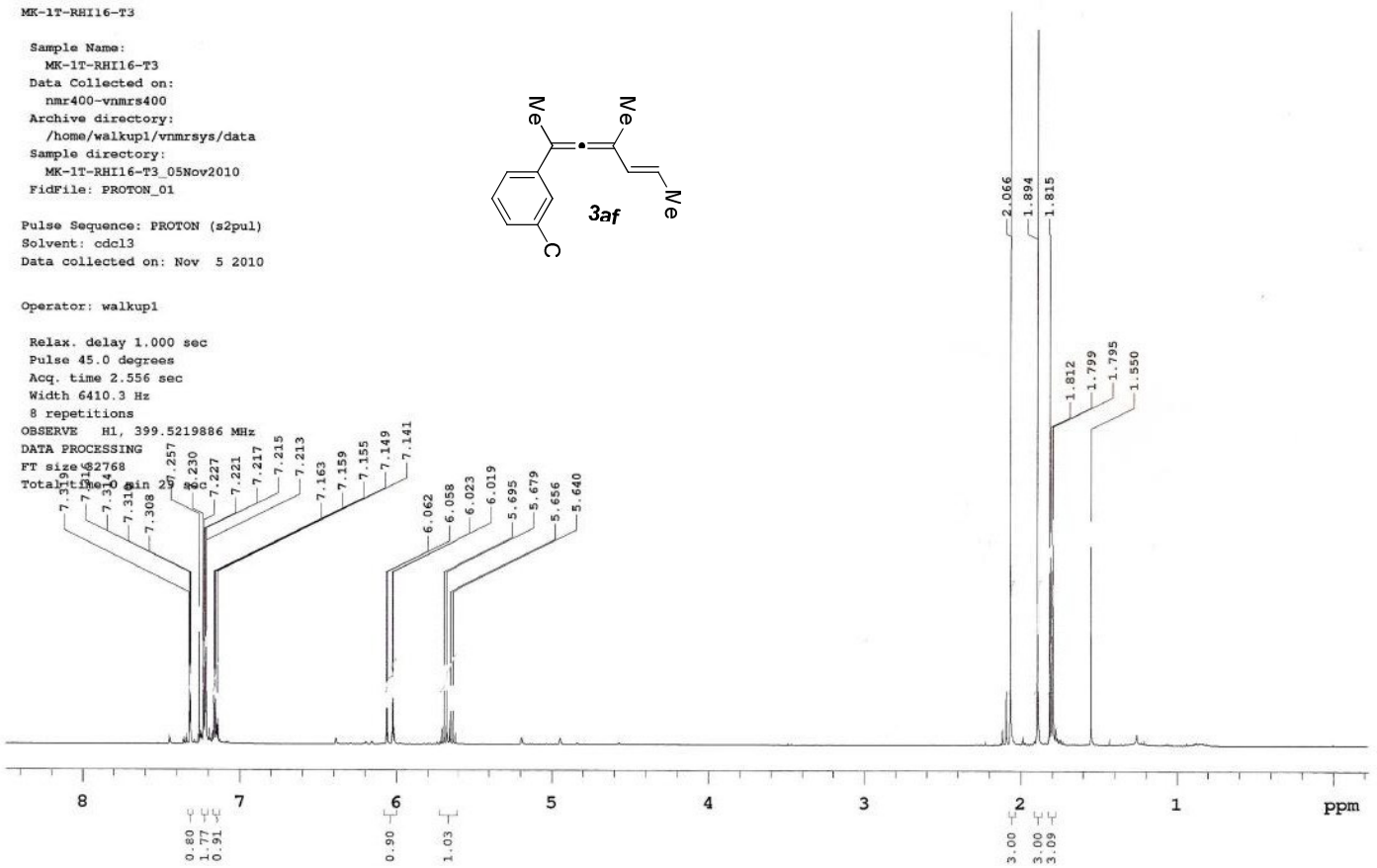

Figure D.11. [1] H NMR of (*E*)-2-(3-chlorophenyl)-4-methylhepta-2,3,5-triene

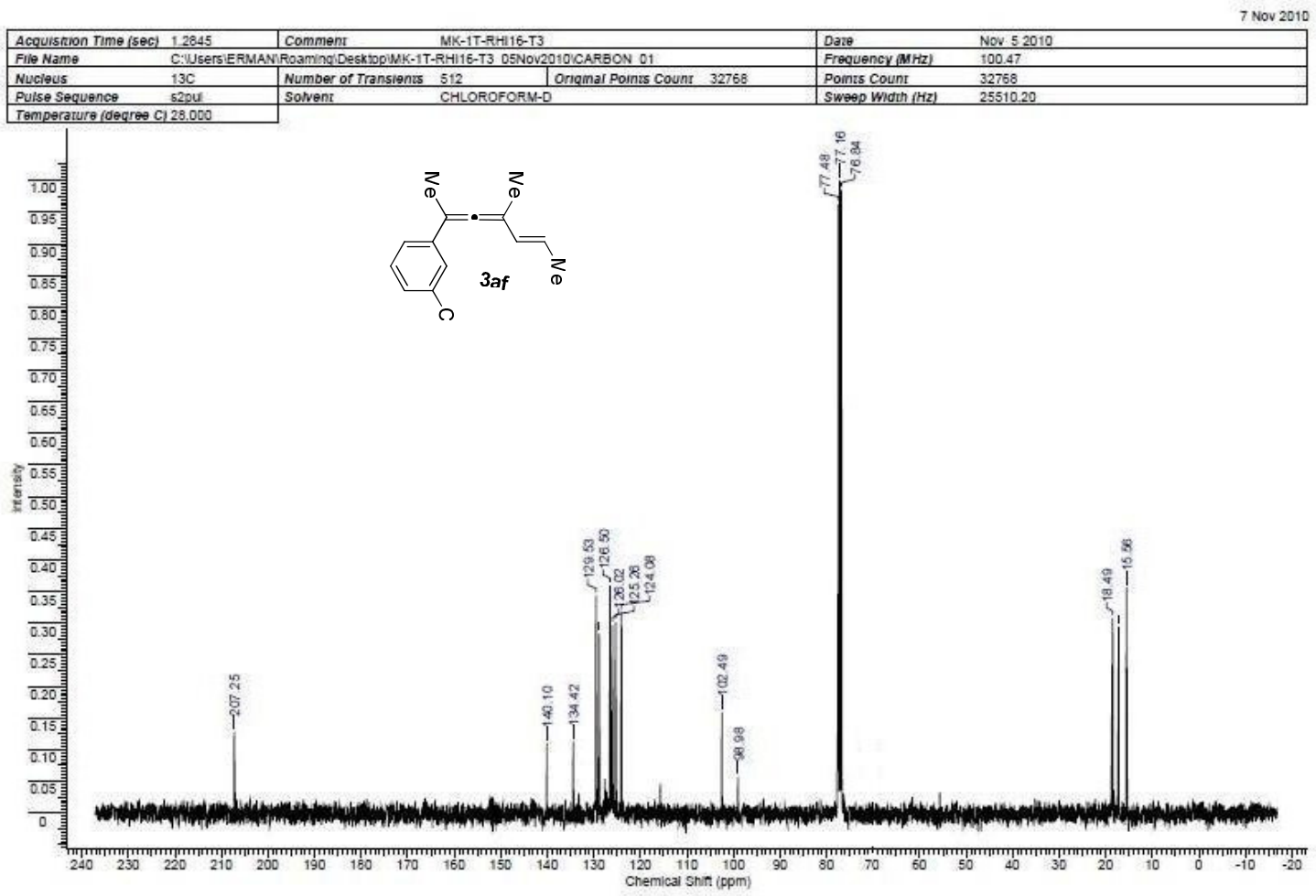

Figure D.12. ^{13} C NMR of (*E*)-2-(3-chlorophenyl)-4-methylhepta-2,3,5-triene

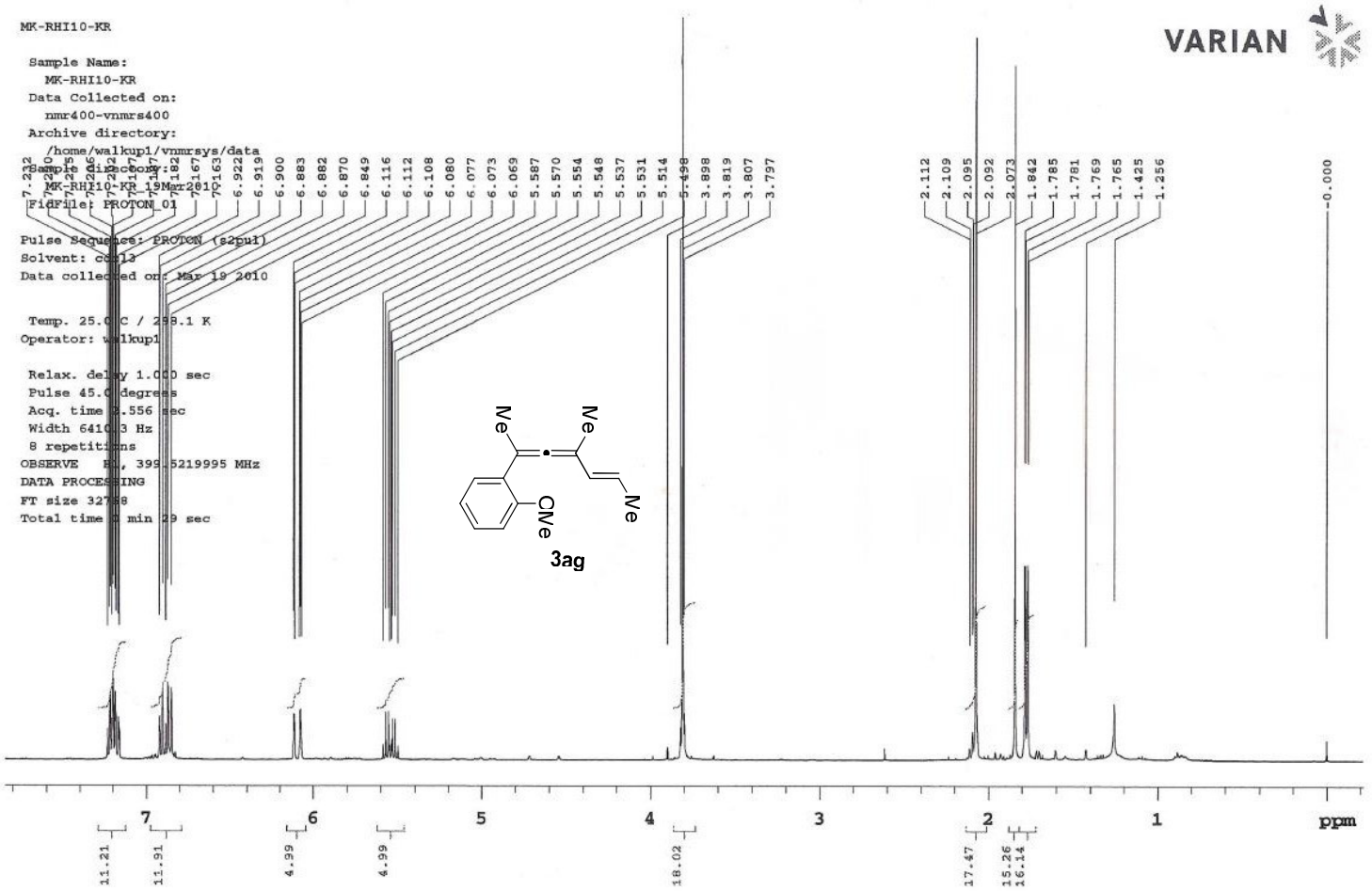

Figure D.13. [1] H NMR of (*E*)-2-(2-methoxyhenyl)-4-methylhepta-2,3,5-triene

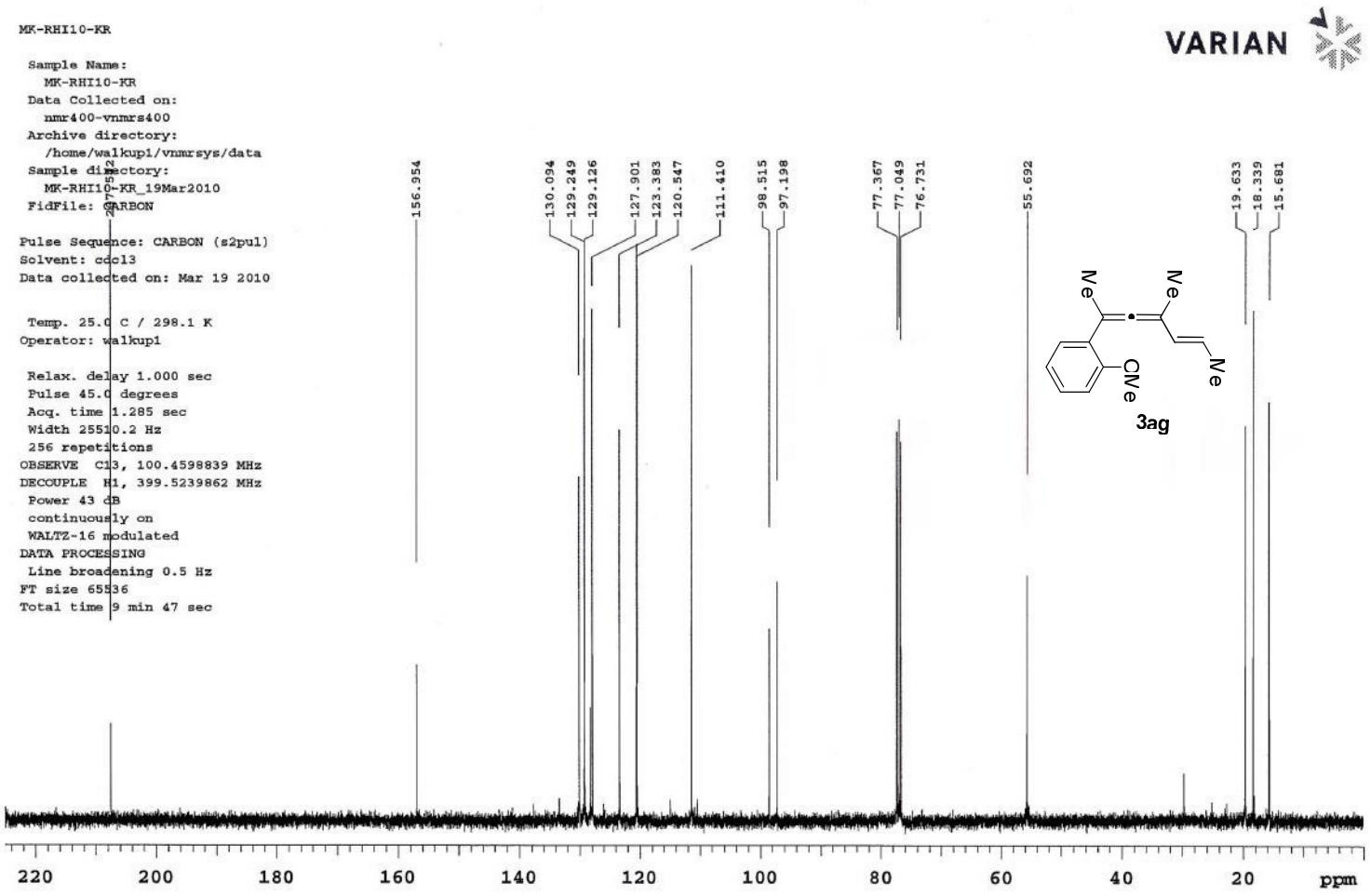

Figure D.14. ^{13} C NMR of (*E*)-2-(2-methoxyhenyl)-4-methylhepta-2,3,5-triene

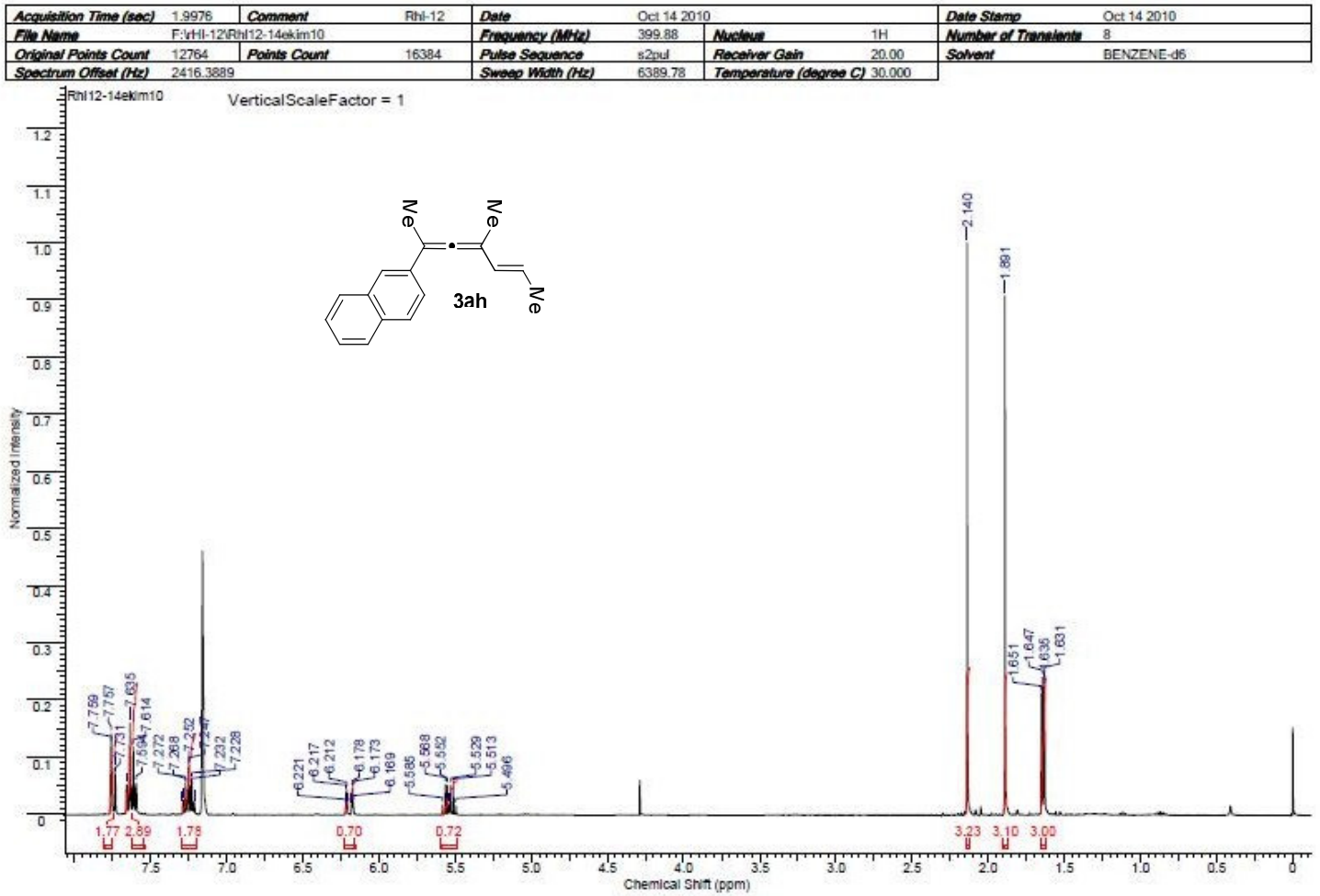

Figure D.15. [1] H NMR of ((*E*)- 2-(2-naphthyl)-4-methylhepta-2,3,5-triene

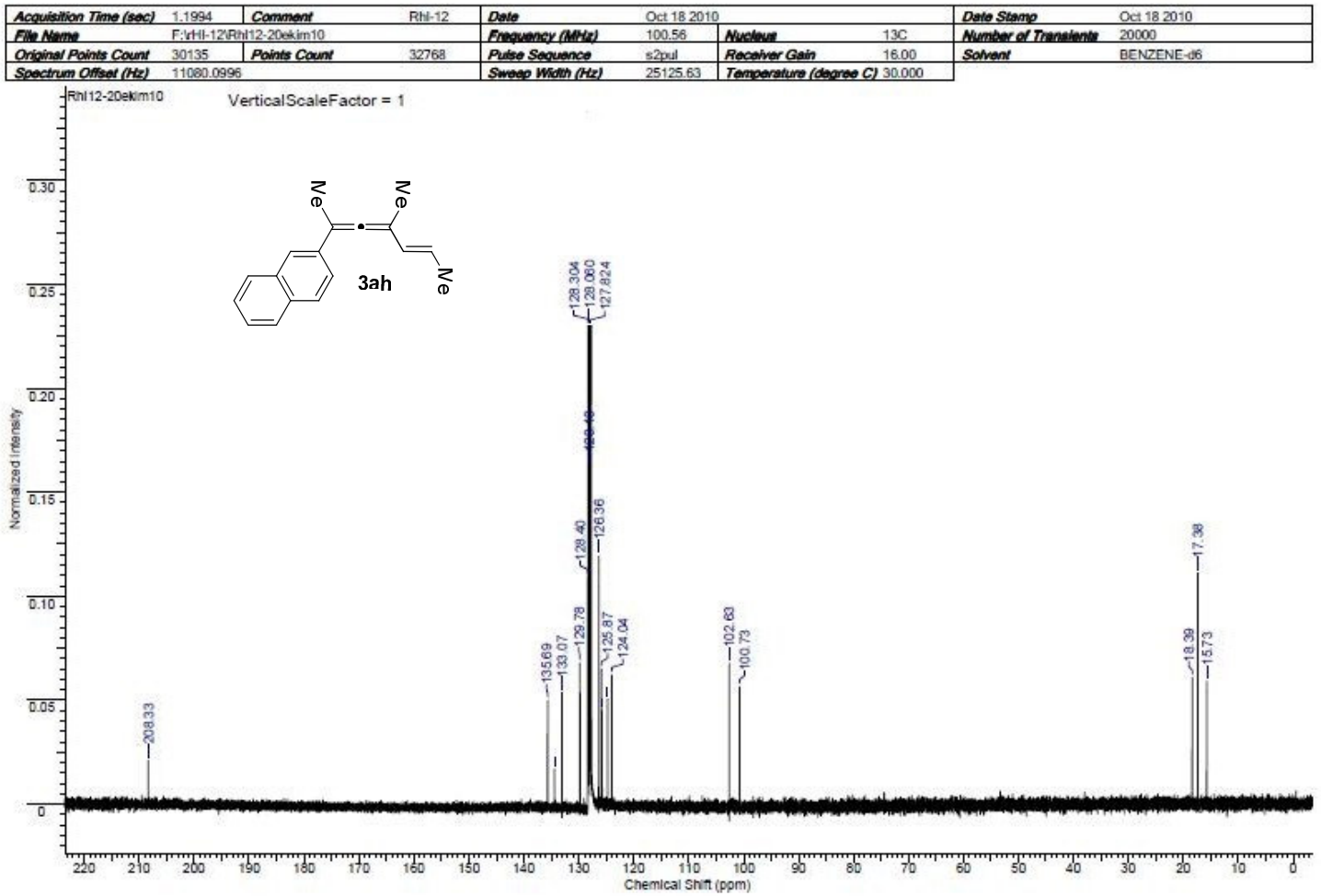

Figure D.16. [13] C NMR of ((*E*)- 2-(2-naphthyl)-4-methylhepta-2,3,5-triene

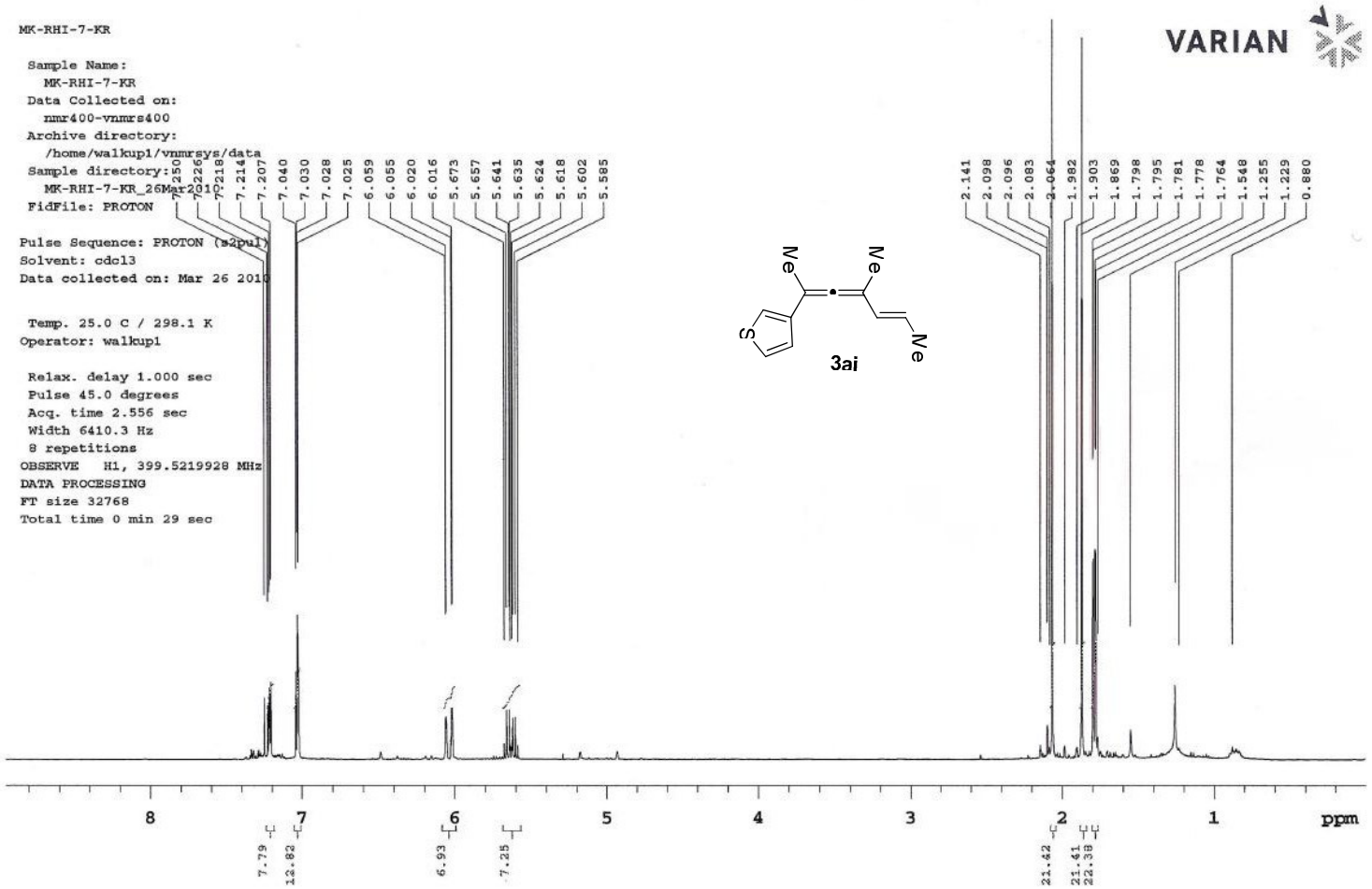

Figure D.17. [1] H NMR of (*E*)- 2-(3-thienyl)-4-methylhepta-2,3,5-triene

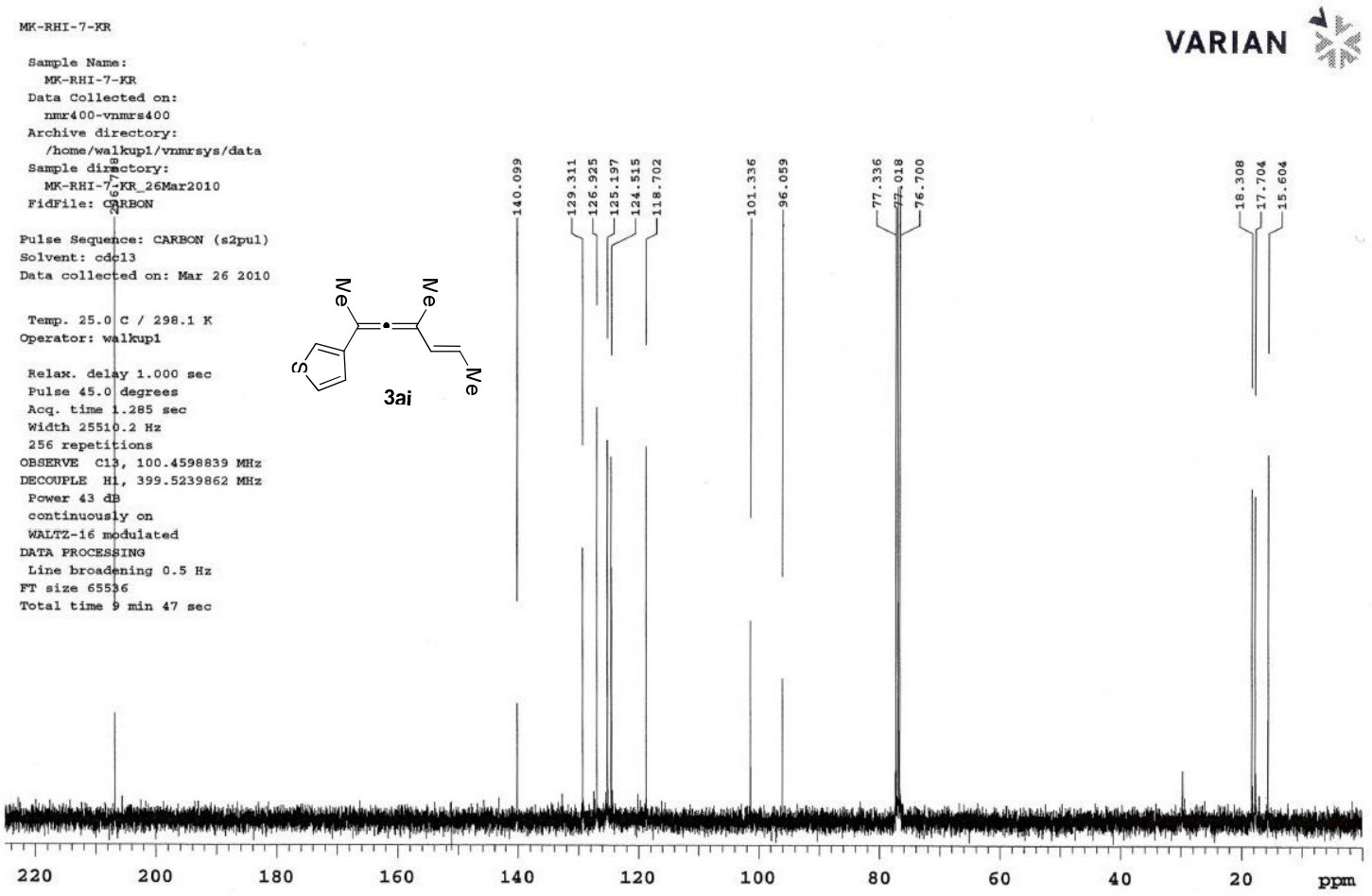

Figure D.18. ^{13} C NMR of (*E*)- 2-(3-thienyl)-4-methylhepta-2,3,5-triene

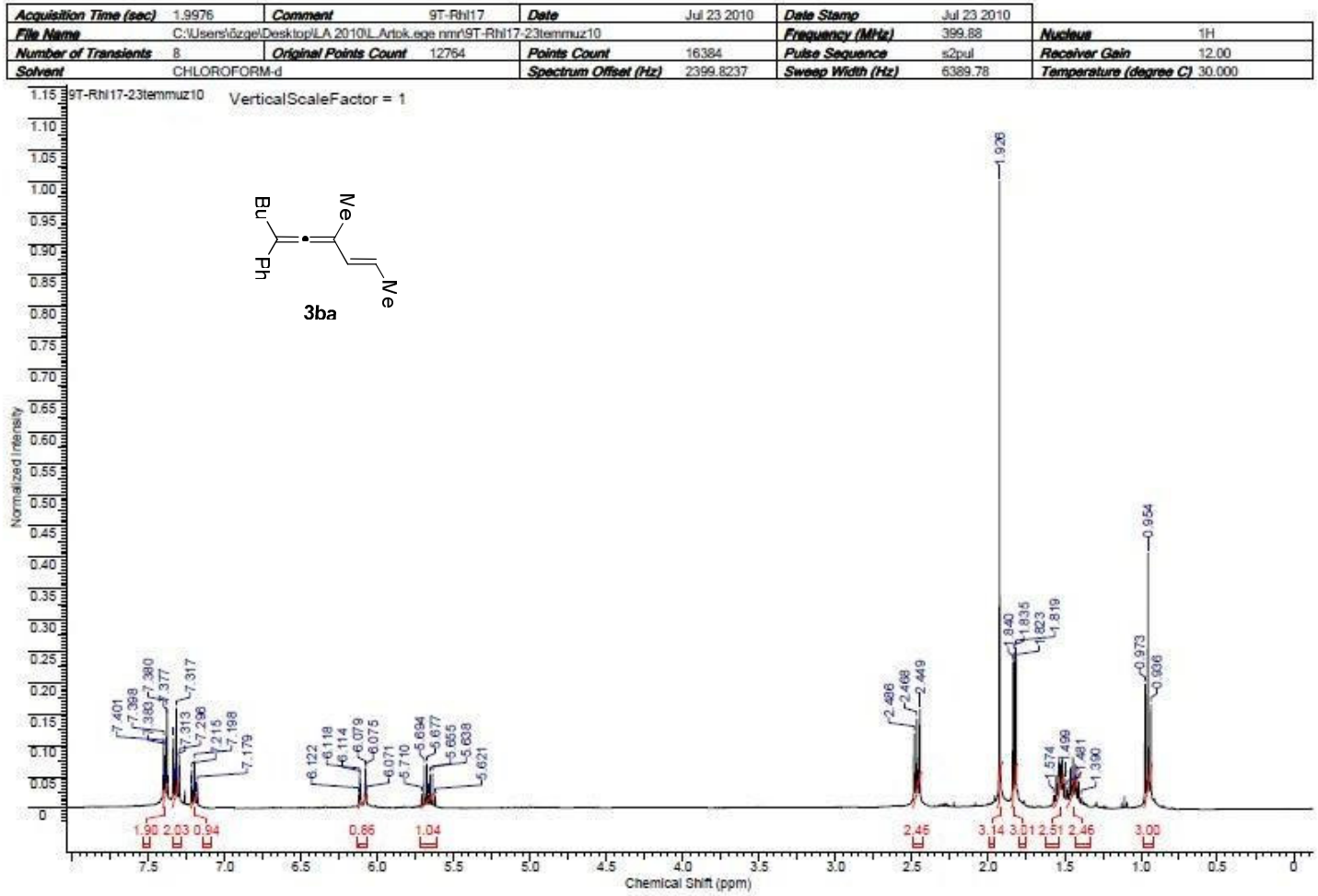

Figure D.19. [1] H NMR of (*E*)- 6-phenyl-4-methyldeca-2,4,5-triene

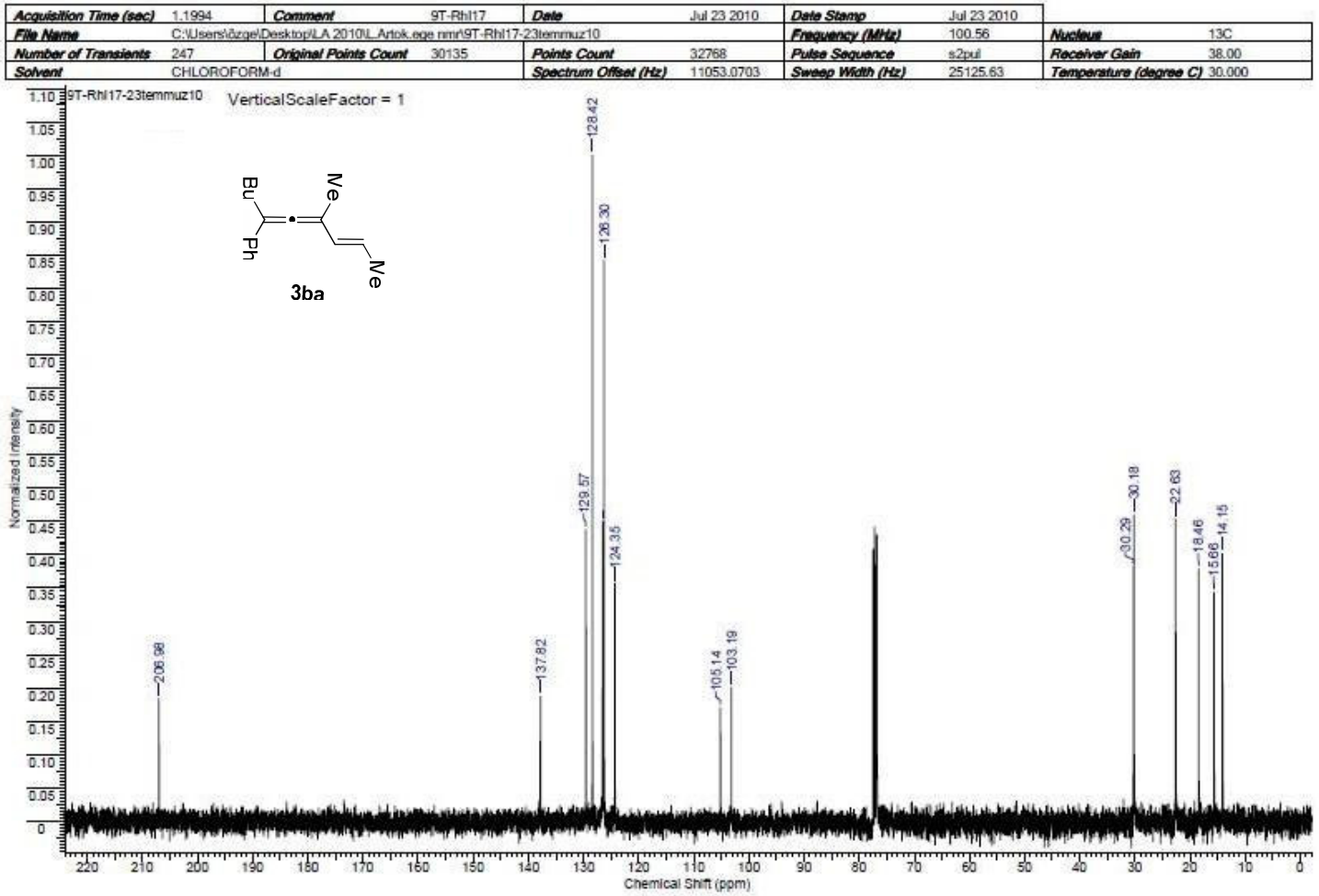

Figure D.20. [13] C NMR of (*E*)- 6-phenyl-4-methyldeca-2,4,5-triene

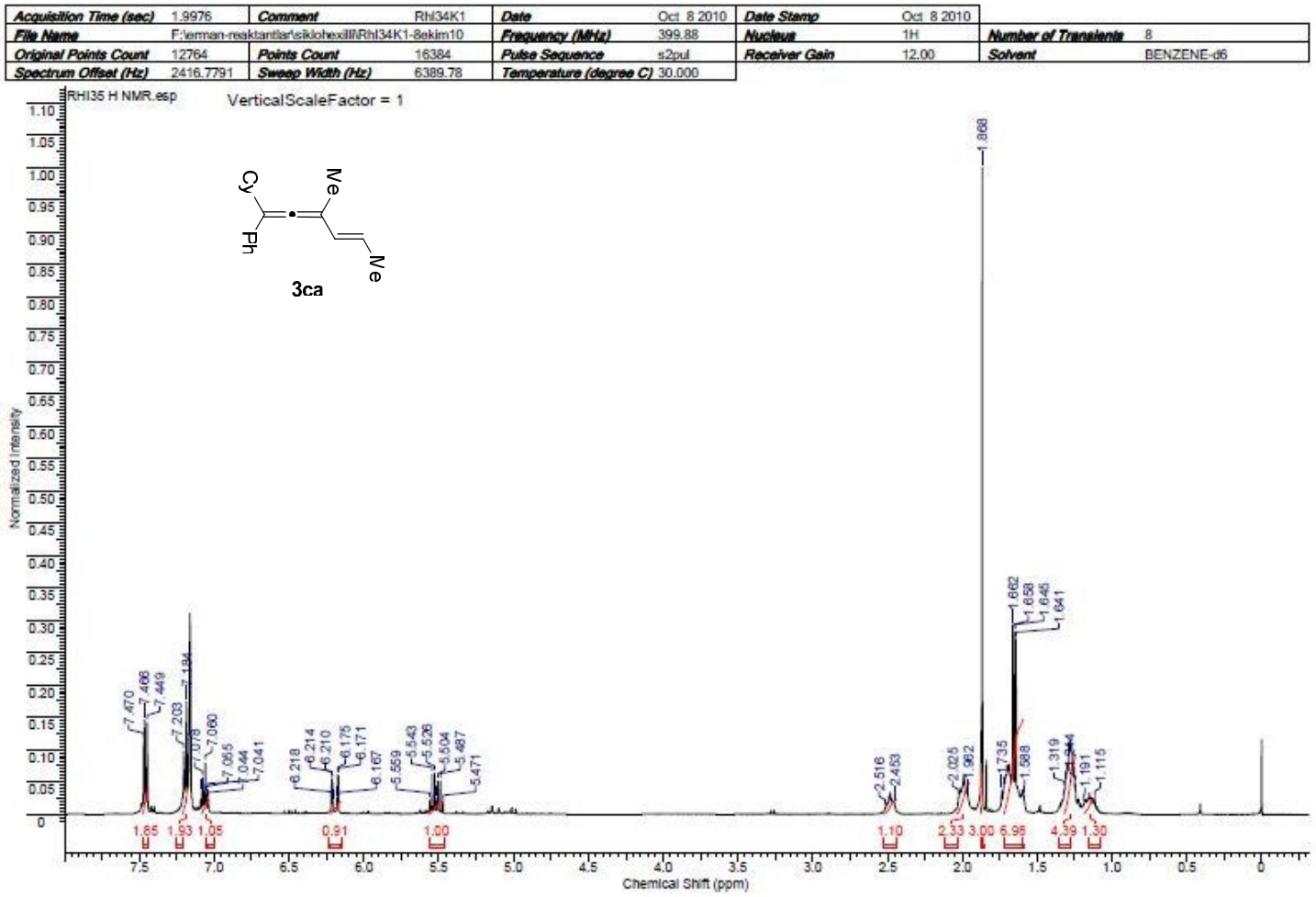

Figure D.21. [1] H NMR of (*E*)-1-cyclohexyl-1-phenyl-3-methyl-hexa-1,2,4-triene

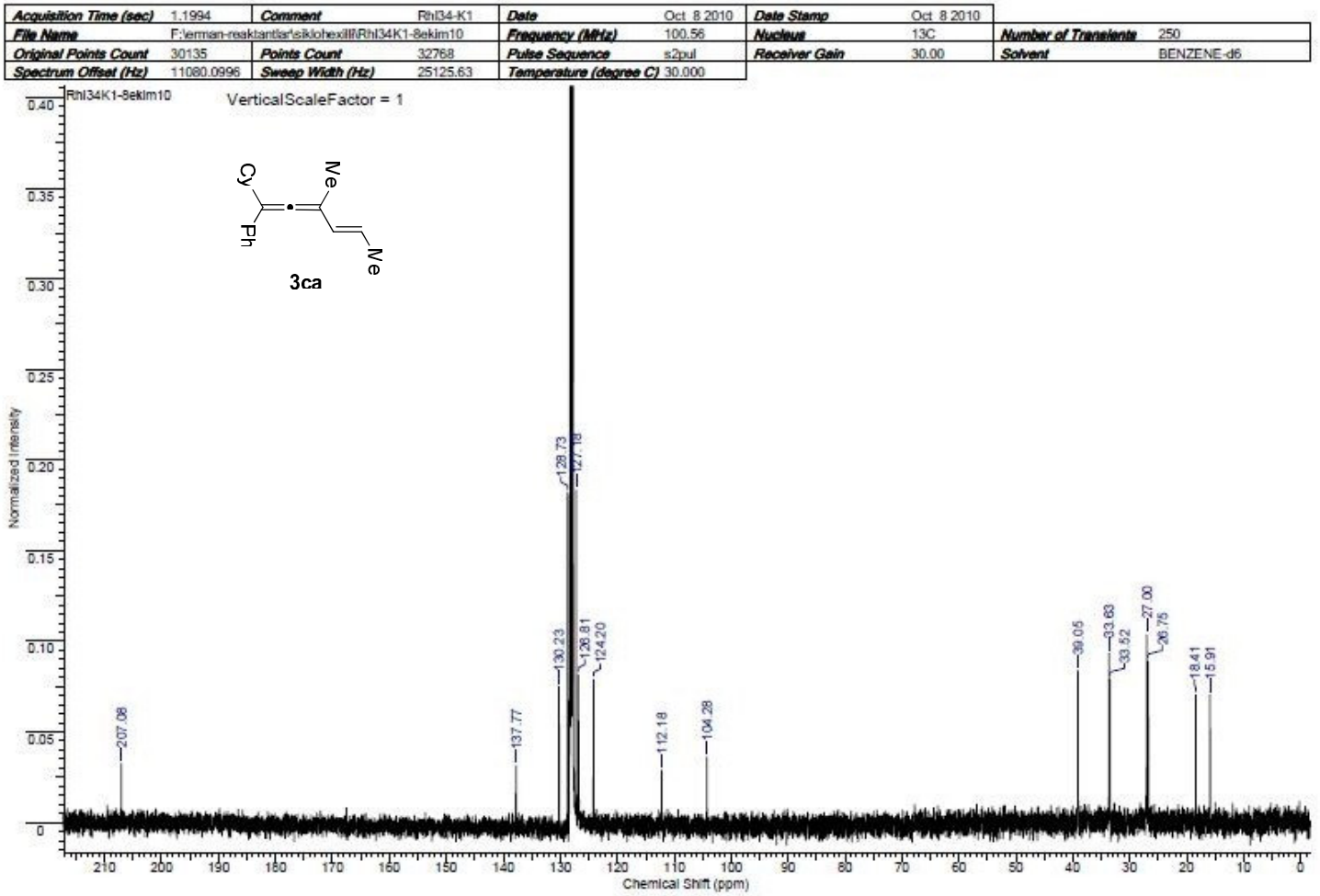

Figure D.22. ^{13} C NMR of (*E*)-1-cyclohexyl-1-phenyl-3-methyl-hexa-1,2,4-triene

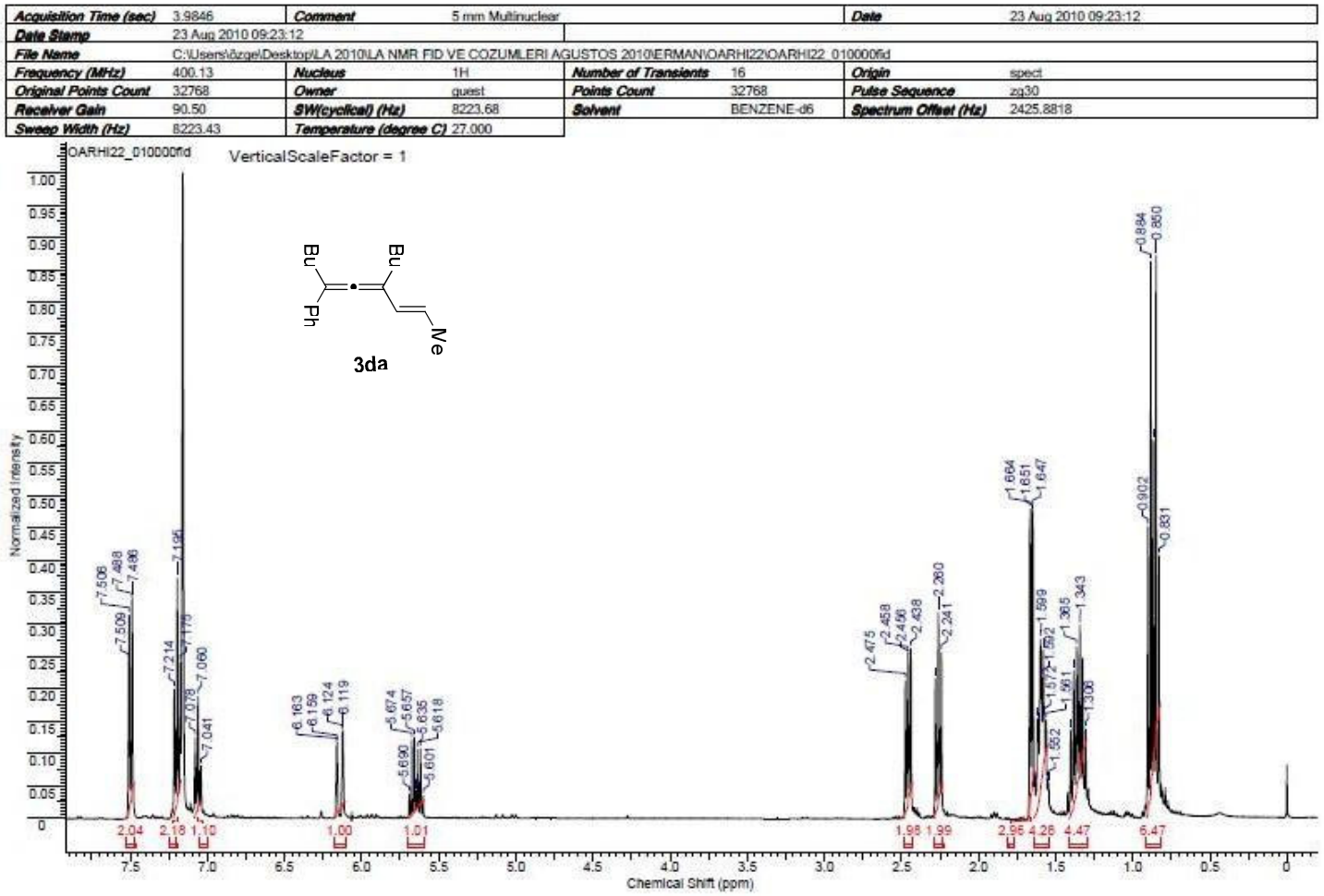

Figure D.23. [1] H NMR of (E)-5-phenyl-7-(prop-1-enyl)undeca-5,6-diene

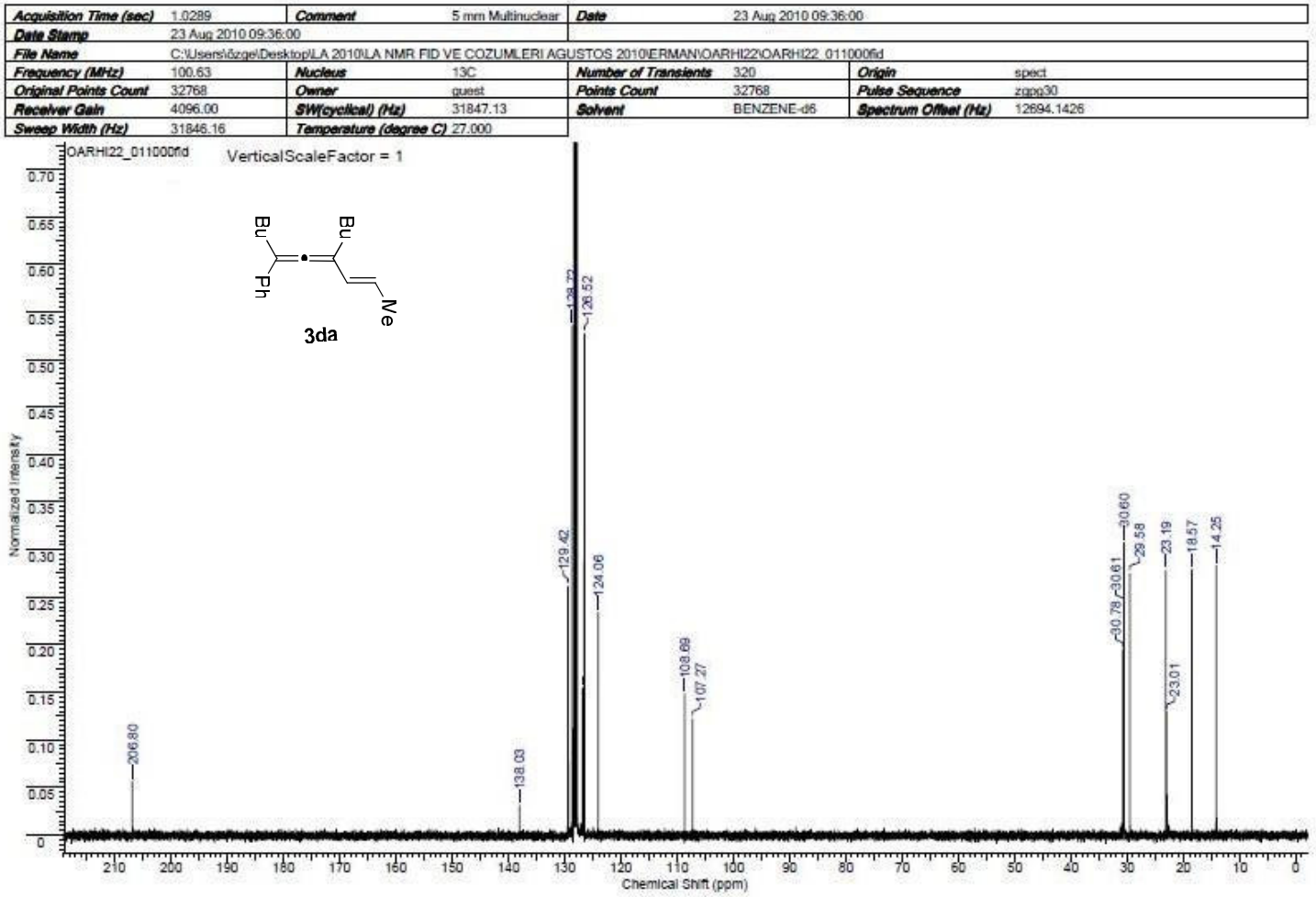

Figure D.24. [1] H NMR of (E)-5-phenyl-7-(prop-1-enyl)undeca-5,6-diene

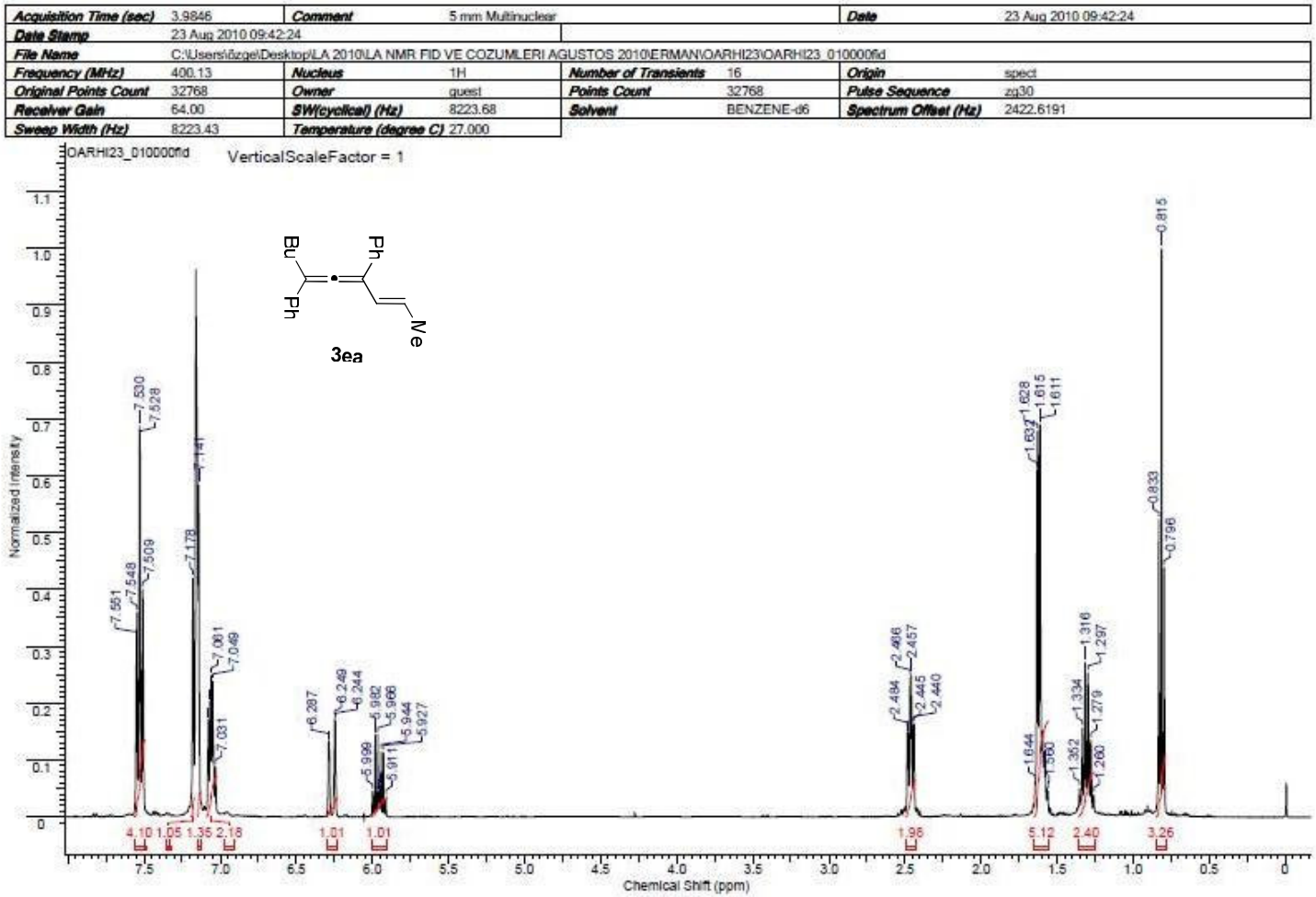

Figure D.25. [1] H NMR of (E)-4,6-diphenyl-deca-2,4,5-triene

Acquisition Time (sec)	1.0289	**Comment**	5 mm Multinuclear	**Date**	23 Aug 2010 09:55:12		
Date Stamp	23 Aug 2010 09:55:12						
File Name	C:\Users\özge\Desktop\LA 2010\LA NMR FID VE COZUMLERI AGUSTOS 2010\ERMAN\OARHI23\OARHI23_0110006d						
Frequency (MHz)	100.63	**Nucleus**	13C	**Number of Transients**	320	**Origin**	spect
Original Points Count	32768	**Owner**	guest	**Points Count**	32768	**Pulse Sequence**	zgpg30
Receiver Gain	4096.00	**SW(cyclical) (Hz)**	31847.13	**Solvent**	BENZENE-d6	**Spectrum Offset (Hz)**	12693.1709
Sweep Width (Hz)	31846.16	**Temperature (degree C)**	27.000				

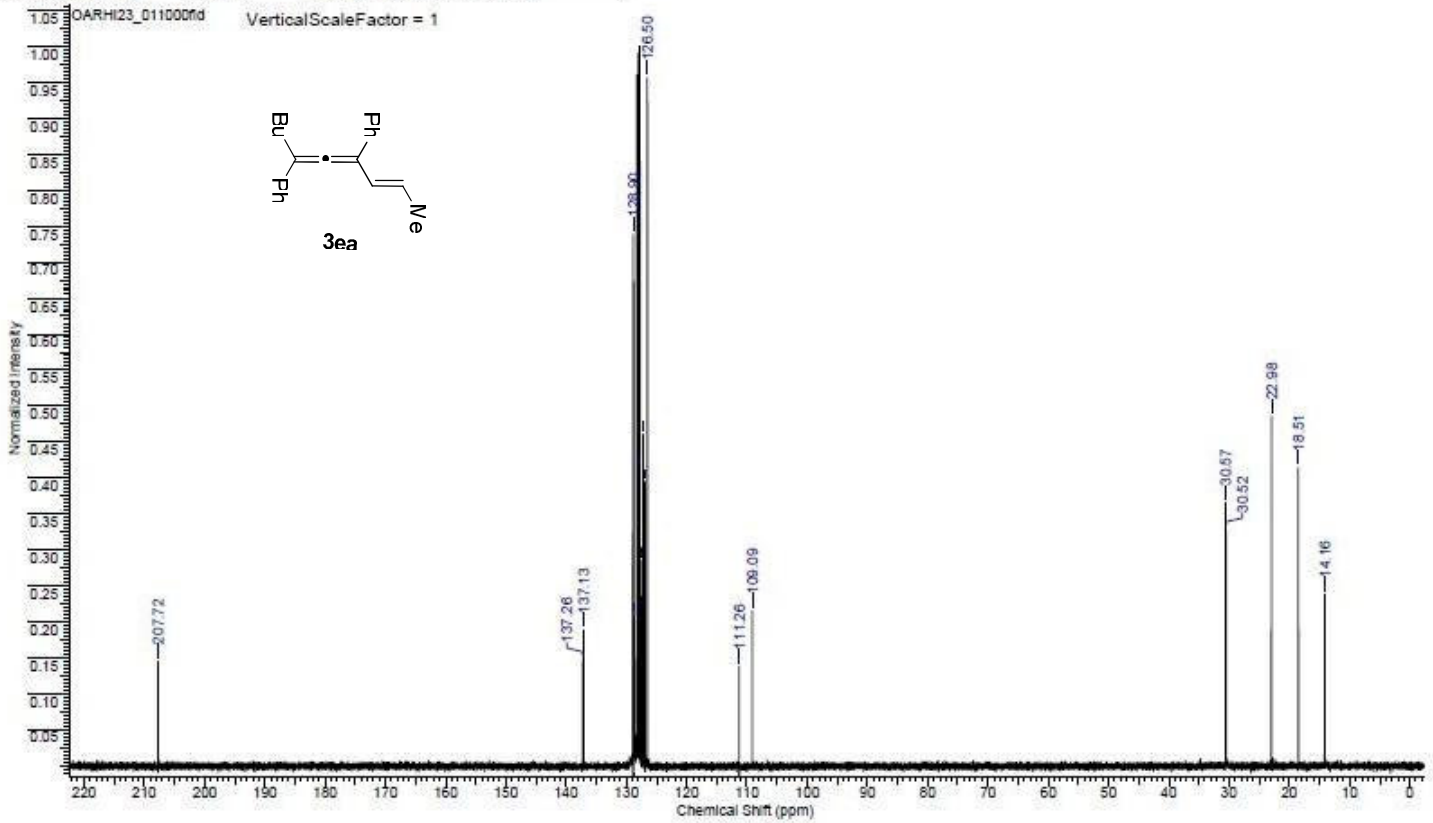

Figure D.26. ^{13} C NMR of (E)-4,6-diphenyl-deca-2,4,5-triene

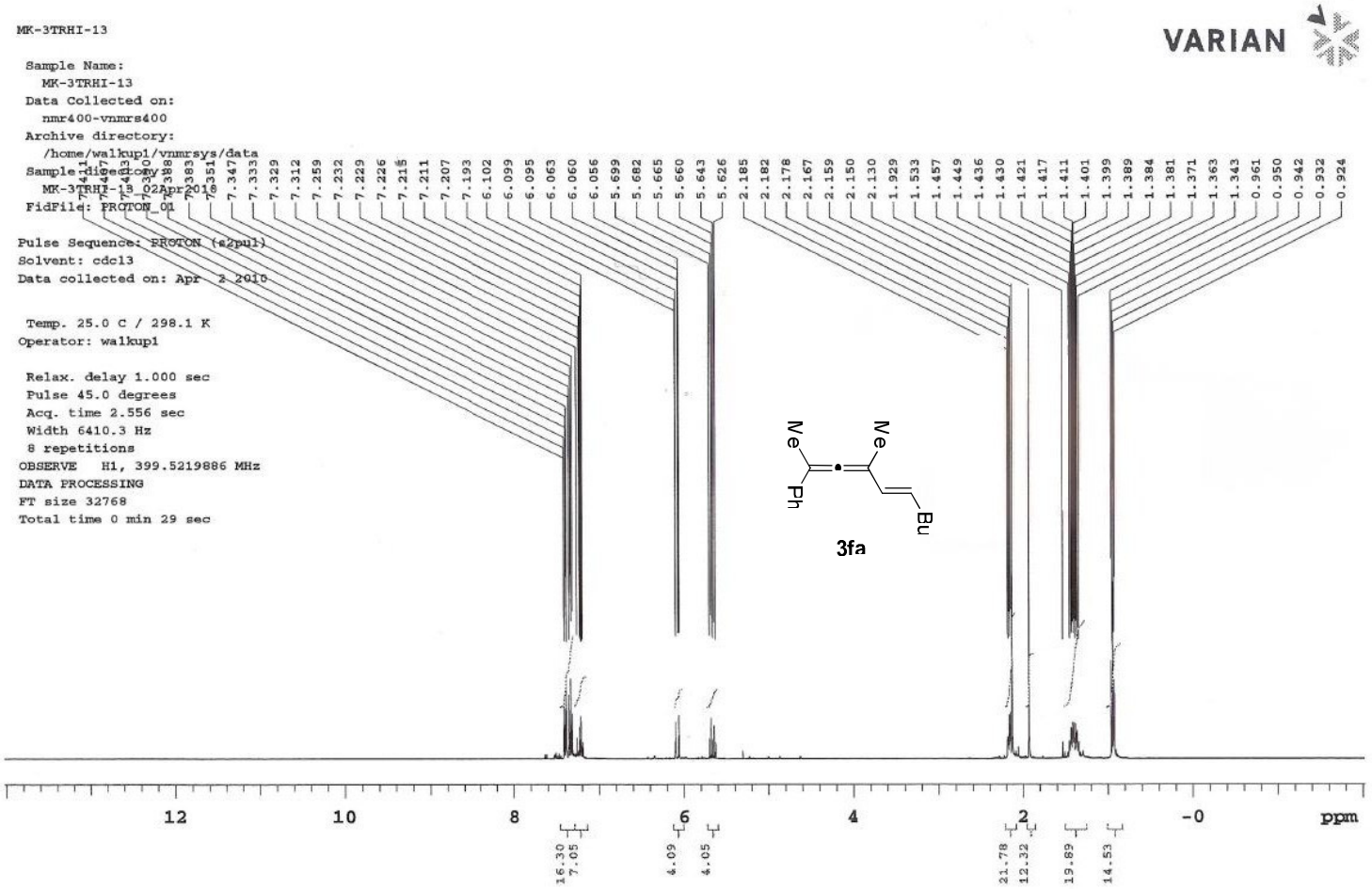

Figure D.27. [1] H NMR of (*E*)-4-methyl-2-phenyl-deca-2,3,5-triene

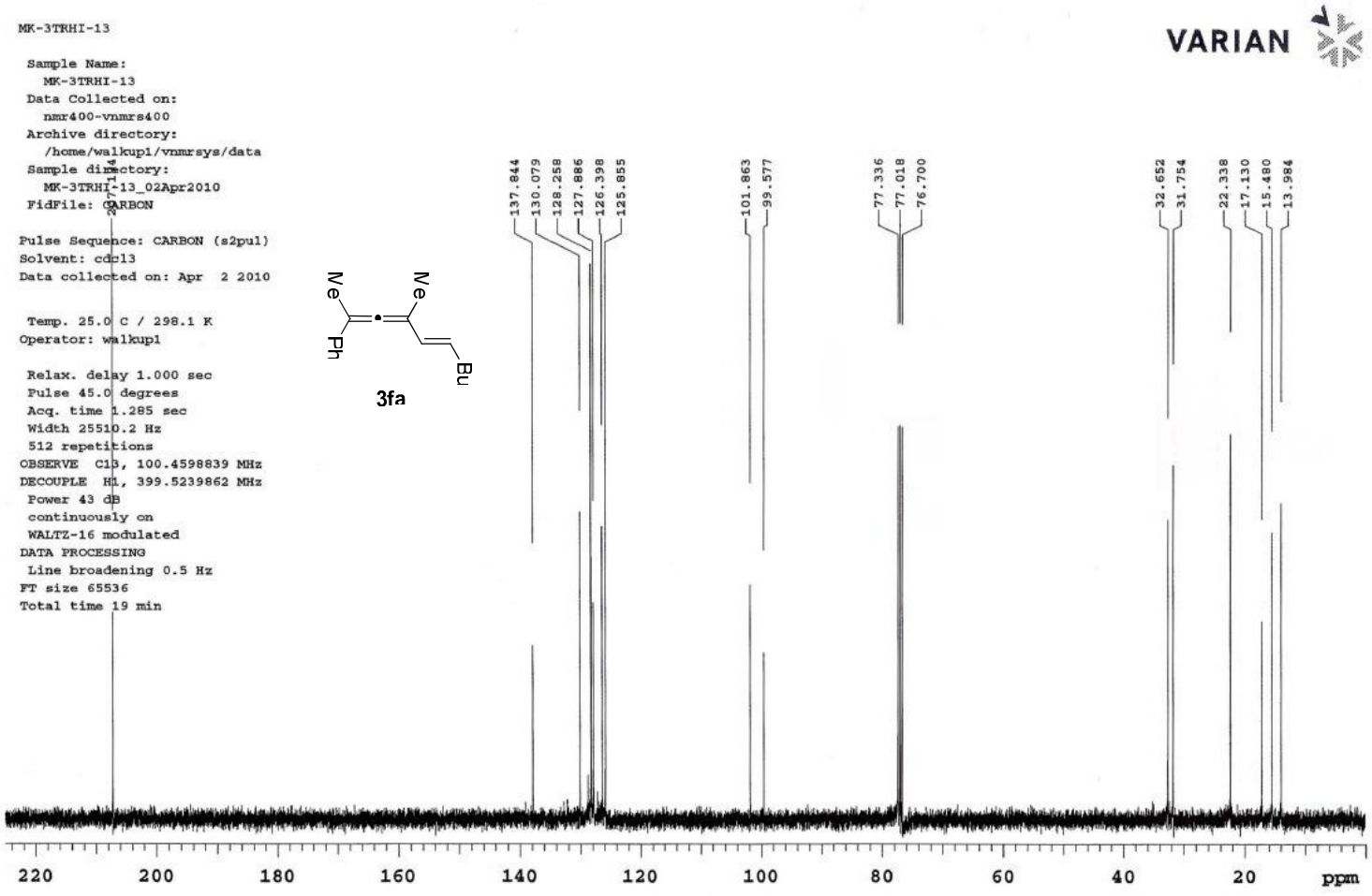

Figure D.28. ^{13} C NMR of (*E*)-4-methyl-2-phenyl-deca-2,3,5-triene

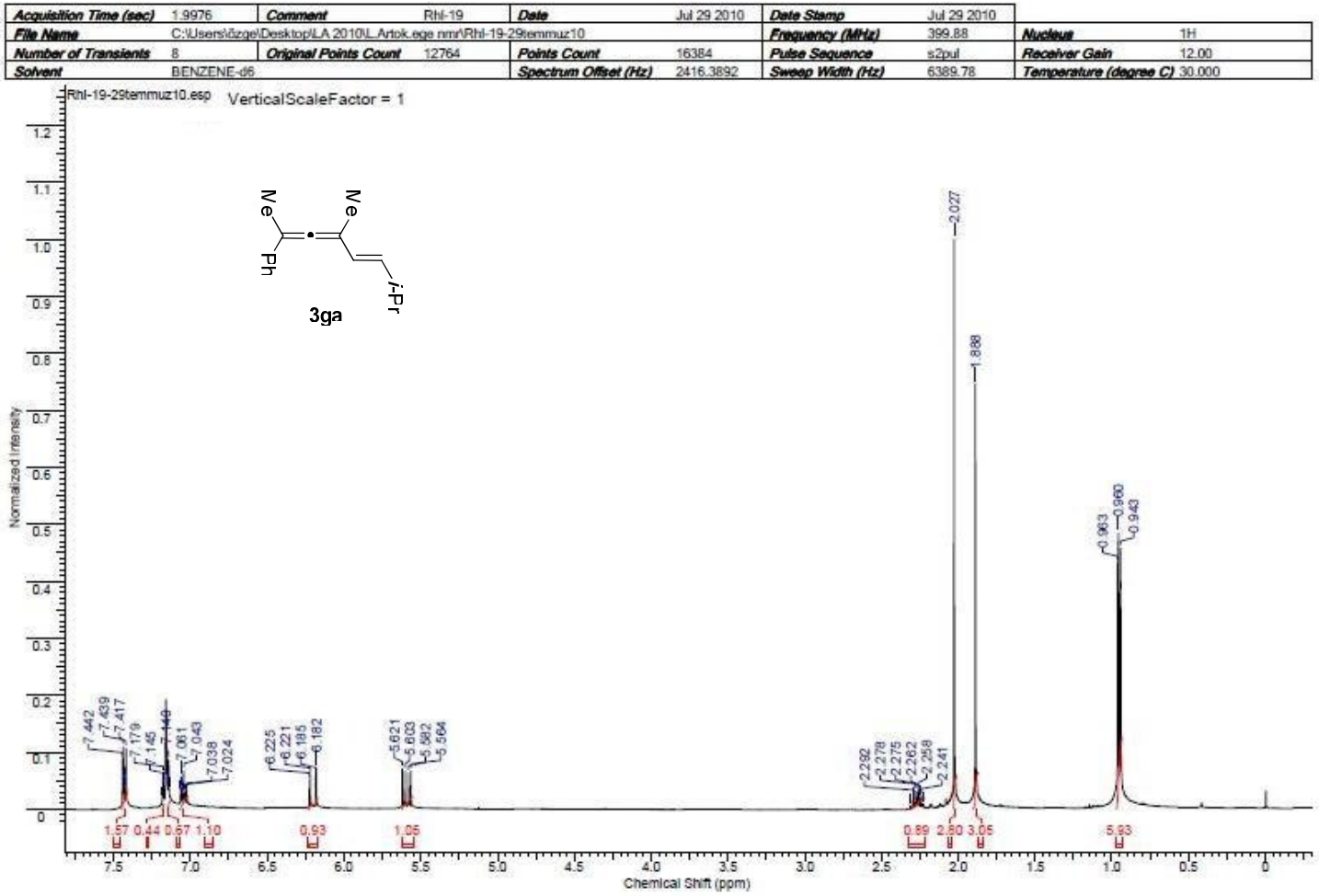

Figure D.29. [1] H NMR of (*E*)-4,7-dimethyl-2-phenyl-octa-2,3,5-triene

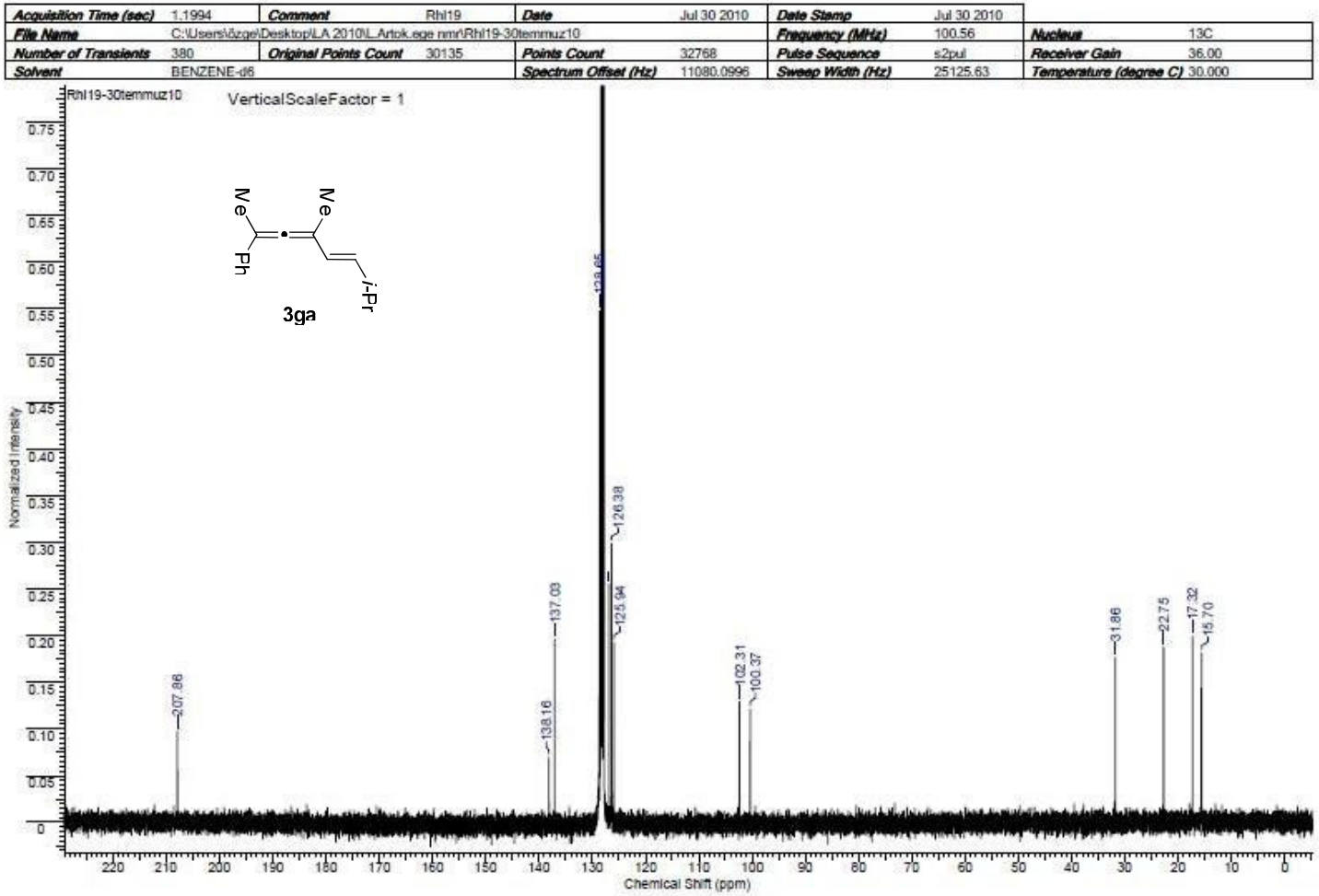

Figure D.30. [13] C NMR of (*E*)-4,7-dimethyl-2-phenyl-octa-2,3,5-triene

APPENDIX E

MASS SPECTRUMS OF PRODUCTS

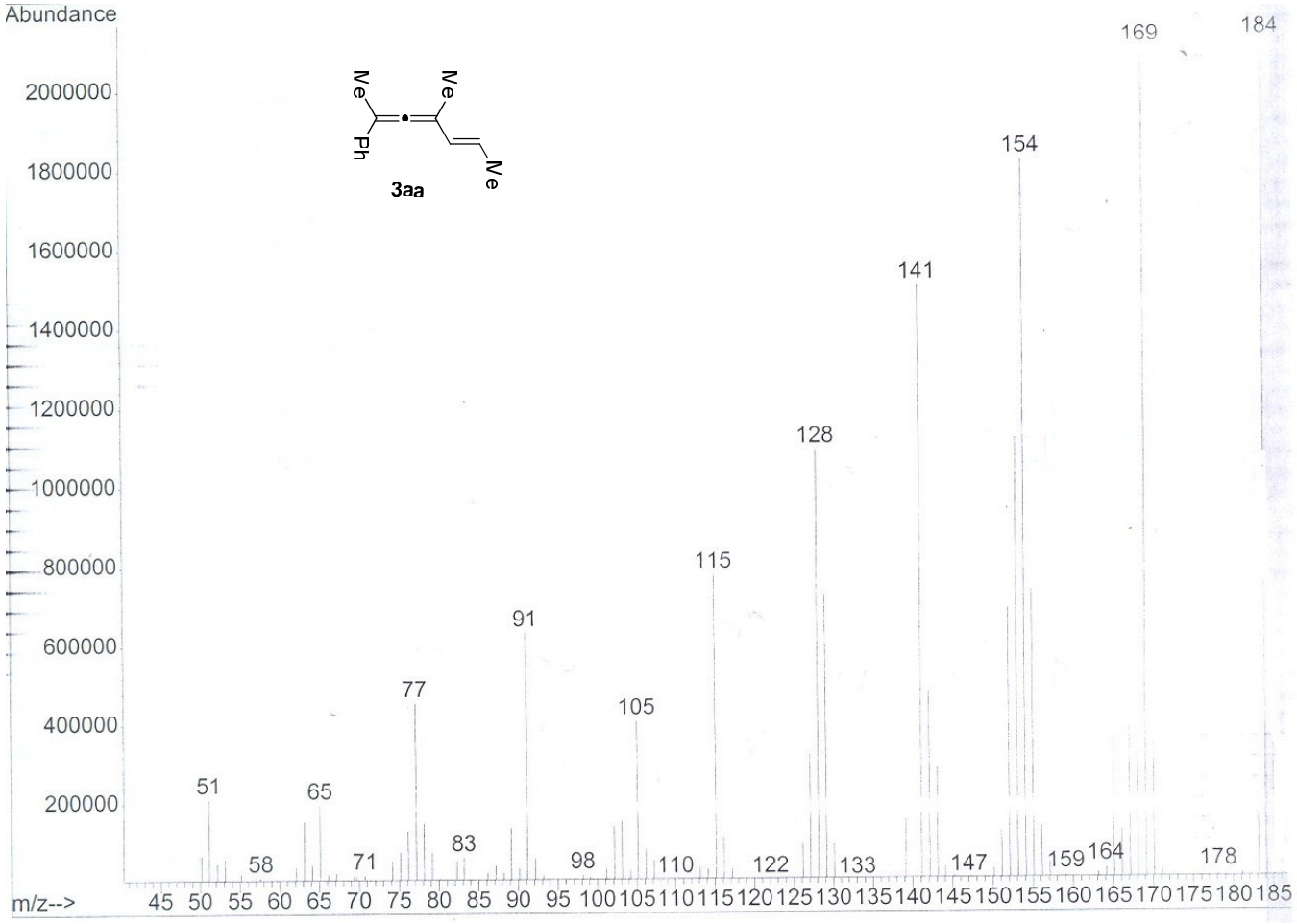

Figure E.1. Mass Spectrum of (*E*)- 2-phenyl-4-methylhepta-2,3,5-triene

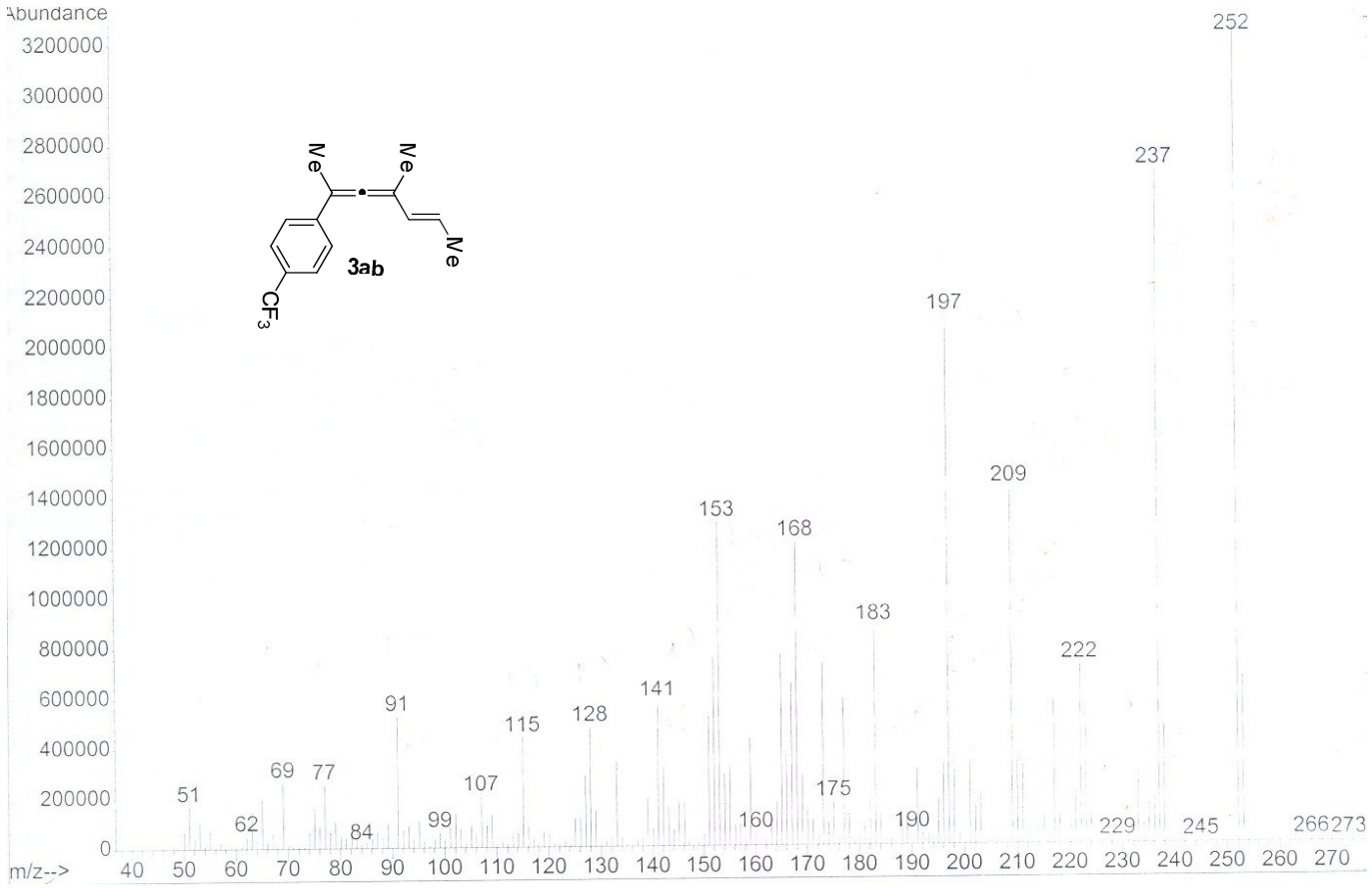

Figure E.2. Mass Spectrum of ((*E*)-2-(4-(trifluoromethyl)-phenyl)-4-methylhepta-2,3,5-triene

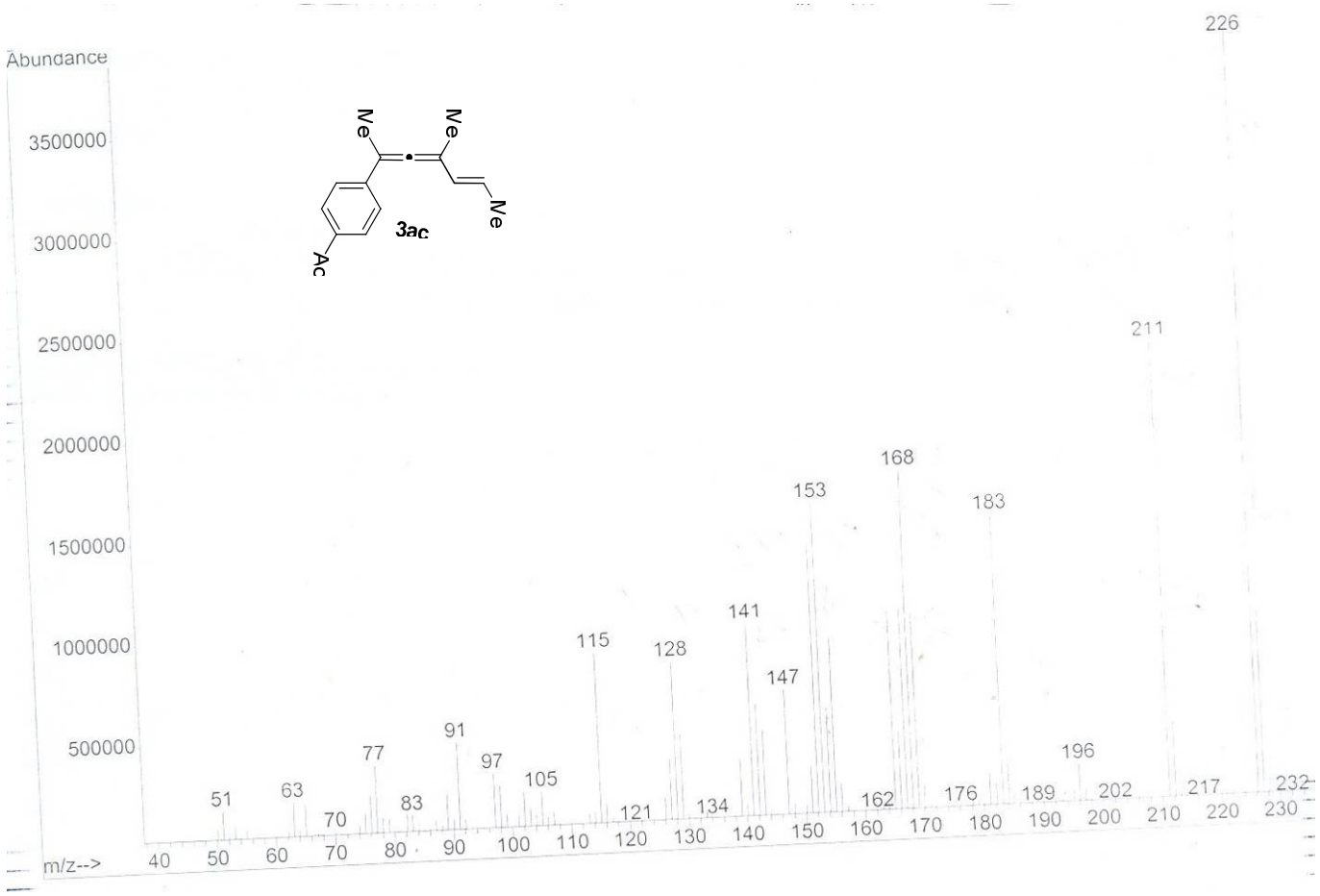

Figure E.3. Mass Spectrum of (*E*)-2-(4-acetylphenyl)-4-methylhepta-2,3,5-triene

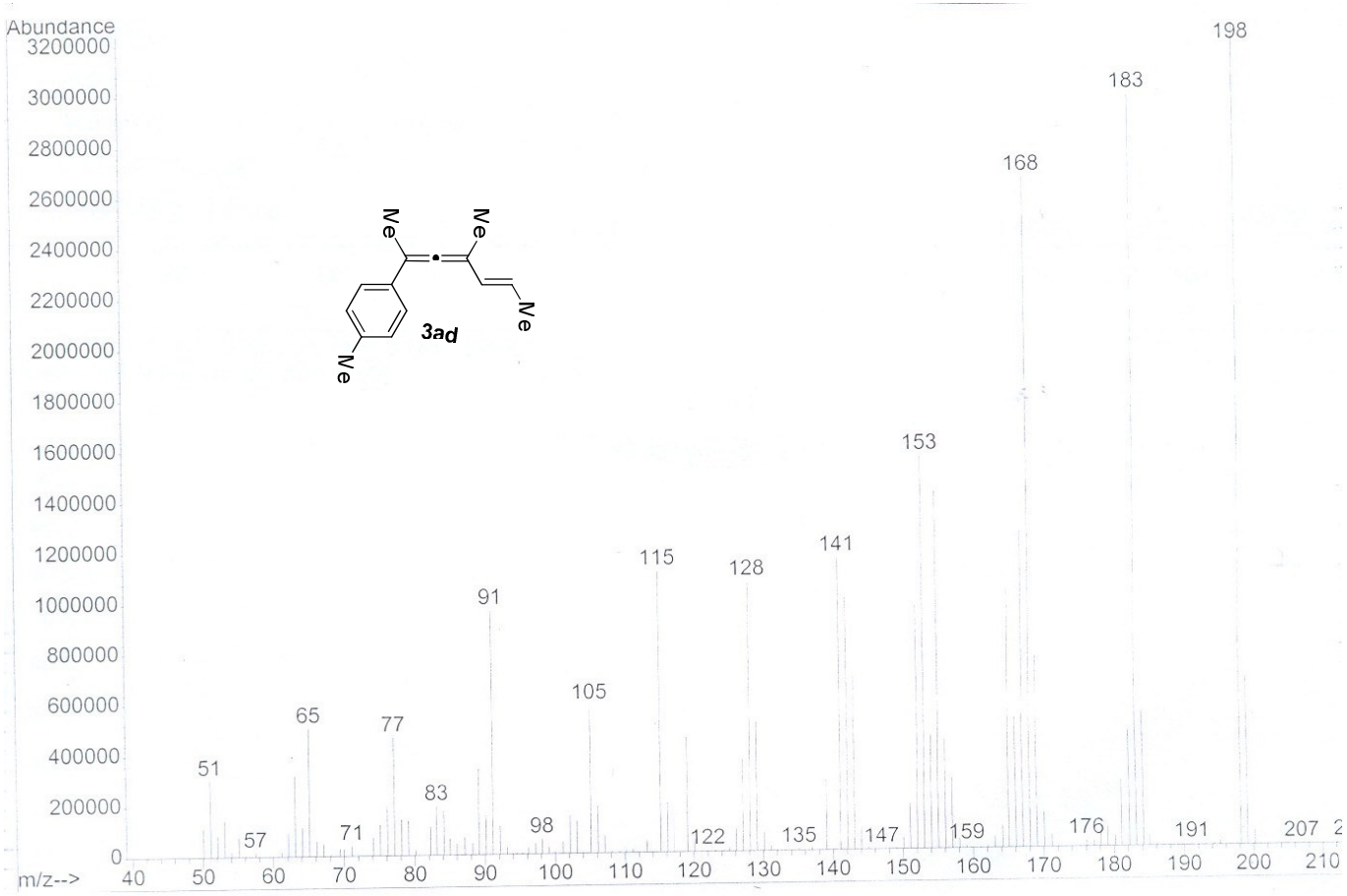

Figure E.4. Mass Spectrum of (*E*)-2-(4-meyhylphenyl)-4-methylhepta-2,3,5-triene

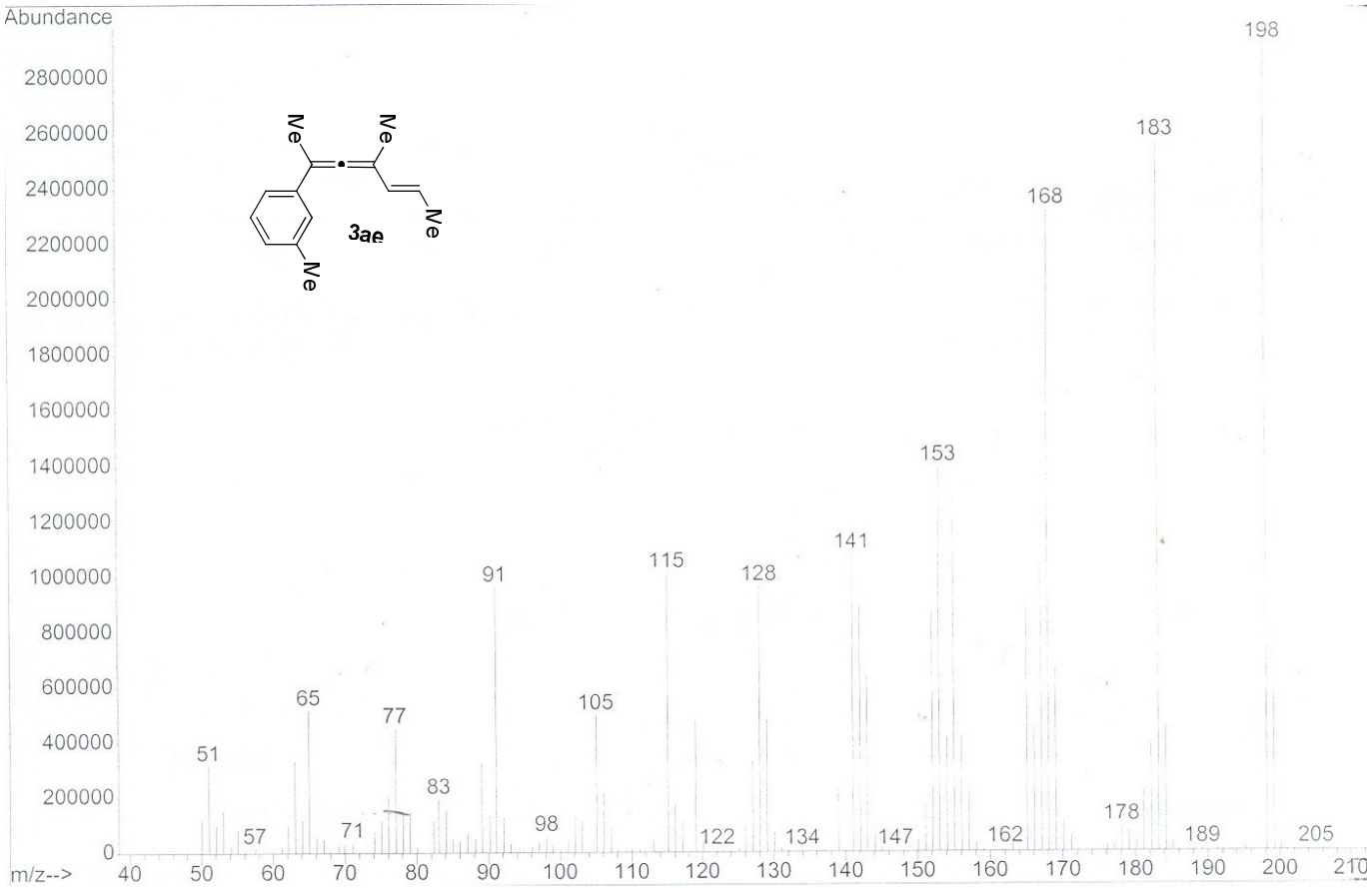

Figure E.5. Mass Spectrum of (*E*)-2-(3-meyhylphenyl)-4-methylhepta-2,3,5-triene

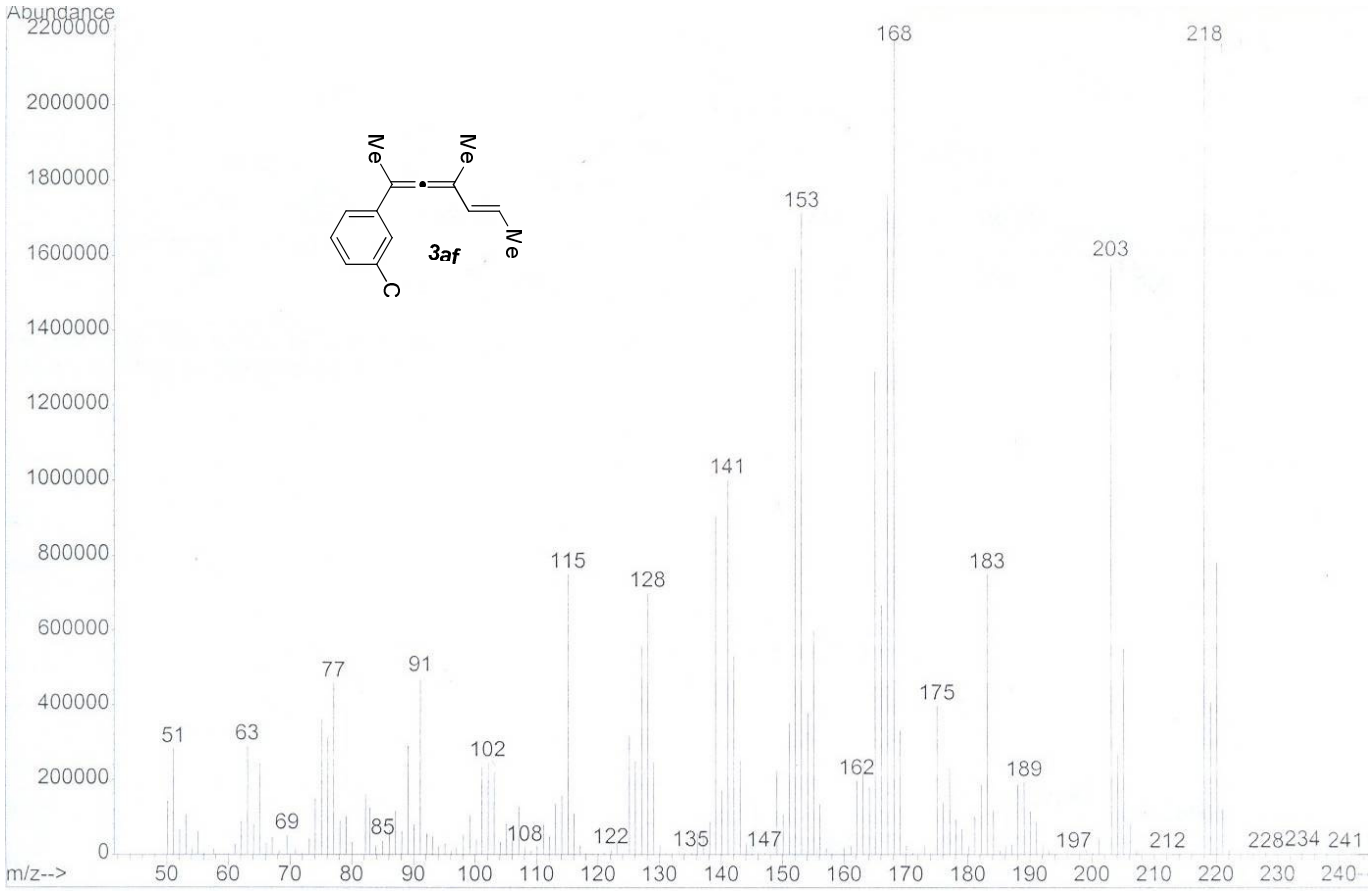

Figure E.6. Mass Spectrum of (*E*)-2-(3-chlorophenyl)-4-methylhepta-2,3,5-triene

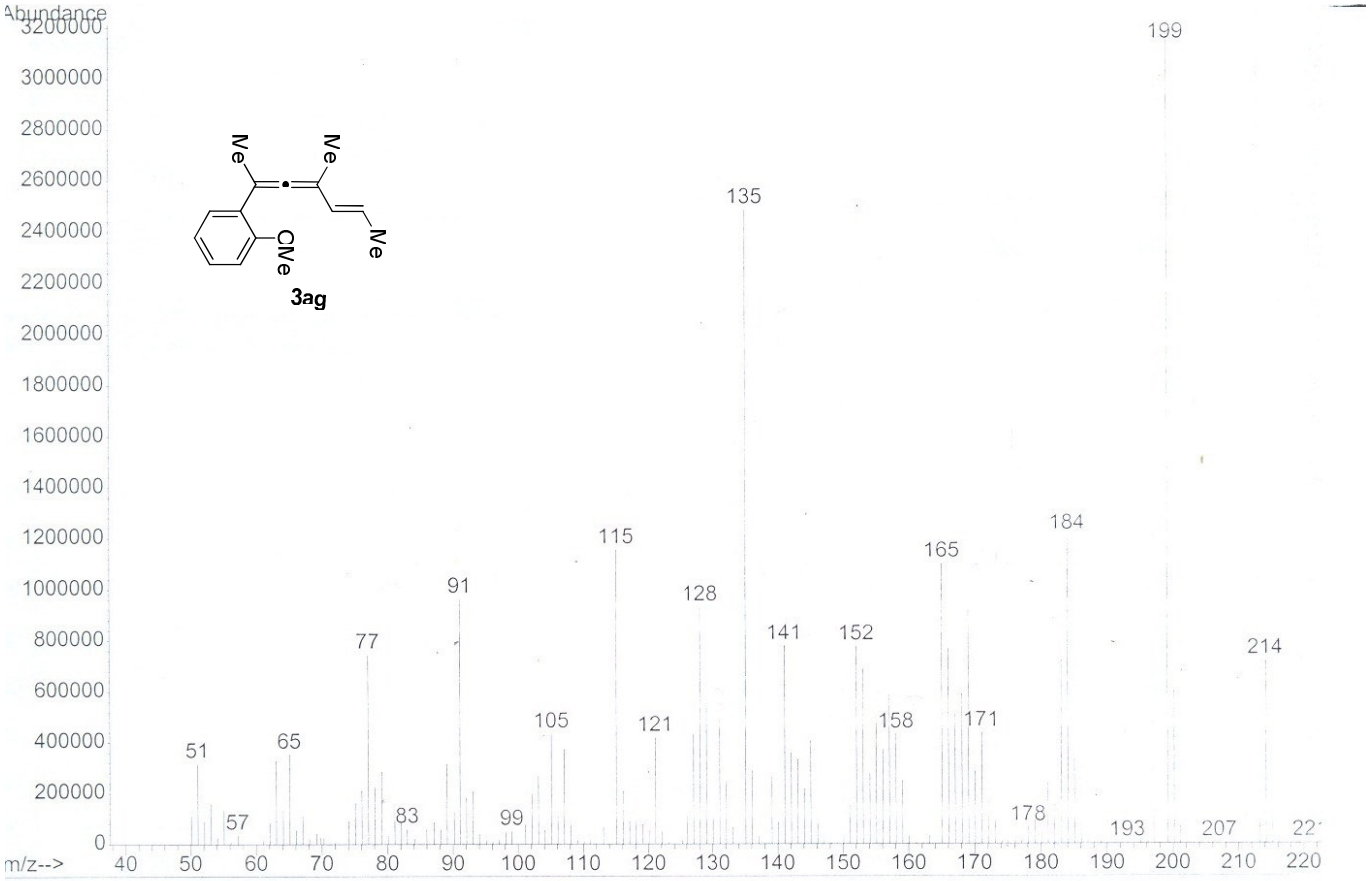

Figure E.7. Mass Spectrum of (*E*)-2-(2-methoxyhenyl)-4-methylhepta-2,3,5-triene

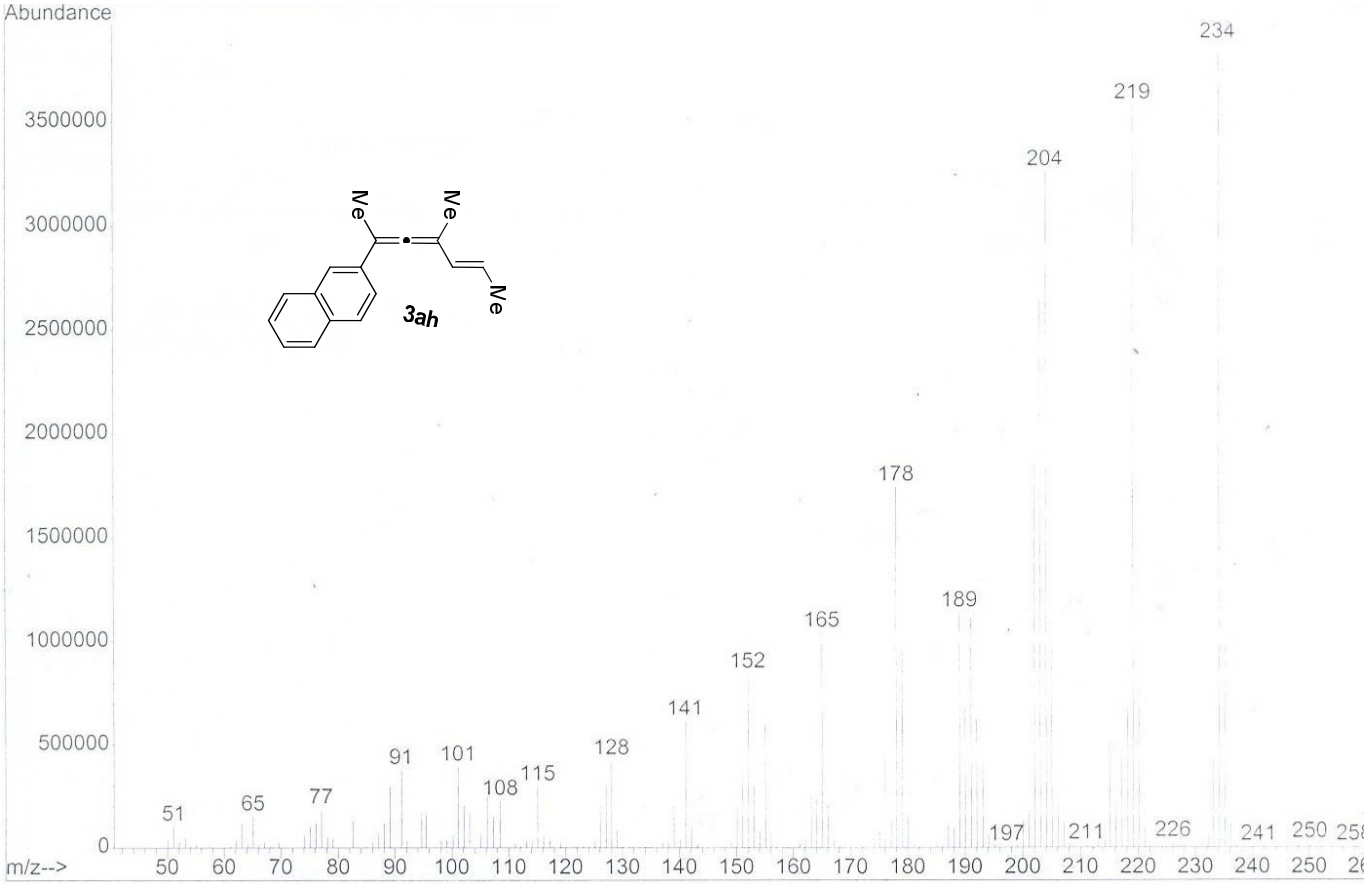

Figure E.8. Mass Spectrum of ((*E*)- 2-(2-naphthyl)-4-methylhepta-2,3,5-triene

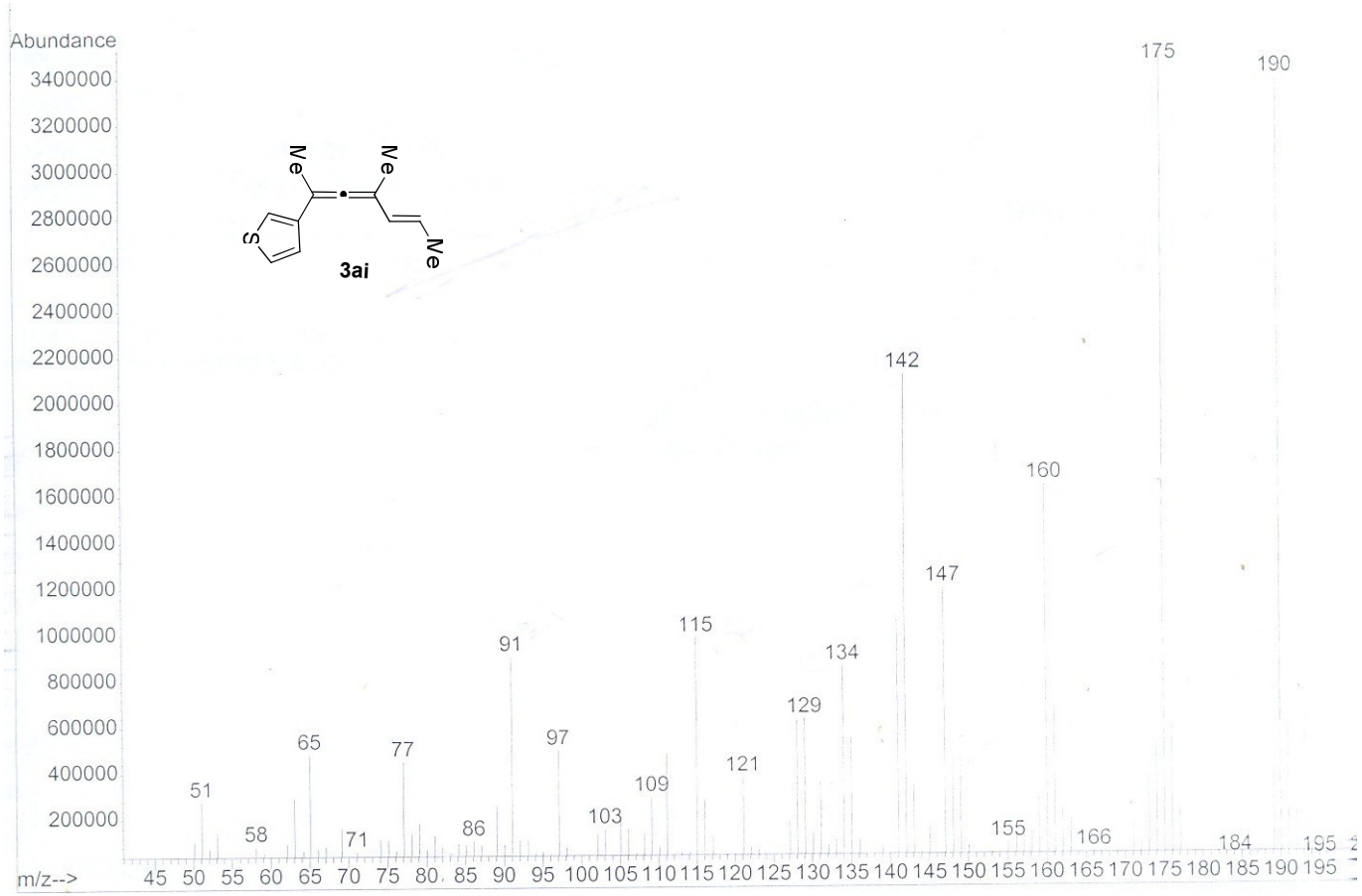

Figure E.9. [1] H NMR of (*E*)- 2-(3-thienyl)-4-methylhepta-2,3,5-triene

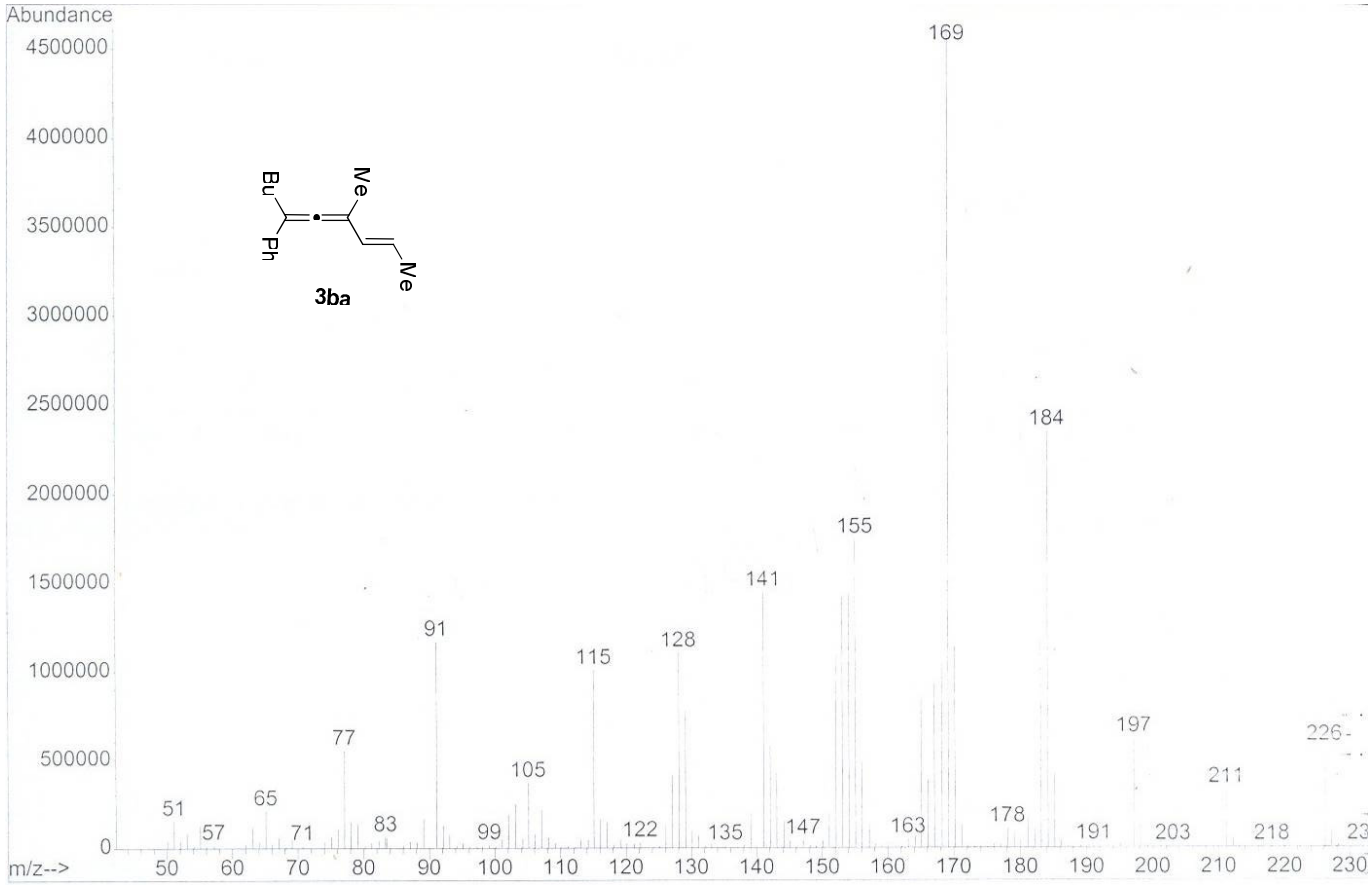

Figure E.10. Mass Spectrum of (*E*)- 6-phenyl-4-methyldeca-2,4,5-triene

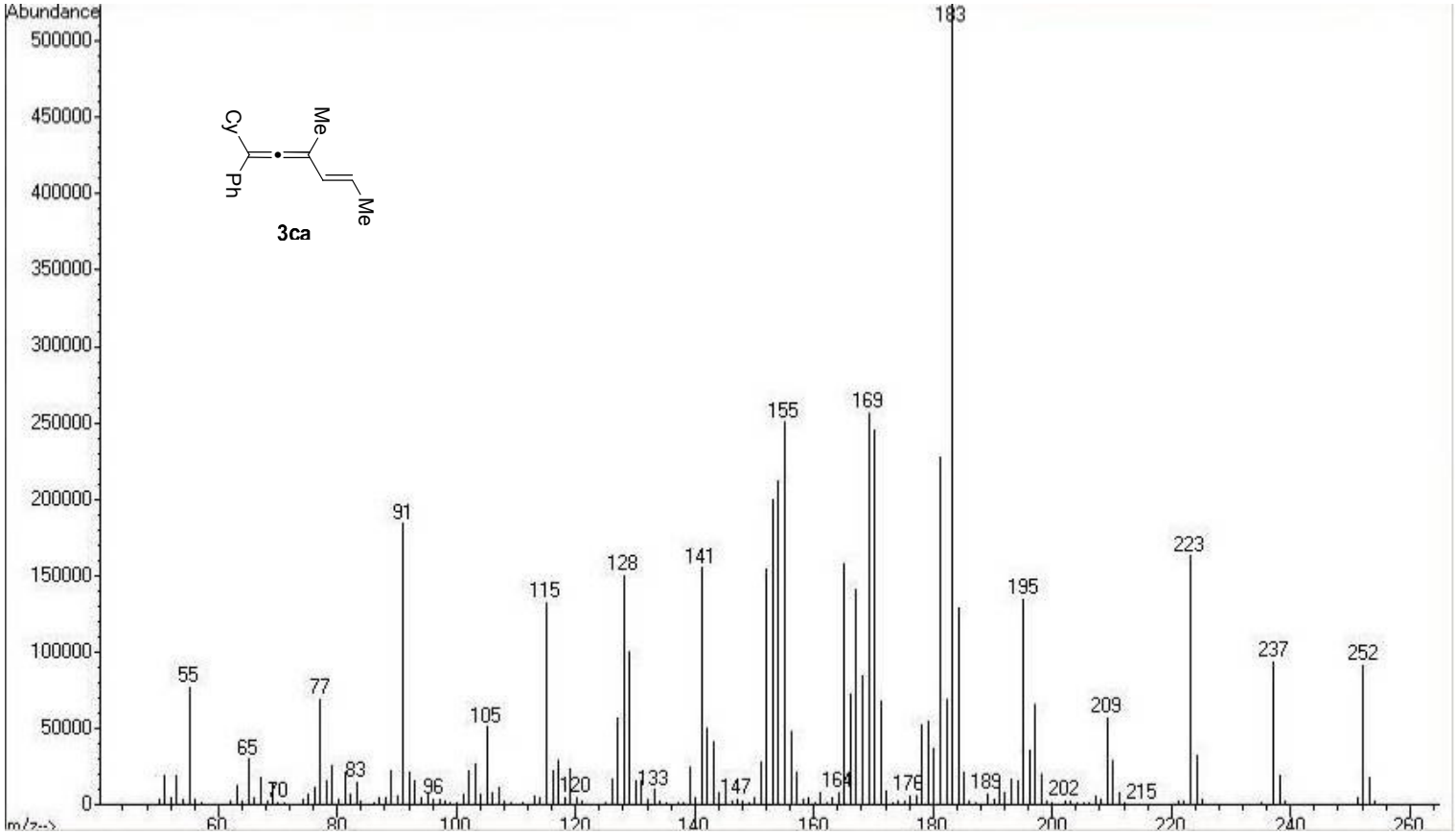

Figure E.11. Mass Spectrum of (*E*)-1-cyclohexyl-1-phenyl-3-methyl-hexa-1,2,4-triene

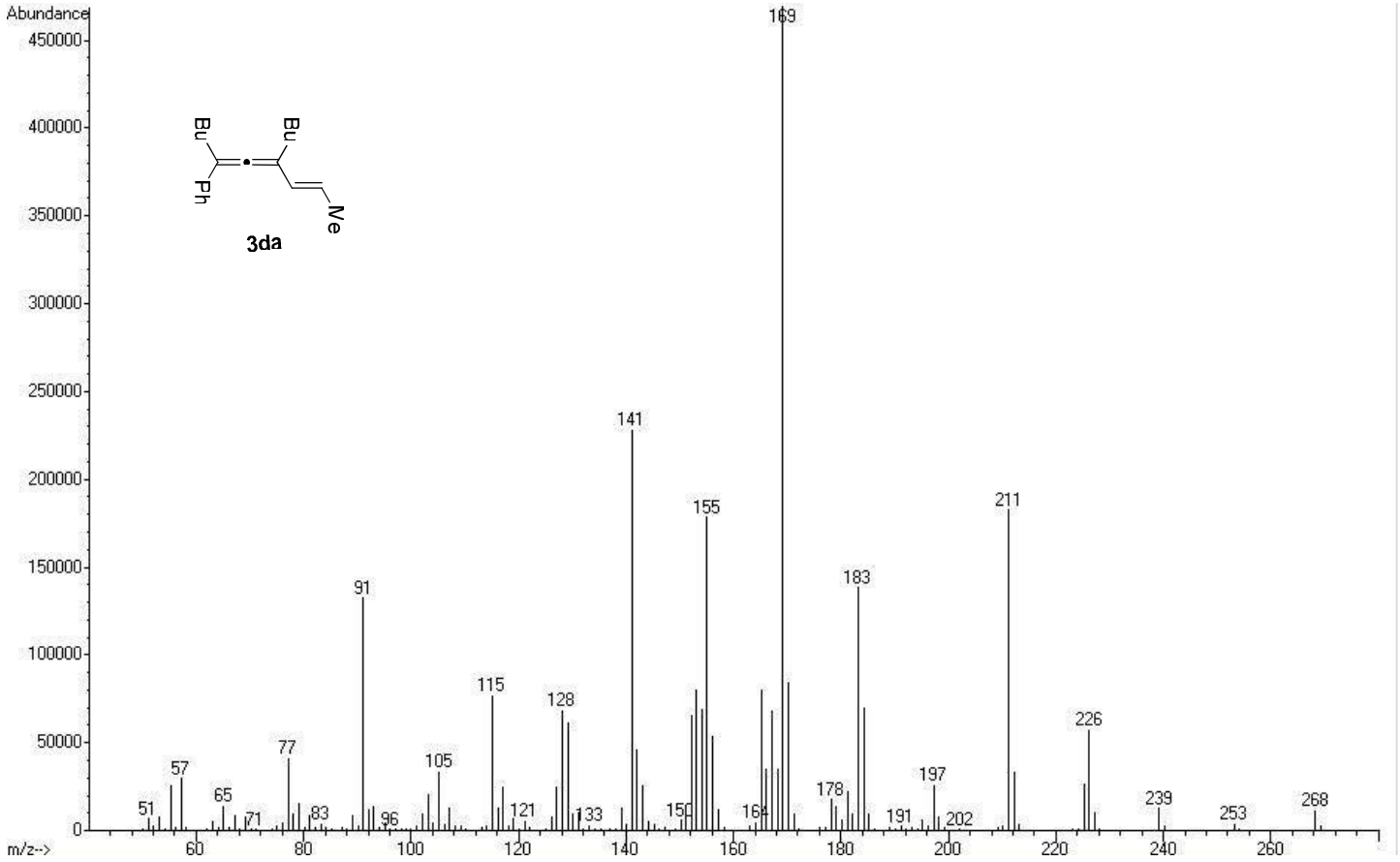

Figure E.12. Mass Specttrum of (E)-5-phenyl-7-(prop-1-enyl)undeca-5,6-diene

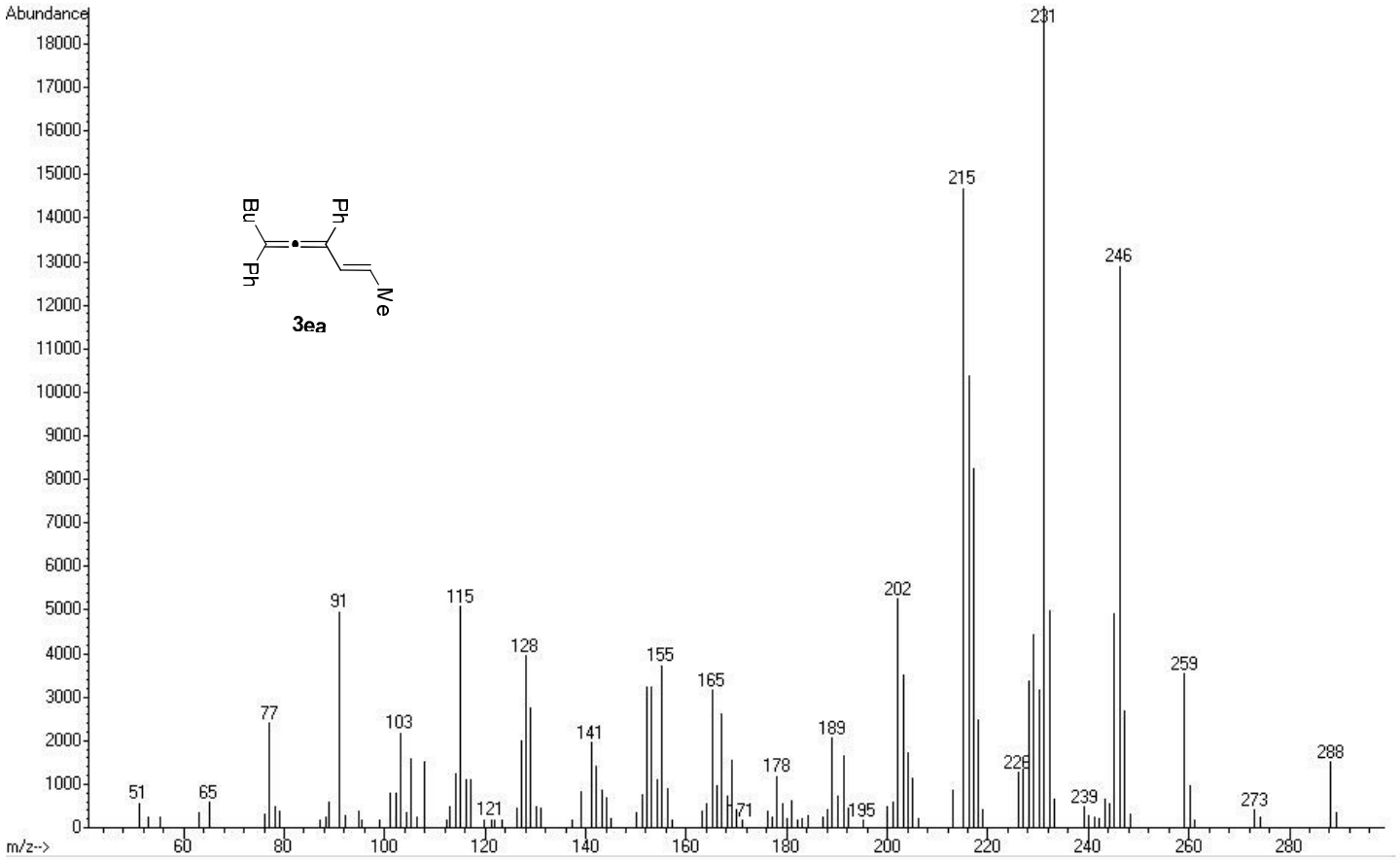

Figure E.13. Mass Spectrum NMR of (E)-4,6-diphenyl-deca-2,4,5-triene

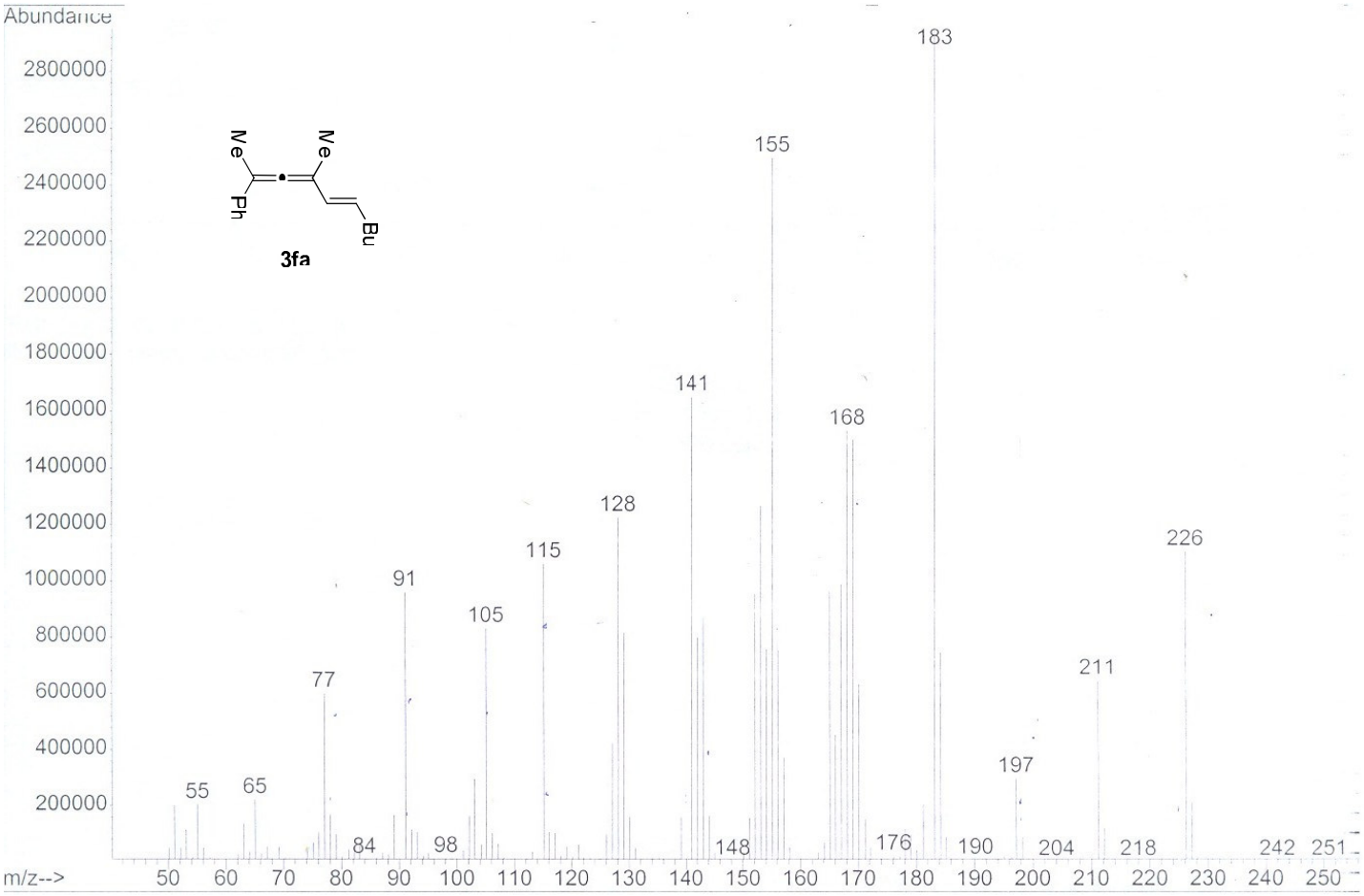

Figure E.14. Mass Spectrum (*E*)-4-methyl-2-phenyl-deca-2,3,5-triene

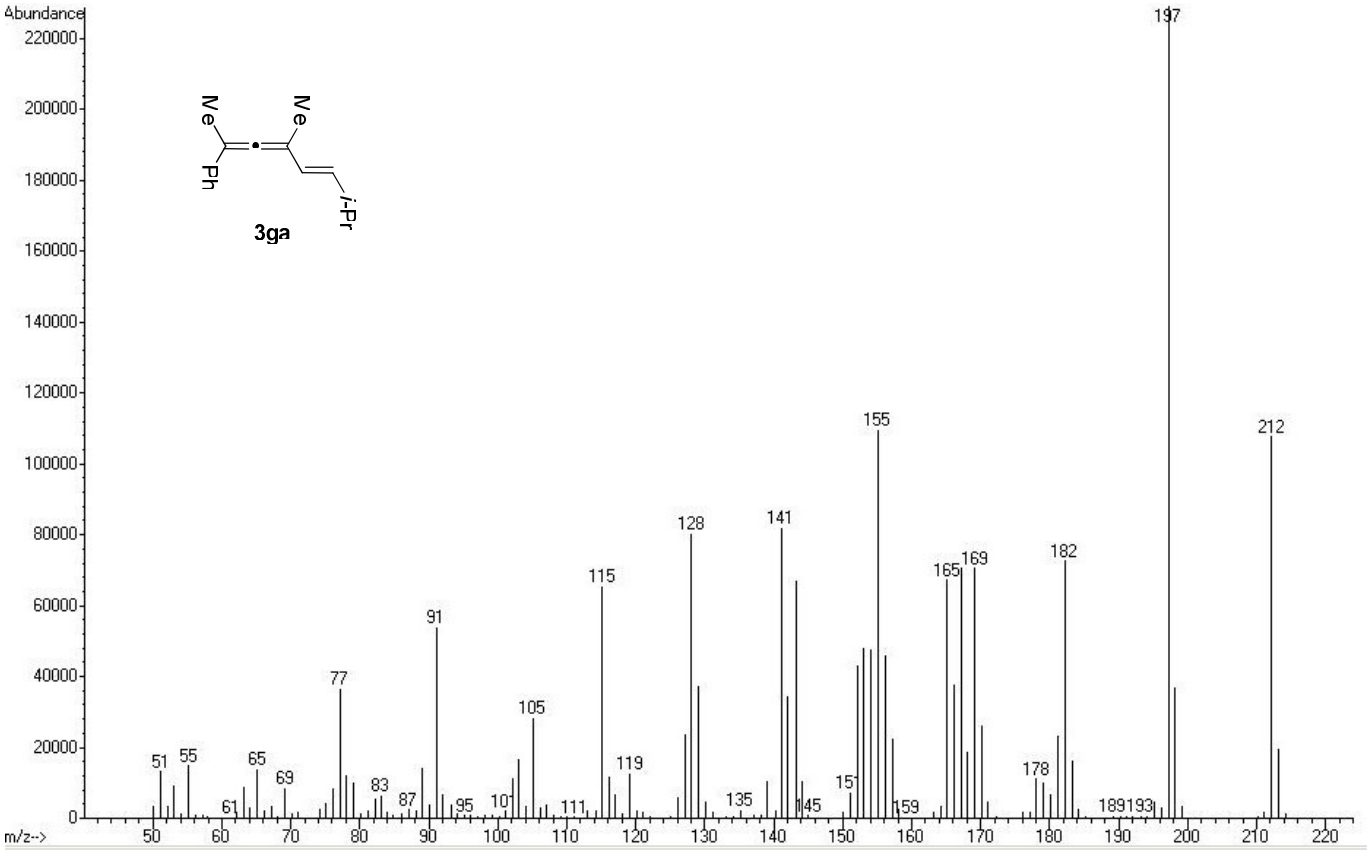

Figure E.15. Mass Spectrum of (*E*)-4,7-dimethyl-2-phenyl-octa-2,3,5-triene

APPENDIX F

FTIR SPECTRUMS OF PRODUCTS

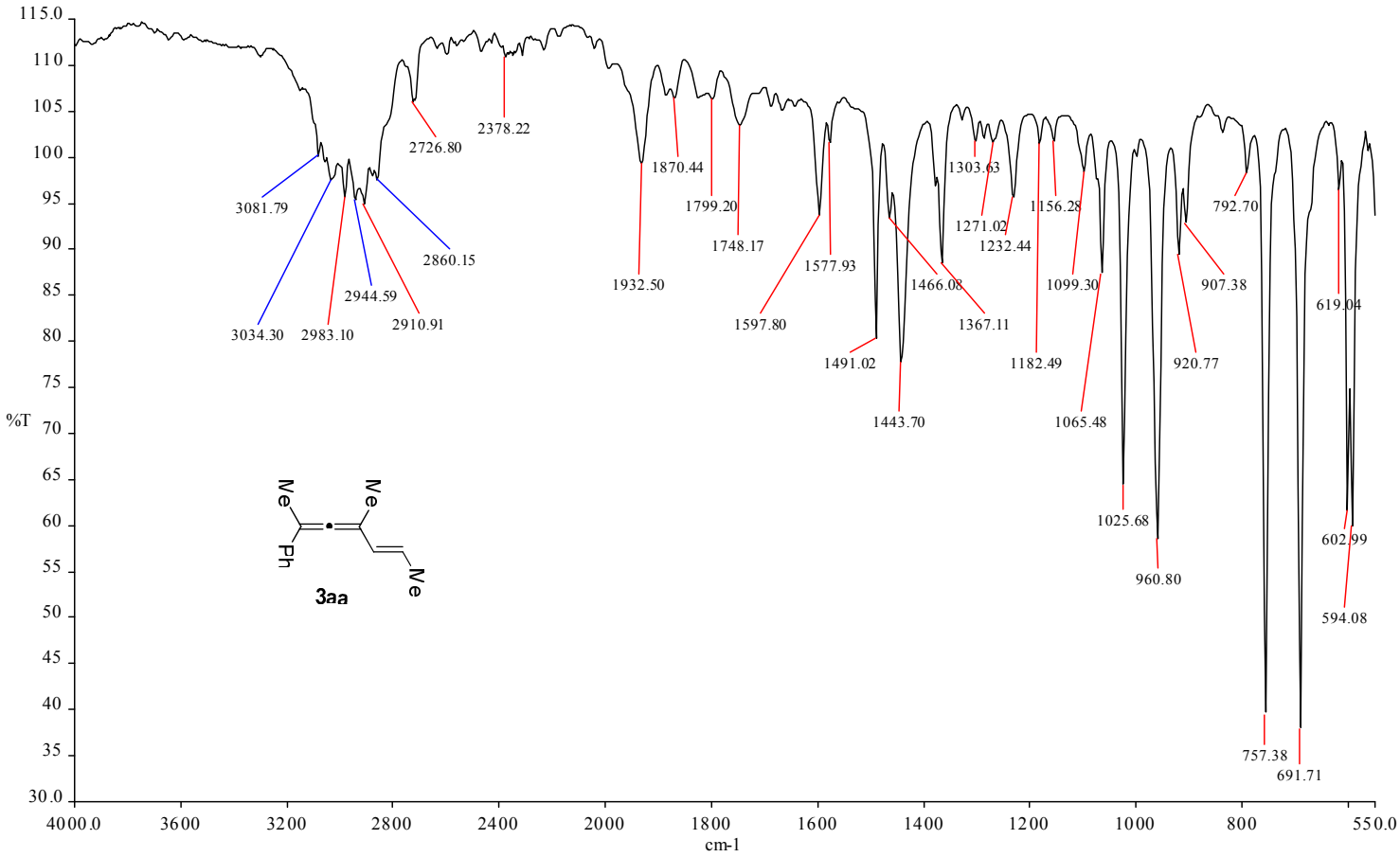

Figure F.1. FTIR Spectrum of (*E*)- 2-phenyl-4-methylhepta-2,3,5-triene

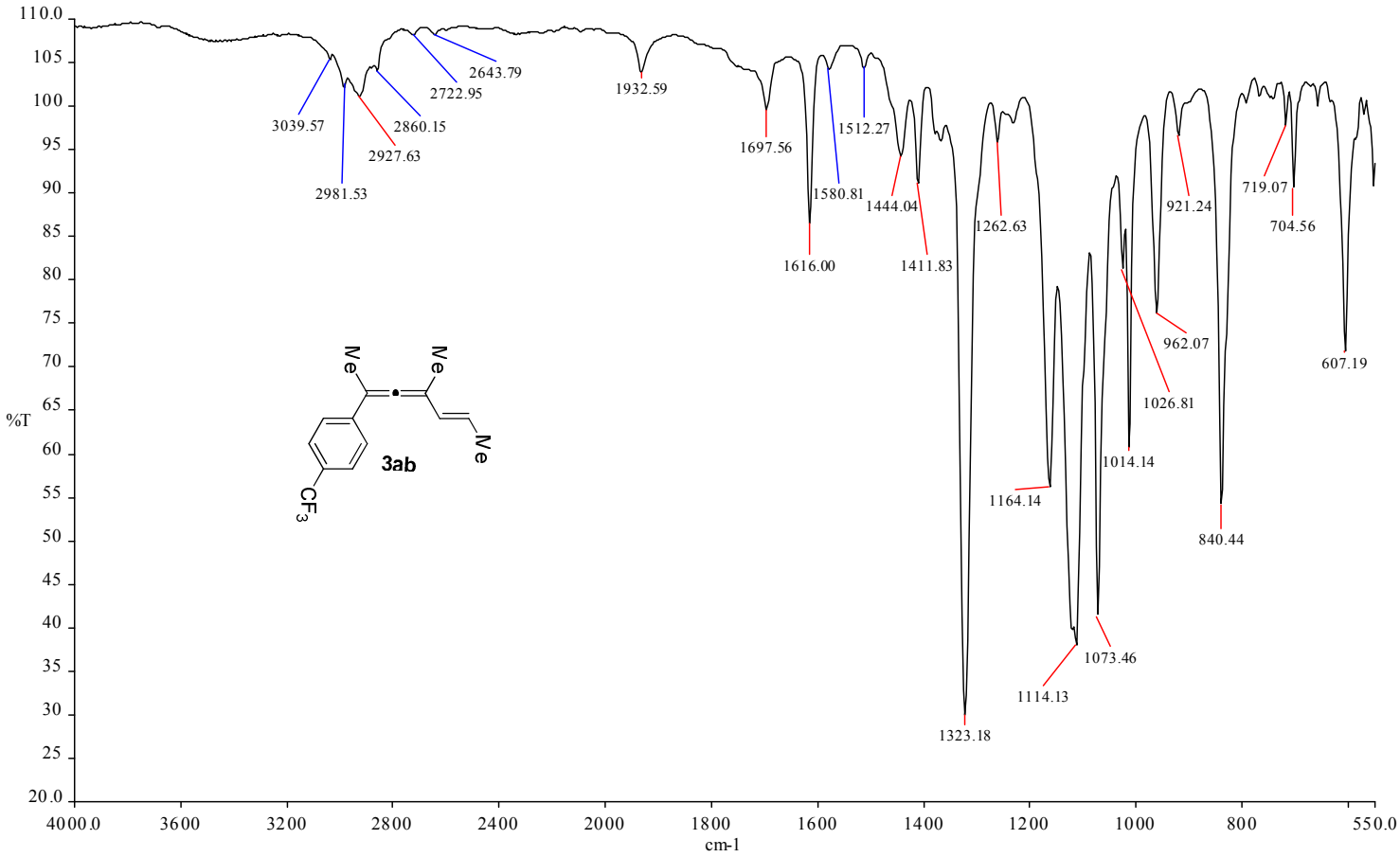

Figure E.2. FTIR Spectrum of ((*E*)-2-(4-(trifluoromethyl)-phenyl)-4-methylhepta-2,3,5-triene

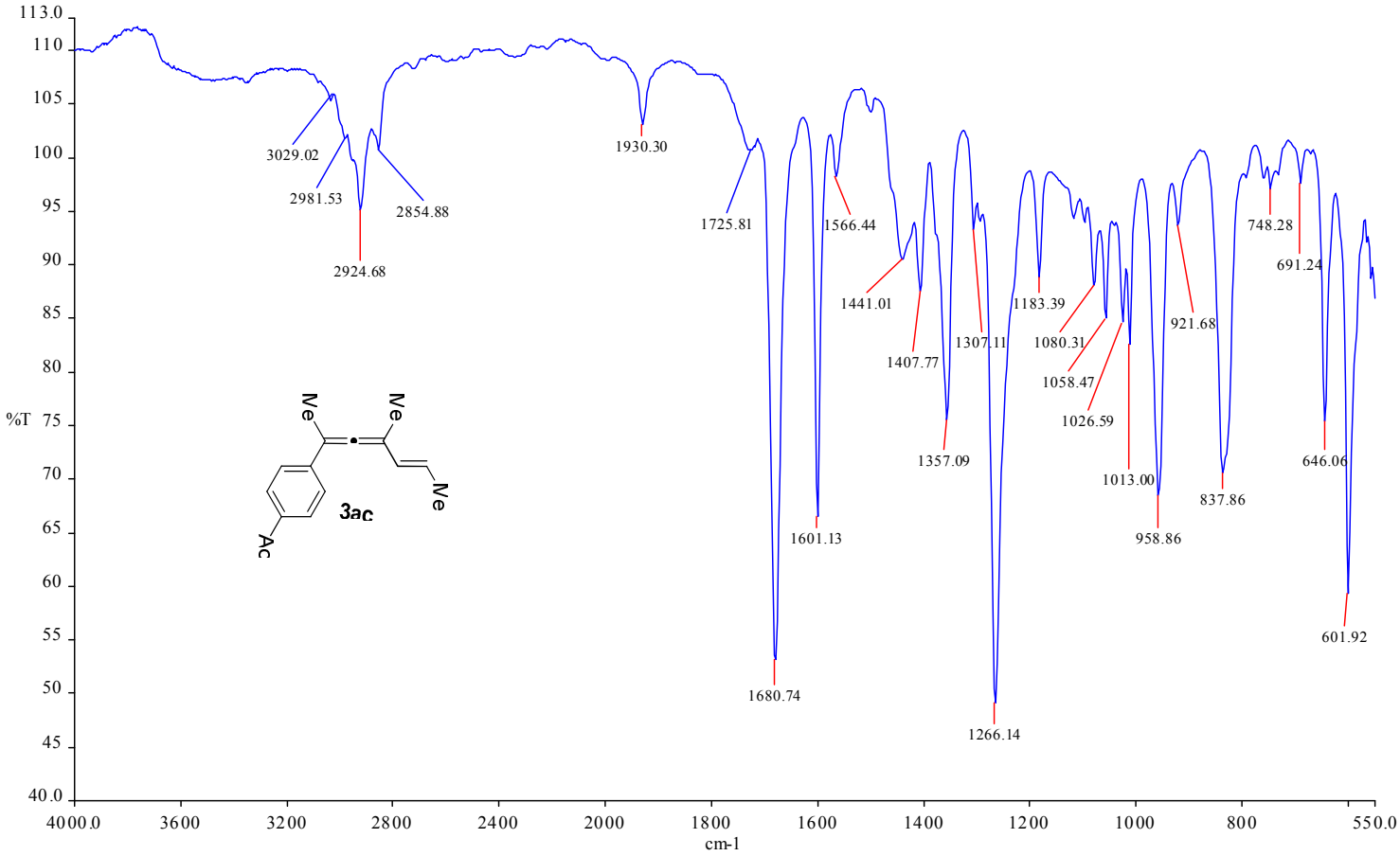

Figure F.3. FTIR Spectrum of (*E*)-2-(4-acetylphenyl)-4-methylhepta-2,3,5-triene

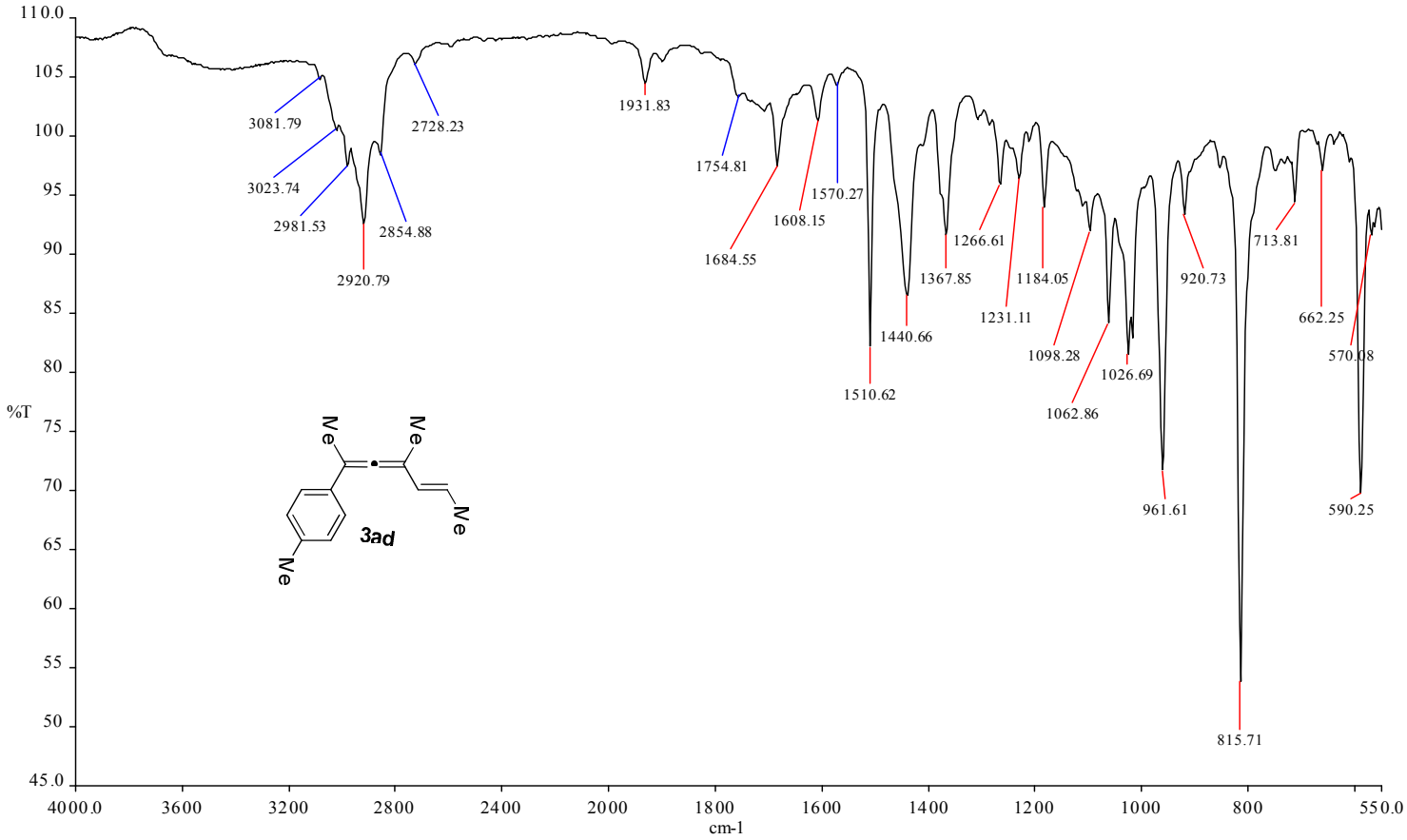

Figure F.4. FTIR Spectrum of (*E*)-2-(4-acetylphenyl)-4-methylhepta-2,3,5-triene

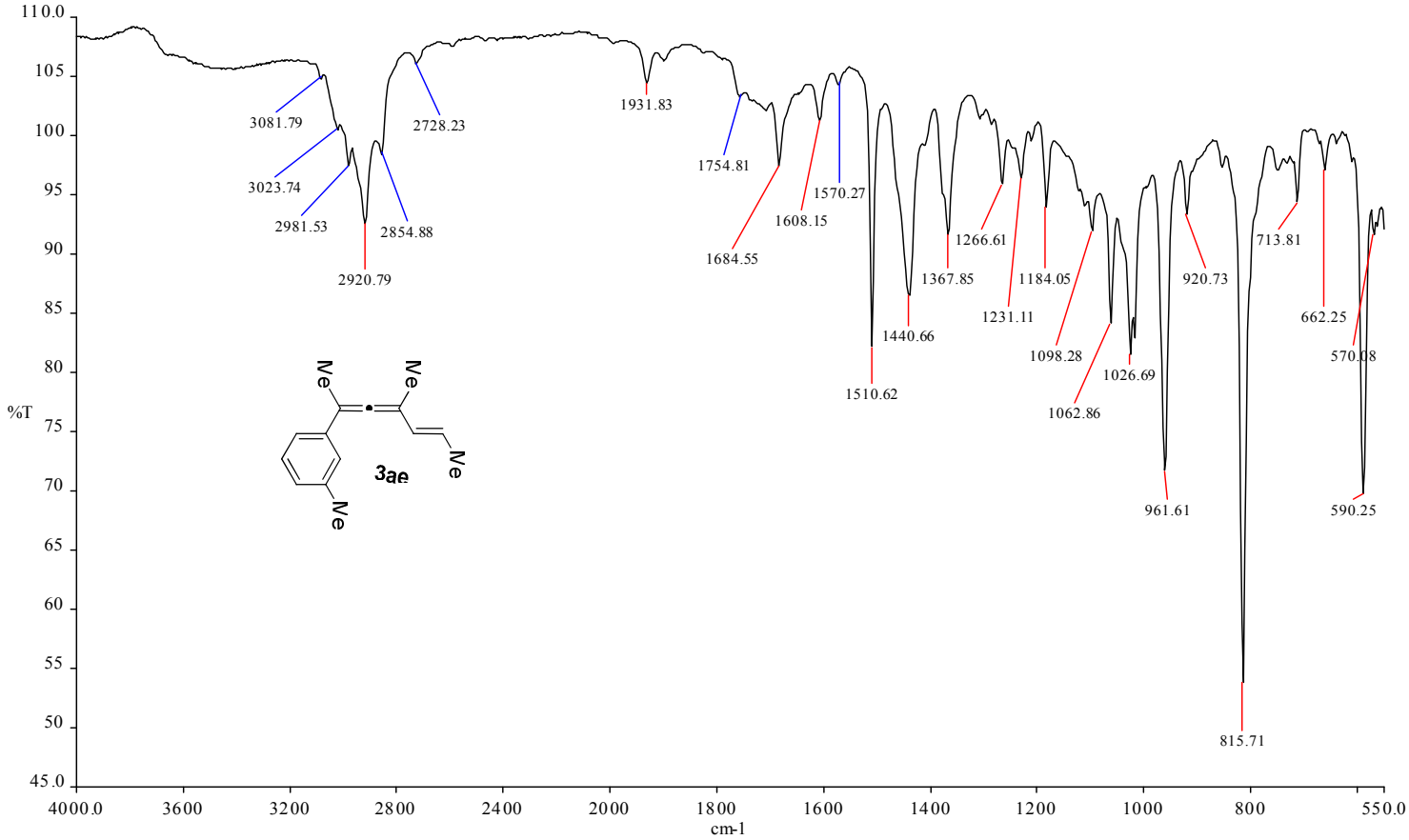

Figure F.5. FTIR Spectrum of (*E*)-2-(3-meyhylphenyl)-4-methylhepta-2,3,5-triene

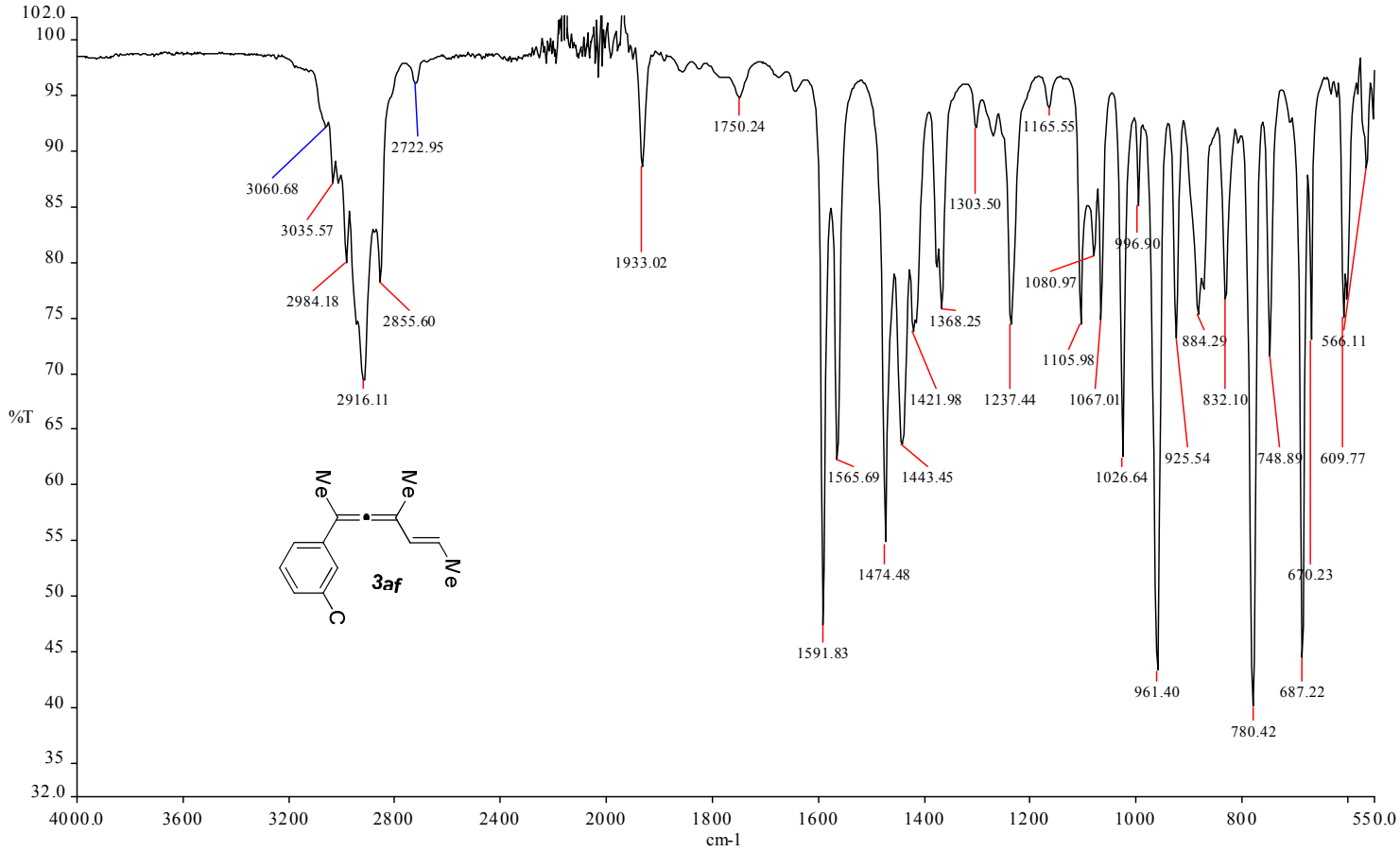

Figure F.6. FTIR Spectrum of (*E*)-2-(3-chlorophenyl)-4-methylhepta-2,3,5-triene

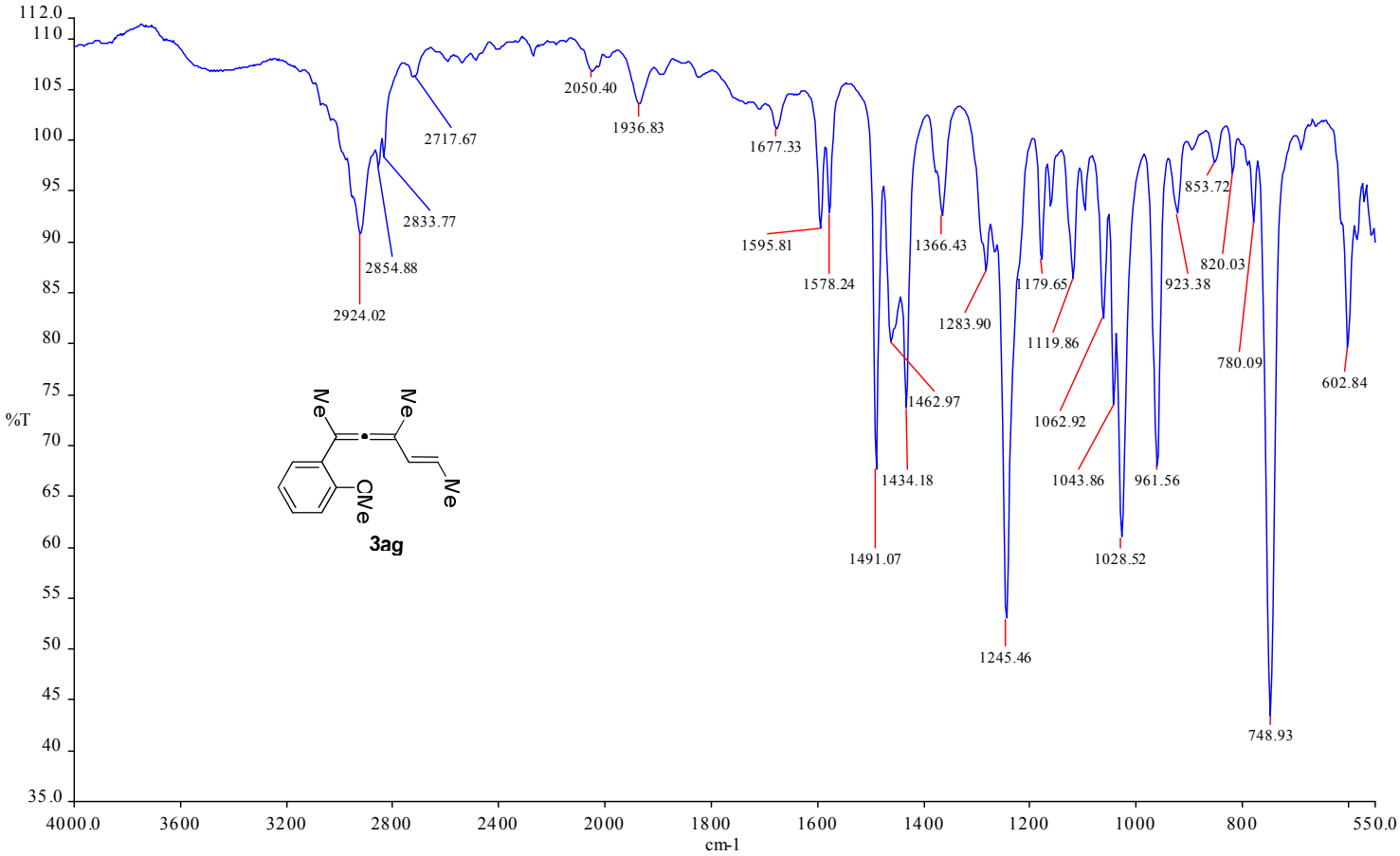

Figure F.7. FTIR Spectrum of (*E*)-2-(2-methoxyhenyl)-4-methylhepta-2,3,5-triene

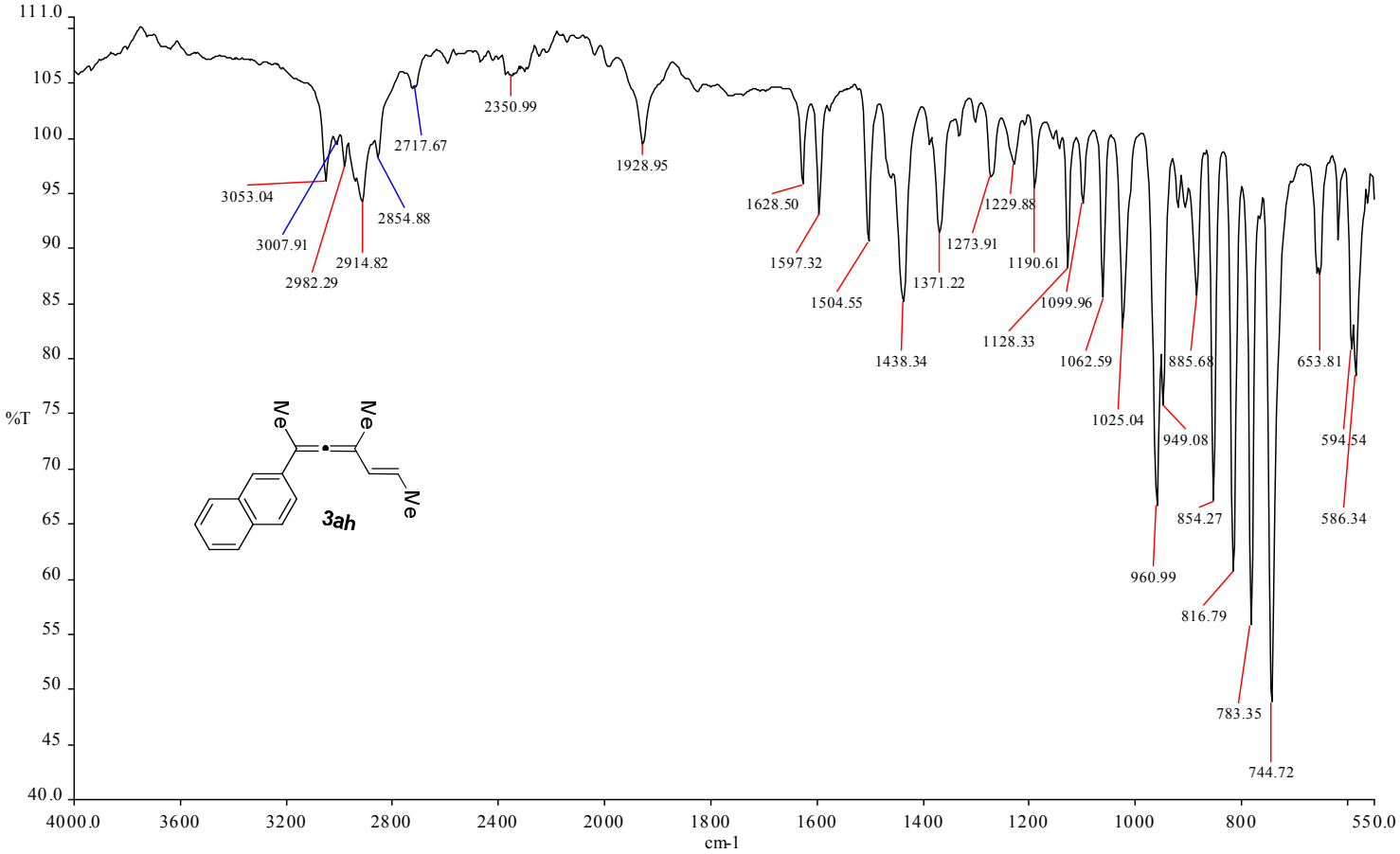

Figure F.8. FTIR Spectrum of ((*E*)- 2-(2-naphthyl)-4-methylhepta-2,3,5-triene

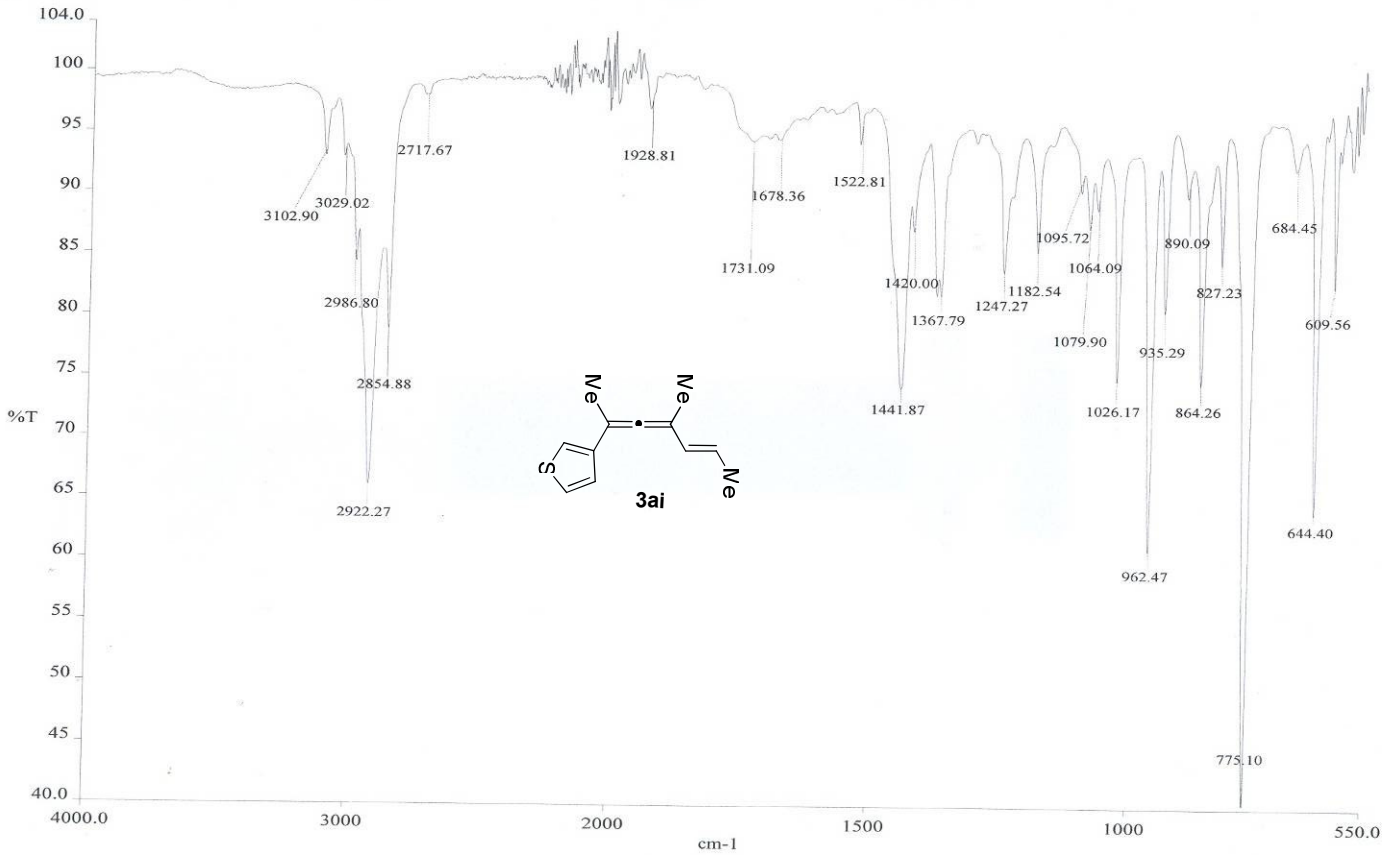

Figure F.9. FTIR Spectrum of (*E*)- 2-(3-thienyl)-4-methylhepta-2,3,5-triene

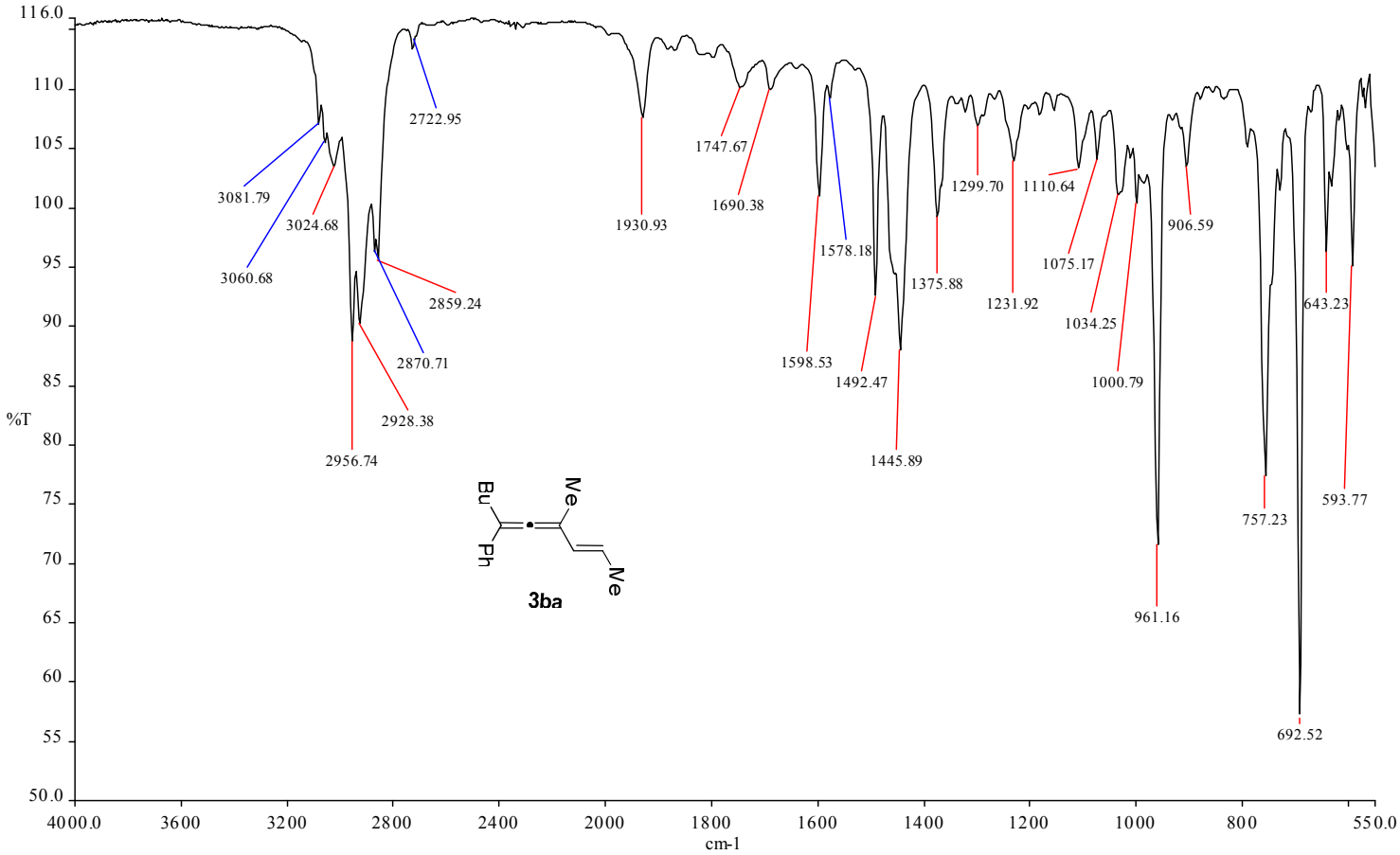

Figure F.10. FTIR Spectrum of (*E*)- 6-phenyl-4-methyldeca-2,4,5-triene

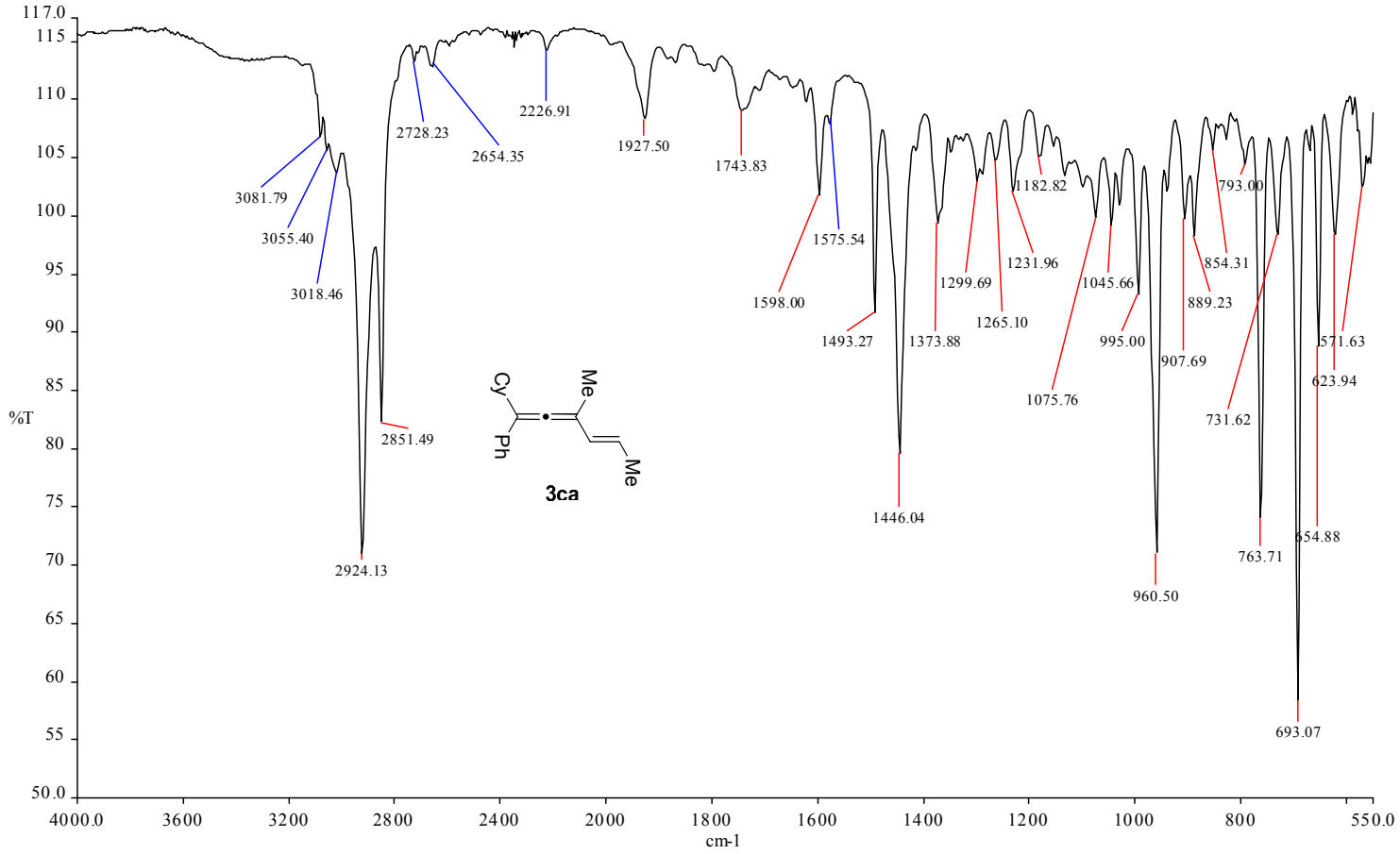

Figure F.11. FTIR Spectrum of (*E*)-1-cyclohexyl-1-phenyl-3-methyl-hexa-1,2,4-triene

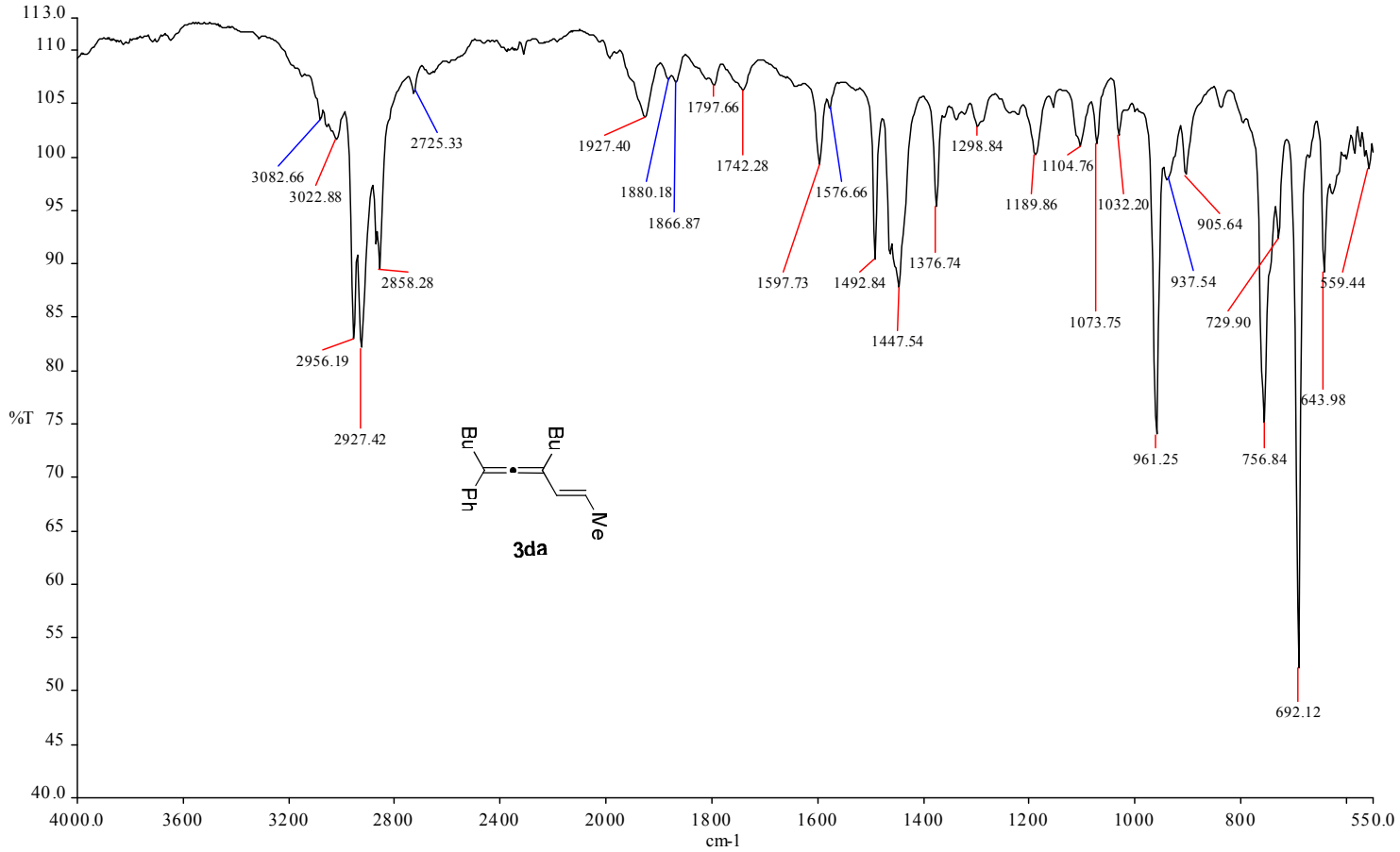

Figure F.12. FTIR Spectrum of (E)-5-phenyl-7-(prop-1-enyl)undeca-5,6-diene

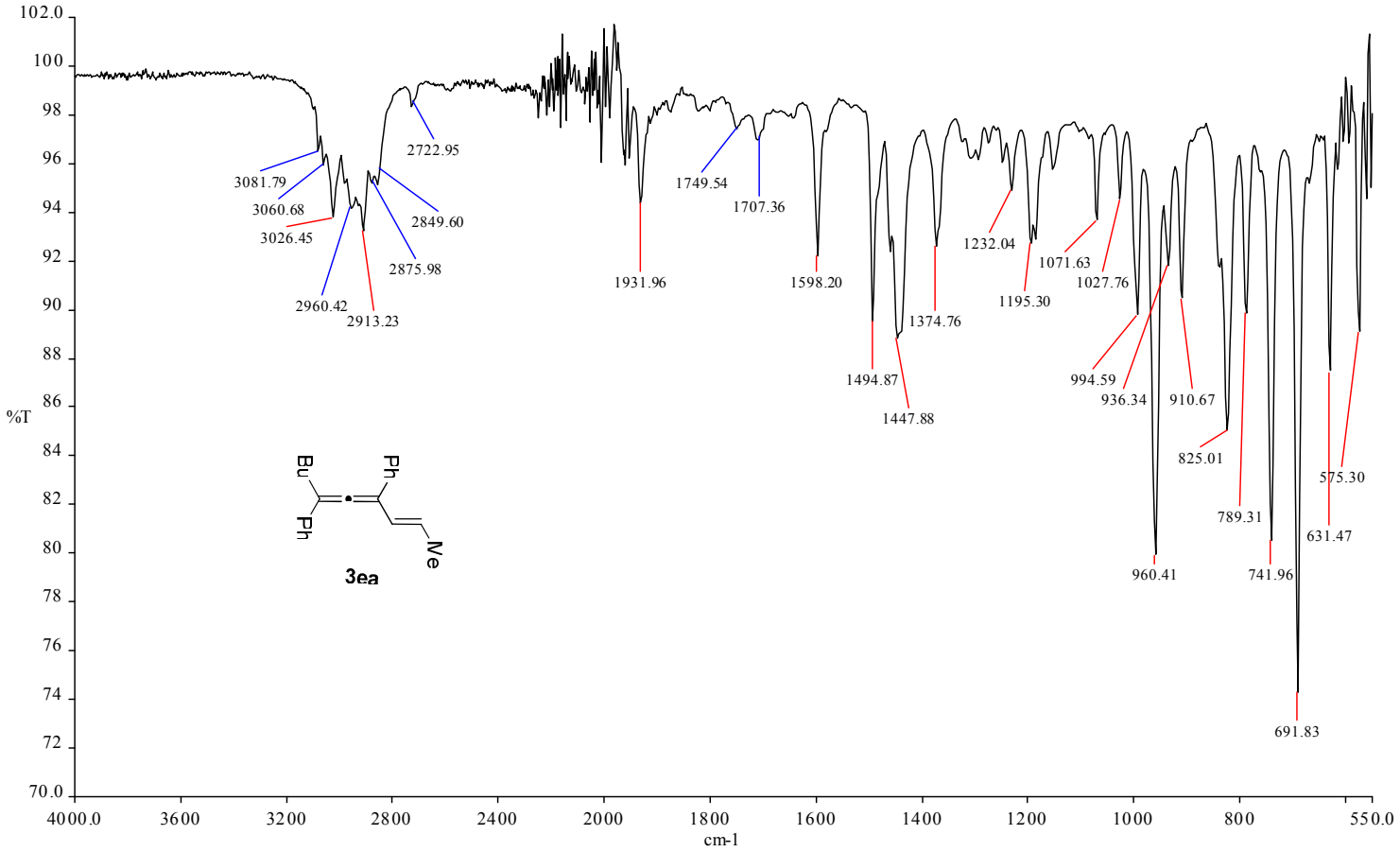

Figure F.13. FTIR Spectrum of (E)-4,6-diphenyl-deca-2,4,5-triene

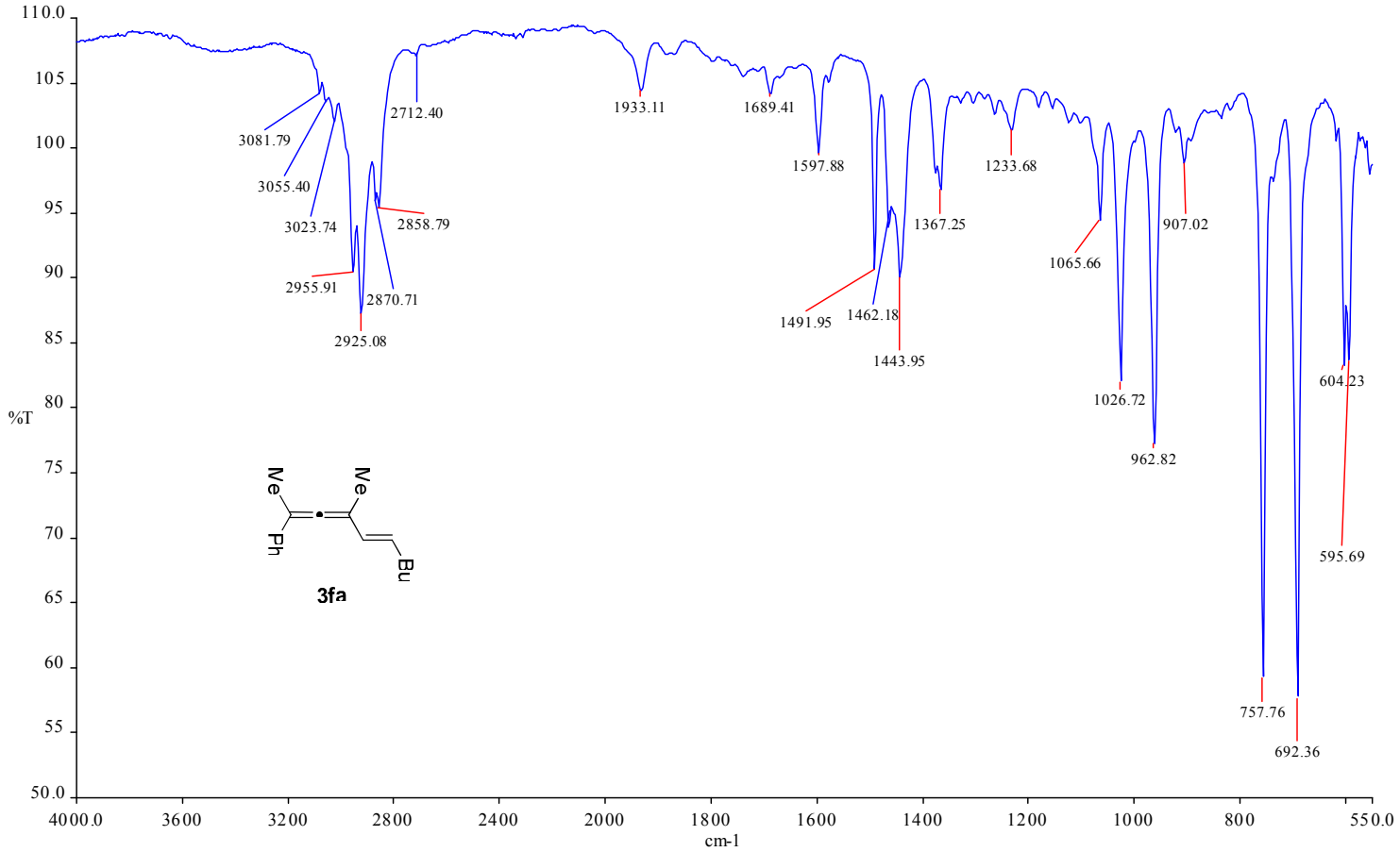

Figure F.14. FTIR Spectrum of (*E*)-4-methyl-2-phenyl-deca-2,3,5-triene

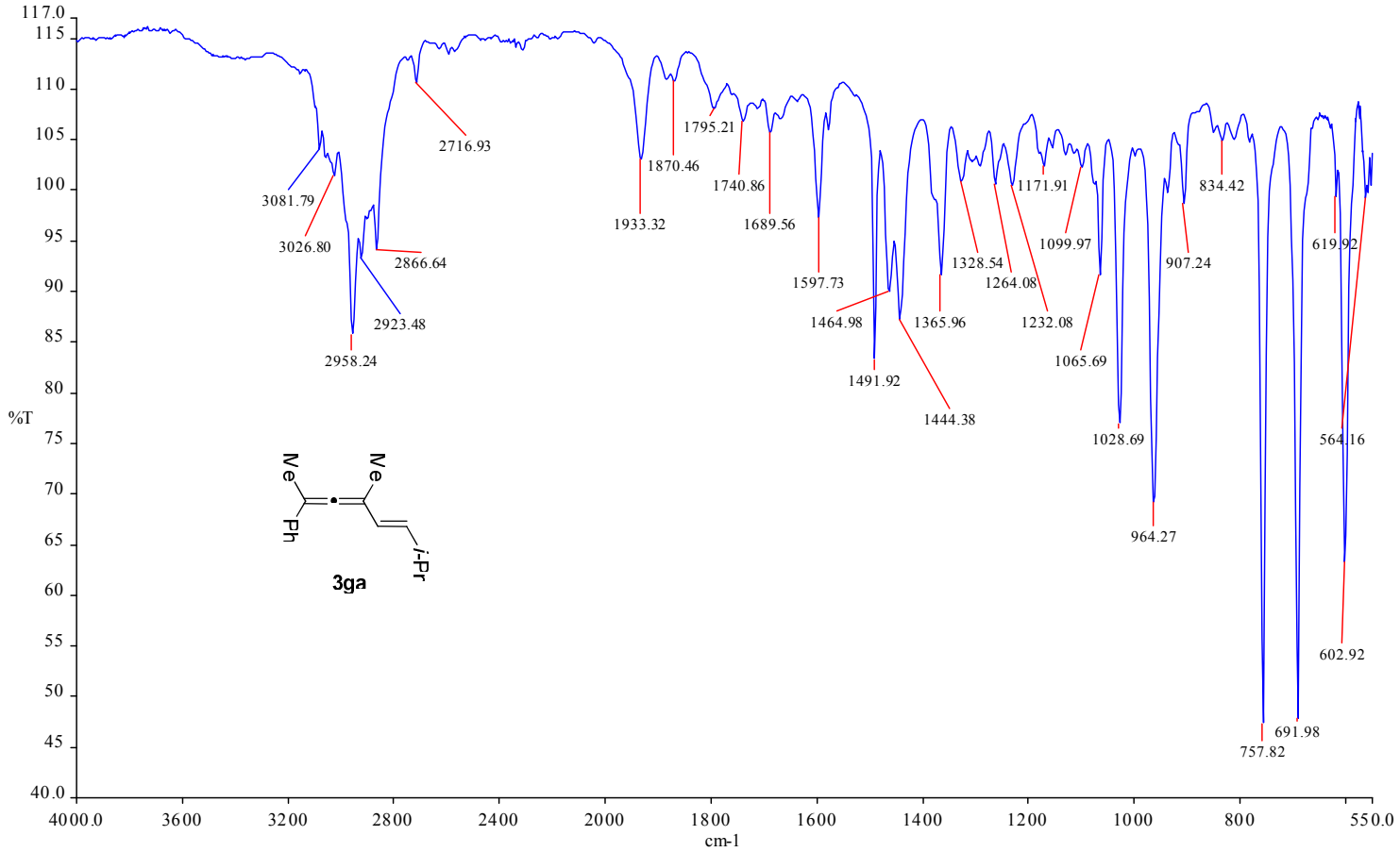

Figure F.15. FTIR Spectrum of (*E*)-4,7-dimethyl-2-phenyl-octa-2,3,5-triene

APPENDIX G

HPLC CHROMATOGRAMS OF REACTANT AND PRODUCTS

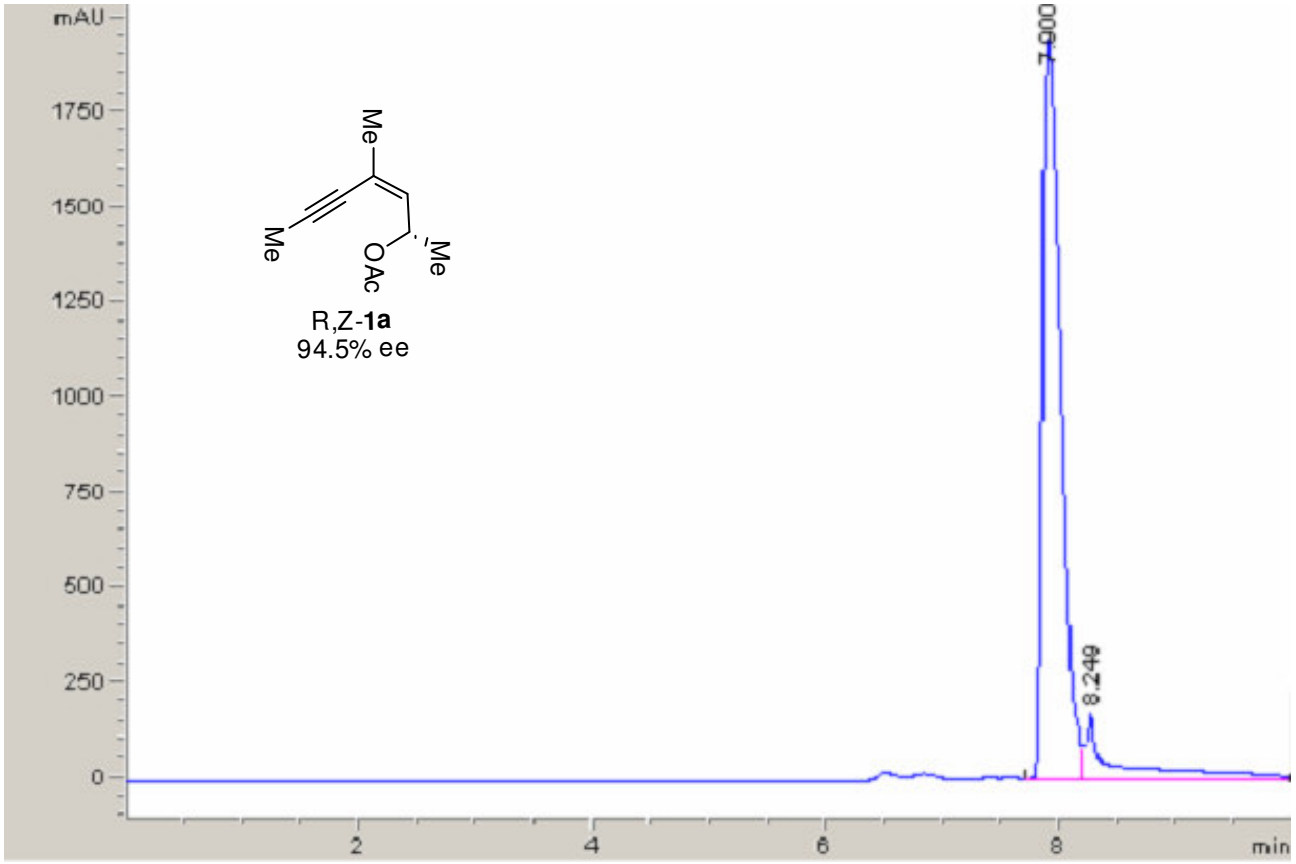

Figure G.1. HPLC Spectrum of (R,*Z*)-4-methylhept-3-en-5-yn-2-yl acetate

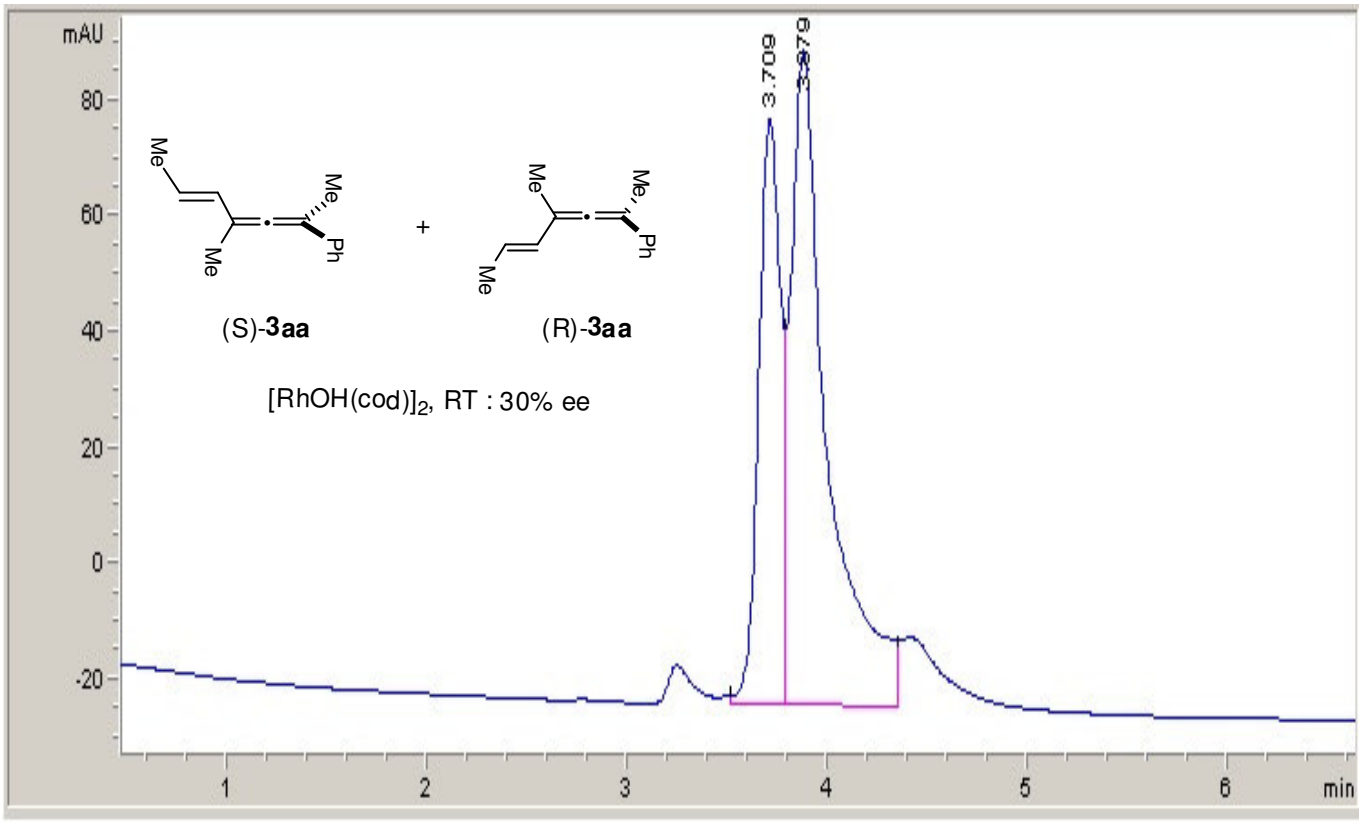

Figure G.2. HPLC Spectrum for racemic mixture of (*E*)- 2-phenyl-4-methylhepta-2,3,5-triene

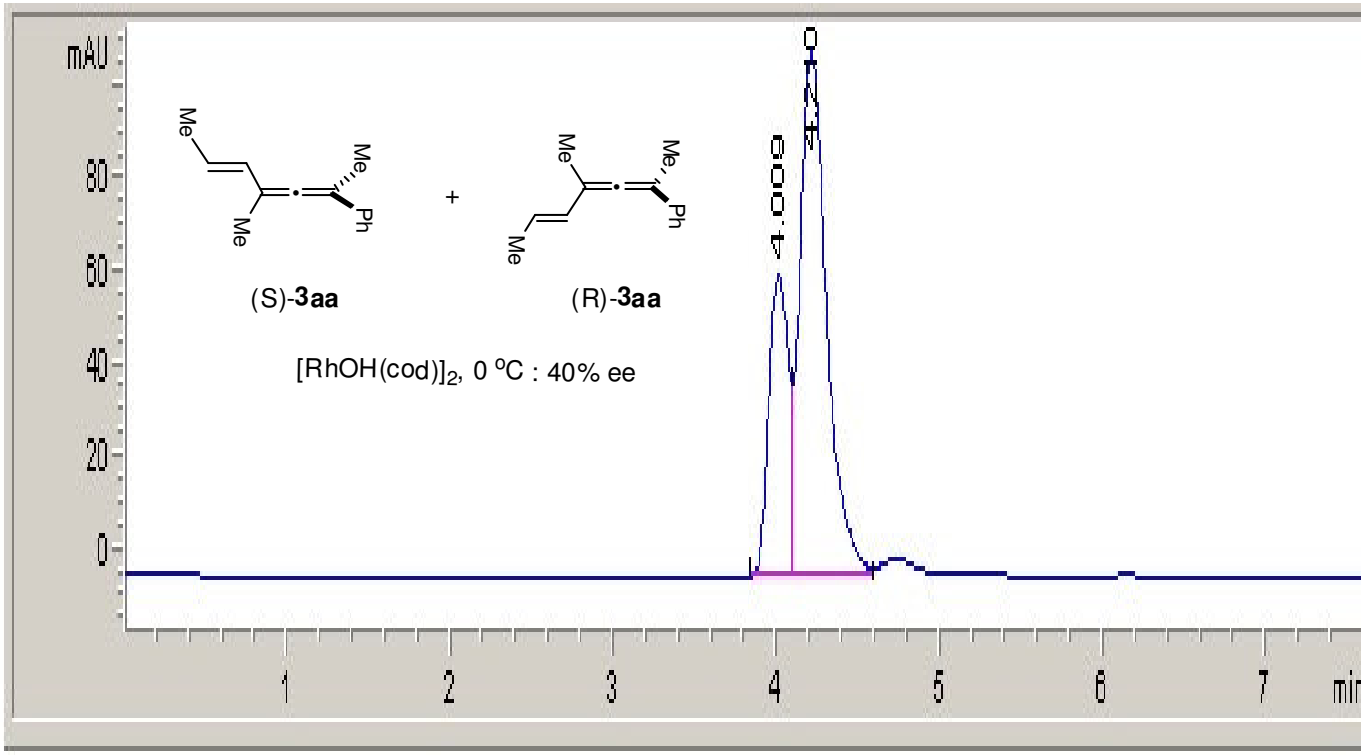

Figure G.3. HPLC Spectrum for racemic mixture of (*E*)- 2-phenyl-4-methylhepta-2,3,5-triene

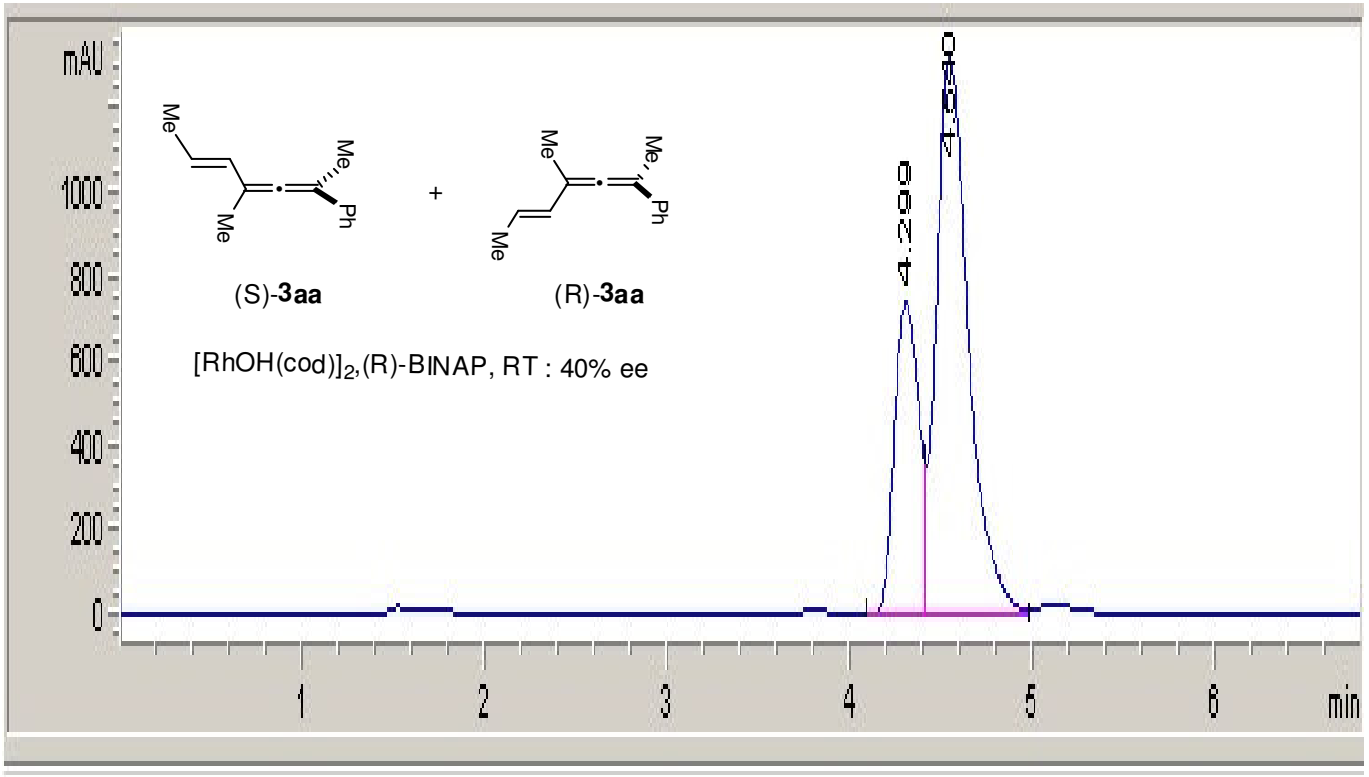

Figure G.4. HPLC Spectrum for racemic mixture of (*E*)- 2-phenyl-4-methylhepta-2,3,5-triene

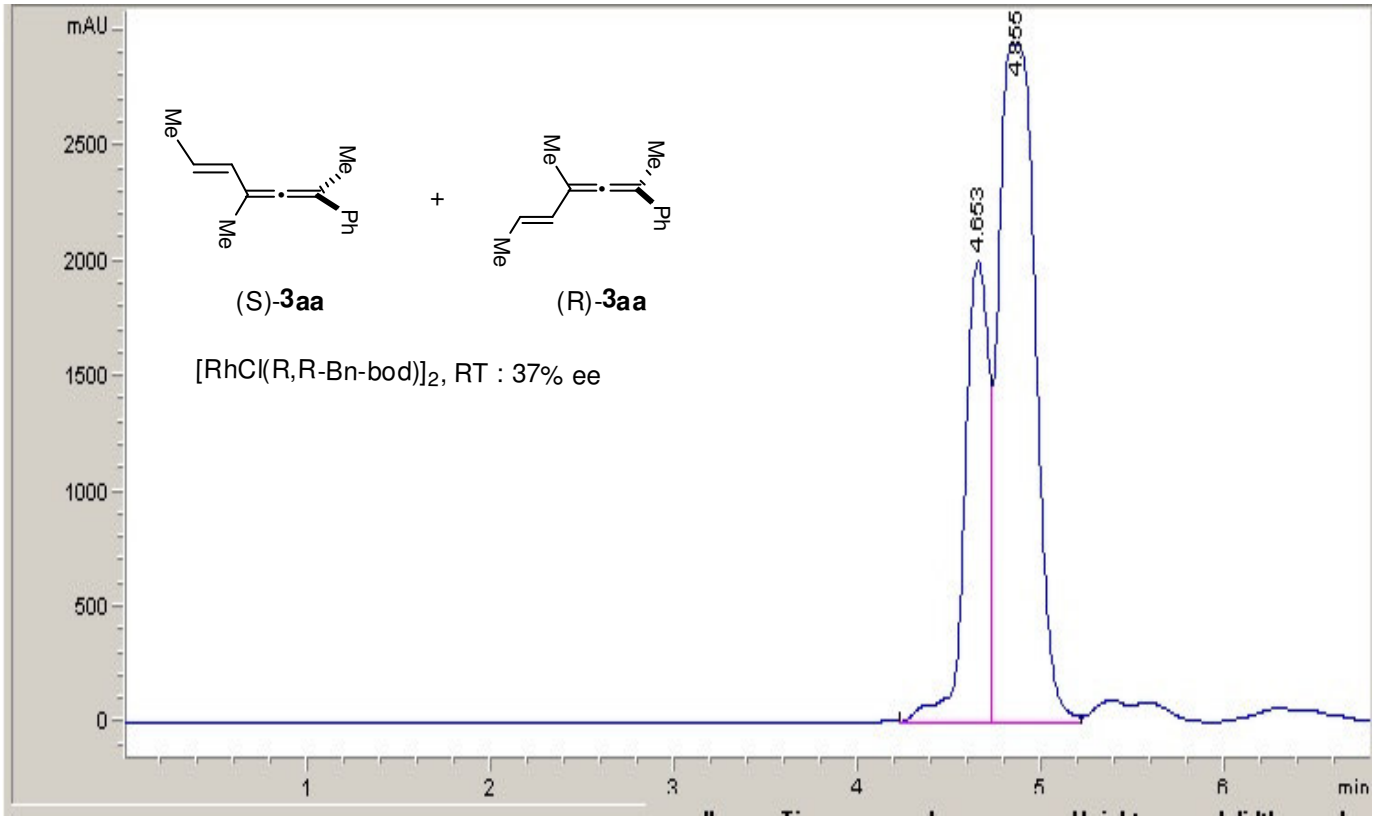

Figure G.4. HPLC Spectrum for racemic mixture of (*E*)- 2-phenyl-4-methylhepta-2,3,5-triene

APPENDIX H

GC CHROMATOGRAMS OF RACEMIC AND ENANTIOMERICALLY PURE (Z)-4-METHYLHEPT-3-EN-5-YN-2-OL

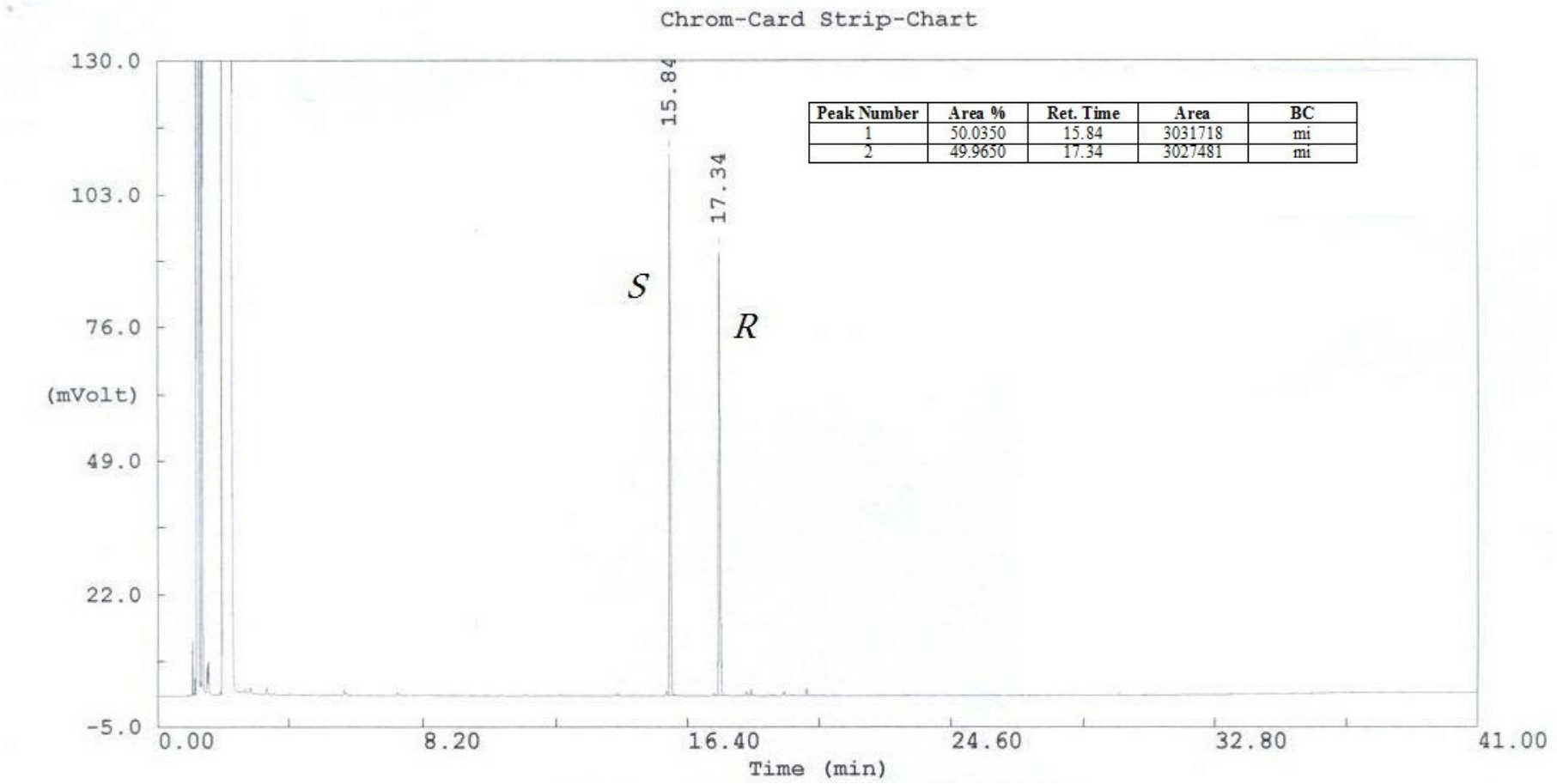

Figure H.1. GC Spectrum of Racemic 4-methylhept-3-en-5-yn-2-ol

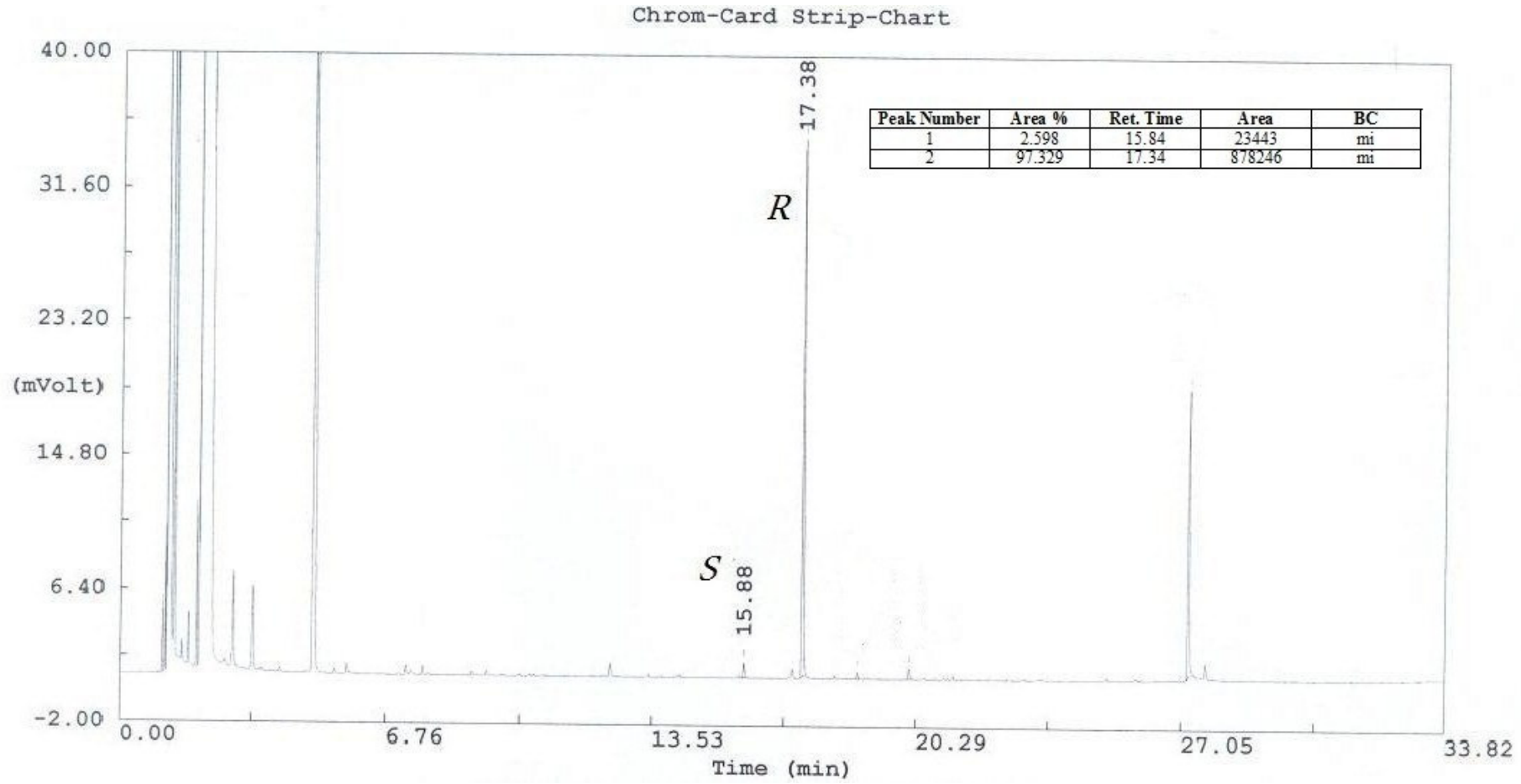

Figure H.2. GC Spectrum of Enantiomerically Pure 4-methylhept-3-en-5-yn-2-ol

APPENDIX I

COMPUTATIONAL CALCULATIONS DATA

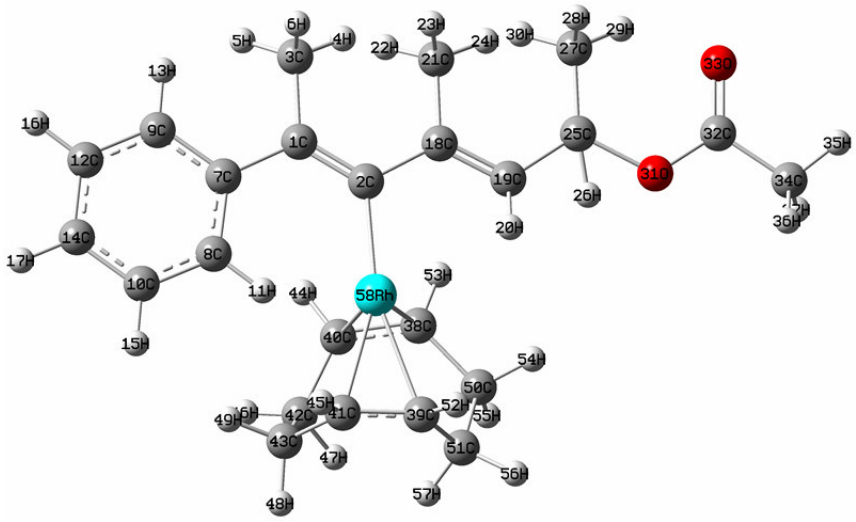

Figure I.1. The structure of the intermediate II which was subjected to conformational analysis by DFT calculation

Table I.1. Some Selected Geometrical Parameters for the Optimized Conformers of the Intermediate **II**[a]

	ES	**ER**	**ZS**	**ZR**
Rh58-C2	2.0608	2.0769	2.0656	2.0710
Rh58-C38	2.1381	2.1358	2.1362	2.1386
Rh58-C40	2.1480	2.1401	2.1507	2.1584
Rh58-C39	2.3124	2.3166	2.2961	2.3154
Rh58-C41	2.2708	2.2596	2.2699	2.2630
Rh58-C3	4.5488	4.5130	4.5431	4.5519
Rh58-C21	3.6354	4.1694	3.8739	3.6509
Rh58-C27	5.4462	4.7614	3.9633	4.2148
Rh58-C34	4.5146	4.5238	4.3586	4.5249
Rh58-O33	2.2862	2.2521	2.2399	2.2706
Rh58-O31	4.1065	3.7225	3.8532	4.1887
O33-C32	1.2568	1.2610	1.2581	1.2547
O33-C27	4.2443	4.0630	3.0171	3.1583
O33-C38	4.3106	4.3193	4.2240	4.3285
O33-C40	4.3959	4.3328	4.3776	4.3684
O33-C39	3.1974	3.3631	3.2584	3.2098
O33-C41	3.1456	3.1999	3.2958	3.0810
C32-O31	1.3517	1.3492	1.3498	1.3497
C25-O31	1.5397	1.5364	1.5114	1.5535
C1-C2	1.3691	1.3727	1.3724	1.3687
C2-C18	1.4910	1.4962	1.4962	1.4887
C18-C19	1.3678	1.3651	1.3625	1.3693
C3-C21	3.6901	3.2297	3.3743	3.6018
C3-C27	4.4296	6.1353	5.8712	3.7638

C3-C34	7.2882	4.8906	4.7043	7.4435
C21-C27	4.9153	4.9737	4.8474	4.7275
C21-C34	6.2662	6.3260	6.2940	6.1987
C27-C34	4.7401	4.6623	4.4240	4.4924
C27-C7	5.5588	6.8677	6.3048	4.1578
O31-C32-O33	124.5	124.4	124.8	125.3
C2-Rh58-C38	93.5	92.8	94.5	91.7
C7-C1-C18-C21	-114.9	112.3	-108.9	114.7
C3-C1-C7-C8	-32.4	-135.9	152.4	-144.1
C1-C2-C18-C19	-86.8	123.4	-105.4	93.5
C7-C1-C2-Rh58	-3.9	-10.3	5.8	7.6
C8-C7-C2-Rh58	130.6	27.3	-18.3	33.7
H20-C19-C25-H26*	-173.3	-124.2	-41.8	29.5

a Distances are given in angstrom, angles in degrees.

Table I.2. The Natural Bond Orbital (NBO) Charge Analysis for the Optimized Conformers of the Intermediate **II**

	ES	ER	ZS	ZR
1 C	-0.07284	-0.05770	-0.07039	-0.06755
2 C	-0.17116	-0.19526	-0.17233	-0.17630
3 C	-0.65531	-0.66407	-0.66213	-0.65852
4 H	0.22071	0.22450	0.22576	0.22210
5 H	0.22087	0.21383	0.22283	0.21670
6 H	0.21554	0.22568	0.21401	0.22078
7 C	-0.04490	-0.03468	-0.04207	-0.04447
8 C	-0.21720	-0.20932	-0.21009	-0.20225
9 C	-0.20097	-0.21630	-0.21882	-0.21680
10 C	-0.21330	-0.21458	-0.21667	-0.21484
11 H	0.21216	0.22296	0.21724	0.21840
12 C	-0.21681	-0.21296	-0.21193	-0.21344
13 H	0.22262	0.21224	0.21299	0.21234
14 C	-0.22832	-0.22865	-0.22909	-0.22880
15 H	0.21455	0.21335	0.21377	0.21379
16 H	0.21459	0.21468	0.21465	0.21469
17 H	0.21427	0.21422	0.21426	0.21429
18 C	0.02100	0.03214	-0.00154	0.02735
19 C	-0.30188	-0.29285	-0.29094	-0.31114
20 H	0.20771	0.20693	0.21277	0.20828
21 C	-0.63389	-0.63353	-0.61976	-0.63162
22 H	0.22606	0.22277	0.22398	0.22404
23 H	0.22627	0.22332	0.21553	0.22517
24 H	0.21628	0.21439	0.21218	0.21610
25 C	0.11453	0.12656	0.12278	0.11883

26 H	0.23011	0.21497	0.23351	0.23077
27 C	-0.63984	-0.64338	-0.64778	-0.65757
28 H	0.21967	0.22565	0.22995	0.23727
29 H	0.22685	0.22521	0.22192	0.22309
30 H	0.23103	0.22810	0.23014	0.23527
31 O	-0.58922	-0.57925	-0.57864	-0.59308
32 C	0.89372	0.90212	0.90805	0.89272
33 O	-0.62956	-0.62822	-0.62898	-0.63029
34 C	-0.71117	-0.70636	-0.70584	-0.70960
35 H	0.24739	0.25802	0.24565	0.24595
36 H	0.24307	0.24551	0.26371	0.24017
37 H	0.24609	0.24440	0.24378	0.24739
38 C	-0.19146	-0.20057	-0.20047	-0.20771
39 C	-0.23192	-0.23596	-0.23003	-0.23572
40 C	-0.22493	-0.21507	-0.21744	-0.20590
41 C	-0.22846	-0.21991	-0.23036	-0.22292
42 C	-0.42944	-0.42877	-0.42816	-0.43070
43 C	-0.43400	-0.43475	-0.43327	-0.43429
44 H	0.22859	0.24103	0.21899	0.24211
45 H	0.22759	0.23654	0.22969	0.23666
46 H	0.22482	0.22972	0.22499	0.23179
47 H	0.21015	0.20735	0.20895	0.20818
48 H	0.22390	0.22338	0.22336	0.22363
49 H	0.22066	0.22720	0.22120	0.22345
50 C	-0.43223	-0.43010	-0.43154	-0.43072
51 C	-0.43294	-0.43150	-0.43255	-0.43192
52 H	0.23468	0.22951	0.23475	0.22807
53 H	0.24315	0.22643	0.24417	0.23212
54 H	0.22946	0.21968	0.22748	0.21827
55 H	0.22380	0.22275	0.22319	0.22392
56 H	0.22749	0.22621	0.22711	0.22653
57 H	0.20839	0.21044	0.20923	0.21055
58 Rh	0.14399	0.10195	0.11825	0.14537

Table I.3 HOMO-LUMO energies of intermediates

Intermediates	ES	ER	ZS	ZR
LUMO	-0.03578	-0.03981	-0.03637	-0.0341
HOMO	-0.1753	-0.17222	-0.17122	-0.17522
E(LUMO-HOMO) (au)	0.13952	0.13241	0.13485	0.14112
E(LUMO-HOMO) (kj/mol)	366.3	347.6	354.0	370.5

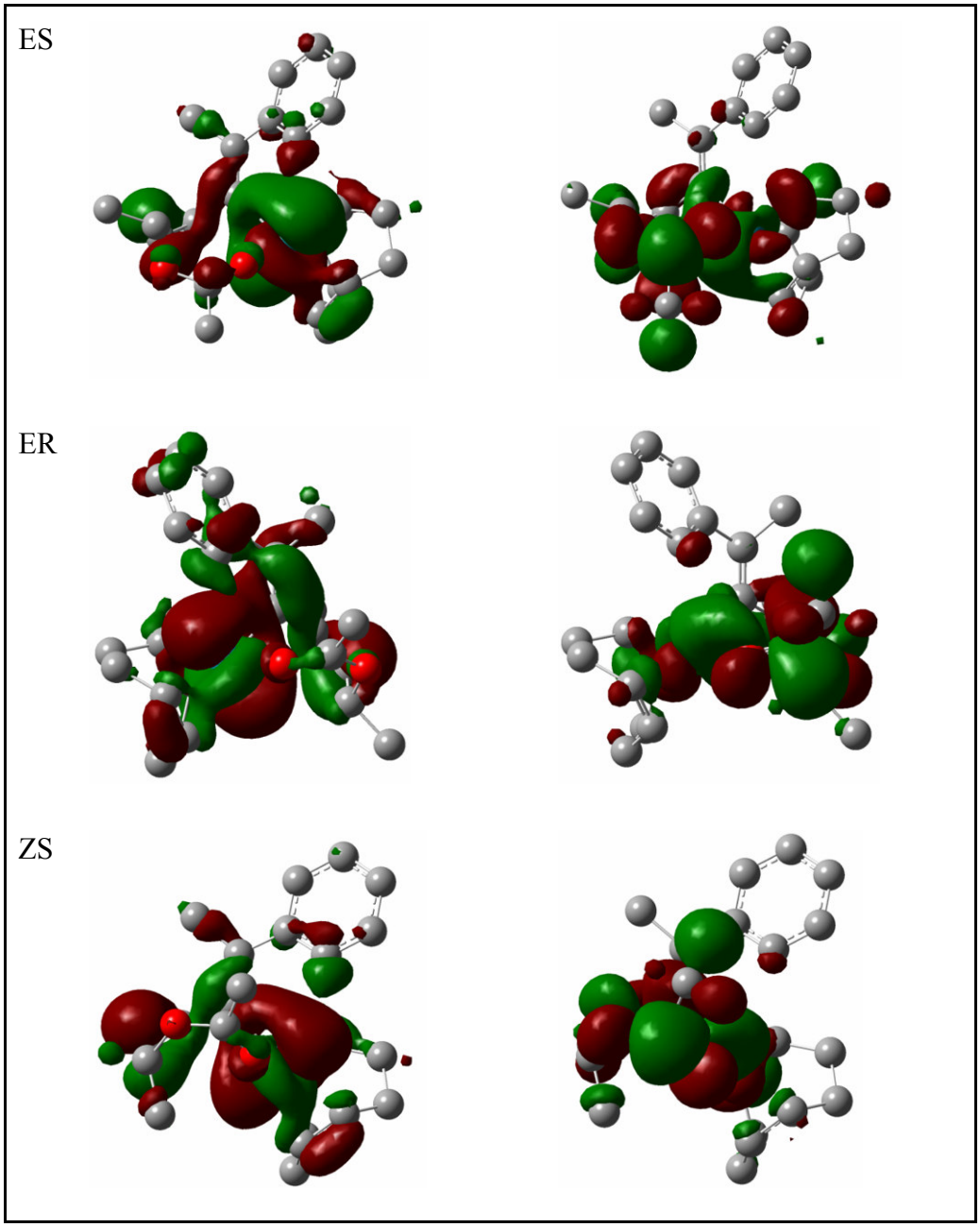

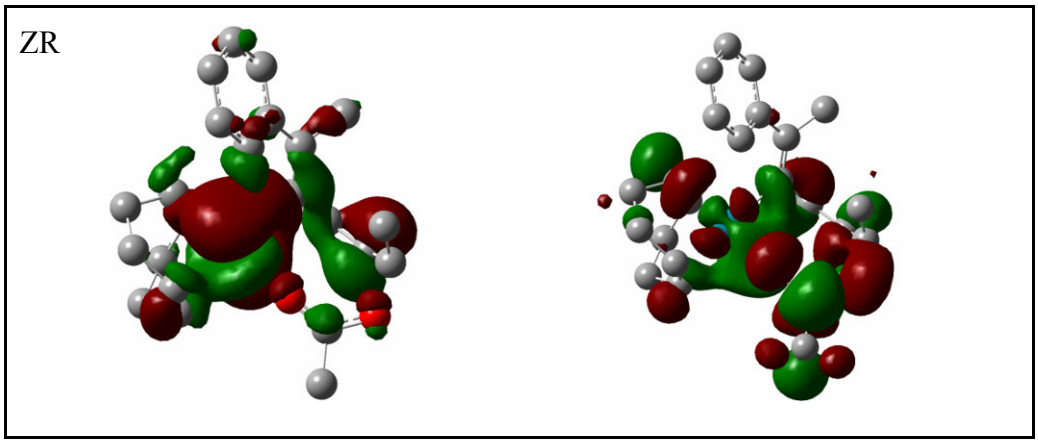

Figure I.2 HOMO-LUMO figures of intermediates

Table I.4 HOMO-LUMO energies of products

Products	ES	ER	ZS	ZR
LUMO	-0.02777	-0.02771	-0.028	-0.02867
HOMO	-0.21387	-0.21388	-0.21626	-0.21717
E(LUMO-HOMO) (au)	0.1861	0.18617	0.18826	0.1885
E(LUMO-HOMO) (kj/mol)	488.6	488.8	494.3	494.9

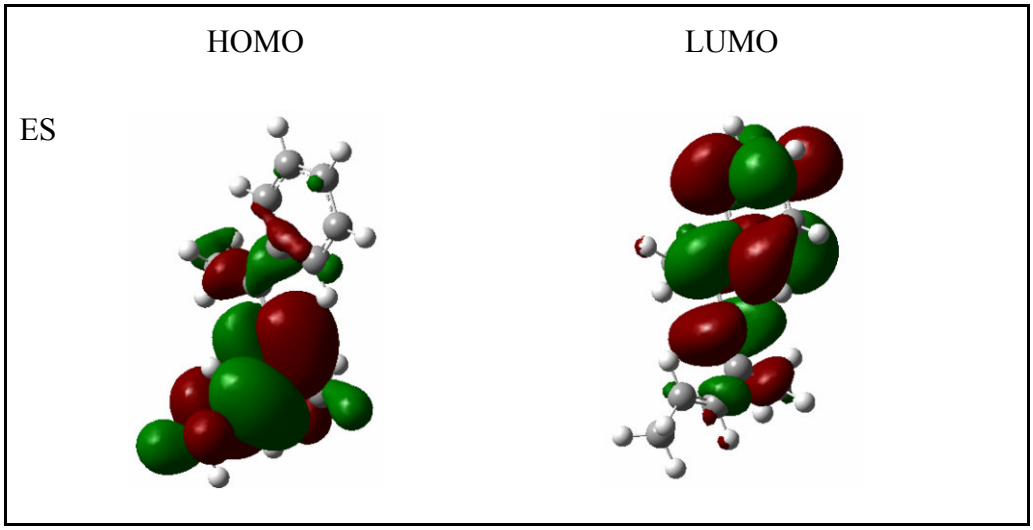

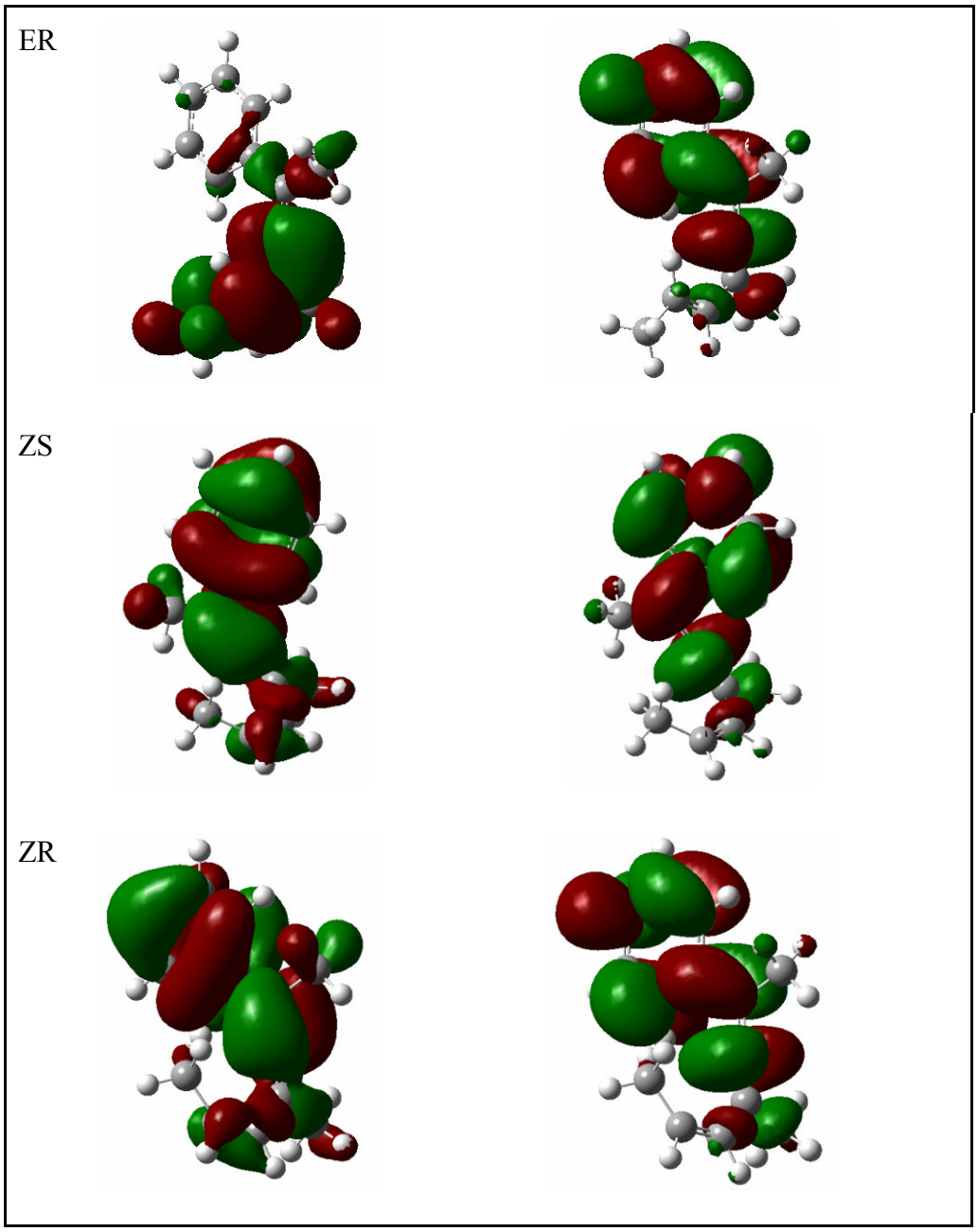

Figure I.3 HOMO-LUMO figures of products